APPENDIX 3.9.4
EOS-HSM STRUCTURAL ANALYSIS

Table of Contents

List of Tables

List of Figures

3.9.4 EOS-HSM STRUCTURAL ANALYSIS

The purpose of this appendix is to present the structural evaluation of the EOS-HSM due to all applied loads during storage, loading and unloading operation. The NUHOMS® EOS System consists of the dual-purpose (transportation and storage) EOS-37PTH and EOS-89BTH dry shielded canister (DSC), a horizontal storage module (EOS-HSM), an onsite transfer cask (EOS-TC), and associated ancillary equipment.

3.9.4.1 General Description

General description and operational features for the NUHOMS® EOS System is provided in Chapter 1. The EOS-HSM is a freestanding, reinforced concrete structure, designed to provide environmental protection and radiological shielding for the EOS-37PTH DSC or EOS-89BTH DSC. The drawings of the EOS-HSM, showing different components and overall dimensions, are provided in Chapter 1.

The EOS-HSM consists of a base unit and a roof unit. The roof unit rests mainly on the front and rear walls, and partly on the side walls of the base unit. The roof and the base are connected by bolts/embedments to form a single module via four steel brackets located at each of the interior upper corners of base unit.

Alternate designs of horizontal storage modules may be used in lieu of EOS-HSM as part of NUHOMS® EOS System. The EOS-HSMS is a multi-segment design of horizontal storage module which consists of two segments of the base unit and a roof unit. The two segments of the base unit of EOS-HSMS are connected by grouted, high-strength, threaded bars/embedments, and the base and roof are connected in a similar way to that of EOS-HSM.

An alternate Flat Plate Support (FPS) Rail design of horizontal storage module, the EOS-HSM-FPS, may also be used in lieu of EOS-HSM as a part of the NUHOMS® EOS System. EOS-HSM-FPS is modified from the EOS-HSM to support the FPS DSC Support Structure with concrete pedestals spaced along the length of the DSC Support Structure.

EOS-HSMS-FPS is a multi-segment design of the EOS-HSM-FPS which consists of two segments of the base unit and a roof unit. The alternate Base front wall thickness is 42" uniform thickness, as opposed to the original design which expanded from 42" to 54" at the bottom portion of the alternate front wall. The 42" thick lower portion of the rear wall is replaced with 24" thick (12" thick rear wall plus 12" thick rear pedestal) support pedestals.

The two segments of the base unit of EOS-HSMS-FPS are connected by grouted, high-strength, threaded bars/embedments, and the base and roof are connected in a similar way to that of EOS-HSM-FPS. EOS-HSM is used herein for all alternatives unless a unique situation is presented. EOS-HSM-FPS is used herein for both the EOS-HSM-FPS and EOS-HSMS-FPS unless a unique situation is presented. The EOS-HSM storage modules can be arranged either in a single-row array, or in back-to-back double-row arrays by placing a module next to, and in contact with, adjacent module(s) with thick end shield walls connected to the EOS-HSM at the end of the arrays. The thick rear shield walls are also connected to the back wall of the EOS-HSM, if the modules are placed in a single-row array.

The EOS-37PTH DSC or EOS-89BTH DSC is supported inside the EOS-HSM by DSC support structure. The DSC support structure is comprised of two main support beams, two extension plates and two nitronic sliding rails and it spans between the front wall and the rear wall of the base unit. The web of the main support beams has openings to allow the air flow around the DSC. The DSC support structure provides support for the DSC during storage and also acts as a sliding surface during the insertion and retrieval of DSC.

DSC support structure is used herein for both DSC support structure and FPS DSC support structure unless a unique situation is presented.

The EOS-37PTH DSC or EOS-89BTH DSC is supported inside the EOS-HSM-FPS by the FPS DSC support structure. The FPS DSC support structure is comprised of a stiffened flat-plate design that is supported at the front and rear walls of the EOS-HSM-FPS and additionally at two intermediate concrete support pedestals. The FPS DSC support structure provides support for the DSC during storage and also acts as a sliding surface during the insertion and retrieval of DSC. The FPS DSC support structure is only an option for the medium EOS-HSM.

The width of EOS-HSM is 116 inches. The overall height of EOS-HSM is 240 inches including the outlet vent cover. Three different EOS-HSM lengths are available in order to accommodate DSCs of different lengths. The internal cavity of the EOS-HSM accommodates DSCs of variable length by varying the location of the axial retainer and by variation of gap between the DSC and the EOS-HSM back wall.

The air inlet vents located at the front lower corners of base unit extend through the bottom of side wall on both sides, which ultimately lead to the cavity of base unit. The air outlet vents are provided in the roof at both sides of the module.

The front wall of EOS-HSM base unit has round access door opening provided for transferring EOS-37PTH DSC or EOS-89BTH DSC into the module or retrieving it from the module. The door opening is closed by a shield door after the insertion of EOS-37PTH DSC or EOS-89BTH DSC. The EOS-HSM shield door is a combination of rectangular and cylindrical concrete block with steel backing plate on the inside face. The shield door provides environmental protection, including missile and shielding protection.

End shield walls are installed at each end of a module array to provide the required missile and shielding protection. Similarly, a rear shield wall is installed at the rear of each module of the single row module array for same purpose.

For thermal protection of the EOS-HSM concrete, a thin stainless steel heat shield is installed inside the EOS-HSM. The interior surface of the upper part of the side wall is protected with side heat shields, and the underside of the roof unit is protected with a roof heat shield. The roof heat shield has an upward slope at 10 degrees from center towards outlet vent. The heat shield guides the cooling air flow through the EOS-HSM.

During DSC insertion and retrieval operations, the EOS-TC is docked with the EOS-HSM docking surface and mechanically secured to the cask restraint embedments provided in the front wall of the base unit. These embedments are equally spaced on either side of the door opening and located near the lower embedment for door attachment.

3.9.4.2 Material Properties

The material properties used in the analysis and design of EOS-HSM and its components are discussed in detail in Chapter 8.

3.9.4.3 Design Criteria

The reinforced concrete EOS-HSM and the DSC support structure are important to safety components of NUHOMS® EOS System. Consequently, they are designed and analyzed to perform their intended functions under the extreme environmental and natural phenomena specified in 10 CFR 72.122 [3.9.4-1] and American National Standards Institute (ANSI) 57.9 [3.9.4-10]. These include tornado and wind, seismic, and flood design criteria. The design wind pressure is determined as per American Society of Civil Engineers (ASCE) 7-10 [3.9.4-15].

The concrete EOS-HSM and steel DSC support structures are designed to the requirements of American Concrete Institute (ACI) 349-06 [3.9.4-12] and the American Institute of Steel Construction (AISC) Manual of Steel Construction [3.9.4-14], respectively, using the load combinations prescribed by ANSI 57.9 [3.9.4-10]. When ACI-349-06 does not have enough information, ACI-318-08 [3.9.4-11] is used as supplement. The following table summarizes the Codes and Standards for design and fabrication of these components.

Component	Material	Applicable Code
EOS-HSM Concrete Components	Concrete	ACI 349-06 (Design) ACI 318-08 (Fabrication) ASCE 7-10 (Loads) ANSI/ANS 57.9-84 (Loads & Load Combination)
DSC Support Structure, Heat Shields and other Steel Components	Steel	AISC Manual of Steel Construction,13th Edition (Structural Steel) AWS D1.1, March 2010 *(or later editions)* (Structural Weld) ASCE 7-10 (Loads) ANSI/ANS 57.9-84 (Loads & Load Combination)

The ultimate strength method of ACI 349-06 [3.9.4-12] is used for the design of the EOS-HSM reinforced concrete structural components. The reinforcement is provided to meet the minimum flexural and shear reinforcement requirement of ACI 349-06 and to ensure that the provided design strength exceeds the required strength. Alternatively, for some cases, the minimum reinforcement area requirement can be waived for components with a flexural stress ratio of less than 0.66 as per Section 10.5.3 of ACI 349-06 [3.9.4-12].

The axial, shear and moment capacities for all the concrete components of the EOS-HSM calculated based on ACI 349-06 are provided in Table 3.9.4-11, Table 3.9.4-12*, Table* 3.9.4-26*, and Table* 3.9.4-27 *for EOS-HSM and Table* 3.9.4-26a *and Table* 3.9.4-27a *for EOS-HSM-FPS*. The capacities for blocked vent accident condition consider the strength reduction at elevated temperature.

The comparison of the Highest Combined Shear Force/Moment with the capacities for the EOS HSM is provided in Table 3.9.4-13 *and the comparison of the Highest Combined Shear Force/Moment with the capacities for the Alternate Front wall is provided in Table* 3.9.4-28.

Similarly, the comparison of the highest combined axial force/moment with capacities for the EOS HSM is provided in Table 3.9.4-14 *and comparison of the highest combined axial force/moments with capacities for the alternate front wall is provided in Table* 3.9.4-29.

The required steel strength, S, and required steel shear strength, S_v, for critical section of steel structure are calculated in accordance with the requirements of AISC Steel Construction Manual [3.9.4-14] using the Allowable Strength Design (ASD) method.

3.9.4.4 Load Cases

A summary of the design loads for EOS-HSM concrete component evaluation is provided in Table 3.9.4-4. This table also presents the applicable codes and standards for specific load. A summary of the design loads for DSC support structure is provided in Table 3.9.4-15.

3.9.4.5 Load Combination

The load combinations used in the structural analysis of EOS-HSM and DSC support structure comply with the requirement of 10 CFR 72.122 [3.9.4-1] and ANSI 57.9-84 [3.9.4-10]. Table 3.9.4-5 and Table 3.9.4-16 summarize the load combination requirement of EOS-HSM and DSC support structure, respectively.

3.9.4.6 Finite Element Models

EOS-HSM and EOS-HSMS have variable lengths to store DSCs of different lengths. EOS-HSM Long is analyzed and governs the structural design of EOS-HSM Short, Medium and Long. EOS-HSM-FPS and EOS-HSMS-FPS are only available and analyzed at a Medium length.

3.9.4.6.1 Finite Element Model to Evaluate EOS-HSM Concrete Components for Mechanical Loads

The structural analysis of an individual module provides a conservative estimate of the response of the EOS-HSM structural elements under the postulated static and dynamic loads for any EOS-HSM array configuration. The frame and shear wall action of the EOS-HSM concrete components are considered to be the primary structural system resisting the loads. The analytical model is evaluated for normal operating, off-normal, and postulated accident loads acting on the EOS-HSM.

A three-dimensional (3D) ANSYS finite element model (FEM) of the EOS-HSM, including all the concrete components, is developed. The eight-node brick element (ANSYS element type SOLID185) is used to model the concrete structure. Each node of the eight-node brick element has three translational degrees of freedom. The DSC is modeled using beam elements (ANSYS element type BEAM4). The DSC main support beam, W12x136 and the brace, C3x5 are also modelled using beam elements with appropriate section properties. The mass of the DSC is lumped at eleven discrete nodes of the beam using lumped mass elements (ANSYS element type MASS21). A plot of the ANSYS model of EOS-HSM and EOS-HSMS is shown in Figure 3.9.4-1 and Figure 3.9.4-2, respectively.

A three-dimensional (3D) ANSYS finite element model (FEM) of the EOS-HSM-FPS, including all the concrete components, is developed. The eight-node brick element (ANSYS element type SOLID185) is used to model the concrete structure. Each node of the eight-node brick element has three translational degrees of freedom. The DSC is modeled using beam elements (ANSYS element type BEAM4). The FPS DSC support structure consists of two composite plates (1"x12" and 1"x4").

The mass of the DSC is lumped at 15 discrete nodes using lumped mass elements (ANSYS element type MASS21). A plot of the ANSYS model of EOS-HSM-FPS and EOS-HSMS-FPS are shown in Figure 3.9.4-1a *and* Figure 3.9.4-2a*, respectively.*

The DSC support structure is incorporated into the EOS-HSM analytical model to transfer the load to concrete components. The connections of the support structure to the concrete structure are modeled using rigid beam elements. The various normal, off-normal and accident loads are applied to the analytical model and internal forces and moments are computed by performing a linear elastic finite element analysis.

The node coupling option of ANSYS is used to represent the appropriate connection between the base and roof of the EOS-HSM *and EOS-HSM-FPS models.* For EOS-HSMS *and EOS-HSMS-FPS*, the node to node contact element (ANSYS element type CONTA178) is used across the interface of the upper and lower segment to transfer the load from the roof and upper segment to the lower segment. The counter bore and rail extension baseplate groove at the door opening are not included in the FEM. Conservatively, the nodes at the bottom of EOS-HSM are constrained in all three translational degree of freedom, thus maximizing the EOS-HSM design forces and moments.

3.9.4.6.2 Finite Element Model of the EOS-HSM Concrete Structure for Thermal Stress Analysis

Thermal stress analyses of the EOS-HSM were performed using a 3D FEM, which includes only the concrete components. The connections of the door and the support structure rails to the EOS-HSM concrete structure are designed so that free thermal growth is permitted in these members when the EOS-HSM is subjected to thermal loads. Because of their free thermal growth, the door and the support structure do not induce thermal stresses in the concrete components of the EOS-HSM. Therefore, the analytical model of the EOS-HSM for thermal stress analysis of the concrete components does not include the DSC support structure and the door. The ANSYS models with temperature profile, which is used to perform thermal stress analysis of the concrete components, are shown in Figure 3.9.4-3, Figure 3.9.4-3a, Figure 3.9.4-4, *and* Figure 3.9.4-4a.

For the thermal load analysis, the bottom of the EOS-HSM (y=0 in ANSYS model) was restrained at one set of edge nodes (in axial and lateral directions) and friction forces were applied at the bottom of EOS-HSM base in the axial and lateral directions. One node in the front wall and two nodes in the back wall at y=0 are also restrained in vertical direction.

3.9.4.6.3 Finite Element Model for Structural Analysis of DSC Support Structure

A 3D FEM of the DSC main support beam with stiffener plates and rail extension baseplate is developed in the computer program ANSYS [3.9.4-19]. In the finite element model (FEM) for the DSC main support beam (W12x136), the W section of the main support beam is broken down into flange and web components represented individually by BEAM189 elements.

The beam elements (BEAM189) are arranged in a 2D plane aligned with the centerline of the beam, inclined 30 degrees from vertical along the length of the beam. Each element has three nodes with six degrees of freedom (three translational and three rotational) per node.

The web of the DSC main support beam has triangular openings, allowing for heat flow, resulting in vertical and diagonal web elements. The cross sections of these components are calculated and used to define the assigned cross sections for each component. A plot of the front portion of the model of the DSC main support beam model is shown in Figure 3.9.4-6.

The model is completely restrained at the bottom end of the rail extension baseplate. The ends of the DSC main support beam at the bottom are restrained for vertical displacement and rotation about longitudinal axis to simulate the simple support condition of the concrete pedestals at the front and rear walls. The support beam is also restrained laterally at the location of lateral braces.

The ETAB command of ANSYS is used to extract the beam element results due to individual load cases which then combined to determine the combined load results.

The FPS DSC support structure is a simple design comprised of flat plates. Therefore, hand calculation methodology was employed assuming it as a simply supported beam with concentrated load.

3.9.4.6.4 Finite Element Model for Structural Analysis of Heat Shield Panels and Connection Studs

The heat shields (coupled panel-stud system) are subjected to two loads: a combination of 1g dead load due to its own weight, and a seismic load that is dependent upon its natural frequency as well as the in-structure response spectra (ISRS) at the supports of the plate-stud system.

Modal time-history analysis of the EOS-HSM is performed using ANSYS computer code to determine the ISRS at the nodes at which the studs are supported. Applicable time-histories and modal properties for this evaluation are provided in Section 3.9.4.9.2.

ANSYS is also used to determine the natural vibration frequencies of the coupled panel-stud system. Shell elements (ANSYS element type SHELL63) are used to model the heat shield panel and beam elements (ANSYS element type BEAM4) are used for the studs. The FEM of the coupled panel-stud system is shown in Figure 3.9.4-8 and Figure 3.9.4-9.

The natural frequency of the plate-stud system is used to determine the appropriate g load from the ISRS. It is assumed that the heat shields are dynamically decoupled from the EOS-HSM because the concrete EOS-HSM is much more rigid than the heat shields and the weight of the heat shield is small as compared to the total weight of loaded EOS-HSM. Accordingly, the heat shields are not accounted for in the modal time-history analysis of the EOS-HSM, and the EOS-HSM is not considered in modal analysis of the heat shields.

3.9.4.7 Normal Operation Structural Analysis

The evaluation of the EOS-HSM is performed at normal operating condition. The following table shows the normal operating loads for which the EOS-HSM components are designed. The table also lists the individual EOS-HSM components that are affected by each loading.

	Components	
Load Type	**EOS-HSM**	**DSC Support Structure**
Dead Load	X	X

Live Load	X	X
Normal Handling	X	X
Normal Thermal	X	X
Wind Load	X	

The reinforced concrete and the steel DSC support structure of the EOS-HSM are analyzed for the normal, off-normal, and postulated accident conditions using FEMs described in Section 3.9.4.6. These models are used to evaluate concrete and support structure forces and moments due to dead load, live load, normal handling loads, normal thermal loads, and wind load. The methodology used to evaluate the effects of these normal loads is addressed in the following paragraphs.

3.9.4.7.1 EOS-HSM Dead Load (DL) Analysis

Dead loads are applied to the analytical model by application of 1g acceleration in the vertical direction where g is the gravitational acceleration (386.4 in/sec2). The 5% variation of dead load as indicated in ANSI/ANS 57.9 is not used because the heaviest design weight is used for analysis.

3.9.4.7.2 EOS-HSM Live load (LL) Analysis

Live load analysis is performed by applying 200 psf pressure on the roof. The DSC weight is also applied on the DSC support structure as a live load.

3.9.4.7.3 EOS-HSM Normal Operational Handling Load (R_o) Analysis

Normal operation assumes the canister is sliding over the DSC support structure due to a hydraulic ram force of up to 135,000 lbs (insertion) and 80,000 lbs (extraction) applied at the grapple ring. The normal operation handling load of 70,000 lbs is applied to each DSC main support *structure* in the axial direction resulting in a total applied load of 140,000 lbs on both beams which conservatively envelopes the total insertion/extraction force. The same magnitude of load of 70,000 lbs is also applied at each of the cask restraint embedment in opposite direction. In addition, the DSC weight is applied as a distributed load on both DSC support *structure* of the EOS-HSM.

3.9.4.7.4 EOS-HSM Normal Operating Thermal (T_o) Stress Analysis

The normal operating thermal (T_o) loads on EOS-HSM include the effect of design basis heat load up to 50 kW generated by DSC, plus the effect of normal ambient temperature range. To evaluate the effects of normal thermal loads on the EOS-HSM, heat transfer analyses for a range of normal ambient temperatures (-20 °F and 100 °F) are performed with DSC heat load of 50 kW. The normal thermal cold condition (-20 °F) is bounded by off-normal thermal cold condition (-40 °F). Therefore, off-normal thermal cold condition is used in place of normal thermal cold condition. The ambient condition that causes maximum temperature and maximum gradients in the concrete components is used in the analysis. The normal thermal hot condition is the governing case for this load case. The EOS-HSM thermal stress analysis was performed using thermal profiles and maximum temperatures that bounds those reported in Chapter 4.

3.9.4.7.5 EOS-HSM Design Basis Wind Load (W) Analysis

The DSC support structure and DSC inside the EOS-HSM are not affected by wind load. The concrete structure forces and moments due to design basis wind load (W) are bounded by the result of tornado generated wind load discussed in Section 3.9.4.9.1. Therefore, tornado generated wind load is conservatively used in the off-normal wind load combination C2, as seen in Table 3.9.4-5. Therefore, no separate analysis is performed for the design basis wind load case.

3.9.4.8 Off-Normal Operation Structural Analysis

This section describes the design basis off-normal events for the EOS-HSM components and presents analyses that demonstrate the adequacy of the design safety features of the EOS-HSM.

The following table shows the off-normal operating loads for which the EOS-HSM components are designed.

	Components	
Load Type	**EOS-HSM**	**DSC Support Structure**
Off-Normal Handling	X	X
Off-Normal Thermal	X	X

For an operating NUHOMS® EOS System, off-normal events could occur during fuel loading, TC handling, canister transfer, trailer towing, and other operational events. Two credible off-normal events as listed in the above table are defined that bound the range of off-normal conditions for EOS-HSM. The limiting off-normal events are defined as a jammed DSC during loading or unloading from the EOS-HSM and the extreme ambient temperatures of -40 °F (winter) and +117 °F (summer). These events bound the range of expected off-normal structural loads and off-normal temperatures range acting on the EOS-HSM. ANSYS FEMs described in Section 3.9.4.6 are used to evaluate concrete and support structure forces and moments due to these loads.

The FPS DSC support structure employs hand calculation methodology to calculate forces and moments by assuming it as a simply supported beam with concentrated load.

3.9.4.8.1 EOS-HSM Off-Normal Handling Loads (Ra) Analysis

This load case assumes that the EOS-TC is not accurately aligned with respect to the EOS-HSM resulting in binding of the DSC during a transfer operation causing the hydraulic pressure in the ram to increase. The ram force is limited to a maximum load of 135,000 lbs during insertion, as well as during retrieval. Therefore, for the DSC support structure, the off-normal jammed canister load (R_a) is defined as an axial load of 135 kips on one DSC support *structure*, plus a vertical load of one half the DSC weight (on both rails) at the most critical location.

3.9.4.8.2 EOS-HSM Off-Normal Thermal Loads Analysis

This load case is the same as the normal thermal load, but with an ambient temperature range from -40 °F to 117 °F. The temperature distributions for the extreme ambient conditions are used in the analysis for the concrete component evaluation.

3.9.4.9 Accident Condition Structural Analysis

The design basis accident events specified by ANSI/ANS 57.9-1984, and other credible accidents postulated to affect the normal safe operation of the EOS-HSM are addressed in this section.

Each accident condition is analyzed to demonstrate that the requirements of 10 CFR 72.122 are met and that adequate safety margins exist for the EOS-HSM design. The resulting accident condition stresses in the EOS-HSM components are evaluated and compared with the applicable code limits. The postulated accident conditions addressed in this section include:

- Tornado winds and tornado generated missiles (W_t, W_m)
- Design basis earthquake (E)

- Design basis flood (FL)
- Blocked Vent Accident Thermal (T_a)

ANSYS FEMs described in Section 3.9.4.6 are used to evaluate concrete and support structure forces and moments due to these loads.

The FPS DSC support structure employs hand calculation methodology to calculate forces and moments by assuming it as a simply supported beam with concentrated load.

3.9.4.9.1 Tornado Winds/Tornado Missile Load (W_t, W_m) Analysis

The most severe tornado generated wind and missile loads selected for analysis specified by NRC Regulatory Guide 1.76 [3.9.4-4] and NUREG-0800 [3.9.4-7]. The extreme design basis wind loads are less severe than tornado generated wind loads and, therefore, do not need to be addressed.

The tornado wind intensities used for the EOS-HSM analysis are obtained from NRC Regulatory Guide 1.76, Rev. 0 [3.9.4-4], which bound the design basis requirements. Region I intensities are utilized since they result in the most severe loading parameters. For this region, the maximum wind speed is 360 mph, the rotational speed is 290 mph, and the maximum translational speed is 70 mph. The radius of the maximum rotational speed is 150 ft, the pressure drop across the tornado is 3 psi and the rate of pressure drop is 2 psi per second [3.9.4-4].

The maximum wind speed used of 360 mph provides substantial conservatism relative to the maximum wind speed of 230 mph prescribed in current regulatory guidance in NRC Regulatory Guide 1.76 Revision 1 [3.9.4-22]. For the purposes of the structural evaluation as described in Chapter 3 and its associated appendices, as well as the accident evaluation as described in Chapter 12 the design basis tornado (DBT) refers to the bounding criteria from Regulatory Guide 1.76, Rev. 0 used in the analysis.

Tornado loads are generated for three separate loading phenomena:

- Pressure or suction forces created by drag as air impinges and flows past the EOS-HSM. These pressure or suction forces are due to tornado generated wind with maximum wind speed of 360 mph.
- Pressure or suction forces created by drag due to tornado generated pressure drop or differential pressure load of 3 psi.
- Impact, penetration and spalling forces created by tornado-generated missiles impinging on the EOS-HSM.

The determination of impact forces created by tornado missiles for the EOS-HSM is consistent with that presented in Section 2.3.1.2. The four types of missiles listed below envelope the missile spectrum of NUREG-0800, Revision 2, Section 3.5.1.4 [3.9.4-7]. These missiles also bound the design basis missile spectrum of NRC Regulatory Guide 1.76, Revision 1 [3.9.4-22] and NUREG 0800, Revision 3, Section 3.5.1.4 [3.9.4-8]. Evaluation of the effects of small diameter spherical missiles (artillery) is not required because there are no openings in the EOS-HSM leading directly to the DSC through which such missiles could pass.

1. Utility wooden pole, 13.5" diameter, 35' long, Weight = 1500 lbs, Impact velocity = 294 fps.

2. Armor piercing artillery shell 8" diameter, Weight = 276 lbs, Impact velocity = 185 fps.

3. Steel pipe, 12" diameter, Schedule 40, 30 ft long, Weight = 1500 lbs, Impact velocity = 205 fps.

4. Automobile traveling through the air not more than 25 ft above the ground and having contact area of 20 sq. ft, Weight = 4000 lbs, Impact Horizontal Velocity = 195 fps.

Stability and stress analyses are performed to determine the response of the EOS-HSM to tornado wind pressure loads. The stability analyses are discussed in detail in Appendix 3.9.7. The stress analyses are performed using the ANSYS FEM of a single EOS-HSM to determine design forces and moments. These conservative analyses envelope the effects of wind pressures on the EOS-HSM array. Thus, the requirements of 10 CFR 72.122 are met.

The EOS-HSM is qualified for maximum design basis tornado (DBT) generated design wind loads of 218 psf and 154 psf on the windward and leeward EOS-HSM walls (See Table 3.9.4-1 and Table 3.9.4-2), and a pressure drop of 3 psi.

A single, stand-alone EOS-HSM is protected by shield walls, or an adjacent module on either side and at the rear. For an EOS-HSM array, the critical module is on the windward end of the array. This module has an end shield wall to protect the module from tornado missile impacts. The shield wall is also subjected to the 218 psf windward pressure load. The leeward side of the same end module in the array has no appreciable suction load due to the presence of the adjacent module. The 154 psf suction load is applicable to the end shield wall on the opposite end module in the array. A suction of 326 psf is also applied to the roof of each EOS-HSM in the array.

For the stress analyses, the DBT wind pressures are applied to the EOS-HSM as uniformly distributed loads. The rigidity of the EOS-HSM in the transverse direction, due to frame and shear wall action of the EOS-HSM, is the primary load transfer mechanism assumed in the analysis. The bending moments and shear forces at critical locations in the EOS-HSM concrete components are calculated by performing an analysis using the ANSYS analytical model of the EOS-HSM as described in Section 3.9.4.6. The resulting moments and forces are included in the EOS-HSM load combination results reported in Table 3.9.4-7 to Table 3.9.4-10 *and in the EOS-HSM-FPS load combinations reported in* Table 3.9.4-13a *and* Table 3.9.4-14a.

Conservatively, the design basis extreme wind pressure loads are assumed to be equal to those calculated for the DBT (based on 360 mph wind speed) in the formulation of EOS-HSM load combination results.

In addition, the adequacy of the EOS-HSM to resist tornado missile loads is checked using the modified National Defense Research Committee (NDRC) empirical formulae [3.9.4-13] for local damage evaluation, and response chart solution method [3.9.4-18] for global response. These evaluations are described in Section 3.9.4.10.6.

3.9.4.9.2 Earthquake (Seismic) Load (E) Analysis

The design basis seismic load used for analysis of the EOS-HSM components is as discussed in Section 2.3.4. Based on U.S. NRC (NRC) Regulatory Guide 1.61 [3.9.4-3], a damping value of four percent is used for seismic analysis of steel structural components and a damping value of seven percent is used for seismic analysis of concrete components of EOS-HSM. An evaluation of the frequency content of the loaded EOS-HSM is performed to determine the amplified accelerations associated with the design basis seismic response spectra for EOS-HSM.

The design basis accelerations for the EOS-HSM are amplified based on the results of the frequency analysis of the EOS-HSM. The results of the frequency analysis of the EOS-HSM structure (which includes a simplified model of the DSC) yield a lowest frequency of 18.7 Hz in the transverse direction and 32.7 Hz in the longitudinal direction. The lowest vertical frequency exceeds 45 Hz; therefore the spectral acceleration is not amplified in vertical direction. Thus, based on the Regulatory Guide 1.60 response spectra amplifications, and conservatively using ZPA accelerations of 0.50g and 0.33g in the horizontal and vertical directions, respectively, the corresponding seismic accelerations used for the design of the EOS-HSM are 0.936g and 0.628g in the transverse and longitudinal directions, respectively, and 0.333g in the vertical direction. The resulting amplified accelerations are given in Table 3.9.4-3.

An equivalent static analysis of the EOS-HSM is performed using the ANSYS model described in Section 3.9.4.6 by applying the amplified seismic accelerations load. These amplified accelerations are determined based on the frequency analysis of the EOS-HSM. The frequency analysis of EOS-HSM and multi-segment design EOS-HSMS was performed individually and found that EOS-HSMS yields bounding amplified acceleration. Therefore, the bounding amplified acceleration derived from modal analysis of EOS-HSMS is conservatively used for both EOS-HSM and EOS-HSMS.

Similarly, the frequency analysis of EOS-HSM-FPS and multi-segment design EOS-HSMS-FPS was performed individually and found that EOS-HSMS-FPS yields bounding amplified acceleration. Therefore, the bounding amplified acceleration derived from modal analysis of EOS-HSMS-FPS is conservatively used for both EOS-HSM-FPS and EOS-HSMS-FPS.

The responses for each orthogonal direction are combined using the square root of the sum of the squares (SRSS) method. The resulting moments and forces due to combined seismic load are included in the EOS-HSM load combination results.

For sites where the response spectra at the base of the HSM are larger than analyzed, more than one module may need to tie together to prevent significant sliding or to prevent the modules from banging into each other causing unacceptable damage. The reinforcement requirement may also need to be reviewed, and additional rebar may be added for such sites.

The stability evaluation of the EOS-HSM due to a 0.45g Horizontal/0.30g Vertical seismic load is discussed in Appendix 3.9.7.

For dynamic analysis, the stability evaluation shall be performed using the analysis methodology described in CoC 1029 [3.9.4-21].

Seismic analysis of the EOS-HSM heat shields consists of a modal time-history analysis of the EOS-HSM for obtaining the ISRS at heat shields support locations and an equivalent static analysis of the EOS-HSM heat shields using the seismic acceleration load corresponding to the ISRS obtained in the first step. The earthquake time histories compatible with the RG 1.60 spectra are used as seismic input motion. The acceleration, velocity, and displacement time histories and corresponding spectra of the motion in the two horizontal and vertical directions, all with 1.0g ZPA, are shown in Figure 3.9.4-10 through Figure 3.9.4-15. The ISRS of the side heat shield support nodes are shown in Figure 3.9.4-10, Figure 3.9.4-11, and Figure 3.9.4-12. Modal frequencies and mass participation factors of the EOS-HSMS are shown in Table 3.9.4-23 *for EOS-HSM and* Table 3.9.4-23a *for EOS-HSM-FPS.* From the modal time-history analysis, the ISRS with a damping value of four percent are obtained at the support locations of the heat shields are shown in Figure 3.9.4-16 through Figure 3.9.4-21. Modal participations factors for the roof heat shield and side heat shield are shown in Table 3.9.4-24 and *Table 3.9.4-25*, respectively. The ISRS for the head heat shields is conservatively determined using ground motion based on the RG 1.60 spectra anchored at 0.50g and 0.33g in the horizontal and vertical directions, respectively.

3.9.4.9.3 Flood Load (FL) Analysis

Since the source of flooding is site specific, the exact source, or quantity of flood water, should be established by the licensee. However, for this generic evaluation of the EOS-HSM, bounding flooding conditions are specified that envelope those that are postulated for most plant sites. As described in Section 2.3.3, the design basis flooding load is specified as a 50-foot static head of water and a maximum flow velocity of 15 feet per second. Each licensee should confirm that this represents a bounding design basis for their specific ISFSI site.

Since the EOS-HSM is open to the atmosphere, static differential pressure due to flooding is not a design load.

The maximum drag pressure, D, acting on the EOS-HSM due to a 15 fps flood water velocity is calculated as follows:

$$D = \frac{C_D \rho_w V^2}{2g} \qquad [3.9.4\text{-}20]$$

Where:

V = 15 fps, Flood water velocity

C_D = 2.0, Drag coefficient for flat plate

ρ_w = 62.4 lb/ft^3, Flood water density

g = 32.2 ft/sec^2, Acceleration due to gravity

D = Drag pressure (psf)

The resulting flood induced drag pressure is: D = 436 psf.

The following flood load cases are considered to account for different flow direction:

- Case 1: Flood water flow from front to rear of EOS-HSM
- Case 2: Flood water flow from rear to front of EOS-HSM
- Case 3: Flood water flow from right side to left side of EOS-HSM or vice versa

ANSYS FEM described in Section 3.9.4.6 is used for the structural evaluation. The results for flood load case are obtained by enveloping results from above load cases.

The stability evaluation of EOS-HSM due to flood load is discussed in Appendix 3.9.7.

3.9.4.9.4 Accident Blocked Vent Thermal (T_a) Stress Analysis

This accident conservatively postulates the complete blockage of the EOS-HSM ventilation air inlet and outlet openings.

Since the EOS-HSMs are located outdoors; there is a remote probability that the ventilation air inlet and outlet vent openings could become blocked by debris from events such as flooding, high wind and tornados. Design features, such as the perimeter security fence and the redundant protected location of the air inlet, and outlet vent openings and the screens reduce the probability of occurrence of such an accident. Nevertheless, for this conservative generic analysis, such an accident is postulated to occur and is analyzed.

The postulated accident thermal event occurs due to blockage of the air inlet and outlet vents under off-normal ambient temperatures range from -40 ºF to 117 ºF.

ANSYS FEM described in Section 3.9.4.6 is used for the structural analysis for accident blocked vent condition.

3.9.4.10 Structural Evaluation

The load categories associated with normal operating conditions, off-normal conditions and postulated accident conditions are described previously. The load combination results and design strengths of EOS-HSM components are presented in this section.

3.9.4.10.1 EOS-HSM Concrete Components

To determine the required strength (internal axial forces, shear forces, and bending moments) for each EOS-HSM concrete component, linear elastic finite element analyses are performed for the normal, off-normal, and accident loads using the analytical models described in Section 3.9.4.6 for mechanical and thermal loads.

The concrete design loads are multiplied by load factors and combined to simulate the most adverse load conditions. The load combinations listed in Table 3.9.4-5 are used to evaluate the concrete components. The bounding load combination results for each component are presented in Table 3.9.4-7 to Table 3.9.4-10 *for EOS-HSM and* Table 3.9.4-13a *and* Table 3.9.4-14a *for EOS-HSM-FPS.* Table 3.9.4-11a*,* Table 3.9.4-12a*,* Table 3.9.4-13a*,* Table 3.9.4-14a*, and* Table 3.9.4-14b *provide concrete capacities and demand/capacity comparisons for EOS-HSM-FPS*. The notations for the components of forces and moments and the concrete component planes in which capacities are computed are shown in Figure 3.9.4-5. The thermal stresses of EOS-HSM concrete components used in the load combination results are based on thermal results that bound those reported in Chapter 4. All load combination results are less than computed section capacities.

The required strength, U, for critical sections of concrete is calculated in accordance with the requirements of ANSI 57.9 [3.9.4-10] and ACI 349-06 [3.9.4-12], including the strength reduction factors defined in ACI 349-06, Section 9.3. The design strength of EOS-HSM concrete components exceeds the factored design loads. Thus, the EOS-HSM concrete components are adequate to perform their intended function. EOS-HSM construction details such as construction joints and reinforcement bar splices is detailed on the construction drawings.

3.9.4.10.2 DSC Support Structure

The DSC main support beams, stiffener plates, extension baseplates, DSC stop plates and braces members of the DSC support structure *and 12"x1" plates, tubesteel spacers, stop plates, and extension baseplates of the FPS DSC support structure* are evaluated using the allowable strength design method of the AISC Manual of Steel Construction [3.9.4-14]. The maximum temperature used in the stress analysis of the support steel bounds the maximum temperature reported in Chapter 4.

The load combination results for each of these components are provided in Table 3.9.4-17 to Table 3.9.4-22 *for the DSC support structure and* Table 3.9.4-17a*,*Table 3.9.4-21a*, and* Table 3.9.4-22a *for the FPS DSC support structure.* The maximum value of demand to capacity ratio of DSC support structure is less than 1.0. Thus, DSC support structure is adequately strong to resist the reasonably foreseeable loads applied to it.

3.9.4.10.3 EOS-HSM Shield Door

The shield door is free to grow in the radial direction when subjected to thermal loads. Therefore, there are no stresses in the door due to thermal growth. The dead weight, tornado wind, differential pressure and flood loads cause insignificant stresses in the door compared to stresses due to missile impact load. Therefore, the door is evaluated only for the missile impact load.

The minimum thickness of concrete component to prevent perforation, and scabbing are 18.5 inches and 27.7 inches, respectively. Thus, the 30.5-inch thick door is adequate to protect from local damage due to missile impact. The computed maximum ductility ratio for the door is less than 1, which satisfies the ductility requirement if compared against the allowable ductility ratio of 10 as per ACI 349-06 [3.9.4-12]. Therefore, the concrete door meets the ductility requirement and is adequate to protect from global effect of missile impact.

For the door anchorage, the controlling load is tornado generated differential pressure drop load. The maximum tensile force per bolt (four door attachment bolts), is 7.6 kips. The design strength of door attachment embedment (nonductile) as per Section D.3.6.3 of ACI 349-06 [3.9.4-12] is 17.99 kips, which is greater than 7.6 kips, thus satisfying the ACI 349-06 code requirement.

3.9.4.10.4 EOS-HSM Heat Shield

The roof heat shield assembly consists of four panels. Each panel section is a v-shaped in transverse direction with v-notch at the center of the EOS-HSM width. The roof heat shield panels are connected to the roof by fifteen, ¾-10UNC bolts. The natural lateral frequency of a typical panel/connection stud system is determined from ANSYS computer code. The maximum interaction ratio for combined axial and bending stress in the connection bolts is 0.503, which is less than 1.0. The maximum bending moment in roof heat shield panel is 22.29 in-lb/in., which is also less than the panel moment capacity of 59.59 in-lb/in.

The side wall heat shield assembly also consists of four panels. The side wall heat shield panels are attached to the *EOS-HSM short and long base unit side wall by seventeen 1/2-13UNC bolts on both sides and EOS-HSM medium base unit side wall by fifteen 1/2-13UNC bolts on both sides.* The maximum interaction ratio for combined axial and bending stress in connection bolts is 0.563, which is less than 1.0. The maximum bending moment in side heat shield panel is 46.98 in-lb/in, which is also less than the panel moment capacity of 59.59 in-lb/in.

The maximum temperature used in the stress analysis of the heat shields bounds the maximum temperatures reported in Chapter 4. The size of the slot hole provided in the panel at the connection bolt location is sufficiently large to allow for free thermal expansion. Therefore, neither of roof heat shield panel and side wall heat shield panel is subjected to thermal stress.

3.9.4.10.5 EOS-HSM DSC Axial Restraint

The DSC axial restraint consists of a capped steel tube embedment located within the bottom center of the round access opening of the EOS-HSM front wall, and a 2-inch by 4-inch solid bar steel retainer that drops into the embedment cavity after DSC transfer is complete. The drop-in retainer extends approximately 5 inches above the top of embedment to provide axial restraint of the DSC. The maximum seismically induced shear load in the retainer is 140.5 kips. The allowable shear strength of the axial retainer is 196.0 kips. The maximum seismically induced moment in the retainer is 281.0 in-kips taking a moment arm of 2 inches, conservatively. The allowable flexural strength of axial retainer is 344.9 in-kips. Hence, the DSC axial retainer design is adequate to perform its intended function.

3.9.4.10.6 Evaluation of Concrete Components for Missile Loading

Missile impact effects are assessed in terms of local damage and overall structural response. Local damage that occurs in the immediate vicinity of the impact area is assessed in terms of penetration, perforation, spalling and scabbing. Evaluation of local effects is essential to ensure that protected items (the DSC and fuel) would not be damaged by a missile perforating a protective barrier, or by secondary missiles such as scabbing particles. Evaluation of overall structural response is essential to ensure that protected items are not damaged or functionally impaired by deformation or collapse of the impacted structure.

The tornado-generated missiles are conservatively assumed to strike normal to the surface with the long axis of the missile parallel to the line of flight to maximize the local effects. Plastic deformation to absorb the energy input by the tornado-generated missile load is desirable and acceptable, provided that the overall integrity of the structure is not impaired. Due to complex physical process associated with missile impact effects, the EOS-HSM structure is primarily evaluated conservatively by application of empirical formulae.

3.9.4.10.6.1 Local Damage Evaluation

Local missile impact effects consist of (a) missile penetration into the target, (b) missile perforation through the target, and (c) spalling and scabbing of the target. This also includes punching shear in the region of the target. Per F.7.2.3 of ACI 349-06 [3.9.4-12], if the concrete thickness is at least 20% greater than that required to prevent perforation, the punching shear requirement of the code need not be checked.

The following enveloping missiles are considered for local damage:

- Utility wooden pole
- Armor piercing artillery shell
- 12-inch diameter schedule 40 steel pipe

Large deformable missiles such as automobiles are incapable of producing significant local damage. Concrete thickness satisfying the global structural response requirements including punching shear is considered to preclude unacceptable local damage. Therefore, the local effects from an automobile are evaluated using punching shear criteria of ACI 349-06 [3.9.4-12].

The following empirical formulae are used to determine the local damage effects on reinforced concrete target:

B. Modified NDRC formulas for penetration depth [3.9.4-13]:

$$x = \sqrt{4KNWd\left(\frac{v_o}{1000\ d}\right)^{1.8}}\ , \text{ for } x/d \leq 2.0$$

$$x = \left[KNW\left(\frac{v_o}{1000\ d}\right)^{1.8}\right] + d\ , \text{ for } x/d > 2.0$$

Where,

x = Missile penetration depth, inches

K= concrete penetrability factor = $\frac{180}{\sqrt{f_c'}}$

N = projectile shape factor
= 0.72 flat nosed
= 0.84 blunt nosed
= 1.0 bullet nosed (spherical end)
= 1.14 very sharp nose

W = weight of missile, lb

v_o = striking velocity of missile, fps

d = effective projectile diameter, inches.
for a solid cylinder, d = diameter of projectile and
for a non-solid cylinder, $d = (4A_c/\pi)^{1/2}$

A_c = projectile impact area, in^2

C. Modified NDRC formula for perforation thickness [3.9.4-13]:

$$\frac{e}{d} = 3.19\left(\frac{x}{d}\right) - 0.718\left(\frac{x}{d}\right)^2 \text{, for } x/d \le 1.35$$

$$\frac{e}{d} = 1.32 + 1.24\left(\frac{x}{d}\right) \text{, for } 1.35 \le x/d \le 13.5$$

Where,

e = perforation thickness, in.

In order to provide an adequate margin of safety the design thickness $t_d = 1.2e$ [3.9.4-12]

D. Modified NDRC formula for scabbing thickness [3.9.4-13]:

$$\frac{s}{d} = 7.91\left(\frac{x}{d}\right) - 5.06\left(\frac{x}{d}\right)^2 \text{, for } x/d \le 0.65$$

$$\frac{s}{d} = 2.12 + 1.36\left(\frac{x}{d}\right) \text{, for } 0.65 \le x/d \le 11.75$$

Where,

s = scabbing thickness, in.

In order to provide an adequate margin of safety the design thickness td = 1.2s [3.9.4-12]

The concrete targets of the EOS-HSM that may be subjected to local damage due to missile impact are:

- 44-inch thick roof
- 42-inch thick (minimum) front wall
- 36-inch thick end shield wall
- 36-inch thick rear shield wall
- 30.5-inch thick shielding door

The minimum thickness of concrete target components listed above is 30.5 inches. So, the required perforation thickness and require scabbing thickness is compared against 30.5 inches to ensure the adequacy of design.

3.9.4.10.6.1.1 Local Impact Effects of Utility Wooden Pole Missile

Per section 6.4.1.2.5 of [3.9.4-13], utility wooden pole missiles do not have sufficient strength to penetrate a concrete target and that the scabbing thickness required for wood missiles is substantially less than that required for a steel missile with the same mass and velocity. Practically, wooden pole missiles do not appear to be capable of causing local damage to the 12-inch or thicker walls (also see Section 2.1.1 of [3.9.4-18]). Since none of the concrete targets are less than 12 inches thick, the postulated wood missiles do not cause any local damage to the EOS-HSM concrete component.

3.9.4.10.6.1.2 Local Impact Effects of Armor Piercing Artillery Shell Missile

The penetration depth for this missile is calculated using the NDRC Formula as given in Section 3.9.4.10.6.1 (a) and the parameters used in the formula are as listed below:

d = 8.0 in.	effective diameter of missile
W = 276 lb	weight of missile
v_o = 185 fps	striking velocity of missile
f'_c = 5000 psi	concrete compressive strength
K = 180/√5000 = 2.55	concrete penetrability factor
N = 0.84	projectile shape factor (blunt nosed)
Penetration depth, x = 4.6 in.	for x/d (= 0.58) ≤ 2.0
Perforation thickness, e = 12.9 in.	for x/d (= 0.58) ≤ 1.35

Required perforation thickness = 1.2*12.9 = 15.5 in. < 30.5 in.

Scabbing thickness, s = 23.1 in. for x/d (= 0.58) ≤ 0.65

Required scabbing thickness = 1.2*23.1 = 27.7 in. < 30.5 in.

Therefore, penetration, perforation and scabbing of the concrete components of EOS-HSM do not occur due to this missile impact.

3.9.4.10.6.1.3 Local Impact Effects of 12-Inch Diameter Schedule 40 Steel Pipe Missile

The penetration depth for this missile is calculated using the NDRC Formula as given in Section 3.9.4.10.6.1 (A) and the parameters used in the formula are as listed below:

ϕ = 12.75 in.	outer diameter of 12” dia. schedule 40 steel pipe.
A_c = 15.74 in^2	missile impact area (cross sectional area of steel)

$d = (4*15.74/\pi)^{1/2} = 4.5$ in. effective diameter of missile

W = 750 lb weight of missile

v_o = 154 fps striking velocity of missile

f'_c = 5000 psi concrete compressive strength

K = 180/√5000 = 2.55 concrete penetrability factor

N = 0.72 projectile shape factor (flat nosed)

Penetration depth, x = 7.6 in. for $x/d (= 1.69) \leq 2.0$

Perforation thickness, e = 15.4 in. for $1.35 \leq x/d (= 1.69) \leq 13.5$

Required perforation thickness = 1.2*15.4 = 18.5 in. < 30.5 in. OK

Scabbing thickness, s = 19.9 in. for $0.65 \leq x/d (= 1.69) \leq 11.75$

Required scabbing thickness = 1 .2*19.9 = 23.9 in. < 30.5 in. OK

Therefore, penetration, perforation and scabbing of the concrete components of EOS-HSM do not occur due to this missile impact.

3.9.4.10.6.2 Global Structural Response

When a missile strikes a structure, large forces develop at the missile-structure interface, which decelerate the missile and accelerate the structure. The response of the structure depends on the dynamic properties of the structure and the time dependent nature of the applied loading (interface force-time function). The force-time function is, in turn, dependent on the type of impact (elastic or plastic) and the nature and extent of local damage.

In an elastic impact, the missile and the structure deform elastically, remain in contact for a short period of time (duration of impact), and subsequently disengage due to the action of elastic interface restoring forces.

In a plastic impact, the missile or the structure (or both) may sustain permanent deformation or damage (local damage). Elastic restoring forces are small, and the missile and the structure tend to remain in contact after impact. Plastic impact is much more common than elastic impact, which is rarely encountered. Test data have indicated that the impact from all postulated tornado-generated missiles can be characterized as a plastic impact.

If the interface forcing function can be defined or conservatively idealized, the structure can be modeled mathematically, and conventional analytical or numerical techniques can be used to predict structural response. If the interface forcing function cannot be defined, the same mathematical model of the structure can be used to determine structural response by application of conservation of momentum and energy balance techniques with due consideration for type of impact (elastic or plastic).

In either case, in lieu of a more rigorous analysis, a conservative estimate of structural response can be obtained by first determining the response of the impacted structural element, and then applying its reaction forces to the supporting structure. The predicted structural response enables assessment of structural design adequacy in terms of strain energy capacity, deformation limits, stability and structural integrity.

The overall structural response of each component as a whole (global response) is determined by single degree of freedom analysis using response charts solution method of [3.9.4-18].

The following enveloping missiles are considered for global structural response:

- Utility wooden pole
- Armor piercing artillery shell
- 12-inch diameter schedule 40 steel pipe
- Automobile missile

The peak interface force and impact duration for each missile are calculated as follows:

A. Utility Wooden Pole Missile

For wooden missile, the interface forcing function is a rectangular pulse having a force magnitude of F and duration t_i, per Section 2.3.1 of [3.9.4-18]

$F = PA$

$t_i = M_m \nu_c / F$

Where,

F = interface force (lb)

P = interface pressure (psi) = 2500 psi for wood missiles [3.9.4-18]

A = cross sectional area of the missile (in^2) = π * 13.52/4 = 143.1 in^2

t_i = impact duration (sec)

W_m = weight of missile (lb) = 1124 lb

M_m = missile mass (lb-sec^2/ft) = W_m/g = 1124 lb /32.2 ft/sec^2 = 34.9 lb-sec^2/ft

ν_c = change in velocity during impact (conservatively = ν_s) (fps) = 180 fps

Therefore,

F = 358 kip and t_i = 0.018 sec

B. Armor Piercing Artillery Shell

For solid steel missile, the concrete is a soft target per section 6.4.2 of [3.9.4-13] with a penetration depth of 4.6 in. The interface forcing function is a rectangular pulse per Section 6.4.2.1.1 of [3.9.4-13].

$F = W_m V_0^2/2gX$

$t_i = 2X/V_0$

Where,

F = interface force (lb)

t_i = impact duration (sec)

W_m = missile weight (lb) = 276 lb

V_0 = initial velocity of the missile (fps) = 185 fps

X = penetration depth = 4.6 in.

Therefore,

F = 383 kip and t_i = 0.00414 sec

C. 12-Inch Diameter Schedule 40 Steel Pipe

For steel pipe missile, the interface forcing function is a triangular pulse per Section 2.3.2 of [3.9.4-18].

$t_i = 400M_m /PA$

$F = (2M_m\nu_s)/t_i$

Where,

F = peak interface force (lb)

P = collapse stress of pipe (psi) = 60000 psi

A = cross sectional metal area of the missile (in^2) = 15.74 in^2

t_i = impact duration (sec)

W_m = weight of missile (lb) = 750 lb

M_m = missile mass (lb-sec^2/ft) = W_m/g = 750 lb /32.2 ft/sec^2 = 23.29 lb-sec^2/ft

ν_s = striking velocity of missile = 154 fps

Therefore,

F = 718 kip and t_i = 0.01 sec

D. Automobile Missile

For automobile missile, the interface forcing function per 2.3.3 of [3.9.4-18] is as follows:

$F_t = 0.625\ v_c\ W \sin(20t)$ $0 < t \leq 0.0785$ sec

$F_t = 0$ $t > 0.0785$ sec

Where,

F_t = force as a function of time (lb)

W = weight of automobile (lb) = 4000 lb

v_c = change in velocity during impact (conservatively = v_s) (fps) = 195 fps

Therefore,

F = 488 kip and t_i = 0.0785 sec

The end wall, rear wall, base front wall, roof and door of EOS-HSM are evaluated for global response, since these components may interface with missile loading. The end/rear walls and door are idealized as a simply supported plate while the base front wall and roof are idealized as simply supported beam for structural response. The yield resistance and fundamental period of vibration of concrete components is then determined based on the assumed idealized boundary condition using the equations given in Section 4.4 of [3.9.4-18]. The calculated value of yield resistance, R_y, and fundamental period of vibration, T_n, for different concrete components are tabulated below.

Component	**R_y (kip)**	**T_n (sec)**
End Wall	446.1	0.0180
Rear Wall	919.9	0.0065
Base Front Wall	*1116.1*	0.0045
Roof	402.0	0.0301
Door	1211.0	*0.00208*

In the response chart solution method, the structural response is determined by entering the chart with calculated values of C_T and C_R to determine the ductility ratio, μ, which is compared against the allowable ductility ratio as given in Appendix F of ACI 349-06 [3.9.4-12]. The dimensionless ratios, C_T and C_R, are defined as follows:

$$C_R = \frac{R_y}{F} \qquad C_T = \frac{t_i}{T_n}$$

The maximum value of ductility ratio of all five components is found to be less than 10. The allowable ductility ratio per ACI 349-06 [3.9.4-12] is 10. Hence, the global response of EOS-HSM is within deformation limit meeting the ductility requirement.

Each component is also evaluated for punching shear capacity with interfacing utility wooden pole missile and automobile missile. All the components have punching shear capacity greater than the peak missile interface force.

3.9.4.11 Conclusions

The load categories associated with normal operating conditions, off-normal conditions and postulated accident conditions are described and analyzed in previous sections. The load combination results for EOS-HSM components important-to-safety are also presented. Comparison of the results with the corresponding design capacity shows that the design strength of the EOS-HSM is greater than the strength required for the most critical load combination.

3.9.4.12 References

3.9.4-1 Code of Federal Regulation Title 10, Part 72 (10CFR Part 72), "Licensing Requirements for the Independent Storage of Spent Nuclear Fuel, High-Level Radioactive Waste, and Reactor-Related Greater than Class C Waste."

3.9.4-2 U.S. Nuclear Regulatory Commission, Regulatory Guide 1.60, "Design Response Spectra for Seismic Design of Nuclear Power Plants," Revision 1, 1973.

3.9.4-3 U.S. Nuclear Regulatory Commission, Regulatory Guide 1.61, "Damping Values for Seismic Design of Nuclear Power Plants," Revision 1, March 2007.

3.9.4-4 U.S. Nuclear Regulatory Commission, Regulatory Guide 1.76, "Design Basis Tornado for Nuclear Power Plants," Revision 0, April 1974.

3.9.4-5 U.S. Nuclear Regulatory Commission, Regulatory Guide 1.92, "Combining Modal Responses and Spatial Components in Seismic Response Analysis," Revision 3, October 2012.

3.9.4-6 U.S. Nuclear Regulatory Commission, Regulatory Guide 1.122, "Development of Floor Design Response Spectra for Seismic Design of Floor-Supported Equipment or Components," Revision 1, 1978.

3.9.4-7 NUREG-0800, Standard Review Plan, Section 3.5.1.4, "Missiles Generated by Natural Phenomena," Revision 2, July 1981.

3.9.4-8 NUREG-0800, Standard Review Plan, Section 3.3.1, "Wind Loading," Section 3.3.2 "Tornado Loads," and Section 3.5.1.4 "Missiles Generated by Tornado and Extreme Winds," Revision 3, March 2007.

3.9.4-9 NUREG-1536, "Standard Review Plan for Spent Fuel Dry Storage Systems at a General License Facility," Revision 1, U.S. Nuclear Regulatory Commission, July 2010.

3.9.4-10 ANSI/ANS 57.9-1984, "Design Criteria for an Independent Spent Fuel Storage Installation (Dry Storage Type)," American National Standards Institute, American Nuclear Society.

3.9.4-11 ACI-318-08, "Building Code Requirement for Structural Concrete," American Concrete Institute.

3.9.4-12 ACI 349-06, "Code Requirements for Nuclear Safety Related Concrete Structures," American Concrete Institute.

3.9.4-13 American Society of Civil Engineers, "Structural Analysis and Design of Nuclear Plant Facilities," ASCE Publication No. 58.

3.9.4-14 American Institute of Steel Construction, AISC Manual of Steel Construction, 13th Edition.

3.9.4-15 American Society of Civil Engineers, "Minimum Design Loads for Buildings and Other Structures," ASCE 7-10 (formerly ANSI A58.1).

3.9.4-16 AREVA Inc., "Updated Final Safety Analysis Report for the Standardized NUHOMS® Horizontal Modular Storage System for Irradiated Nuclear Fuel," Revision 14, USNRC Docket Number 72-1004, September 2014.

3.9.4-17 Bechtel Power Corporation, "Design of Structures for Missile Impact," Topical Report BCTOP-9A, Revision 2, San Francisco, California.

3.9.4-18 Bechtel Corporation, "Design Guide Number C-2.45 for Design of Structures for Tornado Missile Impact," Rev. 0, April 1982.

3.9.4-19 "ANSYS Computer Code and User's Manual", Release 14.0.3.

3.9.4-20 Binder, Raymond C., "Fluid Mechanics," 3rd Edition, Prentice-Hall, Inc, 1973.

3.9.4-21 AREVA Inc., "Updated Final Safety Analysis Report For The Standardized Advanced NUHOMS® Horizontal Modular Storage System For Irradiated Nuclear Fuel," Revision 6, US NRC Docket Number 72-1029, August 2014.

3.9.4-22 U.S. Nuclear Regulatory Commission, Regulatory Guide 1.76, "Design Basis Tornado for Nuclear Power Plants," Revision 1, March 2007.

Table 3.9.4-1
Design Pressures for Tornado Wind Flowing from Front Wall to Rear Wall and Vice Versa

Component	Velocity Pressure, q_v (psf)	External Pressure Coefficient, C_p	Internal Pressure Coefficient, (GC_{pi})	Max. Design Pressure, $q_v*(G*C_p-GC_{pi})$ (psf)
Windward(Front/Rear Wall)	254	0.80	±0.18	218
Leeward(Rear/Front Wall)		-0.30(1)		-110
Side(Right Side Wall)		-0.70		-197
Side(Left Side Wall)		-0.70		-197
Roof		-1.30		-326

Notes:

1. The C_p value is taken for L/B = *116"/268" ≈ 0.40 when analyzing EOS-HSM and ≈0.47 when analyzing EOS-HSM-FPS*.
2. The gust effect factor, G=0.85 considering the EOS-HSM as rigid.

Table 3.9.4-2
Design Pressures for Tornado Wind Flowing from Right Side to Left Side Wall and Vice Versa

Component	Velocity Pressure, q_v (psf)	External Pressure Coefficient, C_p	Internal Pressure Coefficient, (GC_{pi})	Max. Design Pressure, $q_v*(G*C_p-GC_{pi})$ (psf)
Side(Front Wall)	254	-0.70	±0.18	-197
Side(Rear Wall)		-0.70		-197
Windward(Right/Left Side Wall)		0.80		218
Leeward(Left/Right Side Wall)		-0.50(1)		-154
Roof		-1.30		-326

Notes:

1. The C_p value is taken for L/B = 116"/268" ≈ 0.4*0 when analyzing EOS-HSM and ≈ 0.47 when analyzing EOS-HSM-FPS.*

2. The gust effect factor, G=0.85 considering the EOS-HSM as rigid.

Table 3.9.4-3
Spectral Acceleration Applicable to Different Components of EOS-HSM for Seismic Analysis

Direction	Frequency (Hz)	Spectral Acceleration Corresponding to ZPA = 0.5g horizontal & 0.333 g vertical(1)		
		at 3% Damping (for DSC)	at 4% Damping (for DSC support structure)	at 7% Damping (for concrete components)
X (Transverse)	18.7	1.229g	1.156g	0.936g
Y (Vertical)	60.3	0.333g	0.333g	0.333g
Z (Longitudinal)	32.7	0.694g	0.677g	0.628g

(1) Seismic loading conservatively exceeds the design basis ZPA values of 0.45g horizontal and 0.30g vertical.

Table 3.9.4-3a
Spectral Acceleration Applicable to Different Components of EOS-HSMS-FPS for Seismic Analysis

Direction	*Frequency (Hz)*	*Spectral Acceleration Corresponding to Design ZPA*		
		at 3% Damping (for DSC)	*at 4% Damping (for DSC support structure)*	*at 7% Damping (for concrete components)*
X (Transverse)	*19.2*	*1.194g*	*1.125g*	*0.917g*
Y (Vertical)	*60.6*	*0.333g*	*0.333g*	*0.333g*
Z (Longitudinal)	*31.4*	*0.724g*	*0.704g*	*0.647g*

Table 3.9.4-4
Load Cases for EOS-HSM Concrete Components Evaluation

Design Load Type	Load Notation	Design Parameters	Applicable Codes / References
Normal			
Dead	DL	Includes self-weight with 160 pcf density for concrete and 0.28 pci for steel support structure.	ANSI/ANS 57.9-1984 [3.9.4-10]
Live	LL	Design live load of 200 psf on roof which includes snow and ice load and DSC weight of 135 kip applied on DSC support rails.	ANSI/ANS 57.9-1984 [3.9.4-10] & ASCE 7-10 [3.9.4-15]
Normal Handling	R_O	The concrete module is evaluated for 140 kip DSC insertion load as a normal handling load. The DSC weight is also applied at both rail support locations (4 points).	
Normal Thermal	T_O	DSC with spent fuel rejecting up to 50.0 kW of decay heat. Extreme ambient air temp. -20 °F and 100 °F. Reference temperature = 70 °F.	
Off-Normal/Accidental			
Off-Normal Handling	R_a	For the steel support structure the magnitude of this load is 135 kip both for DSC insertion and retrieval, applied to one rail. The DSC weight is also applied at one rail support location (two points).	
Accidental Thermal	T_a	Enveloped of Off-Normal and Accidental Thermal (vent blocked) condition. Accidental thermal condition is same as off-normal condition with ambient temperature range of -40 °F to 117 °F. Reference temperature = 70 °F	
Earthquake	E	Zero period acceleration of 0.5g in horizontal and 0.333g in vertical direction with enhancement in frequency above 9 Hz and 7% damping. (1)	NRC Reg. Guide 1.60 [3.9.4-2] & Reg. Guide 1.61 [3.9.4-3]
Flood	FL	Maximum flood height of 50 ft and max. velocity of water 15 ft/sec	10 CFR Part 72 [3.9.4-1]
Wind/Tornado Wind	W/W_t	Maximum wind speed of 360 mph, and a pressure drop of 3 psi	ASCE 7-10 [3.9.4-15] & NRC Reg Guide 1.76 [3.9.4-4]
Tornado Generated Missile	W_m	4 types of tornado-generated missiles	NUREG-0800 Section 3.5.1.4 [3.9.4-7]

(1) Seismic loading conservatively exceeds the design basis ZPA values of 0.45g horizontal and 0.30g vertical.

Table 3.9.4-5
Load Combination for EOS-HSM Concrete Components Evaluation

Combination Number	Load Combination	Event
C1	1.4 DL + 1.7 (LL + R_o)	Normal
C2	1.05 DL + 1.275 (LL + T_o + W)	Off-Normal – Wind
C3	1.05 DL + 1.275 (LL + T_o + R_a)	Off-Normal – Handling
C4	DL + LL + T_o + E	Accident – Earthquake
C5	DL + LL + T_o + W_t	Accident – Tornado
C6	DL + LL + T_o + FL	Accident – Flood
C7	DL + LL + Ta	Accident – Thermal

Note: See Table 3.9.4-4 for notation.

Table 3.9.4-6
Strength Reduction Factors for Concrete

Type of Stress	Strength Reduction Factor, ϕ
Tension - Controlled	0.90
Compression - Controlled	0.65
Shear	0.75
Torsion	0.75
Bearing	0.65

Note: The strength reduction factors are taken from ACI 349-06, Section 9.3 [3.9.4-12].

Table 3.9.4-7
Demand of EOS-HSM Concrete Components for Shear Forces and Moments

Component	Load Combination	M_1 (in-kip/ft)	M_2 (in-kip/ft)	V_{o1} (kip/ft)	V_{o2} (kip/ft)	V_i (kip/ft)
1. Rear Wall Bottom (32")	C1 through C6	338.7	708.7	6.3	9.8	51.6
	C7	232.8	270.8	1.9	2.7	25.3
2. Rear Wall Top (12")	C1 through C6	36.9	106.6	5.1	6.4	13.7
	C7	24.5	69.3	4.2	2.9	7.6
3. Front Wall Bottom (54")	C1 through C6	1024.0	1877.2	14.2	13.0	57.6
	C7	1049.1	1735.2	3.1	3.1	25.2
4. Front Wall Top (42")	C1 through C6	949.7	1768.7	28.5	25.6	90.4
	C7	1353.1	2485.3	26.1	24.4	48.3
5. Side Wall Bottom (24")	C1 through C6	269.3	182.9	15.4	14.8	23.5
	C7	143.4	396.3	14.3	18.6	11.1
6. Side Wall Bottom (14")	C1 through C6	91.4	38.0	11.4	6.1	14.4
	C7	64.0	117.2	12.1	12.7	11.1
7. Side Wall Top (12")	C1 through C6	285.3	195.0	12.3	11.9	38.5
	C7	341.2	151.8	10.6	10.6	46.5
8. Roof (44")	C1 through C6	622.2	1831.5	46.1	49.5	21.5
	C7	283.6	1004.2	11.6	24.3	22.5

Table 3.9.4-8
Demand of EOS-HSM Concrete Components for Axial Forces and Moments

Component	Load Combination	T_1 (kip/ft)	T_2 (kip/ft)	C_1 (kip/ft)	C_2 (kip/ft)	M_{1P} (in-kip/ft)	M_{2P} (in-kip/ft)
1. Rear Wall Bottom (32")	C1 through C6	33.8	32.1	46.4	104.4	299.6	428.3
	C7	13.4	5.5	40.5	44.6	66.4	124.1
2. Rear Wall Top (12")	C1 through C6	9.5	23.6	7.5	29.6	36.9	43.4
	C7	7.1	40.0	15.1	15.8	20.1	45.8
3. Front Wall Bottom (54")	C1 through C6	72.2	65.6	51.3	122.3	1019.5	773.8
	C7	19.8	0.0	32.0	59.8	485.3	0.0
4. Front Wall Top (42")	C1 through C6	97.7	77.5	86.6	256.2	737.5	1137.7
	C7	22.1	32.8	38.7	98.9	1352.7	1796.9
5. Side Wall Bottom (24")	C1 through C6	28.0	37.6	48.2	70.2	267.5	158.6
	C7	22.5	58.7	28.0	38.8	97.1	324.9
6. Side Wall Bottom (14")	C1 through C6	19.4	16.5	47.6	15.9	75.9	37.9
	C7	31.5	62.9	21.9	6.1	64.0	117.2
7. Side Wall Top (12")	C1 through C6	27.5	49.7	157.1	103.7	44.4	49.0
	C7	56.9	11.7	138.0	108.7	64.5	132.3
8. Roof (44")	C1 through C6	24.4	67.5	35.4	107.1	621.8	1817.3
	C7	11.5	59.9	4.8	90.8	239.4	751.2

Table 3.9.4-9
Demand of EOS-HSMS Concrete Components for Shear Forces and Moments

Component	Load Combination	M_1 (in-kip/ft)	M_2 (in-kip/ft)	V_{o1} (kip/ft)	V_{o2} (kip/ft)	V_i (kip/ft)
1. Rear Wall Bottom (32")	C1 through C6	335.6	694.6	6.9	11.3	55.5
	C7	215.2	297.1	2.2	2.5	24.5
2. Rear Wall Top (12")	C1 through C6	69.4	110.3	4.9	7.7	52.9
	C7	25.1	66.2	3.2	3.0	8.5
3. Front Wall Bottom (54")	C1 through C6	970.2	1882.1	13.4	13.0	60.8
	C7	1028.4	1436.7	3.6	3.1	26.2
4. Front Wall Top (42")	C1 through C6	1077.5	1501.8	28.7	28.3	130.5
	C7	1500.8	2424.0	24.8	21.4	46.8
5. Side Wall Bottom (24")	C1 through C6	193.1	161.2	13.3	12.6	20.9
	C7	140.6	409.0	14.6	17.4	13.1
6. Side Wall Bottom (14")	C1 through C6	67.4	38.9	10.9	6.6	15.4
	C7	58.5	115.7	12.0	12.0	9.8
7. Side Wall Top (12")	C1 through C6	265.9	224.6	12.1	12.1	59.3
	C7	307.9	138.6	10.6	10.6	37.7
8. Roof (44")	C1 through C6	623.2	1839.1	39.3	49.8	22.3
	C7	291.1	979.2	10.2	21.8	20.8

Table 3.9.4-10
Demand of EOS-HSMS Concrete Components for Axial Forces and Moments

Component	Load Combination	T_1 (kip/ft)	T_2 (kip/ft)	C_1 (kip/ft)	C_2 (kip/ft)	M_{1P} (in-kip/ft)	M_{2P} (in-kip/ft)
1. Rear Wall Bottom (32")	C1 through C6	25.0	42.4	49.3	108.5	248.3	344.0
	C7	14.6	10.9	39.7	47.3	58.8	295.8
2. Rear Wall Top (12")	C1 through C6	51.4	43.7	306.1	132.2	44.1	29.1
	C7	7.5	34.8	21.9	22.4	21.2	42.4
3. Front Wall Bottom (54")	C1 through C6	54.1	88.6	75.0	117.7	800.5	412.6
	C7	20.5	0.0	35.3	62.5	486.1	0.0
4. Front Wall Top (42")	C1 through C6	111.6	103.8	426.5	336.5	352.2	907.9
	C7	45.6	80.0	65.8	163.9	1500.8	992.9
5. Side Wall Bottom (24")	C1 through C6	34.7	28.2	49.3	60.0	181.8	159.6
	C7	21.0	55.2	26.4	33.8	98.8	342.5
6. Side Wall Bottom (14")	C1 through C6	20.6	15.0	45.9	16.8	64.3	38.9
	C7	29.8	57.3	21.0	10.2	57.2	115.7
7. Side Wall Top (12")	C1 through C6	50.8	62.0	257.1	233.8	40.9	63.2
	C7	51.8	58.5	121.8	240.2	63.3	62.7
8. Roof (44")	C1 through C6	24.9	76.4	38.8	114.5	623.0	1824.9
	C7	10.4	46.9	4.9	94.0	246.1	746.4

Table 3.9.4-11
Ultimate Shear/Moment Capacities of Concrete Components

Component	Thermal Condition	V_{ui} kips/ft	V_{uo1} kips/ft	V_{uo2} kips/ft	M_{u1} kip-in/ft	M_{u2} kip-in/ft
1. Rear Wall Bottom (32")	Normal	90.4	38.3	38.3	886.8	886.8
	Accident	85.6	36.3	36.3	837.1	837.1
2. Rear Wall Top (12")	Normal	65.0	12.8	12.8	290.4	290.4
	Accident	61.4	12.2	12.2	273.8	273.8
3. Front Wall Bottom (54")	Normal	196.0	64.3	64.3	3,791.7	3,791.7
	Accident	185.4	61.0	61.0	3,578.1	3,578.1
4. Front Wall Top (42")	Normal	180.7	49.0	49.0	2,875.6	2,875.6
	Accident	170.9	46.5	46.5	2,712.9	2,712.9
5. Side Wall Bottom (24")	Normal	102.1	27.8	27.8	919.3	919.3
	Accident	96.6	26.4	26.4	867.3	867.3
6. Side Wall Bottom (14")	Normal	89.4	15.1	15.1	489.8	489.8
	Accident	84.5	14.3	14.3	461.7	461.7
7. Side Wall Top (12")	Normal	86.8	12.6	12.6	404.0	404.0
	Accident	82.1	11.9	11.9	380.6	380.6
8. Roof (44")	Normal	151.4	51.5	51.5	2,283.1	2,283.1
	Accident	143.3	48.9	48.9	2,154.6	2,154.6

Notes:
V_{ui} = Minimum of ultimate in plane shear capacities in planes 1 and 2.
V_{uo1} = Minimum ultimate out of plane shear capacity in plane 1.
V_{uo2} = Minimum ultimate out of plane shear capacity in plane 2.
M_{u1} = Minimum ultimate moment capacity in plane 1.
M_{u2} = Minimum ultimate moment capacity in plane 2.
Planes 1 and 2 are defined in Figure 3.9.4-5.
Ultimate shear/moment capacities of alternate front wall rebar layout reported in Table 3.9.4-26.

Table 3.9.4-11a
Ultimate Shear/Moment Capacities of FPS Concrete Components

Component	*Thermal Condition*	V_{ui}	V_{uo1}	V_{uo2}	M_{u1}	M_{u2}
		kips/ft	*kips/ft*	*kips/ft*	*kip-in/ft*	*kip-in/ft*
1. Rear Wall Side (24")	*Normal*	*80.2*	*28.1*	*28.1*	*648.2*	*648.2*
	Accident	*75.9*	*26.6*	*26.6*	*611.8*	*611.8*
2. Rear Wall Mid & Top (12")	*Normal*	*65.0*	*12.8*	*12.8*	*290.4*	*290.4*
	Accident	*61.4*	*12.2*	*12.2*	*273.8*	*273.8*
3. Interior Pedestal (12")	*Normal*	*65.0*	*12.8*	*12.8*	*290.4*	*290.4*
	Accident	*61.4*	*12.2*	*12.2*	*273.8*	*273.8*
4. Front Wall (42")	*Normal*	*180.7*	*49.0*	*49.0*	*2,875.6*	*2,875.6*
	Accident	*170.9*	*46.5*	*46.5*	*2,712.9*	*2,712.9*
5. Side Wall Bottom (24")	*Normal*	*102.1*	*27.8*	*27.8*	*919.3*	*919.3*
	Accident	*96.6*	*26.4*	*26.4*	*867.3*	*867.3*
6. Side Wall Bottom (14")	*Normal*	*89.4*	*15.1*	*15.1*	*489.8*	*489.8*
	Accident	*84.5*	*14.3*	*14.3*	*461.7*	*461.7*
7. Side Wall Top (12")	*Normal*	*86.8*	*12.6*	*12.6*	*404.0*	*404.0*
	Accident	*82.1*	*11.9*	*11.9*	*380.6*	*380.6*
8. Roof (44")	*Normal*	*151.4*	*51.5*	*51.5*	*2,283.1*	*2,283.1*
	Accident	*143.3*	*48.9*	*48.9*	*2,154.6*	*2,154.6*

Notes:
V_{ui} = Minimum of ultimate in plane shear capacities in planes 1 and 2.
V_{uo1} = Minimum ultimate out of plane shear capacity in plane 1.
V_{uo2} = Minimum ultimate out of plane shear capacity in plane 2.
M_{u1} = Minimum ultimate moment capacity in plane 1.
M_{u2} = Minimum ultimate moment capacity in plane 2.
Planes 1 and 2 are defined in Figure 3.9.4-5.

Table 3.9.4-12
Ultimate Axial/Moment Capacities of Concrete Components

Component	Thermal Condition	P_{tu} kips/ft	P_{cu} kips/ft	P_{ub1} kips/ft	P_{ub2} kips/ft	M_{ub1} kip-in/ft	M_{ub2} kip-in/ft
1. Rear Wall Bottom (32")	Normal	59.6	880.4	490.2	490.2	4,802.8	4,802.8
	Accident	56.3	793.9	465.0	465.0	4,367.5	4,367.5
2. Rear Wall Top (12")	Normal	59.6	350.0	163.0	163.0	747.1	747.1
	Accident	56.3	316.5	154.6	154.6	687.3	687.3
3. Front Wall Bottom (54")	Normal	152.7	1,513.4	822.0	822.0	14,501.4	14,501.4
	Accident	144.2	1,365.9	779.7	779.7	13,222.4	13,222.4
4. Front Wall Top (42")	Normal	152.7	1,195.1	625.7	625.7	9,097.3	9,097.3
	Accident	144.2	1,079.5	593.5	593.5	8,318.6	8,318.6
5. Side Wall Bottom (24")	Normal	85.9	682.2	355.5	355.5	2,951.3	2,951.3
	Accident	81.1	616.2	337.2	337.2	2,699.1	2,699.1
6. Side Wall Bottom (14")	Normal	85.9	417.0	191.9	191.9	1,081.2	1,081.2
	Accident	81.1	377.5	182.1	182.1	995.7	995.7
7. Side Wall Top (12")	Normal	85.9	364.0	159.1	159.1	806.6	806.6
	Accident	81.1	329.8	151.0	151.0	744.4	744.4
8. Roof (44")	Normal	114.5	1,227.8	659.5	659.5	9,425.2	9,425.2
	Accident	108.1	1,108.0	625.5	625.5	8,597.8	8,597.8

Notes:

P_{tu} = Minimum of ultimate tensile capacities in planes 1 and 2.
P_{cu} = Minimum of ultimate compressive capacities in plane 1 and 2.
P_{ub1} = Minimum of ultimate balanced section compressive capacity in plane 1.
P_{ub2} = Minimum of ultimate balanced section compressive capacity in plane 2.
M_{ub1} = Minimum of ultimate balanced section moment capacity in plane 1.
M_{ub2} = Minimum of ultimate balanced section moment capacity in plane 2.
Planes 1 and 2 are defined in Figure 3.9.4-5.
Ultimate axial and balanced moment capacities of alternate front wall rebar layout reported in Table 3.9.4-26.

Table 3.9.4-12a
Ultimate Axial/Moment Capacities of FPS Concrete Components

Component	*Thermal Condition*	P_{tu}	P_{cu}	P_{ub1}	P_{ub2}	M_{ub1}	M_{ub2}
		kips/ft	*kips/ft*	*kips/ft*	*kips/ft*	*kip-in/ft*	*kip-in/ft*
1. Rear Wall Side (24")	*Normal*	*59.6*	*668.2*	*359.3*	*359.3*	*2,782.8*	*2,782.8*
	Accident	*56.3*	*602.9*	*340.8*	*340.8*	*2,538.0*	*2,538.0*
2. Rear Wall Mid & Top (12")	*Normal*	*59.6*	*350.0*	*163.0*	*163.0*	*747.1*	*747.1*
	Accident	*56.3*	*316.5*	*154.6*	*154.6*	*687.3*	*687.3*
3. Interior Pedestal (12")	*Normal*	*59.6*	*350.0*	*163.0*	*163.0*	*747.1*	*747.1*
	Accident	*56.3*	*316.5*	*154.6*	*154.6*	*687.3*	*687.3*
4. Front Wall (42")	*Normal*	*152.7*	*1,195.1*	*625.7*	*625.7*	*9,097.3*	*9,097.3*
	Accident	*144.2*	*1,079.5*	*593.5*	*593.5*	*8,318.6*	*8,318.6*
5. Side Wall Bottom (24")	*Normal*	*85.9*	*682.2*	*355.5*	*355.5*	*2,951.3*	*2,951.3*
	Accident	*81.1*	*616.2*	*337.2*	*337.2*	*2,699.1*	*2,699.1*
6. Side Wall Bottom (14")	*Normal*	*85.9*	*417.0*	*191.9*	*191.9*	*1,081.2*	*1,081.2*
	Accident	*81.1*	*377.5*	*182.1*	*182.1*	*995.7*	*995.7*
7. Side Wall Top (12")	*Normal*	*85.9*	*364.0*	*159.1*	*159.1*	*806.6*	*806.6*
	Accident	*81.1*	*329.8*	*151.0*	*151.0*	*744.4*	*744.4*
8. Roof (44")	*Normal*	*114.5*	*1,227.8*	*659.5*	*659.5*	*9,425.2*	*9,425.2*
	Accident	*108.1*	*1,108.0*	*625.5*	*625.5*	*8,597.8*	*8,597.8*

Notes:

P_{tu} = Minimum of ultimate tensile capacities in planes 1 and 2
P_{cu} = Minimum of ultimate compressive capacities in plane 1 and 2
P_{ub1} = Minimum of ultimate balanced section compressive capacity in plane 1
P_{ub2} = Minimum of ultimate balanced section compressive capacity in plane 2
M_{ub1} = Minimum of ultimate balanced section moment capacity in plane 1
M_{ub2} = Minimum of ultimate balanced section moment capacity in plane 2
Planes 1 and 2 are defined in Figure 3.9.4-5

Table 3.9.4-13
Comparison of Highest Combined Shear Forces/Moments with the Capacities of EOS-HSM
3 Pages

Component	Load Combination	Quantity	V_I	V_{o1}	V_{o2}	M_1	M_2
			***kips*/ft**	**kips/ft**	**kips/ft**	**kip-in/ft**	**kip-in/ft**
1. Rear Wall Bottom (32")	C1 through C6	Computed	51.62	6.26	9.79	338.75	708.70
		Capacity	90.43	38.26	38.26	886.79	886.79
		Ratio	0.57	0.16	0.26	0.38	0.80
	C7	Computed	25.29	1.86	2.71	232.79	270.83
		Capacity	85.58	36.30	36.30	837.08	837.08
		Ratio	0.30	0.05	0.07	0.28	0.32
2. Rear Wall Top (12")	C1 through C6	Computed	13.70	5.12	6.40	36.93	106.65
		Capacity	64.97	12.81	12.81	290.38	290.38
		Ratio	0.21	0.40	0.50	0.13	0.37
	C7	Computed	7.64	4.22	2.95	24.52	69.33
		Capacity	61.43	12.15	12.15	273.80	273.80
		Ratio	0.12	0.35	0.24	0.09	0.25
3. Front Wall Bottom (54")	C1 through C6	Computed	57.56	14.24	13.02	1023.97	1877.23
		Capacity	195.97	64.28	64.28	3791.72	3791.72
		Ratio	0.29	0.22	0.20	0.27	0.50
	C7	Computed	25.23	3.12	3.11	1049.12	1735.23
		Capacity	185.37	60.98	60.98	3578.11	3578.11
		Ratio	0.14	0.05	0.05	0.29	0.48

Table 3.9.4-13
Comparison of Highest Combined Shear Forces/Moments with the Capacities of EOS-HSM
3 Pages

Component	Load Combination	Quantity	V_I	V_{o1}	V_{o2}	M_1	M_2
			***kips*/ft**	**kips/ft**	**kips/ft**	**kip-in/ft**	**kip-in/ft**
4. Front Wall Top (42")	C1 through C6	Computed	90.42	28.50	25.62	949.69	1768.70
		Capacity	180.69	49.00	49.00	2875.63	2875.63
		Ratio	0.50	0.58	0.52	0.33	0.62
	C7	Computed	48.32	26.12	24.35	1353.14	2485.27
		Capacity	170.88	46.49	46.49	2712.91	2712.91
		Ratio	0.28	0.56	0.52	0.50	0.92
5. Side Wall Bottom (24")	C1 through C6	Computed	23.50	15.39	14.78	269.28	182.86
		Capacity	102.12	27.84	27.84	919.26	919.26
		Ratio	0.23	0.55	0.53	0.29	0.20
	C7	Computed	11.06	14.31	18.56	143.44	396.28
		Capacity	96.57	26.41	26.41	867.25	867.25
		Ratio	0.11	0.54	0.70	0.17	0.46
6. Side Wall Bottom (14")	C1 through C6	Computed	14.39	11.42	6.10	91.36	38.03
		Capacity	89.39	15.11	15.11	489.85	489.85
		Ratio	0.16	0.76	0.40	0.19	0.08
	C7	Computed	11.13	12.14	12.65	63.98	117.21
		Capacity	84.50	14.34	14.34	461.69	461.69
		Ratio	0.13	0.85	0.88	0.14	0.25

Table 3.9.4-13
Comparison of Highest Combined Shear Forces/Moments with the Capacities of EOS-HSM
3 Pages

Component	Load Combination	Quantity	V_I	V_{o1}	V_{o2}	M_1	M_2
			***kips*/ft**	**kips/ft**	**kips/ft**	**kip-in/ft**	**kip-in/ft**
7. Side Wall Top (12")	C1 through C6	Computed	38.48	12.32	11.88	285.32	195.00
		Capacity	86.84	12.57	12.57	403.96	403.96
		Ratio	0.44	0.98	0.95	0.71	0.48
	C7	Computed	46.54	10.56	10.64	341.15	151.85
		Capacity	82.08	11.92	11.92	380.58	380.58
		Ratio	0.57	0.89	0.89	0.90	0.40
8. Roof (44")	C1 through C6	Computed	21.46	46.12	49.54	622.18	1831.53
		Capacity	151.43	51.55	51.55	2283.14	2283.14
		Ratio	0.14	0.89	0.96	0.27	0.80
	C7	Computed	22.51	11.56	24.29	283.58	1004.18
		Capacity	143.25	48.90	48.90	2154.63	2154.63
		Ratio	0.16	0.24	0.50	0.13	0.47

Notes:

Load Combinations C1 through C6 include normal thermal condition and C7 includes accidental thermal condition.

Comparison of highest combined shear forces/moments with capacities for alternate front wall rebar layout reported in Table 3.9.4-28.

Table 3.9.4-13a
Comparison of Highest Combined Shear Forces/Moments with the Capacities of EOS FPS HSM
3 Pages

Component	*Load Comb.*[1]	*Quantity*	V_1	V_{o1}	V_{o2}	M_1	M_2
			kips/ft	*kips/ft*	*kips/ft*	*kip-in/ft*	*kip-in/ft*
1. Rear Wall Side (24")	*C1 through C6*	*Demand*	*26.8*	*8.5*	*21.7*	*143.9*	*311.7*
		Capacity	*80.2*	*28.1*	*28.1*	*648.2*	*648.2*
		Ratio	*0.33*	*0.30*	*0.77*	*0.22*	*0.48*
	C7	*Demand*	*6.2*	*4.6*	*8.4*	*156.7*	*204.2*
		Capacity	*75.9*	*26.6*	*26.6*	*611.8*	*611.8*
		Ratio	*0.08*	*0.17*	*0.31*	*0.26*	*0.33*
2. Rear Wall Center and Top (12")	*C1 through C6*	*Demand*	*16.2*	*6.7*	*10.2*	*39.2*	*137.7*
		Capacity	*65.0*	*12.8*	*12.8*	*290.4*	*290.4*
		Ratio	*0.25*	*0.52*	*0.80*	*0.13*	*0.47*
	C7	*Demand*	*8.1*	*2.7*	*5.2*	*69.0*	*105.4*
		Capacity	*61.4*	*12.2*	*12.2*	*273.8*	*273.8*
		Ratio	*0.13*	*0.22*	*0.43*	*0.25*	*0.38*
3. Interior Pedestal (12")	*C1 through C6*	*Demand*	*46.3*	*9.4*	*11.3*	*38.7*	*40.1*
		Capacity	*65.0*	*12.8*	*12.8*	*290.4*	*290.4*
		Ratio	*0.71*	*0.74*	*0.88*	*0.13*	*0.14*
	C7	*Demand*	*23.4*	*2.4*	*10.2*	*28.4*	*31.2*
		Capacity	*61.4*	*12.2*	*12.2*	*273.8*	*273.8*
		Ratio	*0.38*	*0.20*	*0.84*	*0.10*	*0.11*

Table 3.9.4-13a
Comparison of Highest Combined Shear Forces/Moments with the Capacities of EOS FPS HSM
3 Pages

Component	*Load Comb.*[1]	*Quantity*	V_I	V_{o1}	V_{o2}	M_1	M_2
			kips/ft	*kips/ft*	*kips/ft*	*kip-in/ft*	*kip-in/ft*
4. Front Wall Top (42")	*C1 through C6*	*Demand*	*96.9*	*27.0*	*43.6*	*1372.2*	*2379.2*
		Capacity	*180.7*	*49.0*	*49.0*	*2875.6*	*2875.6*
		Ratio	*0.54*	*0.55*	*0.89*	*0.48*	*0.83*
	C7	*Demand*	*51.0*	*23.6*	*41.1*	*1377.1*	*2436.3*
		Capacity	*170.9*	*46.5*	*46.5*	*2712.9*	*2712.9*
		Ratio	*0.30*	*0.51*	*0.88*	*0.51*	*0.90*
5. Side Wall Bottom (24")	*C1 through C6*	*Demand*	*28.6*	*14.8*	*14.3*	*204.0*	*233.9*
		Capacity	*102.1*	*27.8*	*27.8*	*919.3*	*919.3*
		Ratio	*0.28*	*0.53*	*0.51*	*0.22*	*0.25*
	C7	*Demand*	*15.9*	*15.9*	*15.8*	*145.2*	*378.9*
		Capacity	*96.6*	*26.4*	*26.4*	*867.3*	*867.3*
		Ratio	*0.16*	*0.60*	*0.60*	*0.17*	*0.44*
6. Side Wall Bottom (14")	*C1 through C6*	*Demand*	*22.0*	*13.6*	*8.5*	*70.6*	*67.9*
		Capacity	*89.4*	*15.1*	*15.1*	*489.8*	*489.8*
		Ratio	*0.25*	*0.90*	*0.56*	*0.14*	*0.14*
	C7	*Demand*	*14.3*	*12.1*	*12.3*	*64.8*	*133.0*
		Capacity	*84.5*	*14.3*	*14.3*	*461.7*	*461.7*
		Ratio	*0.17*	*0.84*	*0.85*	*0.14*	*0.29*

Table 3.9.4-13a
Comparison of Highest Combined Shear Forces/Moments with the Capacities of EOS FPS HSM
3 Pages

Component	*Load Comb.*[1]	*Quantity*	V_1	V_{o1}	V_{o2}	M_1	M_2
			kips/ft	*kips/ft*	*kips/ft*	*kip-in/ft*	*kip-in/ft*
7. Side Wall Top (12")	*C1 through C6*	*Demand*	*43.1*	*11.6*	*11.0*	*315.5*	*159.6*
		Capacity	*86.8*	*12.6*	*12.6*	*404.0*	*404.0*
		Ratio	*0.50*	*0.93*	*0.88*	*0.78*	*0.40*
	C7	*Demand*	*44.1*	*9.5*	*10.2*	*335.4*	*144.9*
		Capacity	*82.1*	*11.9*	*11.9*	*380.6*	*380.6*
		Ratio	*0.54*	*0.80*	*0.86*	*0.88*	*0.38*
8. Roof (44")	*C1 through C6*	*Demand*	*24.6*	*44.8*	*48.4*	*594.5*	*1852.3*
		Capacity	*151.4*	*51.5*	*51.5*	*2283.1*	*2283.1*
		Ratio	*0.16*	*0.87*	*0.94*	*0.26*	*0.81*
	C7	*Demand*	*21.8*	*16.1*	*8.6*	*309.1*	*989.6*
		Capacity	*143.3*	*48.9*	*48.9*	*2154.6*	*2154.6*
		Ratio	*0.15*	*0.33*	*0.18*	*0.14*	*0.46*

Notes:

(1) Comb C1 through C6 include normal thermal, Comb C7 include accident thermal

Table 3.9.4-14
Comparison of Highest Combined Axial Forces/Moments with the Capacities of EOS-HSM
3 Pages

Component	Load Combination	Quantity	P (Comp) kips/ft	P_1 (Tens) kips/ft	P_2 (Tens.) kips/ft	M_{1p} (1) kip-in/ft	M_{2p} (1) kip-in/ft
1. Rear Wall Bottom (32")	C1 through C6	Computed	104.39	33.78	32.11	299.64	428.28
		Capacity	880.39	59.64	59.64	427.42	738.10
		Ratio	0.12	0.57	0.54	0.70	0.58
	C7	Computed	44.56	13.37	5.46	66.43	124.05
		Capacity	793.88	56.33	56.33	826.20	806.31
		Ratio	0.06	0.24	0.10	0.08	0.15
2. Rear Wall Top (12")	C1 through C6	Computed	29.63	9.50	23.56	36.93	43.42
		Capacity	349.99	59.64	59.64	279.91	238.59
		Ratio	0.08	0.16	0.40	0.13	0.18
	C7	Computed	15.84	7.09	40.00	20.08	45.85
		Capacity	316.52	56.33	56.33	249.52	79.84
		Ratio	0.05	0.13	0.71	0.08	0.57
3. Front Wall Bottom (54")	C1 through C6	Computed	122.27	72.22	65.59	1019.49	773.80
		Capacity	1513.35	152.68	152.68	1998.10	3368.23
		Ratio	0.08	0.47	0.43	0.51	0.23
	C7	Computed	59.82	19.82	0.00	485.33	0.00
		Capacity	1365.94	144.20	144.20	3244.10	3578.11
		Ratio	0.04	0.14	0.00	0.15	0.00

Table 3.9.4-14
Comparison of Highest Combined Axial Forces/Moments with the Capacities of EOS-HSM
3 Pages

Component	Load Combination	Quantity	P (Comp) kips/ft	P_1 (Tens) kips/ft	P_2 (Tens.) kips/ft	M_{1p} (1) kip-in/ft	M_{2p} (1) kip-in/ft
4. Front Wall Top (42")	C1 through C6	Computed	256.17	97.70	77.54	737.46	1137.66
		Capacity	1195.11	152.68	152.68	2524.84	1880.68
		Ratio	0.21	0.64	0.51	0.29	0.60
	C7	Computed	98.93	22.08	32.83	1352.68	1796.91
		Capacity	1079.52	144.20	144.20	2297.59	2299.51
		Ratio	0.09	0.15	0.23	0.59	0.78
5. Side Wall Bottom (24")	C1 through C6	Computed	70.20	27.97	37.58	267.46	158.64
		Capacity	682.20	85.88	85.88	664.87	738.53
		Ratio	0.10	0.33	0.44	0.40	0.21
	C7	Computed	38.81	22.46	58.73	97.14	324.92
		Capacity	616.18	81.11	81.11	627.12	331.04
		Ratio	0.06	0.28	0.72	0.15	0.98
6. Side Wall Bottom (14")	C1 through C6	Computed	47.63	19.43	16.50	75.91	37.93
		Capacity	417.00	85.88	85.88	450.17	484.24
		Ratio	0.11	0.23	0.19	0.17	0.08
	C7	Computed	21.85	31.53	62.90	63.98	117.21
		Capacity	377.50	81.11	81.11	337.69	236.42
		Ratio	0.06	0.39	0.78	0.19	0.50

Table 3.9.4-14
Comparison of Highest Combined Axial Forces/Moments with the Capacities of EOS-HSM
3 Pages

Component	Load Combination	Quantity	P (Comp) kips/ft	P_1 (Tens) kips/ft	P_2 (Tens.) kips/ft	M_{1p} (1) kip-in/ft	M_{2p} (1) kip-in/ft
7. Side Wall Top (12")	C1 through C6	Computed	157.07	27.52	49.71	44.42	49.00
		Capacity	363.96	85.88	85.88	386.56	170.14
		Ratio	0.43	0.32	0.58	0.11	0.29
	C7	Computed	138.02	56.91	11.68	64.54	132.35
		Capacity	329.77	81.11	81.11	114.93	358.64
		Ratio	0.42	0.70	0.14	0.56	0.37
8. Roof (44")	C1 through C6	Computed	107.11	24.43	67.55	621.82	1817.34
		Capacity	1227.83	114.51	114.51	2237.29	2106.43
		Ratio	0.09	0.21	0.59	0.28	0.86
	C7	Computed	90.83	11.47	59.85	239.44	751.16
		Capacity	1107.99	108.15	108.15	2085.65	1488.26
		Ratio	0.08	0.11	0.55	0.11	0.50

Notes:

1. M_{1p} and M_{2p} are moments at the same location and for the same load combination as P_1 and P_2. M_{1p} and M_{2p} occur at the same location simultaneously with P_1 and P_2, i.e., $M_1 = [(P_{tu} – P_1)/P_{tu}]*M_{u1}$.
2. Load Combinations C1 to C6 include normal thermal, C7 include accident thermal.
3. *Comparison of highest combined axial forces/moments with capacities for alternate front wall rebar layout reported in Table* 3.9.4-29.

Table 3.9.4-14a
Comparison of Highest Combined Axial Forces/Moments with the Capacities of EOS-HSM-FPS Option
3 Pages

Component	*Load Comb.*[(1)]	*Quantity*	*P (Comp)*	P_1 *(Tens)*	P_2 *(Tens.)*	M_{1p}[(1)]	M_{2p}[(1)]
			kips/ft	*kips/ft*	*kips/ft*	*kip-in/ft*	*kip-in/ft*
1. Rear Wall Side (24")	*C1 through C6*	*Demand*	*61.0*	*20.1*	*18.1*	*139.0*	*202.7*
		Capacity	*668.2*	*59.6*	*59.6*	*430.1*	*515.8*
		Ratio	*0.09*	*0.34*	*0.30*	*0.32*	*0.39*
	C7	*Demand*	*41.9*	*26.4*	*8.1*	*156.7*	*170.1*
		Capacity	*602.9*	*56.3*	*56.3*	*324.9*	*602.2*
		Ratio	*0.07*	*0.47*	*0.14*	*0.48*	*0.28*
2. Rear Wall Center and Top (12")	*C1 through C6*	*Demand*	*31.0*	*10.1*	*24.2*	*39.1*	*48.0*
		Capacity	*350.0*	*59.6*	*59.6*	*241.3*	*247.3*
		Ratio	*0.09*	*0.17*	*0.41*	*0.16*	*0.19*
	C7	*Demand*	*16.8*	*46.7*	*36.5*	*10.9*	*75.7*
		Capacity	*316.5*	*56.3*	*56.3*	*47.0*	*96.8*
		Ratio	*0.05*	*0.83*	*0.65*	*0.23*	*0.78*
3. Interior Pedestal (12")	*C1 through C6*	*Demand*	*167.2*	*49.6*	*34.6*	*27.4*	*39.7*
		Capacity	*350.0*	*59.6*	*59.6*	*57.1*	*225.0*
		Ratio	*0.48*	*0.83*	*0.58*	*0.48*	*0.18*
	C7	*Demand*	*82.3*	*8.6*	*12.5*	*28.4*	*4.3*
		Capacity	*316.5*	*56.3*	*56.3*	*243.4*	*271.8*
		Ratio	*0.26*	*0.15*	*0.22*	*0.12*	*0.02*

Table 3.9.4-14a
Comparison of Highest Combined Axial Forces/Moments with the Capacities of EOS-HSM-FPS Option
3 Pages

Component	*Load Comb.*[1]	*Quantity*	*P (Comp)*	*P_1 (Tens)*	*P_2 (Tens.)*	*M_{1p}*[1]	*M_{2p}*[1]
			kips/ft	*kips/ft*	*kips/ft*	*kip-in/ft*	*kip-in/ft*
4. Front Wall Top (42")	*C1 through C6*	*Demand*	*250.0*	*109.5*	*110.6*	*619.9*	*1205.3*
		Capacity	*1195.1*	*152.7*	*152.7*	*1030.3*	*1360.6*
		Ratio	*0.21*	*0.72*	*0.72*	*0.60*	*0.89*
	C7	*Demand*	*100.8*	*31.0*	*31.4*	*1353.2*	*1733.0*
		Capacity	*1079.5*	*144.2*	*144.2*	*2360.9*	*2293.2*
		Ratio	*0.09*	*0.21*	*0.22*	*0.57*	*0.76*
5. Side Wall Bottom (24")[3]	*C1 through C6*	*Demand*	*53.3*	*56.0*	*68.9*	*204.0*	*168.5*
		Capacity	*682.2*	*85.9*	*85.9*	*632.7*	*191.4*
		Ratio	*0.08*	*0.65*	*0.80*	*0.32*	*0.88*
	C7	*Demand*	*37.0*	*22.1*	*74.8*	*69.8*	*361.5*
		Capacity	*616.2*	*81.1*	*81.1*	*630.9*	*67.2*
		Ratio	*0.06*	*0.27*	*0.92*	*0.11*	*5.38*[4]
6. Side Wall Bottom (14")	*C1 through C6*	*Demand*	*62.0*	*32.0*	*55.8*	*41.3*	*48.0*
		Capacity	*417.0*	*85.9*	*85.9*	*416.7*	*171.8*
		Ratio	*0.15*	*0.37*	*0.65*	*0.10*	*0.28*
	C7	*Demand*	*21.3*	*31.0*	*65.7*	*64.8*	*133.0*
		Capacity	*377.5*	*81.1*	*81.1*	*346.3*	*149.4*
		Ratio	*0.06*	*0.38*	*0.81*	*0.19*	*0.89*

Table 3.9.4-14a
Comparison of Highest Combined Axial Forces/Moments with the Capacities of EOS-HSM-FPS Option
3 Pages

Component	*Load Comb.*[1]	*Quantity*	*P (Comp)*	P_1 *(Tens)*	P_2 *(Tens.)*	M_{1p}[1]	M_{2p}[1]
			kips/ft	*kips/ft*	*kips/ft*	*kip-in/ft*	*kip-in/ft*
7. Side Wall Top (12")	*C1 through C6*	*Demand*	*162.9*	*26.4*	*57.8*	*37.6*	*53.9*
		Capacity	*364.0*	*85.9*	*85.9*	*291.2*	*148.2*
		Ratio	*0.45*	*0.31*	*0.67*	*0.13*	*0.36*
	C7	*Demand*	*138.3*	*44.8*	*5.5*	*90.0*	*113.5*
		Capacity	*329.8*	*81.1*	*81.1*	*171.7*	*378.6*
		Ratio	*0.42*	*0.55*	*0.07*	*0.52*	*0.30*
8. Roof (44")	*C1 through C6*	*Demand*	*142.2*	*41.4*	*66.0*	*434.7*	*1678.1*
		Capacity	*1227.8*	*114.5*	*114.5*	*1457.0*	*1920.3*
		Ratio	*0.12*	*0.36*	*0.58*	*0.30*	*0.87*
	C7	*Demand*	*91.4*	*31.9*	*54.9*	*231.6*	*937.4*
		Capacity	*1108.0*	*108.1*	*108.1*	*2119.8*	*2050.2*
		Ratio	*0.08*	*0.29*	*0.51*	*0.11*	*0.46*

Notes:

1 *Comb C1 through C6 include normal thermal, Comb C7 include accident thermal*

2 *M_{1p} and M_{2p} are moments at the same location and for the same load combination as P_1 and P_2. M_{1p} and M_{2p} occur at the same location simultaneously with P_1 and P_2, i.e., $M_1 = [(P_{tu} – P_1)/P_{tu}]*M_{u1}$*

3 *See* Table 3.9.4-14b *for the results of detailed analysis of side wall local demand to capacity ratio for overstressed region above/adjacent to air vent.*

Table 3.9.4-14b
Comparison of Highest Combined Axial Forces/Moments with the Capacities of EOS-HSM-FPS Option with Supplemental Reinforcement

Component	*Load Comb.*[1]	*Quantity*	P_1 (Tens.)	P_2 (Tens.)	P_1 (Comp)	P_2 (Comp)	M_{1p}[2]	M_{2p}[2]
			kips/ft	*kips/ft*	*kips/ft*	*kips/ft*	*kip-in/ft*	*kip-in/ft*
5B. Side Wall Above/Adjacent Air Vent (24")	*C1 through C6*	*Demand*	*56.0*	*68.9*	*53.3*	*38.7*	*204.0*	*233.9*
		Capacity	*85.9*	*232.0*	*682.2*	*760.0*	*632.7*	*1827.7*
		Ratio	*0.65*	*0.30*	*0.08*	*0.05*	*0.32*	*0.13*
	C7	*Demand*	*22.1*	*74.8*	*37.0*	*21.8*	*69.8*	*361.5*
		Capacity	*81.1*	*219.1*	*616.2*	*689.9*	*630.9*	*1376.2*
		Ratio	*0.27*	*0.34*	*0.06*	*0.03*	*0.11*	*0.26*

Notes:

1 Comb C1 through C6 include normal thermal, Comb C7 include accident thermal

2 M_{1p} and M_{2p} are moments at the same location and for the same load combination as P_1 and P_2. M_{1p} and M_{2p} occur at the same location simultaneously with P_1 and P_2, i.e., $M_1 = [(P_{tu} - P_1)/P_{tu}]*M_{u1}$

Table 3.9.4-15
Load Cases for DSC Support Structure Evaluation

Load Type Nomenclature	Load Type Description
D	Dead load – self weight of rails
L	Live load – weight of the DSC
Ro	Normal handling load
To	Normal thermal load
Ra	Off-normal handling load
Ta	Envelope of off-normal and accident thermal loads
E	Earthquake load

Table 3.9.4-16
Load Combination for DSC Support Structure Evaluation

Load Combination ID	Load Combination	Event
N1	1.0 S > D + L + Ro	Normal
N2	1.0 S > D + L + Ro	Normal – Insertion/Extraction
N3	1.3 S > D + L + Ra + To	Off-normal – Handling
A5S	1.6 S > D + L + E + To	Accident – Earthquake
A5V	1.4 Sv > D + L + E + To	Accident – Earthquake
A8S	1.7 S > D + L + Ta	Accident – Thermal
A8V	1.4 Sv > D + L + Ta	Accident – Thermal

Table 3.9.4-17
Summary of Demand to Capacity Ratio (D/C Ratio) for the Whole Cross Section

Load Combination	Demand/Capacity Ratio	Maximum D/C Ratio and Controlling Action
N3 Strong	0.118	0.729 in Weak Axis Bending in load case A5 Seismic
N1 Weak	0.193	
A5S Weak	0.729	
A8S Weak	0.002	

Table 3.9.4-17a
Summary of Demand to Capacity Ratio of the FPS DSC Support Structure

		Normal			*Off-normal*		
		73" Span	***46" Span***	***40" Span***	***73" Span***	***46" Span***	***40" Span***
Capacities	*Tension, P_{nt} [kips]*	*359*	*359*	*359*	*466*	*466*	*466*
	Compression, P_{nc} [kips]	*449*	*463*	*466*	*584*	*602*	*605*
	Flexure (Weak-Axis), M_n [kips-in]	*596*	*428*	*428*	*775*	*556*	*556*
	Shear, V_n [kips]	*147*	*147*	*147*	*191*	*191*	*191*
Demand	*Tension, P_{nt} [kips]*	*N/A*			*135*	*135*	*135*
	Compression, P_{nc} [kips]				*135*	*135*	*135*
	Flexure (Weak-Axis), M_n [kips-in]				*653*	*416*	*358*
	Flexure (Strong-Axis), M_n [kips-in]				*177*	*876*	*17*
	Shear, V_n [kips]				*36*	*36*	*36*
Demand to Capacity Ratio	*Tension, P_{nt}*	*N/A*			*0.29*	*0.29*	*0.29*
	Compression, P_{nc}				*0.23*	*0.22*	*0.22*
	Flexure (Weak-Axis), M_n [kips-in]				*0.84*	*0.75*	*0.64*
	Shear, V_n				*0.19*	*0.19*	*0.19*
	Combined Compression and Flexure				*0.98*	*0.89*	*0.80*

Table 3.9.4-18
Summary of Demand to Capacity Ratio (D/C Ratio) for the Flange Elements

	Flange Demand/Capacity Type Ratio			Maximum D/C Ratio and Controlling Action
Load Combination	Axial Compression	Strong Bending	Weak Bending	
N1	0.314	0.02	0.228	0.388 Axial Compression in load case N3
N3	0.388	0.226	0.225	
A5S	0.265	0.022	0.229	
A8S	0.114	0.012	0.136	
N2	0.3	0.023	0.271	

Table 3.9.4-19
Summary of Demand to Capacity Ratio (D/C Ratio) for the Web Elements

Load Combination	Web Demand/Capacity Type Ratio			Maximum D/C Ratio and Controlling Action
	Axial Compression	Strong Bending	Weak Bending	
N1	0.747	0.08	0.012	0.761 in Axial Compression in load case A5 Seismic
N3	0.7	0.007	0.007	
A5S	0.761	0.076	0.014	
A8S	0.407	0.038	0.008	
N2	0.693	0.091	0.012	

Table 3.9.4-20
Summary of Demand to Capacity Ratio (D/C Ratio) for the Stiffener Elements

Load Combination	Stiffener Demand/Capacity Type Ratio			Maximum D/C Ratio and Controlling Action
	Axial Compression	Strong Bending	Weak Bending	
N1	0.162	0.023	0.707	0.805 in Weak Axis Bending in load case A5 Seismic
N3	0.059	0.372	0.372	
A5S	0.153	0.026	0.805	
A8S	0.096	0.014	0.434	
N2	0.156	0.02	0.529	

Table 3.9.4-21
Summary of Demand to Capacity Ratio (D/C Ratio) for the Accessories

Item	Demand/Capacity Ratio
Stop plate	0.784
DSC seismic impact	0.027
Extension baseplate	0.864
Lateral braces	0.636

Table 3.9.4-21a
Summary of Demand to Capacity Ratio (D/C Ratio) for FPS DSC Support Structure Accessories

Item	*Demand/Capacity Ratio*
12"x1" Plate	*0.82*
Tubesteel Spacer	*0.63*
Stop Plate	*0.81*
Rail Extension Baseplate	*0.57*

Table 3.9.4-22
Summary of Demand to Capacity Ratio (D/C Ratio) for *DSC Support Structure Welds*

Weld between	Demand/Capacity Ratio
Stop plate and rail	0.363
Extension baseplate and rail	0.141
Stiffener and lateral brace	0.291
Stiffener plate and rail	0.668

Table 3.9.4-22a
Summary of Demand to Capacity Ratio (D/C Ratio) for FPS DSC Support Structure Welds

Weld between	*Demand/Capacity Ratio*
4"x1" Plate and 12"x1" Plate	*0.27*
Stiffener and 12" x 1" Plate	*0.05*
Stop Plate and Support[(1)]	*0.81*
Tubesteel Spacer and 12" x 1" Plate	*0.70*
Extension Baseplate and 12" x 1" Plate	*0.42*
Nitronic Plate to 4"x1" Plate	*0.74*

Notes:

1. *Full penetration weld and qualification of base metal qualifies the welds - see* Table 3.9.4-21a.

Table 3.9.4-23
Modal Frequencies and Mass Participation of EOS-HSMS

Mode	Frequency (Hz)	Mass Participation					
		X-Direction		Y-Direction		Z-Direction	
		Mass (lb-s^2/in)	%	Mass (lb-s^2/in)	%	Mass (lb-s^2/in)	%
1	18.7	696	56%	-	-	-	-
2	31.7	-	-	-	-	-	-
3	32.7	-	-	-	-	711	57%
4	33.6	-	-	-	-	-	-
5	37.6	20	2%	-	-	-	-
6	49.8	291	23%	-	-	-	-
7	60.3	-	-	489	39%	-	-
8	67.3	-	-	-	-	323	26%
9	69.2	-	-	-	-	-	-
10	70.4	-	-	-	-	-	-

Table 3.9.4-23a
Modal Frequencies and Mass Participation of EOS-HSMS-FPS

Mode	*Frequency (Hz)*	*Mass Participation*					
		X-Direction		*Y-Direction*		*Z-Direction*	
		Mass	*%*	*Mass*	*%*	*Mass*	*%*
1	*19.2*	*663.6*	*56.1%*	-	-	-	-
2	*31.4*	-	-	*1.5*	*0.1%*	*797.3*	*67.4%*
3	*34.1*	-	-	-	-	-	-
4	*35.7*	-	-	-	-	-	-
5	*38.8*	*37.1*	*3.1%*	-	-	-	-
6	*44.2*	*251.2*	*21.2%*	-	-	-	-
7	*46.6*	-	-	-	-	*151.8*	*12.8%*
8	*60.6*	-	-	*468.2*	*39.6%*	-	-
9	*75.8*	-	-	*24.0*	*2.0%*	-	-
10	*76.5*	*4.3*	*0.4%*	-	-	-	-

Table 3.9.4-24
Roof Heat Shield Modal Participating Mass Ratios

Frequency (Hz)	Participating Mass Ratio		
	X-Direction	Y-Direction	Z-Direction
5.86	0.026	0.000	0.000
7.40	0.000	0.000	0.573
11.29	0.000	0.000	0.000
12.71	0.003	0.000	0.000
13.77	0.000	0.000	0.000
15.53	0.000	0.000	0.159
20.51	0.003	0.000	0.000
23.54	0.000	0.000	0.000
24.51	0.000	0.974	0.000
25.01	0.943	0.000	0.000
25.89	0.000	0.000	0.000
27.22	0.000	0.004	0.000
32.84	0.000	0.000	0.000
35.49	0.002	0.000	0.000
36.77	0.000	0.000	0.000
40.90	0.000	0.000	0.020
41.06	0.000	0.000	0.000
43.97	0.001	0.000	0.000
44.67	0.000	0.000	0.000
48.45	0.000	0.000	0.000
48.66	0.000	0.000	0.040
51.44	0.000	0.000	0.000
54.01	0.000	0.000	0.006
60.36	0.000	0.000	0.000
66.09	0.000	0.000	0.000
66.19	0.000	0.000	0.000
68.80	0.000	0.000	0.007
74.25	0.000	0.000	0.000
78.30	0.000	0.000	0.000
80.56	0.000	0.000	0.000
80.69	0.000	0.000	0.000
81.37	0.000	0.000	0.046
82.17	0.000	0.000	0.000
86.31	0.000	0.000	0.000
89.52	0.000	0.000	0.006
95.39	0.000	0.000	0.000
97.21	0.000	0.000	0.000

Table 3.9.4-25
Side Heat Shield Modal Participating Mass Ratios
(2 Sheets)

Frequency (Hz)	Participating Mass Ratio		
	X-Direction	Y-Direction	Z-Direction
3.97	0.684	0.000	0.000
4.51	0.154	0.000	0.000
6.57	0.006	0.000	0.000
7.42	0.004	0.000	0.000
7.69	0.000	0.000	0.000
9.21	0.000	0.000	0.000
10.43	0.010	0.000	0.000
15.53	0.000	0.000	0.000
16.55	0.000	0.001	0.000
16.74	0.042	0.000	0.000
17.39	0.000	0.000	0.000
17.78	0.018	0.000	0.001
19.63	0.000	0.001	0.000
22.45	0.000	0.000	0.000
24.59	0.001	0.000	0.000
26.88	0.000	0.000	0.000
29.15	0.000	0.000	0.000
29.75	0.001	0.000	0.001
30.11	0.004	0.000	0.000
32.69	0.016	0.000	0.002
33.60	0.000	0.002	0.000
36.04	0.000	0.000	0.000
38.72	0.014	0.000	0.001
39.05	0.000	0.000	0.000
42.87	0.000	0.000	0.000
43.01	0.000	0.000	0.000
44.44	0.000	0.000	0.000
46.77	0.001	0.000	0.000
48.98	0.001	0.000	0.001
49.35	0.000	0.009	0.000
50.17	0.003	0.000	0.000
53.29	0.005	0.000	0.001
55.11	0.000	0.018	0.000
56.77	0.000	0.000	0.004
59.53	0.000	0.000	0.034
61.20	0.000	0.096	0.000

Table 3.9.4-25
Side Heat Shield Modal Participating Mass Ratios
(2 Sheets)

Frequency (Hz)	Participating Mass Ratio		
	X-Direction	Y-Direction	Z-Direction
64.18	0.000	0.000	0.179
64.44	0.000	0.001	0.000
65.87	0.000	0.000	0.000
66.19	0.001	0.000	0.425
67.23	0.000	0.509	0.000
68.47	0.002	0.000	0.255
70.35	0.000	0.326	0.000
71.92	0.000	0.000	0.009
74.26	0.000	0.001	0.000
75.55	0.000	0.000	0.059
76.08	0.000	0.002	0.000
79.42	0.000	0.000	0.000
81.57	0.002	0.000	0.015
83.62	0.000	0.018	0.000
83.79	0.000	0.000	0.001
86.33	0.001	0.000	0.001
88.01	0.000	0.001	0.000
91.46	0.000	0.002	0.000
92.25	0.000	0.000	0.000
92.56	0.000	0.000	0.000
93.78	0.000	0.001	0.000
96.86	0.003	0.000	0.001
97.14	0.000	0.000	0.000

***Table* 3.9.4-26**
Ultimate Shear/Moment Capacities of Alternate Front Wall

Component	***Thermal Condition***	V_{ui}	V_{uo1}	V_{uo2}	M_{u1}	M_{u2}
		kips/ft	***kips/ft***	***kips/ft***	***kip-in/ft***	***kip-in/ft***
3. Front Wall Bottom (54")	*Normal*	*148.31*	*42.45*	*65.55*	*3,041.40*	*2,599.68*
	Accident	*140.26*	*40.28*	*62.19*	*2,869.52*	*2,453.93*
4. Front Wall Top (42")	*Normal*	*157.09*	*35.58*	*46.69*	*2,566.64*	*2,238.71*
	Accident	*148.61*	*33.75*	*44.29*	*2,420.78*	*2,112.66*
4. Front Wall Middle (42")	*Normal*	*181.44*	*43.59*	*47.58*	*2,565.76*	*2,806.10*
	Accident	*171.58*	*41.36*	*45.14*	*2,420.22*	*2,647.21*
4. Front Wall Bottom (42")	*Normal*	*135.48*	*49.32*	*47.74*	*2,766.98*	*1,819.51*
	Accident	*128.18*	*46.79*	*45.29*	*2,610.56*	*1,717.30*

Notes:
V_{ui} = Minimum of ultimate in plane shear capacities in planes 1 and 2
V_{uo1} = Minimum ultimate out of plane shear capacity in plane 1
V_{uo2} = Minimum ultimate out of plane shear capacity in plane 2
M_{u1} = Minimum ultimate moment capacity in plane 1
M_{u2} = Minimum ultimate moment capacity in plane 2
Planes 1 and 2 are defined in Figure 3.9.4-5

***Table* 3.9.4-26a**
Ultimate Shear/Moment Capacities of EOS-HSM-FPS Alternate Front Wall

Component	*Thermal Condition*	V_{ui} *Kips/ft*	V_{uo1} *Kips/ft*	V_{uo2} *Kips/ft*	M_{u1} *In-kips/ft*	M_{u2} *In-kips/ft*
Front Wall Top (42")	*Normal*	*130.25*	*35.50*	*45.18*	*2,566.64*	*1,612.46*
	Accident	*123.24*	*33.68*	*42.87*	*2,420.78*	*1,521.80*
Front Wall Mid Upper Side (42")	*Normal*	*154.84*	*43.59*	*44.83*	*2,565.76*	*2,153.87*
	Accident	*146.45*	*41.36*	*42.53*	*2,420.22*	*2,032.24*
Front Wall Mid Upper Center (42")	*Normal*	*106.69*	*43.59*	*44.79*	*2,565.76*	*1,218.03*
	Accident	*100.96*	*41.36*	*42.49*	*2,420.22*	*1,149.74*
Front Wall Mid Lower Side (42")	*Normal*	*140.33*	*43.59*	*44.82*	*2,565.76*	*1,909.71*
	Accident	*132.74*	*41.36*	*42.52*	*2,420.22*	*1,802.07*
Front Wall Mid Lower Center (42")	*Normal*	*91.13*	*43.59*	*44.71*	*2,565.76*	*894.29*
	Accident	*86.28*	*41.36*	*42.42*	*2,420.22*	*844.27*
Front Wall Mid Center (42")	*Normal*	*176.35*	*43.59*	*44.87*	*2,565.76*	*2,642.55*
	Accident	*166.75*	*41.36*	*42.56*	*2,420.22*	*2,492.74*
Front Wall Bottom (42")	*Normal*	*130.25*	*49.00*	*50.28*	*2,892.11*	*1,796.75*
	Accident	*123.24*	*46.49*	*47.70*	*2,728.44*	*1,695.85*

Notes:

V_{ui} = Minimum of ultimate in plane shear capacities in planes 1 and 2
V_{uo1} = Minimum ultimate out of plane shear capacity in plane 1
V_{uo2} = Minimum ultimate out of plane shear capacity in plane 2
M_{u1} = Minimum ultimate moment capacity in plane 1
M_{u2} = Minimum ultimate moment capacity in plane 2
Planes 1 and 2 are defined in Figure 3.9.4-5

***Table* 3.9.4-27**
Ultimate Axial and Balanced Moment Capacities of Alternate Front Wall Rebar

Component	*Thermal Condition*	P_{tu}	P_{cu}	P_{ub1}	P_{ub2}	M_{ub1}	M_{ub2}
		kips/ft	*kips/ft*	*kips/ft*	*kips/ft*	*kip-in/ft*	*kip-in/ft*
3. Front Wall Bottom (54")	*Normal*	*102.06*	*1,014.54*	*542.30*	*839.81*	*9,952.43*	*13,776.69*
	Accident	*96.39*	*916.25*	*514.44*	*796.54*	*9,088.71*	*12,515.78*
4. Front Wall Top (42")	*Normal*	*124.36*	*968.35*	*453.12*	*596.68*	*7,119.07*	*8,523.67*
	Accident	*117.47*	*875.40*	*429.90*	*566.00*	*6,546.80*	*7,803.89*
4. Front Wall Middle (42")	*Normal*	*153.58*	*1,195.59*	*556.08*	*607.30*	*8,443.62*	*8,947.22*
	Accident	*145.04*	*1,079.97*	*527.54*	*576.11*	*7,763.11*	*8,193.92*
4. Front Wall Bottom (42")	*Normal*	*98.42*	*1,166.23*	*629.94*	*610.99*	*9,046.99*	*8,334.65*
	Accident	*92.96*	*1,052.14*	*597.57*	*579.54*	*8,266.99*	*7,612.34*

Notes:

P_{tu} *=Minimum of ultimate tensile capacities in planes 1 and 2*
Separate plane 1 and plane 2 values are calculated in "Concapsh_B.xlsx" and used in "EOS-HSM[s]_Demand_Rev.0_0221R2.xlsx"

P_{cu} *= Minimum of ultimate compressive capacities in plane 1 and 2*

P_{ub1} *= Minimum of ultimate balanced section compressive capacity in plane 1*

P_{ub2} *= Minimum of ultimate balanced section compressive capacity in plane 2*

M_{ub1} *= Minimum of ultimate balanced section moment capacity in plane 1*

M_{ub2} *= Minimum of ultimate balanced section moment capacity in plane 2*

Planes 1 and 2 are defined in Figure 3.9.4-5

***Table* 3.9.4-27a**
Ultimate Axial/Moment Capacities of EOS-HSM-FPS Alternate Front Wall

Component	*Thermal Condition*	P_{tu}		P_{cu}		P_{ub1}	P_{ub2}	M_{ub1}	M_{ub2}
		plane 1 Kips/ft	*plane 2 Kips/ft*	*plane 1 Kips/ft*	*plane 2 Kips/ft*	*Kips/ft*	*Kips/ft*	*In-kips/ft*	*In-kips/ft*
Front Wall Top (42")	*Normal*	*151.21*	*92.15*	*968.55*	*1162.89*	*452.07*	*578.28*	*7,110.37*	*8,036.23*
	Accident	*142.84*	*87.03*	*875.59*	*1048.97*	*428.90*	*548.51*	*6,539.49*	*7,359.85*
Front Wall Mid Upper Side (42")	*Normal*	*153.58*	*124.72*	*1089.51*	*1127.19*	*556.08*	*572.77*	*7,535.83*	*7,833.62*
	Accident	*145.04*	*117.79*	*984.50*	*1017.67*	*527.54*	*543.33*	*6,901.82*	*7,170.99*
Front Wall Mid Upper Center (42")	*Normal*	*153.58*	*69.98*	*1089.51*	*1045.01*	*556.08*	*573.84*	*7,535.83*	*6,725.66*
	Accident	*145.04*	*66.10*	*984.50*	*942.31*	*527.54*	*544.27*	*6,901.82*	*6,121.83*
Front Wall Mid Lower Side (42")	*Normal*	*153.58*	*110.36*	*1089.51*	*1066.50*	*556.08*	*573.02*	*7,535.83*	*7,181.25*
	Accident	*145.04*	*104.23*	*984.50*	*962.69*	*527.54*	*543.55*	*6,901.82*	*6,552.64*
Front Wall Mid Lower Center (42")	*Normal*	*153.58*	*51.32*	*1089.51*	*1035.08*	*556.08*	*573.39*	*7,535.83*	*6,512.28*
	Accident	*145.04*	*48.47*	*984.50*	*932.89*	*527.54*	*543.82*	*6,901.82*	*5,920.78*
Front Wall Mid Center (42")	*Normal*	*153.58*	*153.58*	*1089.51*	*1089.51*	*556.08*	*572.45*	*7,535.83*	*7,672.60*
	Accident	*145.04*	*145.04*	*984.50*	*984.50*	*527.54*	*543.06*	*6,901.82*	*7,017.02*
Front Wall Bottom (42")	*Normal*	*153.58*	*92.15*	*1195.59*	*1162.89*	*625.63*	*643.74*	*9,108.20*	*8,454.89*
	Accident	*145.04*	*87.03*	*1079.97*	*1048.97*	*593.49*	*610.58*	*8,328.86*	*7,694.69*

Notes:

P_{tu} = *Minimum of ultimate tensile capacities in planes 1 and 2*
P_{cu} = *Minimum of ultimate compressive capacities in plane 1 and 2*
P_{ub1} = *Minimum of ultimate balanced section compressive capacity in plane 1*
P_{ub2} = *Minimum of ultimate balanced section compressive capacity in plane 2*
M_{ub1} = *Minimum of ultimate balanced section moment capacity in plane 1*
M_{ub2} = *Minimum of ultimate balanced section moment capacity in plane 2*
Planes 1 and 2 are defined in Figure 3.9.4-5

***Table* 3.9.4-28**
Comparison of Highest Combined Shear Forces/Moments with the Capacities of the Alternate Front Wall
2 Pages

Component	*Load Comb.*	*Quantity*	V_1	V_{o1}	V_{o2}	M_1	M_2
			Kips/ft	***kips/ft***	***kips/ft***	***kip-in/ft***	***kip-in/ft***
3. Front Wall Bottom (54")	*C1 through C6*	*Computed*	*57.6*	*14.2*	*13.0*	*1024.0*	*1877.2*
		Capacity	*148.3*	*42.5*	*65.6*	*3041.4*	*2599.7*
		Ratio	*0.39*	*0.34*	*0.20*	*0.34*	*0.72*
	C7	*Computed*	*25.2*	*3.1*	*3.1*	*1049.1*	*1735.2*
		Capacity	*140.3*	*40.3*	*62.2*	*2869.5*	*2453.9*
		Ratio	*0.18*	*0.08*	*0.05*	*0.37*	*0.71*
4. Front Wall Top (42")	*C1 through C6*	*Computed*	*28.8*	*28.5*	*14.0*	*949.7*	*1453.5*
		Capacity	*157.1*	*35.6*	*46.7*	*2566.6*	*2238.7*
		Ratio	*0.18*	*0.80*	*0.30*	*0.37*	*0.65*
	C7	*Computed*	*9.8*	*26.1*	*13.0*	*1353.1*	*1584.6*
		Capacity	*148.6*	*33.8*	*44.3*	*2420.8*	*2112.7*
		Ratio	*0.07*	*0.77*	*0.29*	*0.56*	*0.75*
4. Front Wall Middle (42")	*C1 through C6*	*Computed*	*90.4*	*6.4*	*25.6*	*938.6*	*1768.7*
		Capacity	*181.4*	*43.6*	*47.6*	*2565.8*	*2806.1*
		Ratio	*0.50*	*0.15*	*0.54*	*0.37*	*0.63*
	C7	*Computed*	*48.3*	*6.3*	*24.4*	*1326.9*	*2485.3*
		Capacity	*171.6*	*41.4*	*45.1*	*2420.2*	*2647.2*
		Ratio	*0.28*	*0.15*	*0.54*	*0.55*	*0.94*

***Table* 3.9.4-28**
Comparison of Highest Combined Shear Forces/Moments with the Capacities of the Alternate Front Wall
2 Pages

Component	*Load Comb.*	*Quantity*	V_1	V_{o1}	V_{o2}	M_1	M_2
			Kips/ft	***kips/ft***	***kips/ft***	***kip-in/ft***	***kip-in/ft***
4. Front Wall Bottom (42")	*C1 through C6*	*Computed*	*48.0*	*8.8*	*13.1*	*463.1*	*399.4*
		Capacity	*135.5*	*49.3*	*47.7*	*2767.0*	*1819.5*
		Ratio	*0.35*	*0.18*	*0.27*	*0.17*	*0.22*
	C7	*Computed*	*12.1*	*3.9*	*6.0*	*1058.0*	*509.5*
		Capacity	*128.2*	*46.8*	*45.3*	*2610.6*	*1717.3*
		Ratio	*0.09*	*0.08*	*0.13*	*0.41*	*0.30*

Notes:

1. Load Combinations C1 through C6 include normal thermal condition, C7 includes accidental thermal condition.

***Table* 3.9.4-28a**
Comparison of Highest Combined Shear Forces/Moments with Capacities of the EOS-HSM-FPS Alternate Front Wall
3 Pages

Component	*Load Comb.*[1]	*Quantity*	V_1	V_{o1}	V_{o2}	M_1	M_2[2]
			Kips/ft	***kips/ft***	***kips/ft***	***kip-in/ft***	***kip-in/ft***
4A. Front Wall Top (42")	*C1 through C6*	*Demand*	*28.8*	*14.6*	*31.2*	*984.6*	*1471.7*
		Capacity	*130.2*	*35.5*	*45.2*	*2566.6*	*1612.5*
		Ratio	*0.22*	*0.41*	*0.69*	*0.38*	*0.91*
	C7	*Demand*	*11.2*	*12.4*	*29.6*	*1377.1*	*1215.0*
		Capacity	*123.2*	*33.7*	*42.9*	*2420.8*	*1521.8*
		Ratio	*0.09*	*0.37*	*0.69*	*0.57*	*0.80*
4B. Front Wall Mid Upper Side (42")	*C1 through C6*	*Demand*	*83.4*	*0.0*	*38.7*	*876.9*	*1257.2*
		Capacity	*154.8*	*43.6*	*44.8*	*2565.8*	*2153.9*
		Ratio	*0.54*	*0.00*	*0.86*	*0.34*	*0.58*
	C7	*Demand*	*45.3*	*0.0*	*36.8*	*995.3*	*1827.7*
		Capacity	*146.5*	*41.4*	*42.5*	*2420.2*	*2032.2*
		Ratio	*0.31*	*0.00*	*0.87*	*0.41*	*0.90*
4C. Front Wall Mid Upper Center (42")	*C1 through C6*	*Demand*	*38.0*	*27.0*	*27.1*	*938.7*	*513.8*
		Capacity	*106.7*	*43.6*	*44.8*	*2565.8*	*1218.0*
		Ratio	*0.36*	*0.62*	*0.60*	*0.37*	*0.42*
	C7	*Demand*	*17.7*	*23.6*	*25.1*	*1289.3*	*544.0*
		Capacity	*101.0*	*41.4*	*42.5*	*2420.2*	*1149.7*
		Ratio	*0.18*	*0.57*	*0.59*	*0.53*	*0.47*

***Table* 3.9.4-28a**
Comparison of Highest Combined Shear Forces/Moments with Capacities of the EOS-HSM-FPS Alternate Front Wall
3 Pages

Component	*Load Comb.*[1]	*Quantity*	V_1	V_{o1}	V_{o2}	M_1	M_2[2]
			Kips/ft	***kips/ft***	***kips/ft***	***kip-in/ft***	***kip-in/ft***
4D. Front Wall Mid Lower Side (42")	*C1 through C6*	*Demand*	*84.1*	*0.0*	*38.0*	*965.6*	*1283.7*
		Capacity	*140.3*	*43.6*	*44.8*	*2565.8*	*1909.7*
		Ratio	*0.60*	*0.00*	*0.85*	*0.38*	*0.67*
	C7	*Demand*	*19.3*	*0.0*	*28.6*	*766.6*	*1212.7*
		Capacity	*132.7*	*41.4*	*42.5*	*2420.2*	*1802.1*
		Ratio	*0.15*	*0.00*	*0.67*	*0.32*	*0.67*
4E. Front Wall Mid Lower Center (42")	*C1 through C6*	*Demand*	*73.6*	*16.0*	*14.7*	*1372.2*	*901.2*
		Capacity	*91.1*	*43.6*	*44.7*	*2565.8*	*894.3*
		Ratio	*0.81*	*0.37*	*0.33*	*0.53*	*1.01(2)*
	C7	*Demand*	*51.0*	*9.3*	*4.9*	*1190.5*	*736.2*
		Capacity	*86.3*	*41.4*	*42.4*	*2420.2*	*844.3*
		Ratio	*0.59*	*0.23*	*0.11*	*0.49*	*0.87*
4F. Front Wall Mid Center (42")	*C1 through C6*	*Demand*	*87.5*	*0.0*	*35.9*	*455.4*	*1832.5*
		Capacity	*176.3*	*43.6*	*44.9*	*2565.8*	*2642.5*
		Ratio	*0.50*	*0.00*	*0.80*	*0.18*	*0.69*
	C7	*Demand*	*47.5*	*0.0*	*30.2*	*602.1*	*2350.1*
		Capacity	*166.8*	*41.4*	*42.6*	*2420.2*	*2492.7*
		Ratio	*0.28*	*0.00*	*0.71*	*0.25*	*0.94*

***Table* 3.9.4-28a**
Comparison of Highest Combined Shear Forces/Moments with Capacities of the EOS-HSM-FPS Alternate Front Wall
3 Pages

Component	*Load Comb.*[1]	*Quantity*	V_1	V_{o1}	V_{o2}	M_1	M_2[2]
			Kips/ft	***kips/ft***	***kips/ft***	***kip-in/ft***	***kip-in/ft***
4G. Front Wall Bottom (42")	*C1 through C6*	*Demand*	*48.1*	*10.1*	*43.6*	*327.8*	*603.3*
		Capacity	*130.2*	*49.0*	*50.3*	*2892.1*	*1796.8*
		Ratio	*0.37*	*0.21*	*0.87*	*0.11*	*0.34*
	C7	*Demand*	*16.1*	*2.6*	*20.5*	*445.3*	*489.5*
		Capacity	*123.2*	*46.5*	*47.7*	*2728.4*	*1695.9*
		Ratio	*0.13*	*0.06*	*0.43*	*0.16*	*0.29*

Notes:

1. *Load Combinations C1 through C6 include normal thermal, Comb C7 includes accident thermal*
2. *The maximum load ratio from front wall mid lower center is 1.01 based on lower moment capacity. The maximum load ratio (M_2) excluding the critical section is 0.87. The load ratio M_2 for the critical section using weighted average for a section across both mid lower center and mid lower side is 0.67.*

***Table* 3.9.4-29**
Comparison of Highest Combined Axial Forces/Moments with the Capacities of the Alternate Front Wall
2 Pages

Component	*Load Comb.*	*Quantity*	*P (Comp)*	*P_1 (Tens)*	*P_2 (Tens.)*	*$M_{1p}^{(1)}$*	*$M_{2p}^{(1)}$*
			kips/ft	*kips/ft*	*kips/ft*	*kip-in/ft*	*kip-in/ft*
3. Front Wall Bottom (54")	*C1 through C6*	*Computed*	*122.3*	*72.2*	*65.6*	*1019.5*	*773.8*
		Capacity	*1014.5*	*123.3*	*102.1*	*1260.1*	*2165.3*
		Ratio	*0.12*	*0.59*	*0.64*	*0.81*	*0.36*
	C7	*Computed*	*59.8*	*19.8*	*0.0*	*485.3*	*0.0*
		Capacity	*916.3*	*116.5*	*96.4*	*2537.9*	*2453.9*
		Ratio	*0.07*	*0.17*	*0.00*	*0.19*	*0.00*
4. Front Wall Top (42")	*C1 through C6*	*Computed*	*58.5*	*97.7*	*33.5*	*737.5*	*788.5*
		Capacity	*968.4*	*150.8*	*124.4*	*2249.7*	*1982.4*
		Ratio	*0.06*	*0.65*	*0.27*	*0.33*	*0.40*
	C7	*Computed*	*18.7*	*22.1*	*31.7*	*1352.7*	*1439.2*
		Capacity	*875.4*	*142.5*	*117.5*	*2045.7*	*1543.4*
		Ratio	*0.02*	*0.15*	*0.27*	*0.66*	*0.93*
4. Front Wall Middle (42")	*C1 through C6*	*Computed*	*256.2*	*94.0*	*77.5*	*721.7*	*1137.7*
		Capacity	*1195.6*	*153.6*	*153.6*	*2337.3*	*1840.9*
		Ratio	*0.21*	*0.61*	*0.50*	*0.31*	*0.62*
	C7	*Computed*	*98.9*	*13.8*	*32.8*	*1326.9*	*1796.9*
		Capacity	*1080.0*	*145.0*	*145.0*	*2209.2*	*2246.2*
		Ratio	*0.09*	*0.09*	*0.23*	*0.60*	*0.80*

***Table* 3.9.4-29**
Comparison of Highest Combined Axial Forces/Moments with the Capacities of the Alternate Front Wall
2 Pages

Component	***Load Comb.***	***Quantity***	***P (Comp)***	***P_1 (Tens)***	***P_2 (Tens.)***	***M_{1p} (1)***	***M_{2p} (1)***
			kips/ft	***kips/ft***	***kips/ft***	***kip-in/ft***	***kip-in/ft***
4. Front Wall Bottom (42")	*C1 through C6*	*Computed*	*66.4*	*77.3*	*33.8*	*450.5*	*177.3*
		Capacity	*1166.2*	*145.8*	*98.4*	*1612.9*	*1422.3*
		Ratio	*0.06*	*0.53*	*0.34*	*0.28*	*0.12*
	C7	*Computed*	*31.9*	*18.8*	*1.0*	*453.5*	*405.9*
		Capacity	*1052.1*	*137.7*	*93.0*	*2566.1*	*1700.6*
		Ratio	*0.03*	*0.14*	*0.01*	*0.18*	*0.24*

Notes:

1 M_{1p} and M_{2p} are moments at the same location and for the same load combination as P_1 and P_2. M_{1p} and M_{2p} occur at the same location simultaneously with P_1 and P_2.

2 C1 through C6 include normal thermal, C7 includes accident thermal

***Table* 3.9.4-29a**
Comparison of Highest Combined Axial Forces/Moments with Capacities of the EOS-HSM-FPS Alternate Front Wall
3 Pages

Component	*Load Comb.*[1]	*Quantity*	P_1 *(Tens.)*	P_2 *(Tens.)*	P_1 *(Comp)*	P_2 *(Comp)*	M_{1p}[2]	M_{2p}[2]
			kips/ft	*kips/ft*	*kips/ft*	*kips/ft*	*kip-in/ft*	*kip-in/ft*
4A. Front Wall Top (42")	*C1 through C6*	*Demand*	*95.9*	*38.0*	*38.6*	*53.3*	*789.0*	*662.5*
		Capacity	*151.2*	*92.1*	*968.5*	*1162.9*	*2077.5*	*1007.5*
		Ratio	*0.63*	*0.41*	*0.04*	*0.05*	*0.38*	*0.66*
	C7	*Demand*	*18.7*	*0.3*	*15.3*	*20.2*	*1353.2*	*101.8*
		Capacity	*142.8*	*87.0*	*875.6*	*1049.0*	*2103.7*	*1521.2*
		Ratio	*0.13*	*0.00*	*0.02*	*0.02*	*0.64*	*0.07*
4B. Front Wall Mid Upper Side (42")	*C1 through C6*	*Demand*	*45.2*	*51.2*	*73.5*	*122.3*	*416.5*	*737.8*
		Capacity	*153.6*	*124.7*	*1089.5*	*1127.2*	*1811.2*	*1319.1*
		Ratio	*0.29*	*0.41*	*0.07*	*0.11*	*0.23*	*0.56*
	C7	*Demand*	*7.8*	*0.0*	*39.1*	*54.6*	*536.1*	*0.0*
		Capacity	*145.0*	*117.8*	*984.5*	*1017.7*	*2344.2*	*2032.2*
		Ratio	*0.05*	*0.00*	*0.04*	*0.05*	*0.23*	*0.00*
4C. Front Wall Mid Upper Center (42")	*C1 through C6*	*Demand*	*97.9*	*17.6*	*56.4*	*29.0*	*763.5*	*252.9*
		Capacity	*153.6*	*70.0*	*1089.5*	*1045.0*	*2185.2*	*981.8*
		Ratio	*0.64*	*0.25*	*0.05*	*0.03*	*0.35*	*0.26*
	C7	*Demand*	*12.6*	*0.1*	*24.1*	*14.2*	*1282.0*	*70.3*
		Capacity	*145.0*	*66.1*	*984.5*	*942.3*	*2209.5*	*1148.3*
		Ratio	*0.09*	*0.00*	*0.02*	*0.02*	*0.58*	*0.06*

***Table* 3.9.4-29a**
Comparison of Highest Combined Axial Forces/Moments with Capacities of the EOS-HSM-FPS Alternate Front Wall
3 Pages

Component	*Load Comb.*[1]	*Quantity*	P_1 *(Tens.)*	P_2 *(Tens.)*	P_1 *(Comp)*	P_2 *(Comp)*	M_{1p}[2]	M_{2p}[2]
			kips/ft	*kips/ft*	*kips/ft*	*kips/ft*	*kip-in/ft*	*kip-in/ft*
4D. Front Wall Mid Lower Side (42")	*C1 through C6*	*Demand*	*98.0*	*76.7*	*68.2*	*98.0*	*619.9*	*420.3*
		Capacity	*153.6*	*110.4*	*1089.5*	*1066.5*	*928.9*	*682.8*
		Ratio	*0.64*	*0.70*	*0.06*	*0.09*	*0.67*	*0.62*
	C7	*Demand*	*20.4*	*17.2*	*33.8*	*68.6*	*275.2*	*895.0*
		Capacity	*145.0*	*104.2*	*984.5*	*962.7*	*2381.6*	*1504.4*
		Ratio	*0.14*	*0.17*	*0.03*	*0.07*	*0.12*	*0.59*
4E. Front Wall Mid Lower Center (42")	*C1 through C6*	*Demand*	*100.0*	*30.2*	*139.2*	*63.6*	*1372.2*	*321.8*
		Capacity	*153.6*	*51.3*	*1089.5*	*1035.1*	*2262.5*	*408.3*
		Ratio	*0.65*	*0.59*	*0.13*	*0.06*	*0.61*	*0.79*
	C7	*Demand*	*2.0*	*0.0*	*61.0*	*34.0*	*323.5*	*0.0*
		Capacity	*145.0*	*48.5*	*984.5*	*932.9*	*2387.0*	*844.3*
		Ratio	*0.01*	*0.00*	*0.06*	*0.04*	*0.14*	*0.00*
4F. Front Wall Mid Center (42")	*C1 through C6*	*Demand*	*38.6*	*98.4*	*57.8*	*232.3*	*270.0*	*997.7*
		Capacity	*153.6*	*153.6*	*1089.5*	*1089.5*	*2185.4*	*1214.7*
		Ratio	*0.25*	*0.64*	*0.05*	*0.21*	*0.12*	*0.82*
	C7	*Demand*	*5.0*	*17.7*	*30.8*	*48.7*	*157.4*	*1635.1*
		Capacity	*145.0*	*145.0*	*984.5*	*984.5*	*2408.1*	*2354.3*
		Ratio	*0.03*	*0.12*	*0.03*	*0.05*	*0.07*	*0.69*

***Table* 3.9.4-29a**
Comparison of Highest Combined Axial Forces/Moments with Capacities of the EOS-HSM-FPS Alternate Front Wall
3 Pages

Component	*Load Comb.*[1]	*Quantity*	P_1 *(Tens.)*	P_2 *(Tens.)*	P_1 *(Comp)*	P_2 *(Comp)*	M_{1p}[2]	M_{2p}[2]
			kips/ft	***kips/ft***	***kips/ft***	***kips/ft***	***kip-in/ft***	***kip-in/ft***
4G. Front Wall Bottom (42")	*C1 through C6*	*Demand*	*40.1*	*60.7*	*35.9*	*87.5*	*327.8*	*236.3*
		Capacity	*153.6*	*92.1*	*1195.6*	*1162.9*	*2684.9*	*883.0*
		Ratio	*0.26*	*0.66*	*0.03*	*0.08*	*0.12*	*0.27*
	C7	*Demand*	*31.0*	*6.4*	*9.5*	*19.5*	*318.6*	*449.9*
		Capacity	*145.0*	*87.0*	*1080.0*	*1049.0*	*2145.7*	*1651.9*
		Ratio	*0.21*	*0.07*	*0.01*	*0.02*	*0.15*	*0.27*

Notes:

1 Load Combinations C1 through C6 include normal thermal, Combination C7 includes accident thermal

2 M_{1p} and M_{2p} are moments at the same location and for the same load combination as P_1 and P_2. M_{1p} and M_{2p} occur at the same location simultaneously with P_1 and P_2, i.e. $M_1 = [(P_{tu} - P_1)/P_{tu}]*M_{u1}$

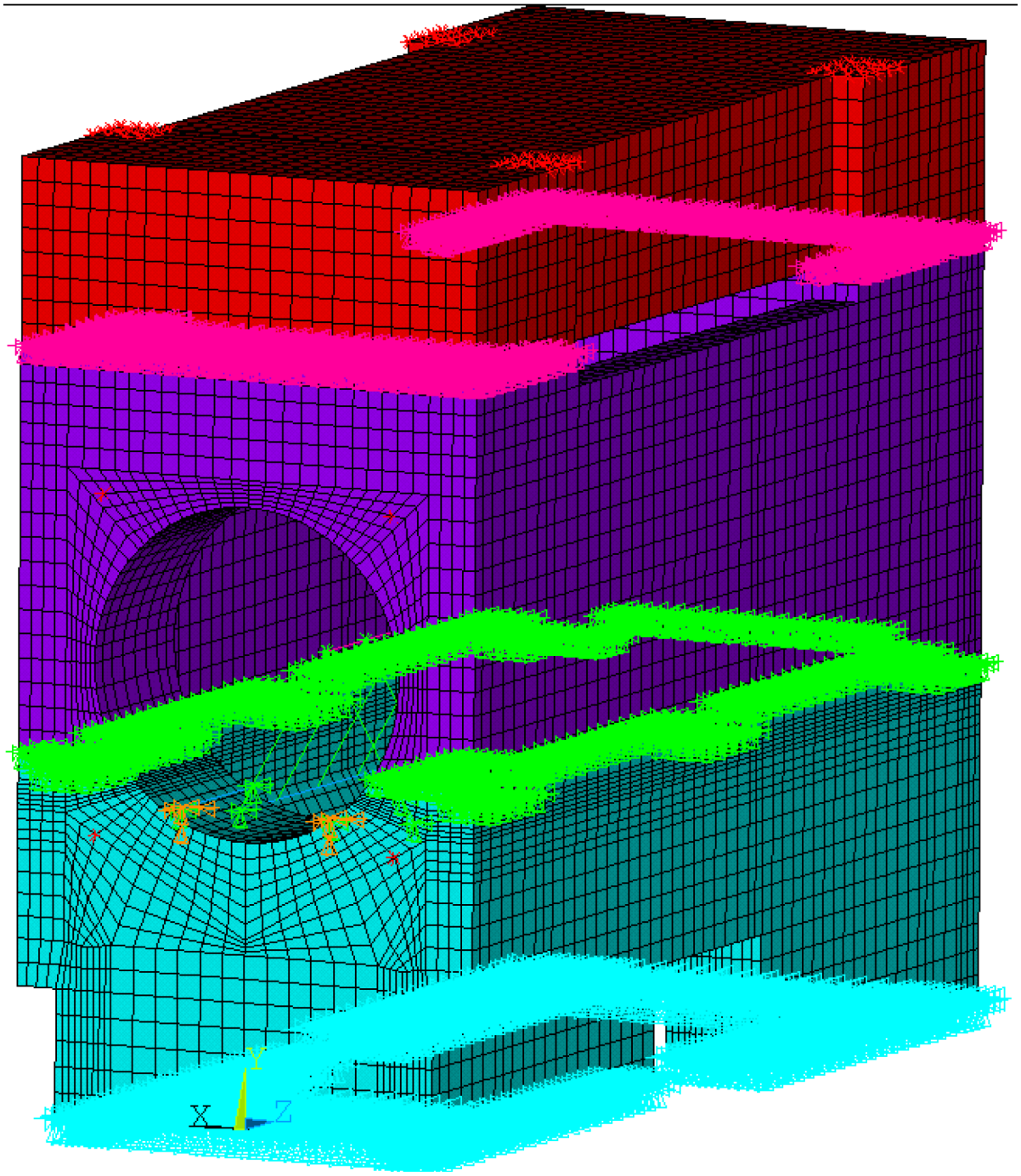

Figure 3.9.4-1
Analytical Model of EOS-HSM for Mechanical Load Analysis

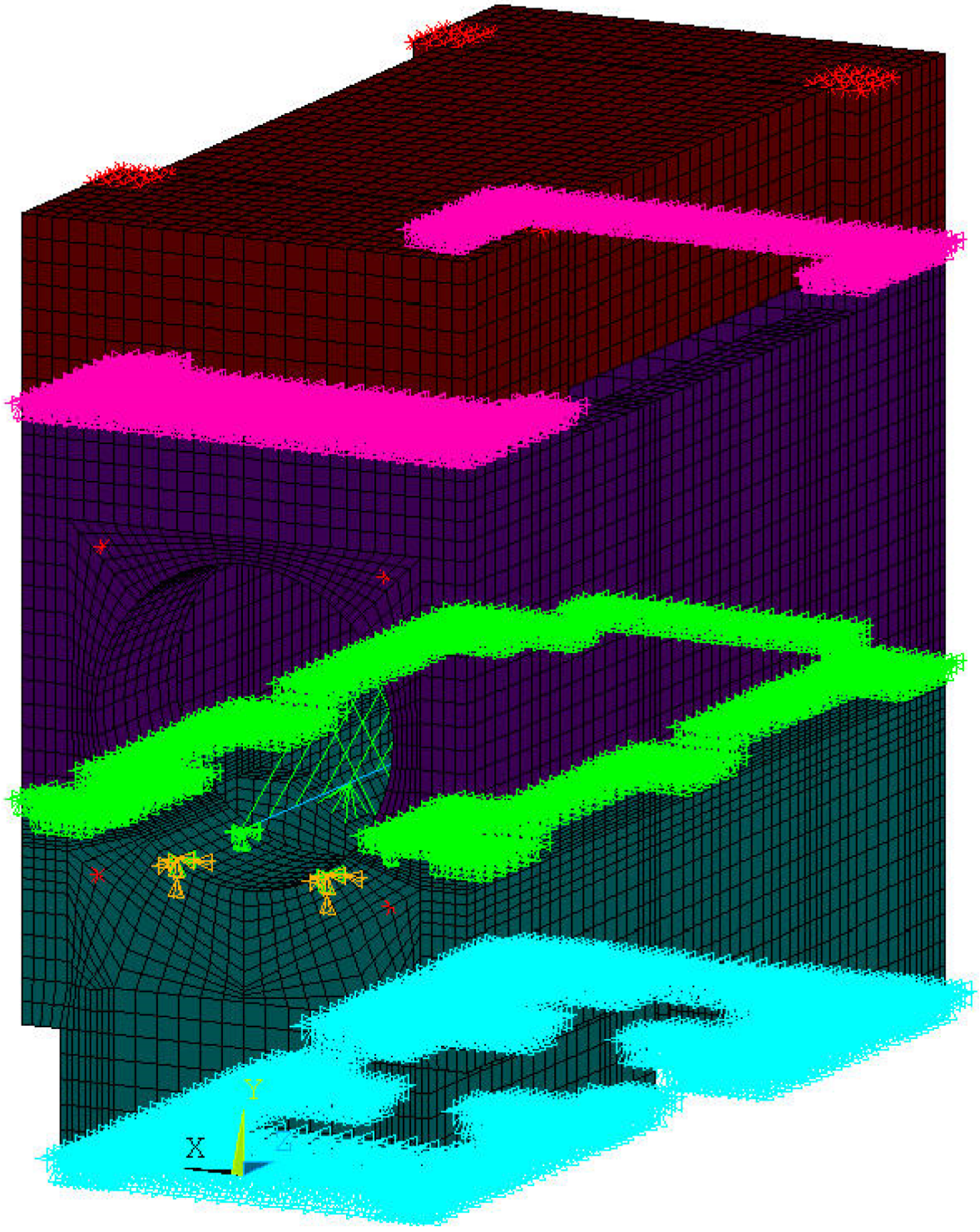

Figure 3.9.4-1a
Analytical Model of EOS-HSM-FPS for Mechanical Load Analysis

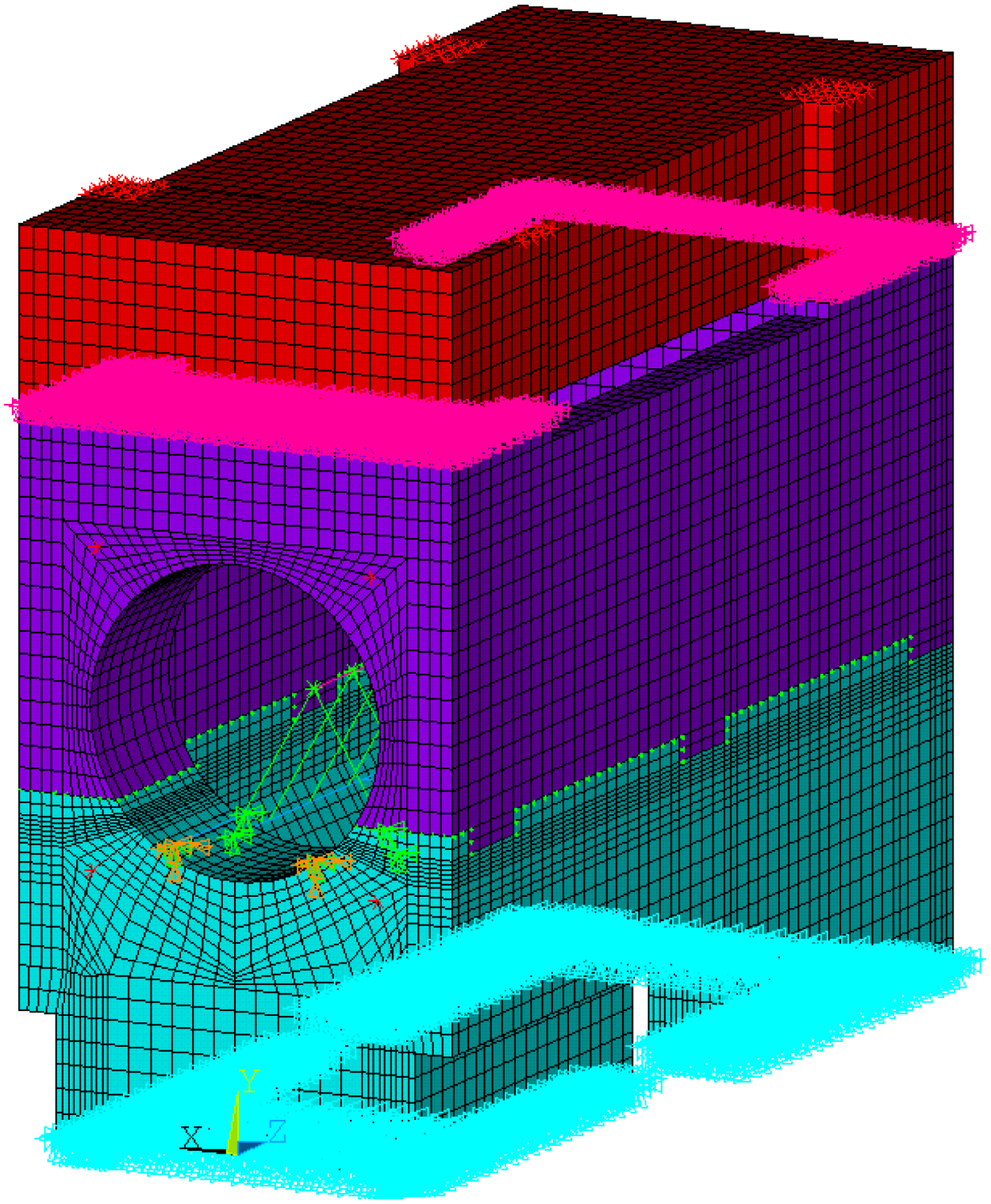

Figure 3.9.4-2
Analytical Model of EOS-HSMS for Mechanical Load Analysis
(Node to Node Contact at Segment Joint interface)

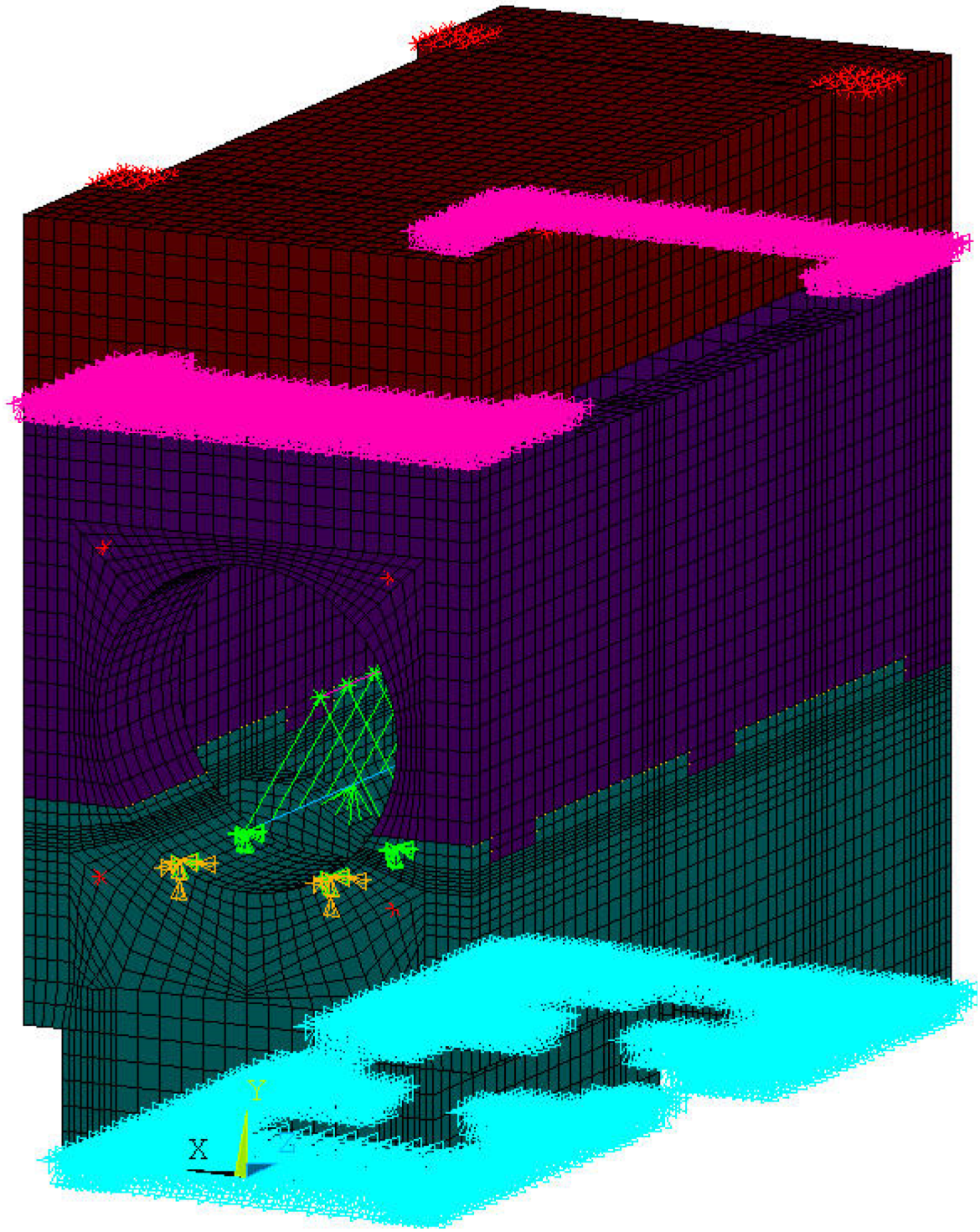

Figure 3.9.4-2a
Analytical Model of EOS-HSMS-FPS for Mechanical Load Analysis
(Node to Node Contact at Segment Joint Interface)

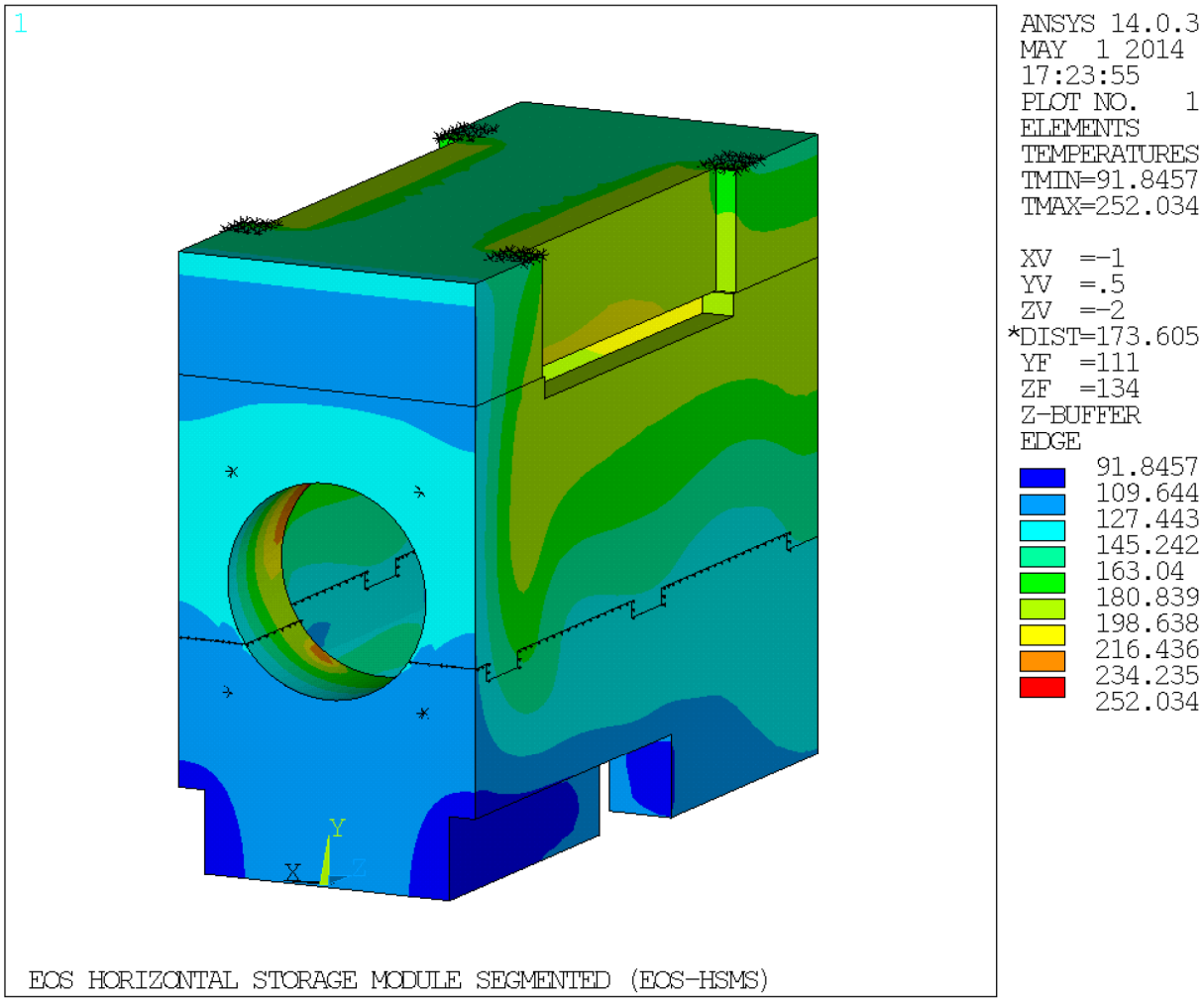

Figure 3.9.4-3
Temperature distribution of EOS-HSMS for Normal Thermal Hot Condition

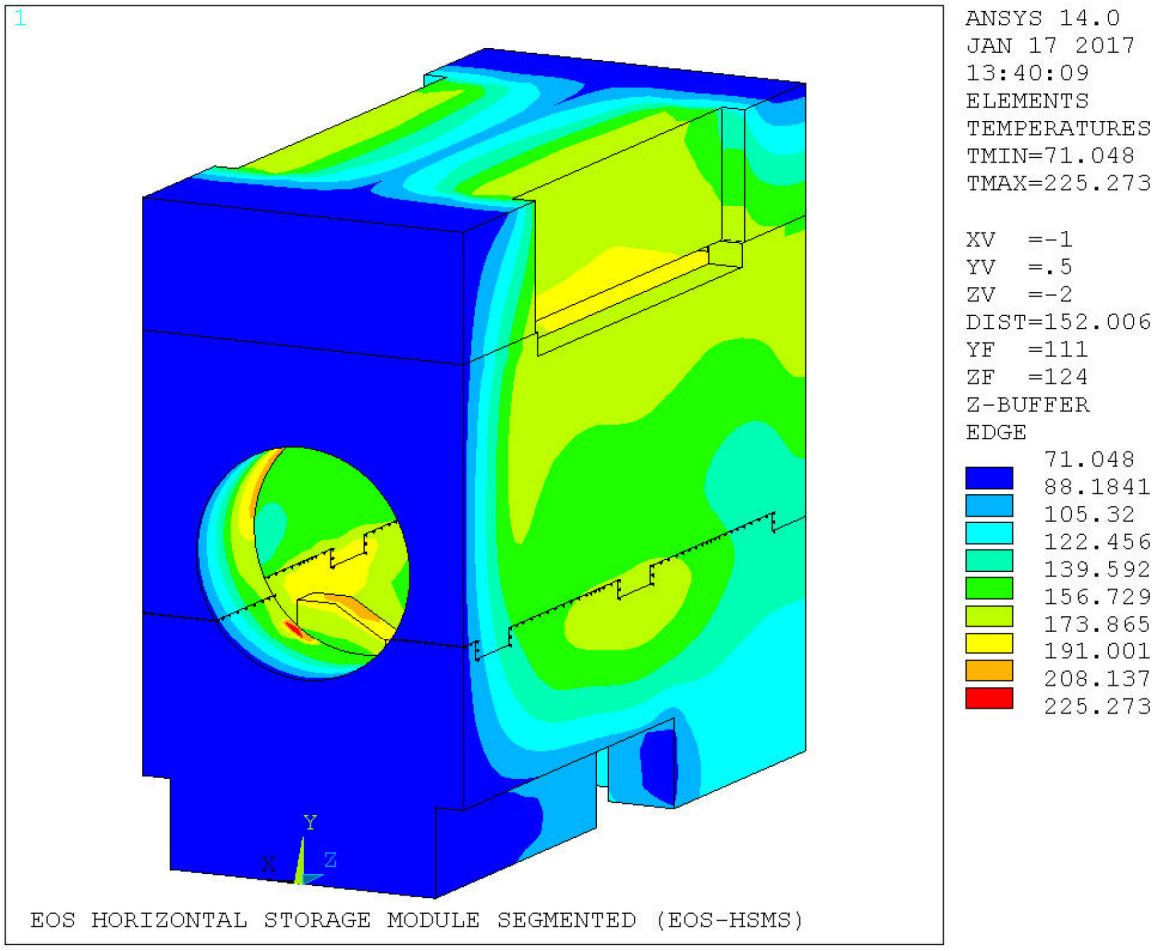

Figure 3.9.4-3a
Temperature distribution of EOS-HSMS-FPS for Normal Thermal Hot Condition

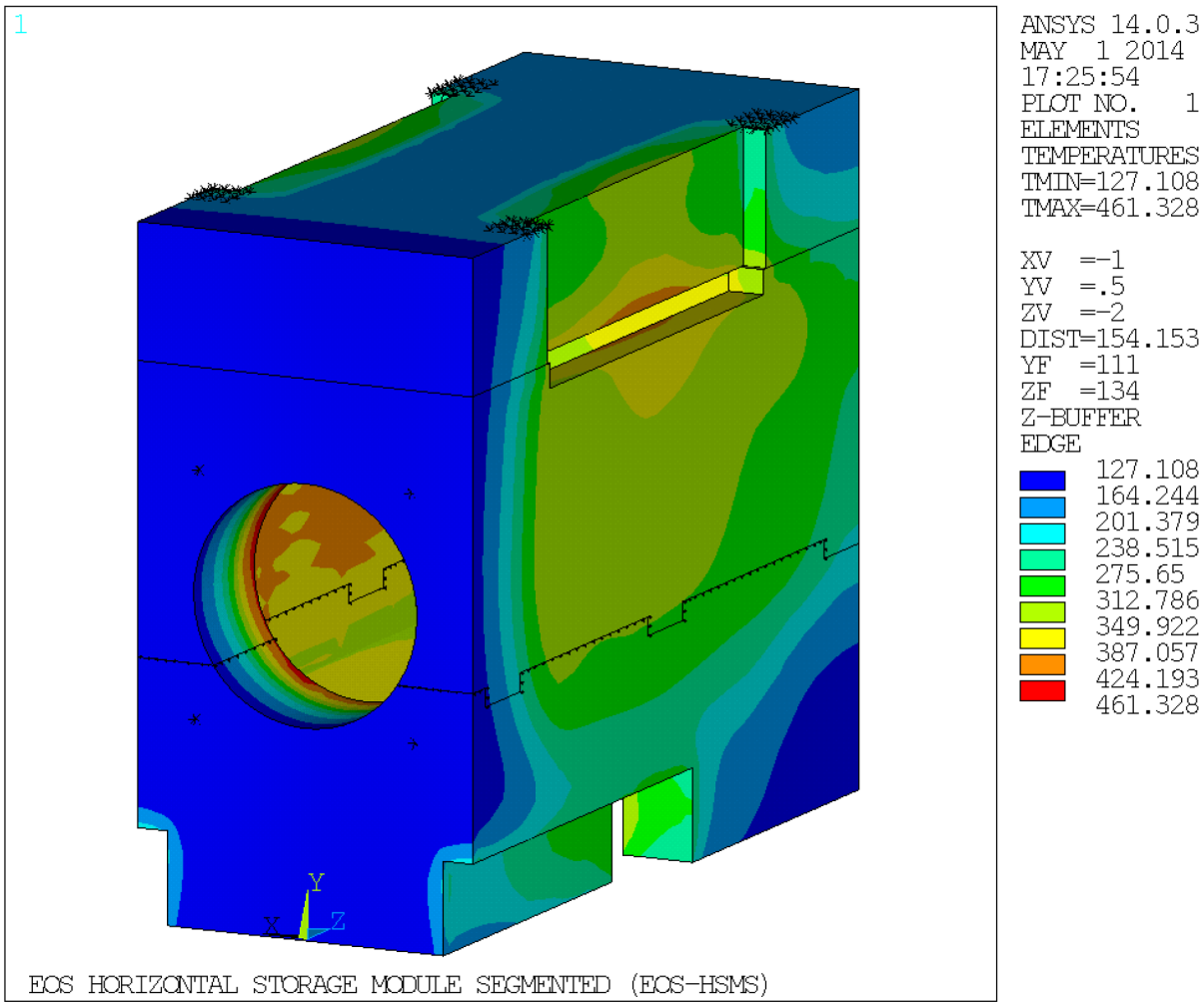

Figure 3.9.4-4
Temperature distribution of EOS-HSMS for Blocked Vent Accident Thermal Condition

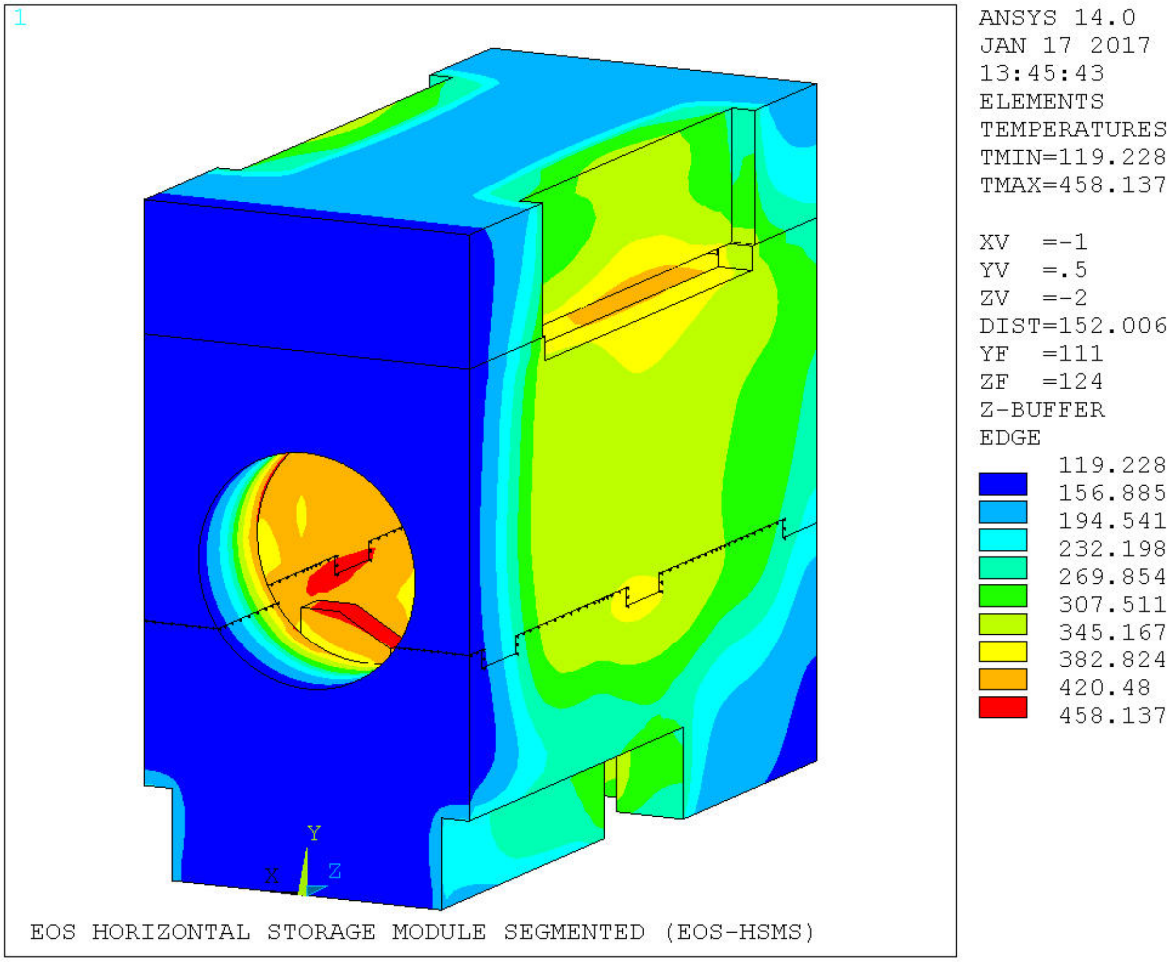

Figure 3.9.4-4a
Temperature distribution of EOS-HSMS-FPS for Blocked Vent Accident Thermal Condition

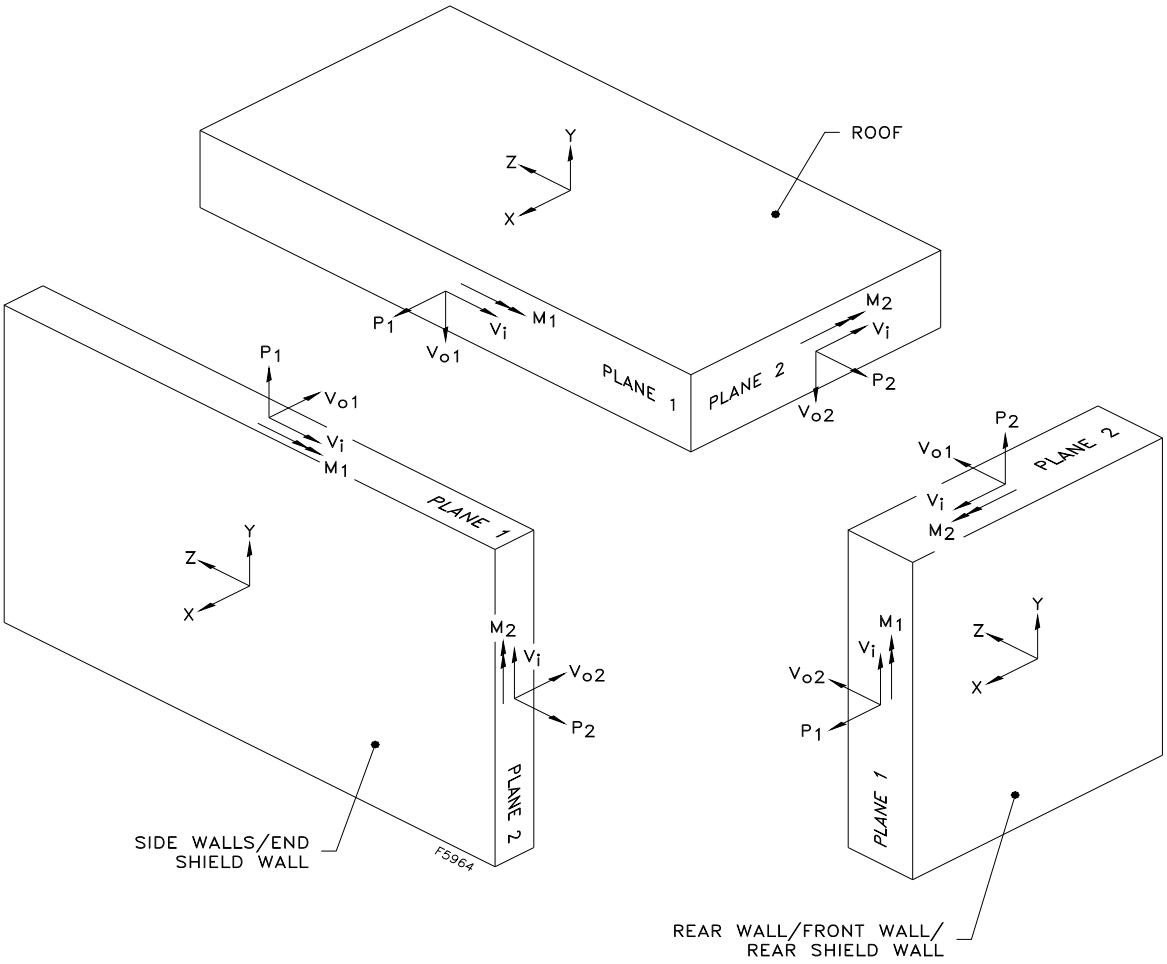

Figure 3.9.4-5
Symbolic Notation of Forces and Moments of EOS-HSM Concrete Components

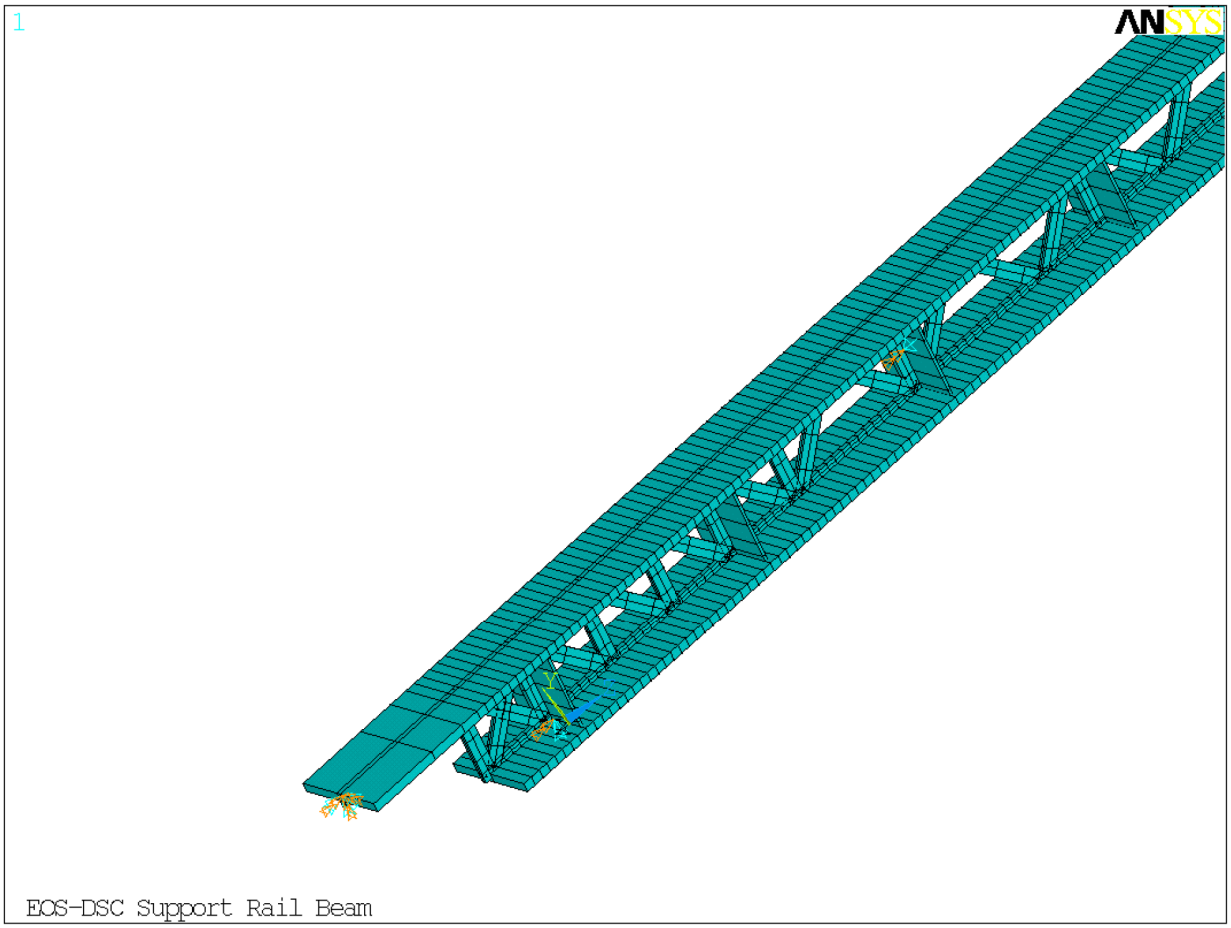

Figure 3.9.4-6
Analytical Model of the W12x136 DSC Main Support Beam with Stiffeners and Open Web

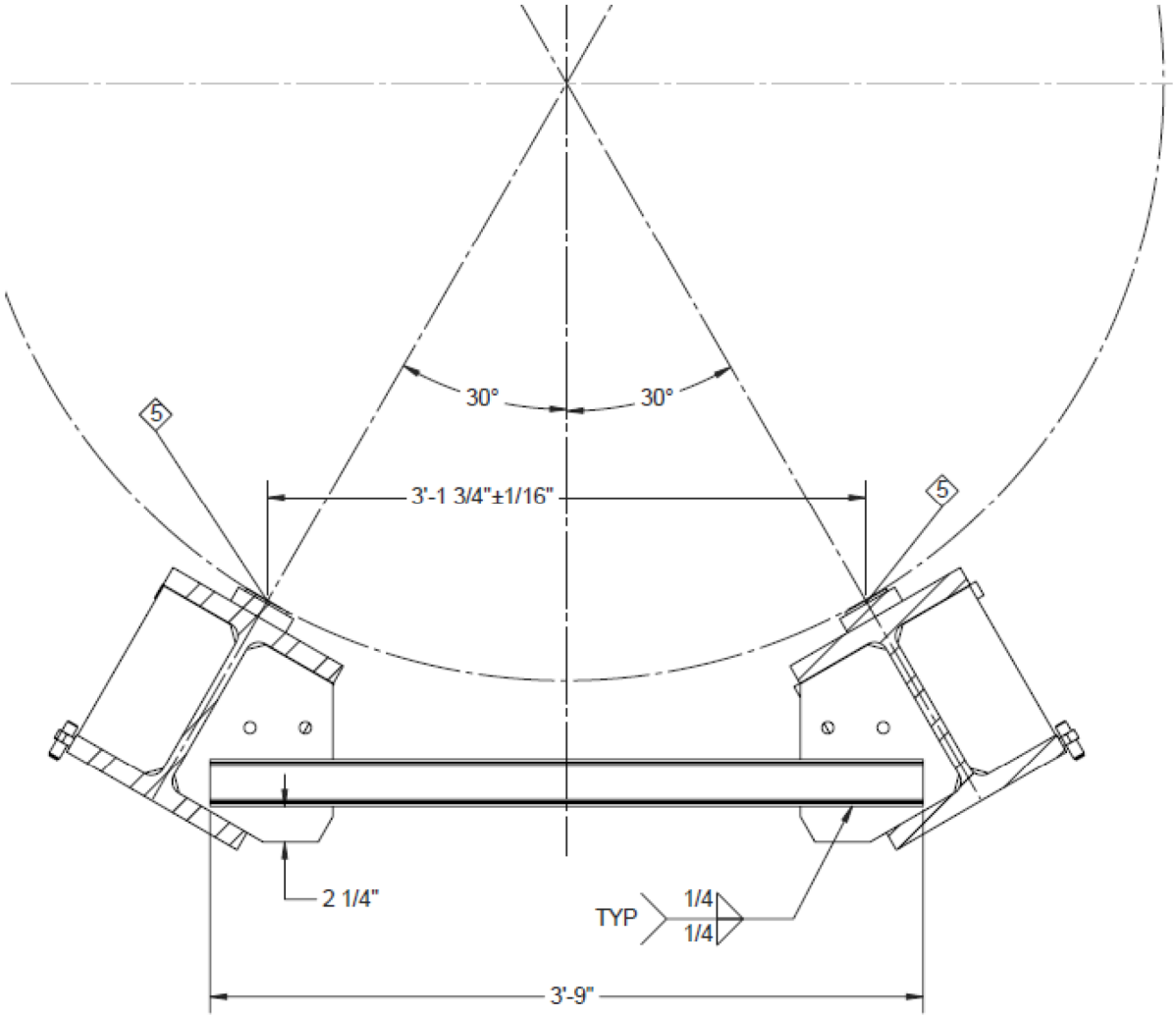

Figure 3.9.4-7
Components of DSC Support Structure

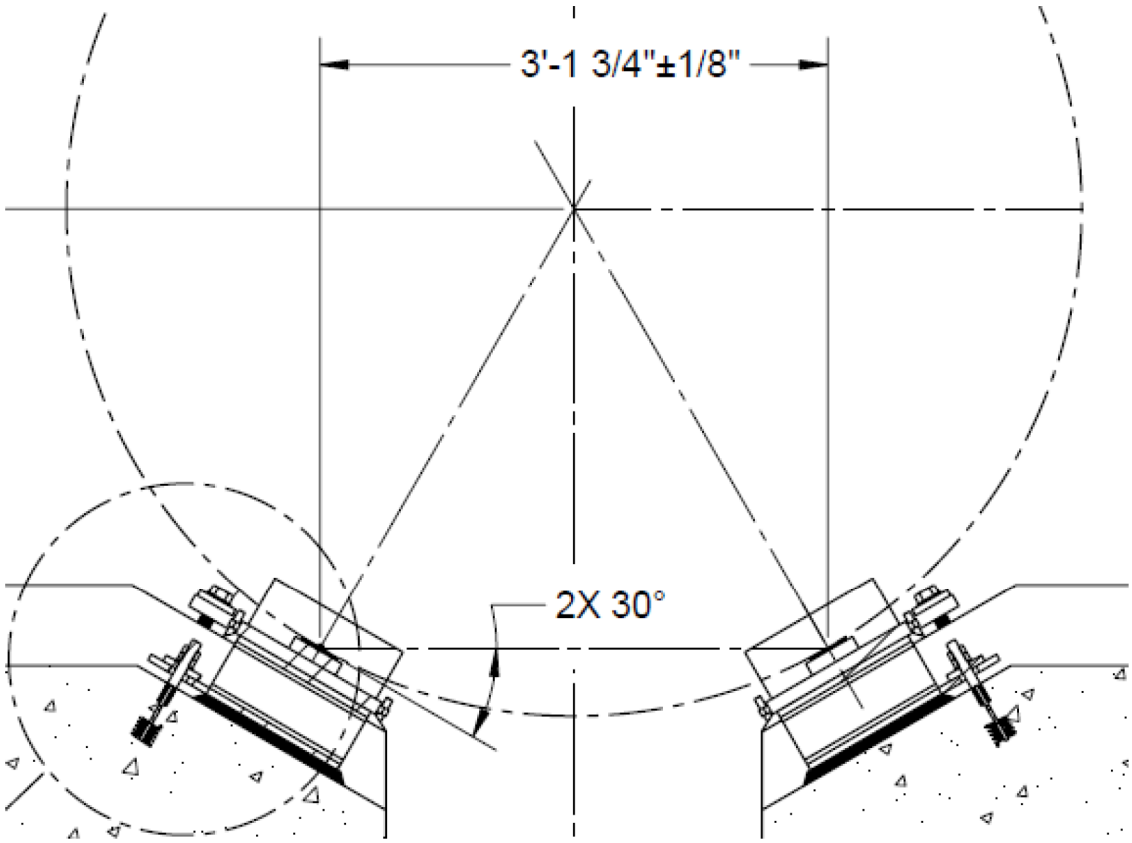

Figure 3.9.4-7a
Components of FPS DSC Support Structure

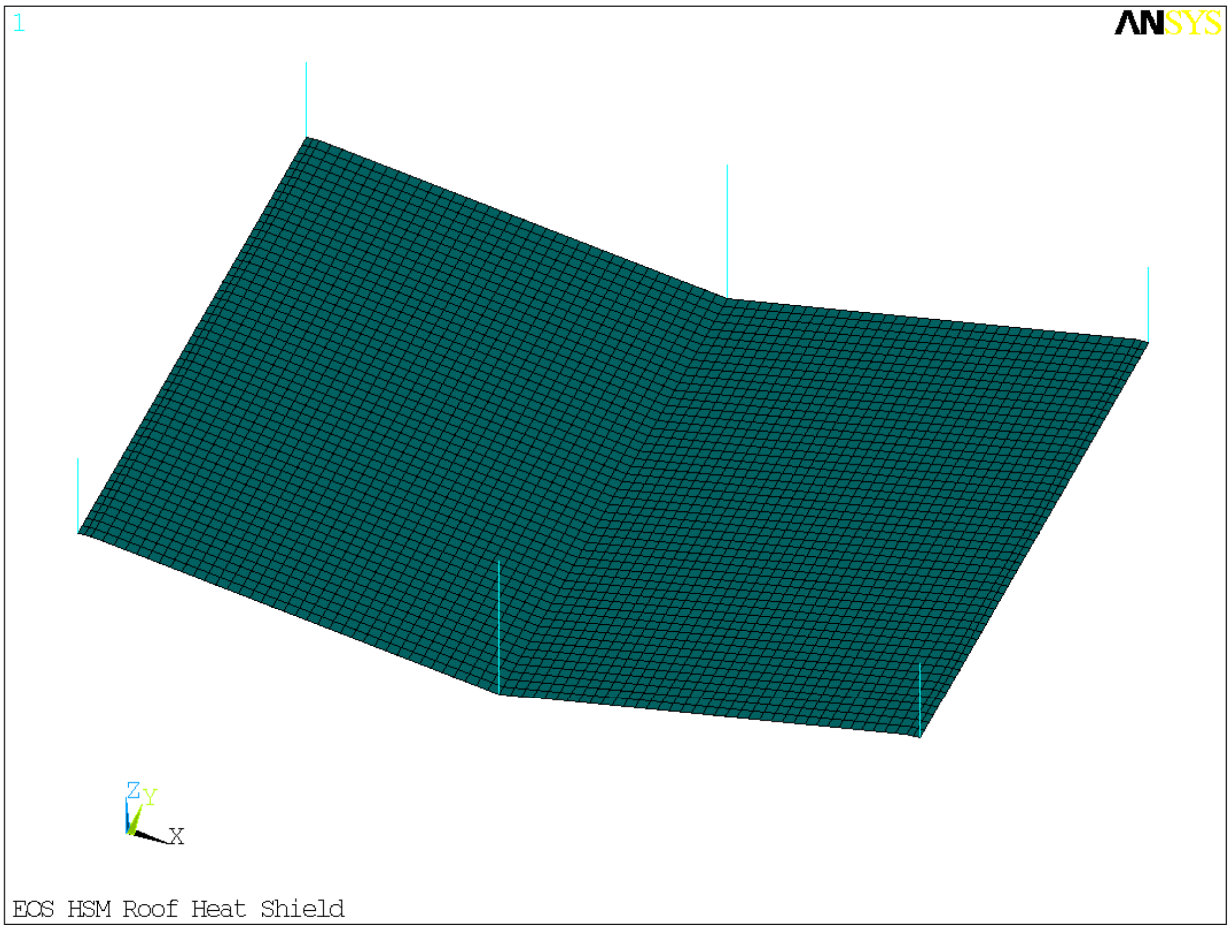

Figure 3.9.4-8
Analytical Model of Coupled Roof Heat Shield and Connection Studs

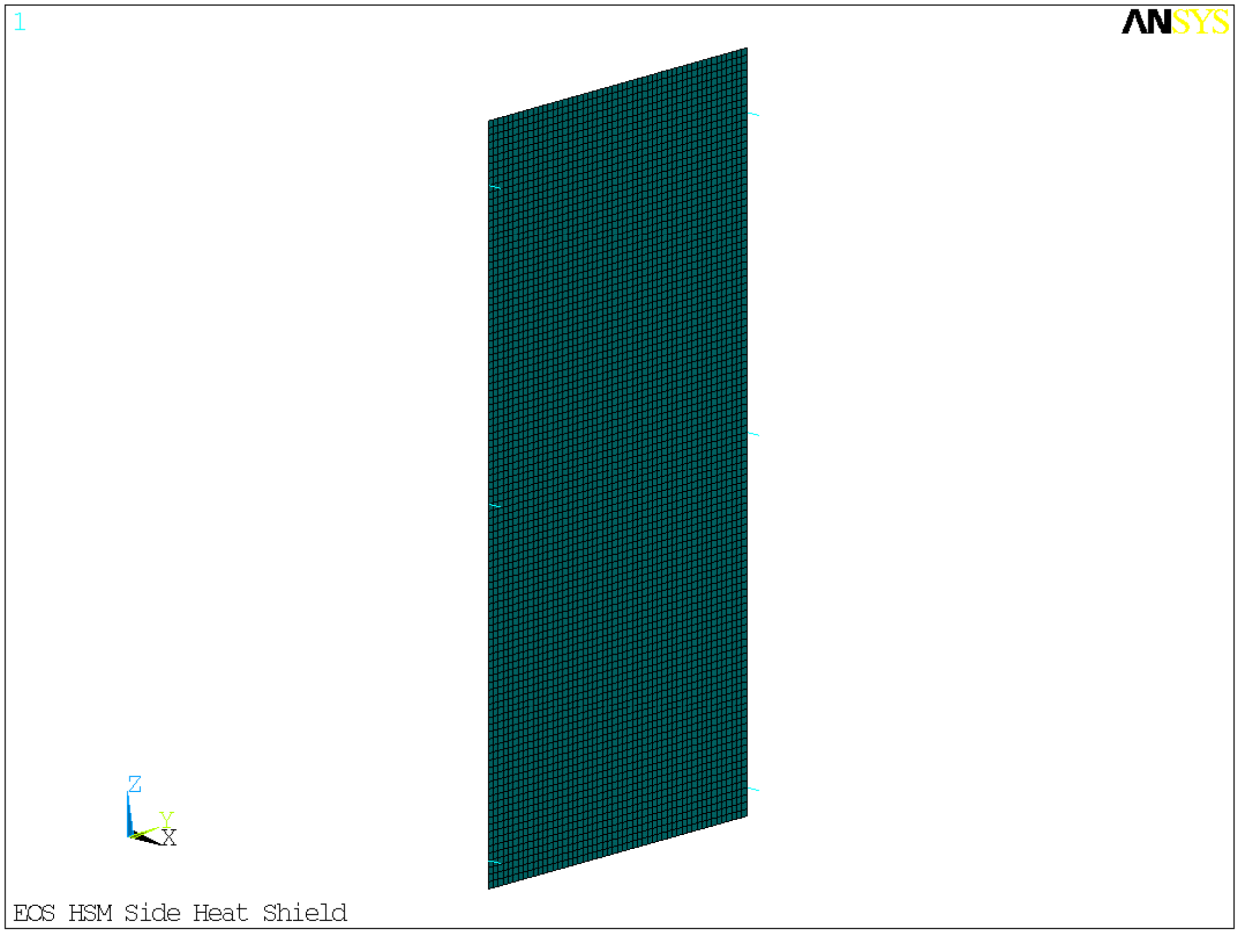

Figure 3.9.4-9
Analytical Model of Coupled Side Heat Shield and Connection Studs

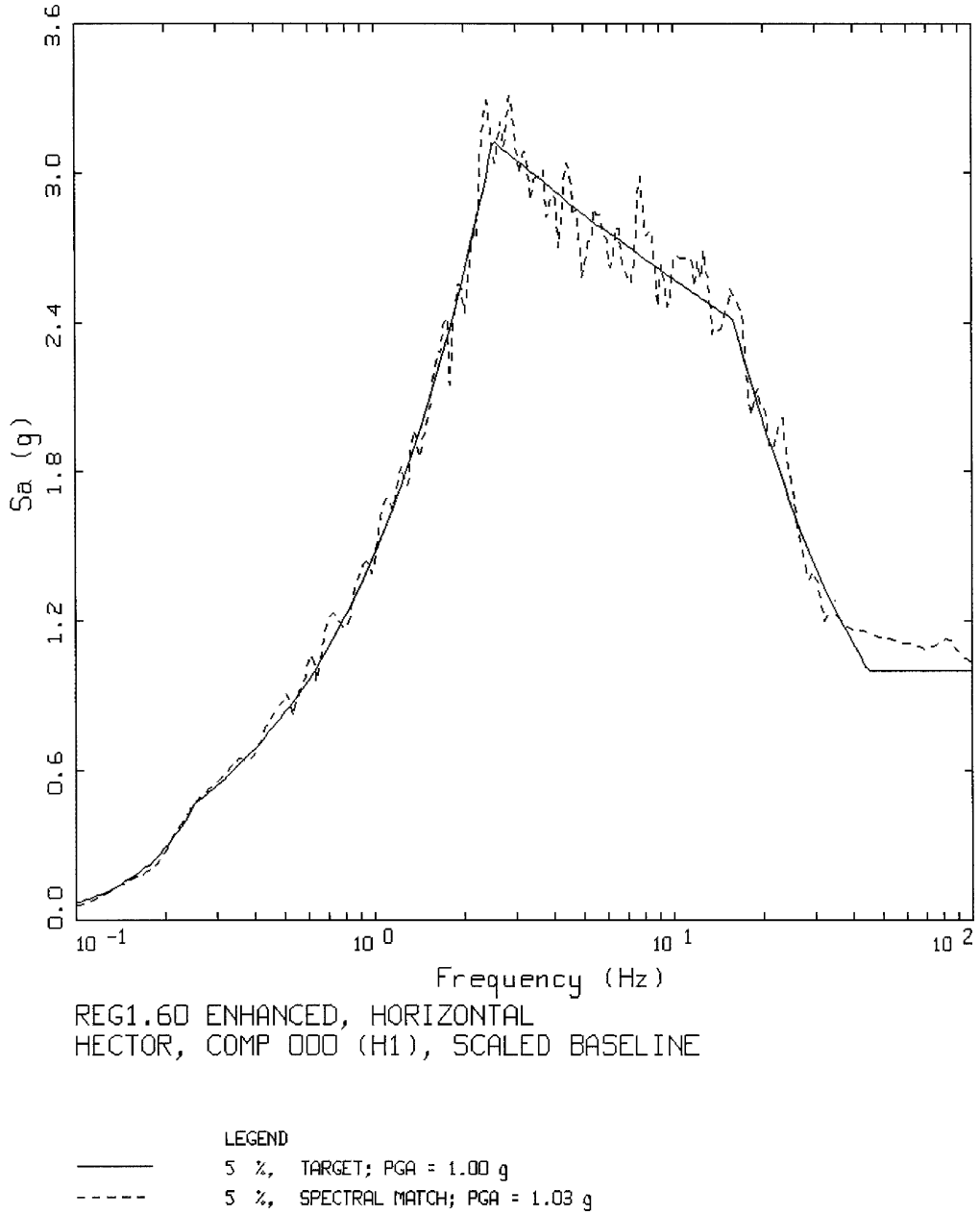

Figure 3.9.4-10
Horizontal Target and 5% Spectral Match (Horizontal 1, Hector Mine Earthquake)

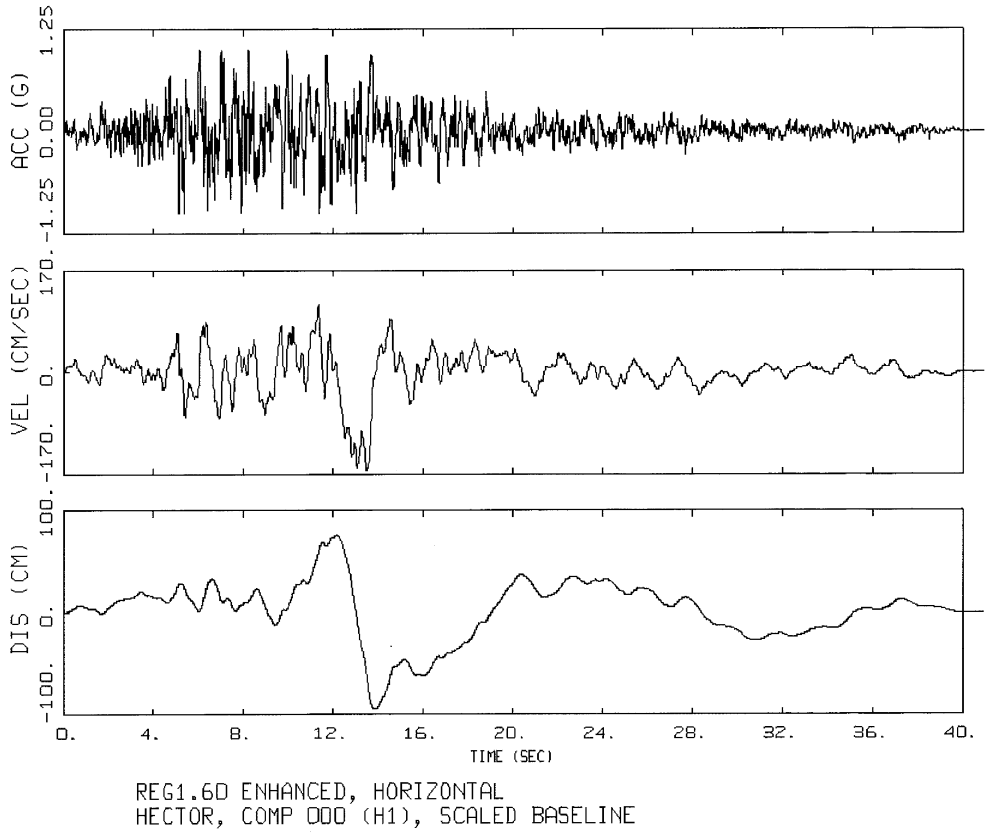

Figure 3.9.4-11
Baseline Corrected Acceleration, Velocity and Displacement Time Histories
(Horizontal 1, Hector Mine Earthquake)

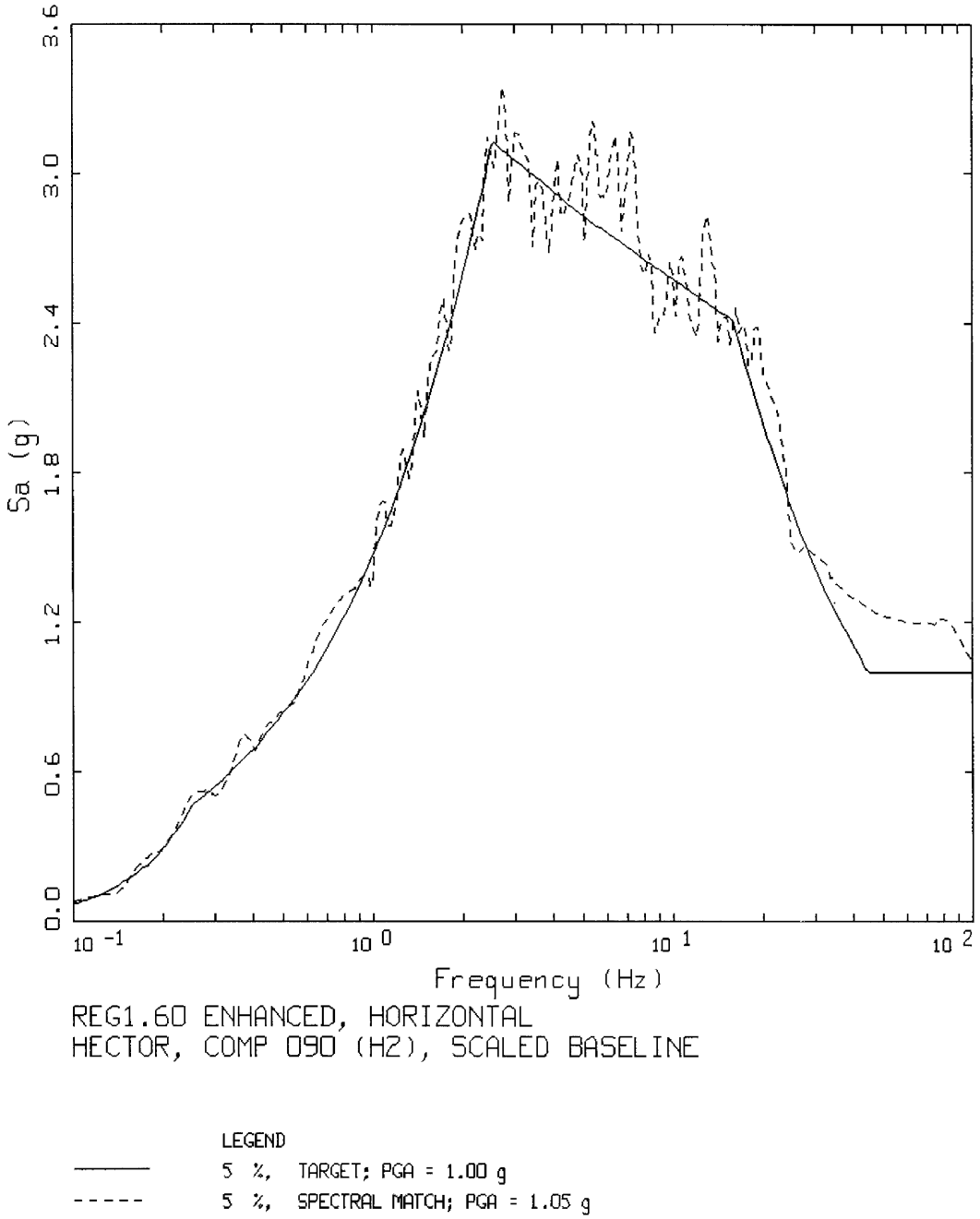

Figure 3.9.4-12
Horizontal Target and 5% Spectral Match (Horizontal 2, Hector Mine Earthquake)

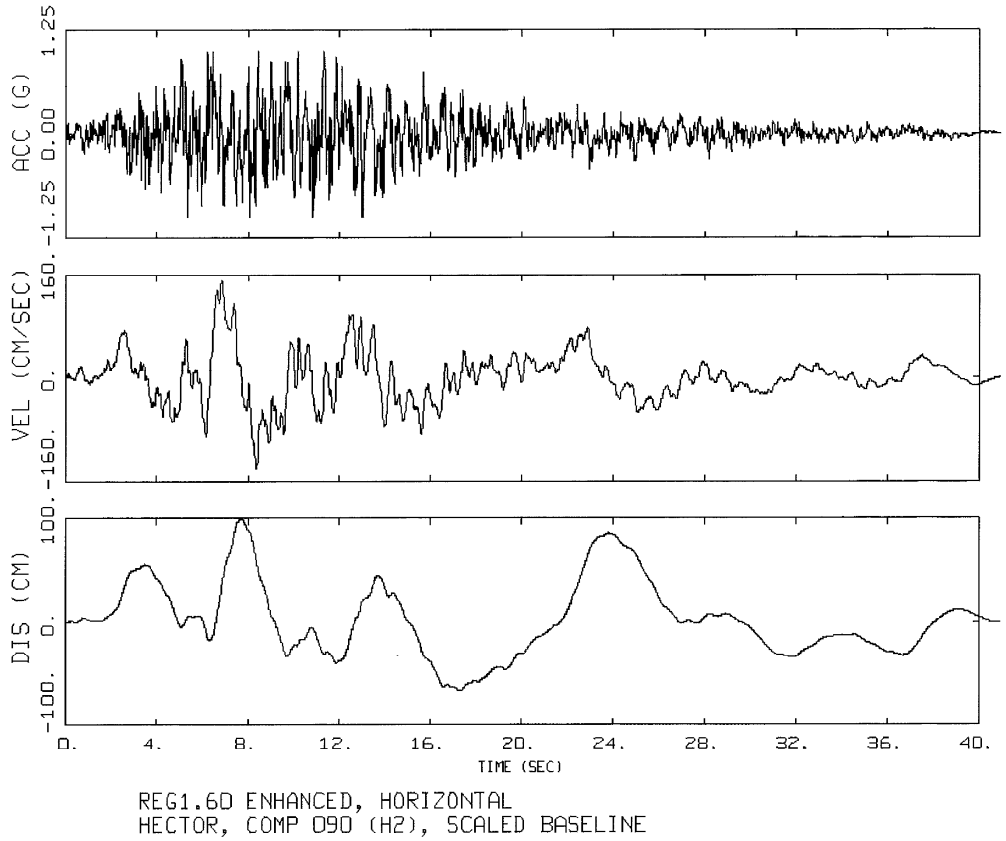

Figure 3.9.4-13
Baseline Corrected Acceleration, Velocity and Displacement Time Histories
(Horizontal 2, Hector Mine Earthquake)

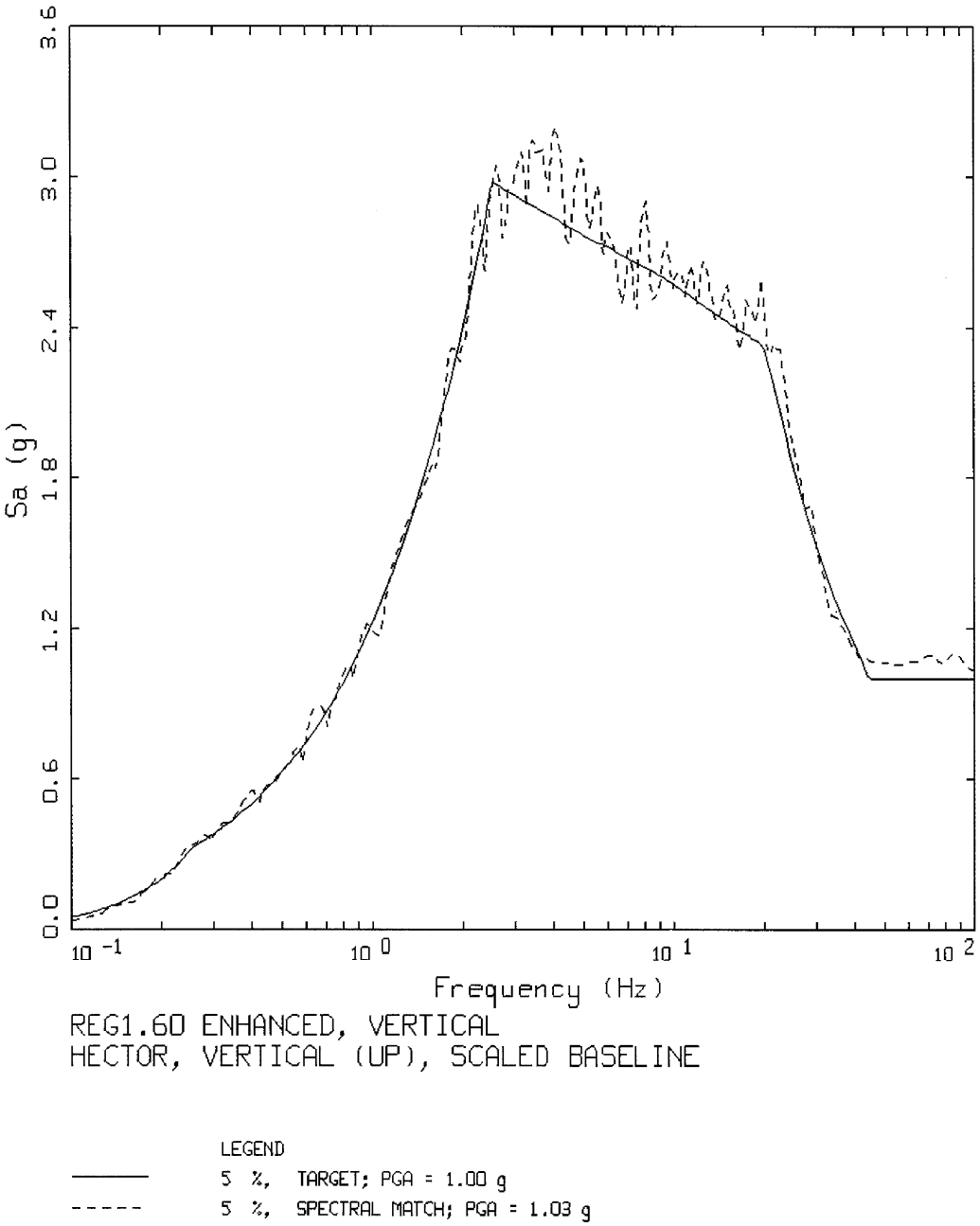

Figure 3.9.4-14
Vertical Target and 5% Spectral Match (Vertical Up, Hector Mine Earthquake)

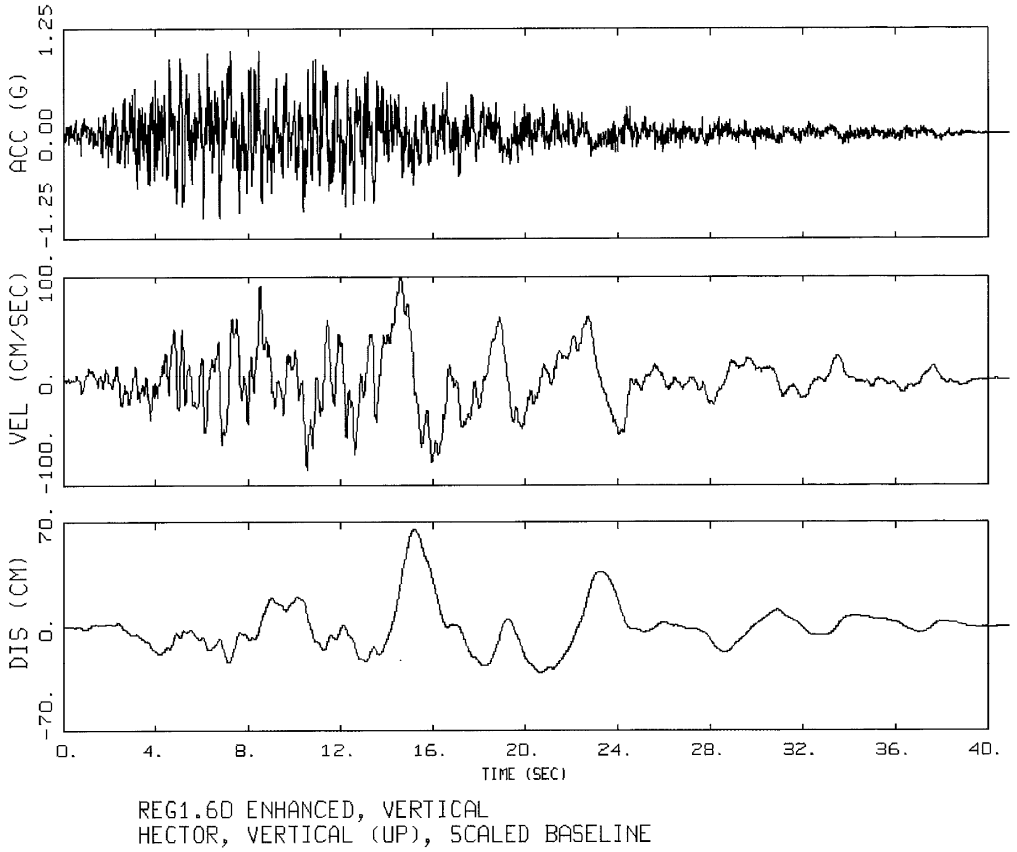

Figure 3.9.4-15
Baseline Corrected Acceleration, Velocity and Displacement Time Histories
(Vertical Up, Hector Mine Earthquake)

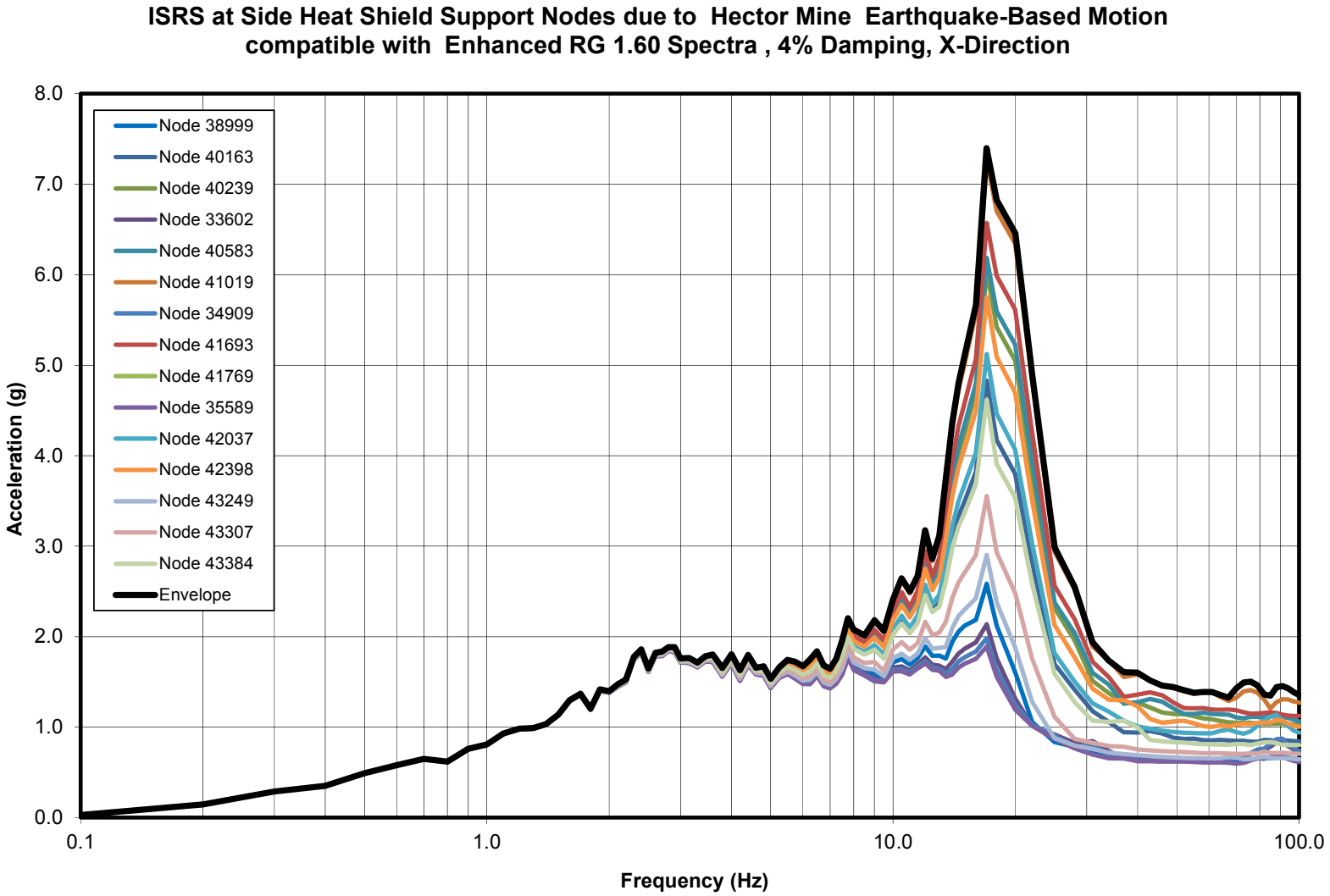

Figure 3.9.4-16
ISRS at Side Heat Shield Support Nodes due to Hector Mine Earthquake-Based Motion compatible with Enhanced RG 1.60 Spectra, 4% Damping, X-Direction

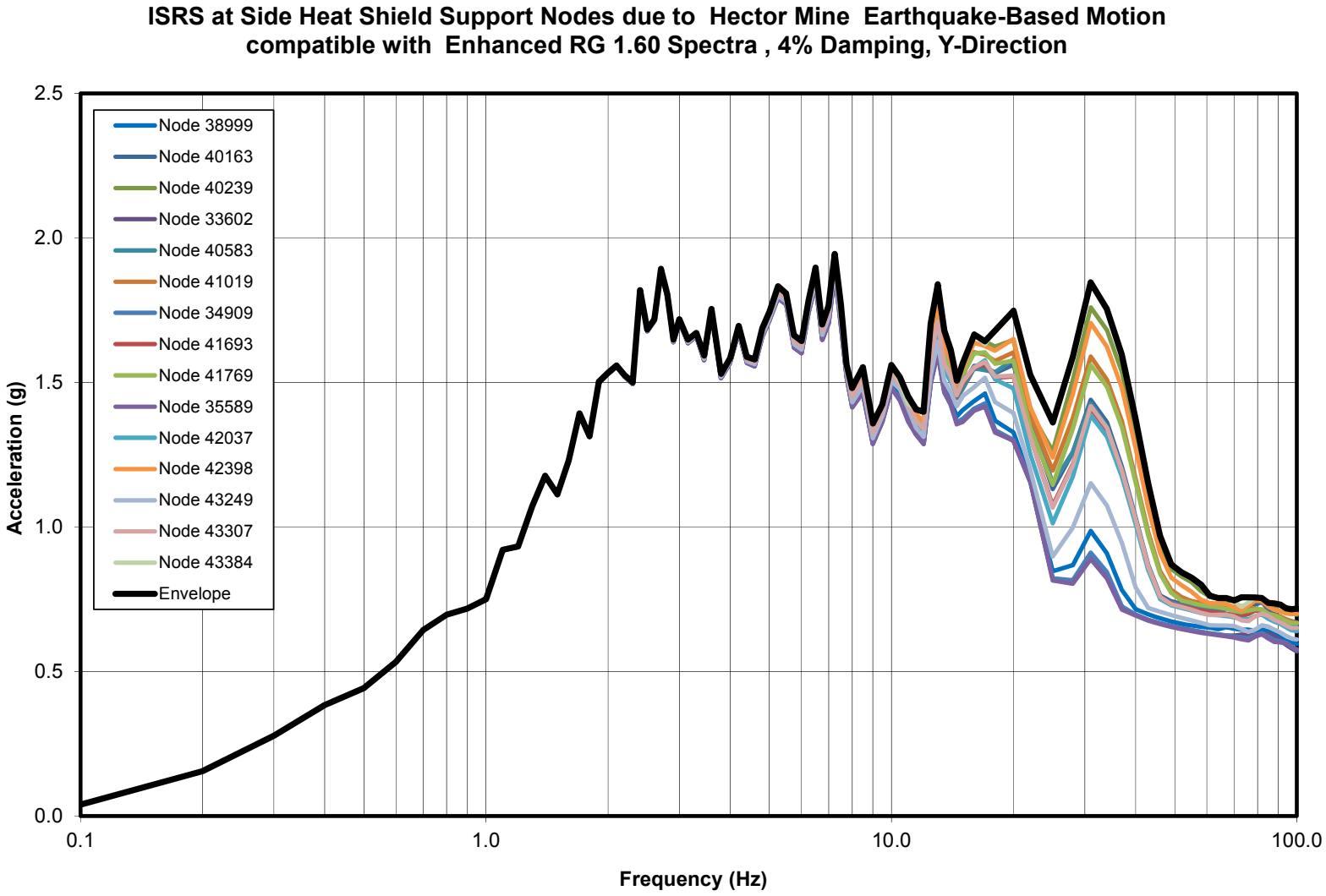

Figure 3.9.4-17
ISRS at Side Heat Shield Support Nodes due to Hector Mine Earthquake-Based Motion compatible with Enhanced RG 1.60 Spectra, 4% Damping, Y-Direction

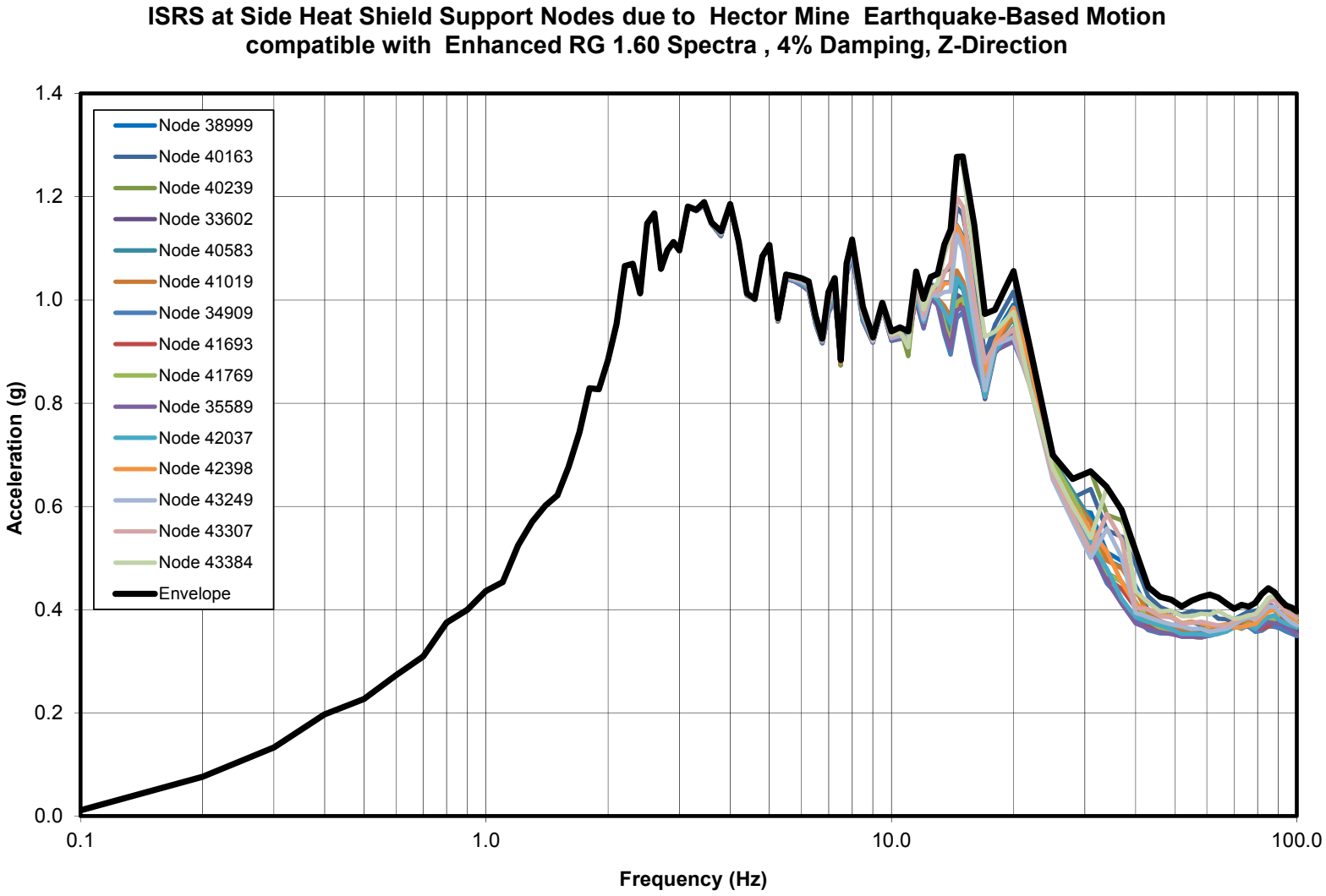

Figure 3.9.4-18
ISRS at Side Heat Shield Support Nodes due to Hector Mine Earthquake-Based Motion compatible with Enhanced RG 1.60 Spectra, 4% Damping, Z-Direction

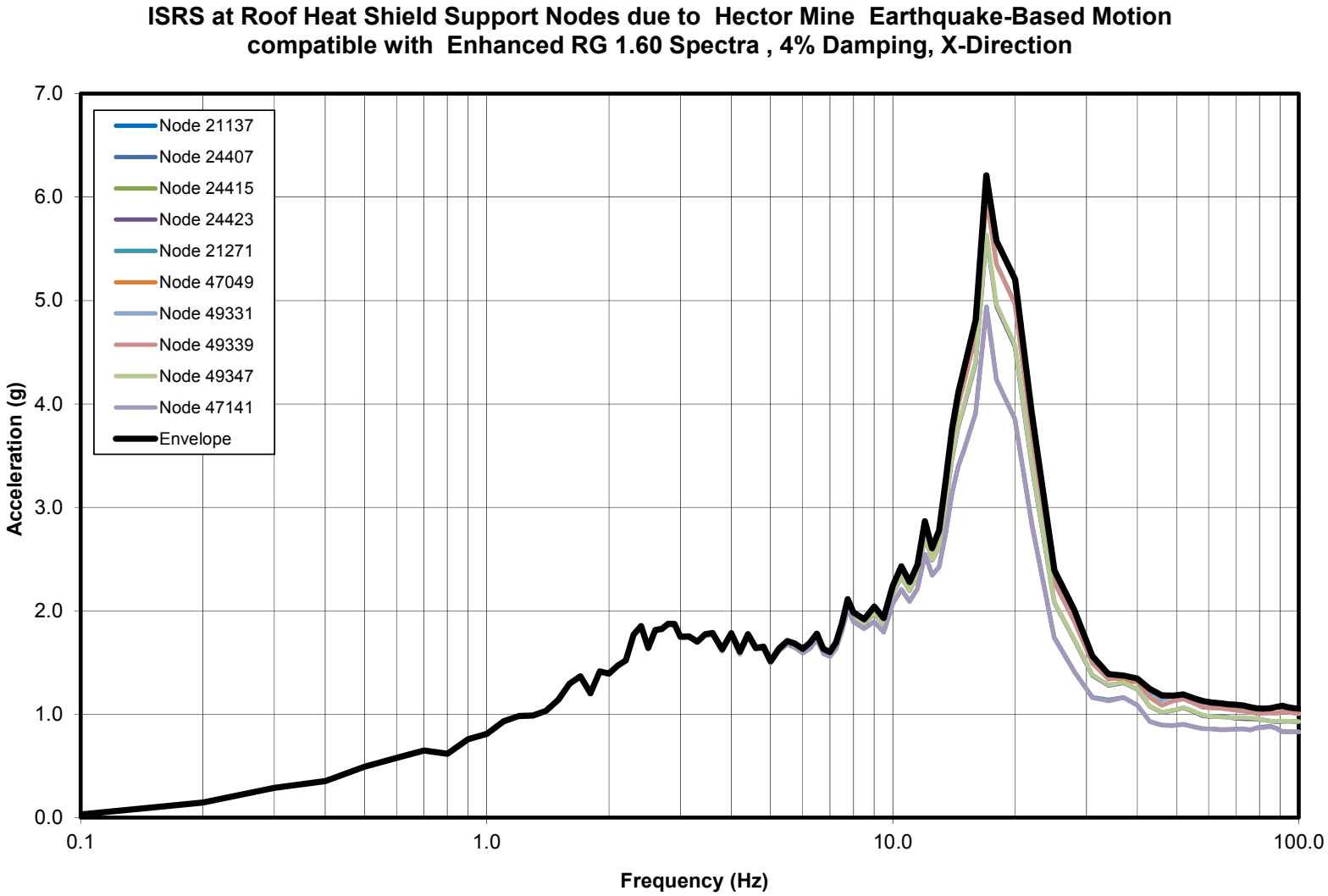

Figure 3.9.4-19
ISRS at Roof Heat Shield Support Nodes due to Hector Mine Earthquake-Based Motion compatible with Enhanced RG 1.60 Spectra, 4% Damping, X-Direction

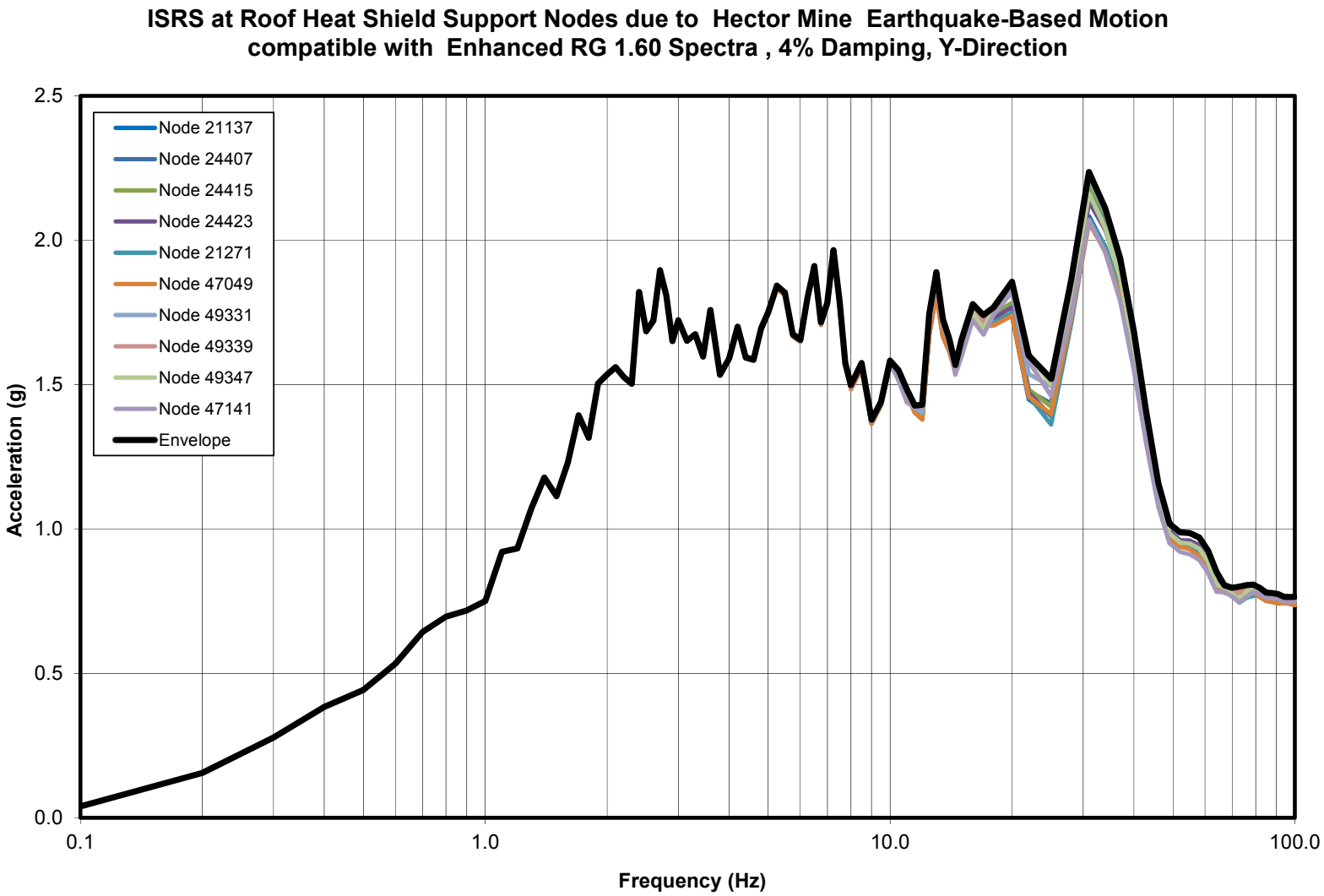

Figure 3.9.4-20
ISRS at Roof Heat Shield Support Nodes due to Hector Mine Earthquake-Based Motion compatible with Enhanced RG 1.60 Spectra, 4% Damping, Y-Direction

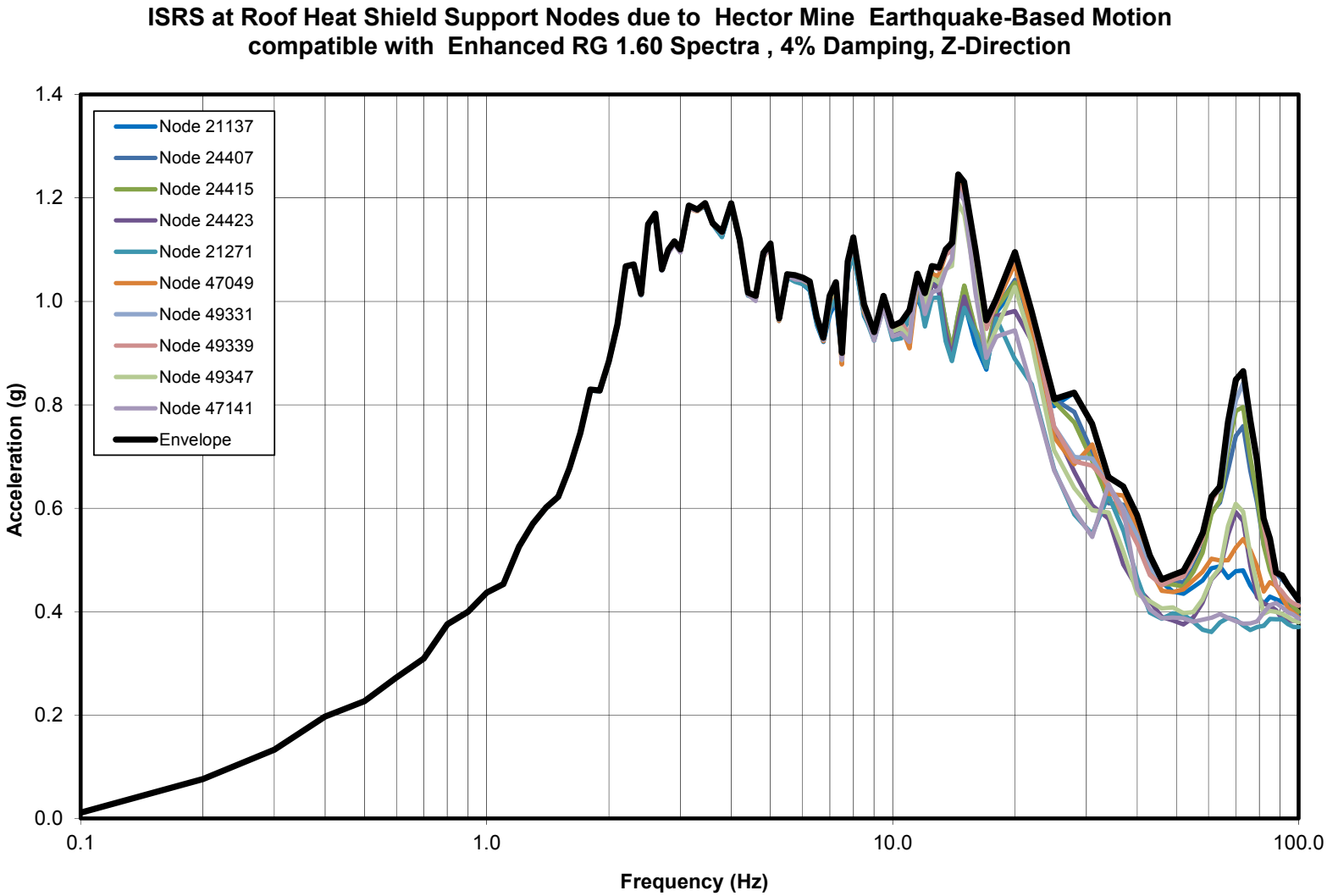

Figure 3.9.4-21
ISRS at Roof Heat Shield Support Nodes due to Hector Mine Earthquake-Based Motion compatible with Enhanced RG 1.60 Spectra, 4% Damping, Z-Direction

APPENDIX 3.9.5
NUHOMS® EOS-TC BODY STRUCTURAL ANALYSIS

Table of Contents

List of Tables

List of Figures

3.9.5 NUHOMS® EOS-TC BODY STRUCTURAL ANALYSIS

3.9.5.1 General Information

This appendix covers the structural evaluation of the transfer cask (TC) when carrying a loaded DSC. The TC structure is designed to American Society of Mechanical Engineers (ASME) NF-3200 [3.9.5-3] stress limits to the greatest degree practical. The trunnions and trunnion welds to the TC top ring are designed to American National Standards Institute (ANSI) N14.6 [3.9.5-2] stress limits for non-redundant lifting. Structural evaluation of the TC for the missile impact load cases is covered in Appendix 3.9.7, and not presented in this Appendix.

A geometric- and load-bounding representation, enveloping the three EOS-TCs (EOS-TC108, EOS-TC125 and EOS-TC135), is referred to as EOS-TCMAX in this evaluation. The geometric dimensions for this bounding model are selected to yield the most bounding stresses and deformations.

3.9.5.2 EOS Transfer Cask Accident (Side and End) Drop Evaluation for 65g Static Load

The purpose of this section is to summarize the structural evaluation of the EOS-TC for the postulated accident side and end drop conditions. The Service Level D drop evaluations are done by means of 3-D elastic-plastic model. Structural integrity of the design is evaluated by means of plastic analysis criteria of Reference [3.9.5-3].

3.9.5.2.1 Material Properties

Mechanical properties of cask components are evaluated at a temperature of 400 °F, except for the trunnions, which are evaluated at 367 °F. These temperatures exceed the maximum temperature of cask body for all cask designs. A bilinear stress-strain curve with a 5% tangent modulus is used for steel components. The lead material is modeled by bilinear kinematic hardening method. All the EOS-TC material properties are listed in Chapter 8.

3.9.5.2.2 Design Criteria

The EOS-TC is analyzed using ASME code, Section III, Appendix F requirements service level D allowable stresses for plastic analysis.

3.9.5.2.3 Methodology

ANSYS [3.9.5-4] is used for the evaluation of side and end drop loads. A static load of 65g is applied and a plastic evaluation is performed for the postulated accident drop loads and compared against the Level D stress allowables.

A 65g drop load is considered bounding for the cask design in the accident conditions. Combination of side and end drop are considered bounding for the corner drop, since the corner accidents decelerations are significantly below 65g magnitude.

3.9.5.2.3.1 Finite Element Model

A 3D half symmetric model is used to perform accident drop evaluations. ANSYS SOLID185 elements were used to model the EOS-TC components. ANSYS Surface to Surface contact CONTA173 were used to model the contacting surface. Top cover bolts were modeled using COMBIN39 spring elements. Welds are modeled by means of nodal couples in all three directions. The finite element model is shown in Figure 3.9.5-1.

3.9.5.2.3.2 Loads and Boundary Conditions

For the side drop evaluation the DSC weight is specified using a cosine distributed pressure load for an angle span of 90°. Symmetry boundary conditions are applied on the cut plane. On the impact side the EOS-TC structural shell is fixed for a small 15° arc in radial direction and over total length. The applied pressure load and the boundary conditions are shown in Figure 3.9.5-2.

For the end drop evaluation the DSC weight is uniformly distributed on the lid/inner bottom end plate. Symmetry boundary conditions are applied on the cut plane. The cask is supported at the impacting surface for the top and bottom end drop. The applied pressure load and the boundary conditions are shown in Figure 3.9.5-3.

3.9.5.2.3.3 Results

The maximum stress intensity and the deformation plots for the 65g side drop are shown in Figure 3.9.5-4 and Figure 3.9.5-5. As shown in Table 3.9.5-1, all stresses are within allowable limits for the side drop condition.

The maximum stress intensity for the 65g top and bottom end drop are shown in Figure 3.9.5-6 and Figure 3.9.5-7. As shown in Table 3.9.5-2 and Table 3.9.5-3, all stresses are within allowable limits for the both top and bottom end drop condition.

3.9.5.3 Lead Gamma Shielding Slump Evaluation

The extent of lead slump in the TC during a vertical/end drop scenario is presented exclusive of side drop results, as a side drop would induce only negligible amounts of slump in the lead shielding.

The lead material conforms to the ASTM B29 specification for standard commercial lead, except that the density is increased from the reference 0.41 lb/in^3 to 0.615 lb/in^3 in order to conservatively bound the largest weight of shielding available.

The lead is assumed to fill the available cavity in the TC, such that any deformation of the inner shell will be carried into the lead shielding. The material is modeled with a multi-linear, kinematic hardening stress response to applied strains as detailed in Chapter 8.

The lead slump is modeled as subjected to a conservative 65g vertical load. This load induces a maximum slump of 2.2 inches in the vertical direction. The mesh for this vertical load is shown in Figure 3.9.5-3, while the displacements of the lead under top and bottom 65g accelerations are shown in Figure 3.9.5-21.

See Chapter 12 for the shielding evaluation of this slump.

3.9.5.4 EOS Transfer Cask Trunnions and Local Shell Stress Evaluation

The purpose of this section is to summarize the structural evaluation of the EOS-TC upper trunnions, the welds between the top/bottom rings and the upper/lower trunnions, respectively, and the shell stresses during lifting and handling operations for transfer conditions.

The EOS-TC is lifted by the two upper trunnions. Two lower pocket trunnions in the bottom ring of the cask form the rotational axis for the cask on the support skid during up-ending and down-ending of the cask. These lower pocket trunnions also provide support for the bottom end of the cask during transfer operations.

A geometric- and load-bounding representation, enveloping the three EOS-TCs (EOS-TC108, EOS-TC125 and EOS-TC135), is referred to as EOS-TCMAX in this evaluation. The geometric dimensions for this bounding model are selected to yield the most bounding stresses and deformations.

The evaluation is performed in the following steps:

- The upper trunnions, bottom ring and the welds between the trunnions and the shell are evaluated using hand calculations.
- The cask shell stresses are evaluated using ANSYS code [3.9.5-4].

3.9.5.4.1 Methodology and Acceptance Criteria

The conservatively bounding weights of the EOS-TC and DSC components employed for the analysis are as follows:

- Unloaded EOS-TC135 136,000 lb
- Loaded EOS-37PTH DSC 134,000 lb

- Total 270,000 lb

The upper trunnions and trunnion welds to the cask top ring are designed in accordance with the allowable stresses defined by ANSI N14.6 [3.9.5-2] for a non-redundant lifting device.

For the vertical configuration, the dead weight load includes the self-weight of the loaded EOS-TC with the bounding EOS-37PTH DSC payload full of water. This load considers the EOS-TC hanging vertically by the two upper trunnions. The weight of the DSC is applied as a uniform pressure on the bottom end plate of the EOS-TCMAX. A dynamic load factor (DLF) of 1.15 is used to include the effects of dynamic interactions.

During transfer of the EOS-TC on the trailer, the EOS-37PTH DSC will rest on the EOS-TC inner shell. The EOS-37PTH DSC weight is therefore applied as a pressure to the inner shell using a cosine shaped load amplitude variation. The EOS-TC will be in contact with the saddle, latch and the lower trunnion pockets; the lower trunnion pocket was modeled in ANSYS as vertically constrained nodes. Similarly, the semicircular half section of the upper trunnion is constrained in radial direction. See Figure 3.9.5-10 for a diagram showing the boundary conditions for various loading conditions.

During down-ending operations on the transfer trailer, the EOS-TC will rotate about the lower trunnion pockets, at which time, the contact between the lifting yoke and the upper trunnion will separate and the total load will be supported by the lower trunnion pockets.

For thermal stress analysis, temperature profiles and maximum component temperatures are based on the thermal analyses described in Chapter 4. Only two load cases are evaluated for thermal stress analysis, depending on the bounding cases, based on the maximum reported temperatures for normal and off-normal conditions. Displacement constraints are applied simply to prevent rigid body motion.

For all analyses except thermal analysis material properties are taken at a conservative temperature of 400 °F. For all analyses, except thermal analysis, material properties are taken at a conservative temperature of 400 °F for the entire cask, except for the trunnions, which are taken at a conservative 367 °F. The allowable stresses for the EOS-TC components are obtained from Chapter 3, Table 3-3 and is reproduced for the pertaining load cases in Table 3.9.5-4.

3.9.5.4.2 Trunnion and Weld Evaluation

The EOS-TC has two upper trunnions to lift the cask during the lifting and handling operations. The upper trunnions are welded to the cask through partial penetration groove welds with fillet covers.

The upper trunnions are single shoulder trunnions as shown in Figure 3.9.5-8. The upper trunnions are evaluated for its critical section, Section A-A shown in Figure 3.9.5-8, for the maximum total weight of the TC.

The maximum total weight is calculated as:

$$F_v = W_L \text{ x } DLF / N_{tr} = 155{,}250 \text{ lb}$$

Where,

F_v = Maximum lift weight
W_L = Total weight of the TC and DSC = 270,000 lb
DLF = Dynamic load factor = 1.15
N_{tr} = Number of trunnions = 2

The shear stress in Section A-A for 1g is:

$$\text{Shear Stress (ksi)} = F_v/S_{AA} = 3.29 \text{ ksi}$$

Where S_{AA} is the section area and the bending stress is:

$$\frac{M_{AA}}{I_{AA}} \times \frac{D_1}{2} = 6.59 \text{ ksi}$$

Where,

M_{AA} = Bending moment at Section A-A
I_{AA} = Moment of Inertia at Section A-A, and
D_1 = Trunnion diameter.

At a service load level of 1g the maximum stress intensity within the upper trunnion itself is 9.31ksi, leading to 6g and 10g stress intensities of 55.9 ksi and 93.1 ksi, respectively.

The upper trunnion is welded to the top ring via a 1.25 inch partial penetration groove weld with a 3/8 inch fillet cover. These welds are also evaluated per the ANSI 14.6 criteria. The direct shear load on the trunnion is considered to be resisted by contact/bearing due to the very tight tolerances to which the parts are machined.

Per Paragraph 4.2.1.1 of ANSI N14.6 [3.9.5-2], the combined shear stress and the maximum tensile stress are compared to the material yield and ultimate strengths considering safety factors of 6 and 10, respectively. Both the base metal and weld metal stresses are evaluated. Only the ultimate stress of the weld metal is considered. For the base metal, both yield and ultimate stress checks are performed.

The normal stress, f_n, and shear stress, f_v, components on each critical plane of the weld are calculated and then the combined maximum equivalent stress is calculated and compared to the bounding allowable stress for the trunnion base metal, weld metal, and top ring base metal. The maximum equivalent stress is calculated as:

$$f_{eqv} = \sqrt{(f_n)^2 + 3(f_v)^2}$$

The bending moment considered in the weld is calculated as the shear load, F_v times the moment arm of 2.62, which is the distance from the load application to the top ring:

$$M = F_v \times 2.62 = 155{,}250 \text{ lbs} \times 2.62 \text{ in} = 406{,}755 \text{ in} - \text{lbs}$$

Therefore, the bending load on the weld is

$$f_b = \frac{M}{I_{weld}} = \frac{406{,}755}{78.54} = 5{,}179\ lb/in$$

Where,

$$I_{weld} = \frac{\pi}{4}(D_2)^2 = 78.54 in^2$$

The trunnion base metal shear stress, f_{vTBM}, is caused by the bending load of 5,179 lb/in calculated above. The base metal length is the depth of the J-groove, 1.25 inch, plus the 3/8 inch cover, for a total length of 1.625 inches.

$$f_{vTBM} = \frac{5{,}179\ lb/in}{1.625\ in} = 3{,}187\ psi$$

The maximum equivalent stress is, therefore:

$$f_{eqv,TBM} = \sqrt{3} f_{vTBM} = 5{,}520\ psi$$

The minimum throat distance through the weld metal is $\sqrt{1.25^2 + 0.375^2} = 1.305$ inches. The weld throat is inclined at an angle of $\tan^{-1}\frac{0.375}{1.25} = 16.7$ degrees. The stress on the minimum throat is a combination of tension and shear.

$$f_{v,weld} = \frac{5{,}179\ lb/in}{1.305\ in}\cos(16.7) = 3{,}801\ psi$$

$$f_{n,weld} = \frac{5{,}179\ lb/in}{1.305\ in}\sin(16.7) = 1{,}140\ psi$$

The weld metal maximum equivalent stress is:

$$f_{eqv,weld} = \sqrt{\left(f_{n,weld}\right)^2 + 3\left(f_{v,weld}\right)^2} = \sqrt{(1{,}140)^2 + 3(3{,}801)^2} = 6{,}682\ psi$$

The cask top ring base metal stress components are conservatively calculated considering a 45-degree weld bevel. The actual length of base metal for the J-groove geometry is larger. The length of the beveled edge is, therefore, taken as 1.414*1.25=1.77 inches. The top ring base metal shear stress is:

$$f_{vTRBM} = \frac{5{,}179\frac{lb}{in}}{1.77\ in}\cos(45) = 2{,}069\ \text{psi}$$

The top ring base metal normal stress is:

$$f_{nTRBM} = \frac{5{,}179\frac{lb}{in}}{1.77in} \times \sin(45) = 2{,}069\ \text{psi}$$

The base metal maximum equivalent stress is, therefore:

$$f_{eqv,TRBM} = \sqrt{(f_{nTRBM})^2 + 3(f_{vTRBM})^2} = \sqrt{2{,}069^2 + 3 \times 2{,}069^2} = 4{,}138\ psi$$

The allowable stresses for each of these stress components are as follows:

Trunnion base metal allowable stress:

$$F_{TBM} = \min\left(\frac{S_y}{6}, \frac{S_u}{10}\right) = \min\left(\frac{82.8}{6}, \frac{113.7}{10}\right) = \min(13.8, 11.4) = 11.4\ ksi$$

Top ring base metal allowable stress:

$$F_{TRBM} = \min\left(\frac{S_y}{6}, \frac{S_u}{10}\right) = \min\left(\frac{32.0}{6}, \frac{70.0}{10}\right) = \min(5.33, 7.0) = 5.33\ ksi$$

Weld metal allowable stress:

$$F_w = \min\left(\frac{S_y}{6}, \frac{S_u}{10}\right) = \min\left(NA, \frac{68.6}{10}\right) = 6.86\ ksi$$

The ultimate stress of the weld metal, ER308L, at 250 °F is 68.6 ksi to match the weaker of the two joined base metals. Using material properties at 250 °F is conservative as the maximum temperature at the weld zone between the top ring and trunnion is 225 °F.

The calculated stresses and comparisons to allowable values for the 1g critical lift (including a dynamic load factor of 1.15) are summarized in Table 3.9.5-4.

The lower trunnion pockets provided in the bottom ring support the EOS-TC during the various handling and transfer operations. The bearing stress in the bottom ring is analyzed for a bounding load of (1g vertical + 1g horizontal + 1g transverse + 1g dead weight). The maximum bearing stress between the bottom trunnions and the bottom ring is 10.8 ksi.

3.9.5.4.3 Shell Evaluation

A single 3D FEM is prepared for the bounding dimensions of the EOS-TCs, which accounts for the minimum thickness, longest length and bounding DSC weight. The following components were modeled with SOLID185 elements:

- Top ring
- Bottom ring
- Inner shell
- Outer shell
- Lead shielding
- Upper trunnions
- Bottom end plate
- Ram access penetration ring
- Top lid

The parts that are not modeled include the EOS-TC rails, bottom neutron shields, inner and outer neutron shield panel, bottom neutron shield plate, and the bottom cover plate, since these components will not significantly affect the evaluation.

Because all of the components of the EOS-TC are not modeled in the FEM, the densities of various components are modified in order to achieve the overall weight of the EOS-TC135. The total weight of the EOS-TCMAX model is 136,000 lb, which is conservatively higher than the overall weight of the EOS-TC135.

The weld between the top trunnions and top ring is modeled by coupling the nodes in all degrees of freedom. The nodes between inner/outer shell with top/bottom rings are merged together as these locations are not in the high stress locations. Contact between components is created using CONTA173 and TARGE170 surface-to-surface contact elements.

The finite element model for the EOS-TCMAX is shown in Figure 3.9.5-9.

3.9.5.4.4 Results

The stress values in the upper trunnions, shell welds and top and bottom ring are below the allowable values. Table 3.9.5-4 summarizes the calculated stress, allowable stress, and safety margin for each item and load case.

There are two upper trunnion and two lower trunnion pockets on the transfer cask. The upper trunnions are used for lifting and are welded to the cask top ring. The maximum stress in the trunnion and the trunnion to cask top ring weld are evaluated in accordance with the allowables defined by ANSI N14.6.

The maximum stress intensity for the upper trunnion is 93.1 ksi with a margin of 0.22 (10g load). The maximum weld stress is 6.68 ksi with a margin of 0.*03* (1g critical lift with 1.15 DLF). The maximum bearing stress for the lower trunnion pocket is 10.8 ksi with a margin of 1.97. The maximum shell stress in the top ring (3g test load) is 32.6 ksi with a margin of 0.31. The maximum stress intensity in the bottom ring (load case HBOT) is 56.3 ksi with a margin of 0.14. The stress contour plots for the 3g test load case and the horizontal transfer load case are shown in Figure 3.9.5-11 and Figure 3.9.5-12, respectively. Since all margins are above zero, the system is shown to be capable of withstanding the prescribed loads.

3.9.5.5 EOS Transfer Cask Neutron Shield Shell Structural Evaluation

The purpose of this section is to summarize the evaluation of the stresses in the neutron shield shell structure of the NUHOMS® EOS-TCs (EOS-TC108, EOS-TC125 and EOS-TC135) due to prescribed loads during fuel loading and transfer operations.

Neutron shield shell is evaluated for all the applied loads during fuel loading and transfer operations as summarized Chapter 2, Table 2-8, except the accident drop loads as the complete loss of neutron shield is assumed in calculating the maximum combined gamma and neutron dose rates. Due to the differences in designs, separate finite element models are setup for the EOS-TC108, EOS-TC125, and EOS-TC135. The evaluation is performed using ANSYS [3.9.5-4].

Material properties, where not explicitly stated, are conservatively taken at 300 °F from the tables in Chapter 8 and the resulting stresses in the neutron shield shell components are compared with the stress criteria listed in Chapter 3, Table 3-5.

3.9.5.5.1 EOS-TC108 Neutron Shield Shell

A 120° segment of the neutron shield shell assembly for EOS-TC108 is modeled. The FEMs are developed using the nominal dimensions per the drawings in Chapter 1, Section 1.3.

Components (neutron shield panel, upper/lower flanges and the I-beams) are modeled using ANSYS SHELL181 3-D shell elements. The elements have 6 degrees of freedom (3 translational and 3 rotational) at each of the four nodes. The interfaces between the mating surfaces are modeled using ANSYS CONTA173 and TARGE170 surface to surface contact elements that allow the transfer of loads. EOS-TC is not modeled explicitly in this model, it is assumed fixed and the interaction between the neutron shield shell inner panel and EOS-TC is simulated using ANSYS CONTA178 node to node contact elements. The interaction between the I-beam faces and the seam plates is simulated using RBE3 constrained equations and ANSYS CONTA175, and TARGE170 node-to-surface contact elements, wherein the RBE3 constrained equation is created between the nodes of the I-beam face to transfer all the forces to the center node onto a single node at the center of the I-beam face. This node is then used to create a node to surface contact between the seam plate surface.

The fillet welds for EOS-TC108 neutron shield assembly are simulated using couplings at the interface of neutron shield inner panel to I-beams and at interface of the neutron shield outer panel to I-beam welds. Welds at other locations are full penetration welds, thus nodes at these weld locations are merged in order to achieve the appropriate behavior.

The FEM for the EOS-TC108 neutron shield assembly is shown in Figure 3.9.5-13.

Horizontal Transfer / Seismic Loads

The horizontal transfer and seismic loads are enveloped by analyzing the neutron shield shell for an internal pressure load of 20 psig and (1g DW + 1g vertical + 1g lateral + 1g axial) accelerations.

Along with this load, the annulus of the neutron shield shell is also subjected to hydrostatic pressure load, which varies linearly with height with maximum at the bottom. Conservatively, a uniform internal pressure equal to the maximum hydrostatic pressure ($p = \rho g d_1 = 0.0361 \times 2.24 \times 90.25 = 7.30$psig) is added. Therefore, the equivalent uniform pressure of 27.5 psig is applied to the model.

This equivalent pressure is applied on the inner walls of the annulus created between the inner neutron shield panel and the outer neutron shield panel. It is also applied on the faces of the I-beams that are exposed to the water.

The neutron shield shell assembly will rest on the EOS-TC. Thus, in order to simulate the effect, ANSYS CONTA178 node-to- node contacts are created between the inner face of the inner panel and the EOS-TC. The EOS-TC surface is not modeled explicitly and the degrees of freedom of free nodes representing the outer surface of the EOS-TC are constrained in all translational directions (UX, UY and UZ).

Nodes at the cut face of 120° segment are constrained in the hoop (UY) direction.

Test Pressure

The EOS-TC108 neutron shield is analyzed in the vertical position and at the room temperature (70 °F) for the test pressure load case.

In addition to hydrostatic pressure due to the water in the neutron shield, an internal pressure of 25 psig (~125% of 20 psig pressure) is also applied for this analysis. The hydrostatic pressure will vary with the height, maximum pressure being at the bottom of the neutron shield shell. This pressure is applied as the triangular varying load. Therefore, the maximum equivalent pressure applied to the model is 31.14 psig.

This equivalent pressure is applied on the inner walls of the annulus between the inner neutron shield panel and the outer neutron shield panel. It is also applied on the faces of the I-beams that are exposed to water.

For pressure test, the neutron shield shell is in the vertical orientation and the nodes at the location of the leg supports are constrained in all directions.

The stresses due to this equivalent pressure in test pressure load are compared with the level B allowable at room temperature.

Vertical Lift

The vertical lift load includes a DLF of 1.15 for pressure load, so the equivalent pressure applied during vertical transfer is 27.06 psig.

This equivalent pressure is applied on the inner walls of the annulus between the inner neutron shield panel and the outer neutron shield panel. It is also applied on the faces of the I-beams that are exposed to the neutron shield.

Thermal Loads

For thermal stress analysis, two temperature distributions from the thermal evaluations documented in Chapter 4 are used. The first load case corresponds to the EOS-TC108 loaded with EOS-37PTH DSC, heat load of 41.8 kW, off-normal hot conditions, outdoor and horizontal position of the TC. The second load case corresponds to the EOS-TC108 loaded with the EOS-89BTH DSC, heat load of 34.44 kW, normal hot conditions, indoor and vertical position of the TC. The temperature distributions are shown in Figure 3.9.5-20.

3.9.5.5.2 EOS-TC125 and EOS-TC135 Neutron Shield Shells

The EOS-TC125 / EOS-TC135 neutron shield shell assembly is analyzed for postulated load conditions using a 3D 180° half-symmetric FEMs. The FEMs are developed using the nominal dimensions per the drawings in Chapter 1, Section 1.3.

All components (EOS-TC shells, neutron shield panel, neutron shield panel support ring plates, and the I-beams) are modeled using ANSYS SOLID185 3-D solid elements. The elements have 3 translational degrees of freedom at each of the eight nodes (no rotational degrees of freedom). The interfaces between the mating surfaces are modeled using ANSYS CONTA173 and TARGE170 surface-to-surface contact elements that allow the transfer of loads.

The welds at the interface of outer shell to I-beams and at the interface of neutron shield plate support ring plates to EOS-TC outer shell are modeled using couplings.

The nodes at slot welds between the I-beam and neutron shield panel are merged in order to achieve appropriate behavior. The weld between neutron shield panel and neutron shield panel support ring are full penetration welds. Thus, nodes at these weld locations are merged in order to achieve the appropriate behavior.

The FEM for the EOS-TC125 neutron shield assembly is shown in Figure 3.9.5-14. It is also representative of the EOS-TC135 neutron shield assembly FEM.

The resulting stresses in the neutron shield shell components are compared with the stress criteria listed in Chapter 3, Table 3-5.

Horizontal Transfer / Seismic Loads

The horizontal transfer and seismic loads are enveloped by analyzing the neutron shield shell for an internal pressure load of 25 psig and (2g vertical + 2g lateral + 2g axial) accelerations.

Along with this load the annulus of the neutron shield shell is also subjected to hydrostatic pressure load which varies linearly with height with maximum at the bottom. Conservatively, a uniform internal pressure equal to the maximum hydrostatic pressure is added. Therefore the equivalent pressure of 40 psig is applied to the model.

This equivalent pressure is applied in the annulus of the neutron shield shell. It is also applied on the faces of the I-Beams which are exposed to the water.

During the horizontal transfer, the EOS-TC is supported by the trunnions and saddle. Therefore, in order to simulate the effect, degree of freedom of nodes at the trunnion locations on the outer surface of the EOS-TC are constrained in axial (upper trunnions) direction and in radial (lower trunnion pockets) direction.

Symmetric boundary conditions are applied at the cut face of the model.

Test Pressure and Vertical Lift

The neutron shield is analyzed in the vertical position and at the room temperature (70 °F) for the test pressure load case.

In addition to hydrostatic pressure due to the water in the neutron shield, an internal pressure of 32 psig (~125% of 25 psig pressure) is also applied for this analysis. The hydrostatic pressure will vary with the height, maximum pressure being at the bottom of the neutron shield shell. The maximum equivalent pressure at the bottom of the cask is calculated to be 38.78 psig. The test pressure load case is enveloped by the horizontal transfer / seismic load case and therefore is not evaluated separately.

Similarly, the maximum pressure during the vertical lift is calculated to be 32.79 psig, which is also enveloped by the horizontal transfer / seismic load case and not evaluated separately.

Thermal Loads

For thermal stress analysis, two temperature distributions from the thermal evaluations documented in Chapter 4 are used. The first load case corresponds to the EOS-TC125 loaded with EOS-37PTH DSC, heat load of 50 kW, off-normal hot conditions, outdoor and horizontal position of the TC. The second load case corresponds to the EOS-TC125 loaded with the EOS-37PTH DSC, heat load of 36.35 kW, normal hot conditions, indoor and vertical position of the TC. The temperature distributions are shown in Figure 3.9.5-19.

3.9.5.5.3 Results

The stress results for the neutron shield shells are summarized in Table 3.9.5-6 and Table 3.9.5-7. The stress contour plots of the EOS-TC108 neutron shield shell for the horizontal transfer/seismic load case are shown in Figure 3.9.5-15 and Figure 3.9.5-16. Also the stress contour plots of the EOS-TC135 neutron shield shell for the horizontal transfer / seismic load case are shown in Figure 3.9.5-17 and Figure 3.9.5-18.

3.9.5.6 EOS Transfer Cask, Trunnion, and Neutron Shield Shell Fatigue Requirements

The transfer cask (TC) and trunnion are designed in accordance with the applicable guidelines of the ASME Code, Section III, Division 1, and Subsection NF for Class 1 vessels, except for the neutron shield tank, which is designed to ASME Code, Section III, Division 1, and Subsection ND. Neither one of these subsections require a fatigue evaluation for low cycle loads. Therefore, the fatigue evaluation is not required for the EOS-TC per ASME code criteria.

3.9.5.7 References

3.9.5-1 Blodgett, O.W., "Design of Welded Structure," published by James F. Lincoln Arc Welding Foundation, June 1966.

3.9.5-2 ANSI N14.6, "Special Lifting Devices for Shipping Containers Weighing 10,000 Pounds or more," 1993.

3.9.5-3 American Society of Mechanical Engineers, "ASME Boiler and Pressure Vessel Code, 2010 Edition with 2011 Addenda.

3.9.5-4 ANSYS Computer Code and User's Manual, Version 14.0.

Table 3.9.5-1
EOS-TCMAX Stress Result Summary Table – 65g Side Drop

STRESS CLASSIFICATION- SERVICE LEVEL D – SUMMARY TABLE				
EOS-TC Components	**Stress Category**	**Maximum Stress (ksi)**	**Allowable Stress (ksi)**	**Max. Stress Ratio**
Outer Shell	P_M	44.14	49.0	0.90
	P_L+P_B	54.72	63.0	0.87
Inner Shell	P_M	45.43	49.0	0.93
	P_L+P_B	50.41	63.0	0.80
Top Cover Plate	P_M	41.58	49.0	0.85
	P_L+P_B	55.78	63.0	0.89
Top Ring	P_M	43.45	49.0	0.89
	P_L+P_B	59.93	63.0	0.95
Bottom Ring	P_M	42.24	49.0	0.86
	P_L+P_B	53.70	63.0	0.85
Bottom End Plate	P_M	47.04	49.0	0.96
	P_L+P_B	50.49	63.0	0.80
RAM Access	P_M	39.41	49.0	0.80
	P_L+P_B	49.40	63.0	0.78
Bottom Neutron	P_M	46.21	49.0	0.94
	P_L+P_B	46.67	63.0	0.74

Table 3.9.5-2
EOS-TCMAX Stress Result Summary Table – 65g Top End Drop

#	Component	Max Stress (ksi) /Stress Ratio			Allowable (ksi)		
		PM	PL	PM+PB	PM	PL	PM+PB
1	Outer Shell	24.4 49.7%	36.3 57.6%	36.3 57.6%	49.0	63.0	63.0
2	Inner Shell	25.7 52.4%	37.9 60.1%	37.9 60.1%	49.0	63.0	63.0
3	Top Cover Plate	12.4 25.2%	18.8 29.8%	18.8 29.8%	49.0	63.0	63.0
4	Top Ring	13.0 26.6%	17.8 28.3%	17.8 28.3%	49.0	63.0	63.0
5	Bottom Ring	3.4 7.0%	6.2 9.9%	6.2 9.9%	49.0	63.0	63.0
6	Bottom End Plate	6.1 12.4%	11.8 18.8%	11.8 18.8%	49.0	63.0	63.0
7	RAM Access Penetration Ring	4.8 9.8%	6.4 10.2%	6.4 10.2%	49.0	63.0	63.0
8	Bottom Neutron Shield Pane	3.8 7.8%	7.0 11.1%	7.0 11.1%	49.0	63.0	63.0

Table 3.9.5-3
EOS-TCMAX Stress Result Summary Table – 65g Bottom End Drop

#	Component	Max Stress (ksi) / Stress Ratio			Allowable (ksi)		
		PM	PL	PM+PB	PM	PL	PM+PB
1	Outer Shell	25.1 51.3%	39.3 62.4%	39.3 62.4%	49.0	63.0	63.0
2	Inner Shell	18.1 37.0%	26.7 42.3%	26.7 42.3%	49.0	63.0	63.0
3	Top Cover Plate	4.1 8.5%	10.8 17.2%	10.8 17.2%	49.0	63.0	63.0
4	Top Ring	1.5 3.1%	2.6 4.1%	2.6 4.1%	49.0	63.0	63.0
5	Bottom Ring	22.5 45.8%	32.5 51.6%	32.5 51.6%	49.0	63.0	63.0
6	Bottom End Plate	16.4 33.5%	32.8 52.1%	32.8 52.1%	49.0	63.0	63.0
7	RAM Access Penetration Ring	25.4 51.8%	29.8 47.3%	29.8 47.3%	49.0	63.0	63.0
8	Bottom Neutron Shield Panel	10.2 20.8%	29.9 47.5%	29.9 47.5%	49.0	63.0	63.0

Table 3.9.5-4
Stress Result Summary Table for the Trunnions
(2 Pages)

Description	Calculated Stress (ksi)	Allowable Stress (ksi)	Margin
Manual Calculation for Upper Trunnions			
Stress intensity at A-A at 6g	55.86	82.80	0.48
Stress intensity at A-A at 10g	93.10	113.70	0.22
Manual Calculation for Weld Stresses and Lower Trunnion Pocket			
Trunnion Base Metal Max Equiv. Stress	5.52	11.40(1)	1.07
Weld Metal Max Equiv. Stress	6.68	*6.86*(2)	0.*03*
Top Ring Base Metal Max Equiv. Stress	4.14	5.33(1)	0.29
Load Case :3g (Test Load - Service level B)			
Top Ring Shell Stress (P_m)	16.58	28.46	0.72
Top Ring Shell Stress ($P_m + P_b$)	32.55	42.69	0.31
Bottom Ring Shell Stress (P_m)	10.44	28.46	1.73
Bottom Ring Shell Stress ($P_m + P_b$)	13.37	42.69	2.19
Load Case :DW Upper Trunnion (Service Level A) Vertical TC			
Top Ring Shell Stress (P_m)	6.75	21.40	2.17
Top Ring Shell Stress ($P_m + P_b$)	12.40	32.40	1.61
Top Ring Shell Stress ($P_m + P_b$) + Q	40.13	64.20	0.60
Bottom Ring Shell Stress (P_m)	3.76	21.40	4.69
Bottom Ring Shell Stress ($P_m + P_b$)	4.82	32.40	5.73
Bottom Ring Shell Stress ($P_m + P_b$) + Q	32.54	64.20	0.97
Load Case : DW Lower Trunnion (Service Level A) Vertical TC			
Top Ring Shell Stress (P_m)	1.36	21.40	14.72
Top Ring Shell Stress ($P_m + P_b$)	1.43	32.40	21.59
Top Ring Shell Stress ($P_m + P_b$) + Q	29.16	64.20	1.20
Bottom Ring Shell Stress (P_m)	11.52	21.40	0.86
Bottom Ring Shell Stress ($P_m + P_b$)	23.22	32.40	0.40
Bottom Ring Shell Stress ($P_m + P_b$) + Q	50.94	64.20	0.26
Load Case : Horizontal Transfer on Skid (1g axial) (Service Level B) Horizontal TC			
Top Ring Shell Stress (P_m)	7.39	28.46	2.85
Top Ring Shell Stress ($P_m + P_b$)	13.68	42.69	2.12
Top Ring Shell Stress ($P_m + P_b$) + Q	41.40	64.20	0.55
Bottom Ring Shell Stress (P_m)	17.47	28.46	0.63
Bottom Ring Shell Stress ($P_m + P_b$)	28.56	42.69	0.50

Table 3.9.5-4
Stress Result Summary Table for the Trunnions
(2 Pages)

Description	Calculated Stress (ksi)	Allowable Stress (ksi)	Margin
Bottom Ring Shell Stress $(P_m + P_b) + Q$	56.28	64.20	0.14
Load Case : Horizontal Transfer on Skid (-1g axial) (Service Level B) Horizontal TC			
Top Ring Shell Stress (P_m)	5.25	28.46	4.42
Top Ring Shell Stress $(P_m + P_b)$	8.66	42.69	3.93
Top Ring Shell Stress $(P_m + P_b) + Q$	36.39	64.20	0.76
Bottom Ring Shell Stress (P_m)	16.12	28.46	0.77
Bottom Ring Shell Stress $(P_m + P_b)$	20.43	42.69	1.09
Bottom Ring Shell Stress $(P_m + P_b) + Q$	48.15	64.20	0.33

Notes:

(1) Lower of $S_y/6$ or $S_u/10$

(2) Equal to $S_u/10$

Table 3.9.5-5
Acceptance Criteria for the Stress Evaluation

Item	Stress Type	Service Levels A	Service Level B
Top Ring and Bottom Ring	Primary Membrane (P_m)	S_m	Same as Level A, increased by a factor of 1.33
	Primary Membrane + Bending ($P_m + P_b$)	1.5 S_m	
	Primary Membrane + Bending + Thermal Stress (Q)	3.0 S_m	
Upper Trunnions	Stress Intensity at 6g loads	S_y	
	Stress Intensity at 10g loads	S_u	
	Primary Membrane (P_m)	S_m	Same as Level A, increased by a factor of 1.33
	Primary Membrane + Bending ($P_m + P_b$)	1.5 S_m	
	Primary Membrane + Bending + Thermal Stress (Q)	3.0 S_m	
Welds	Maximum Equivalent Stress for Critical Lift (1g)	$S_u/10$ (Weld Metal and Base Metal)	
		$S_y/6$ (Base Metal)	
	Combined Weld Stress	$\min(0.3xS_u, 0.4xS_y)$	Same as Level A, increased by a factor of 1.33
Bottom Ring	Bearing Stress	S_y	

Table 3.9.5-6
Stress Result Summary for the Neutron Shield Panel model

TC	Load Case(1)	Component	Pm (ksi)	Allowable (ksi)	Ratio	P_m+P_b (ksi)	Allowable (ksi)	Ratio	P_m+P_b+Q (ksi)	Allowable (ksi)	Ratio
125	E2	Neutron Shield Panel	10.92	20.00	0.55	25.57	30.00	0.85	37.69	48.00	0.79
125	E2	I-Beam	4.69	16.60	0.28	6.55	24.90	0.26	16.20	39.84	0.41
135	E2	Neutron Shield Panel	10.92	20.00	0.55	26.18	30.00	0.87	38.30	48.00	0.80
135	E2	I-Beam	5.06	16.60	0.30	6.96	24.90	0.28	16.60	39.84	0.42
108	A1	Neutron Shield Panel	5.18	5.50	0.94	6.77	8.25	0.82	11.40	13.20	0.86
108	A1	I-Beam	1.45	5.50	0.26	7.64	8.25	0.93	12.21	13.20	0.92
108	E1	Neutron Shield Panel	5.23	5.50	0.95	7.07	8.25	0.86	11.70	13.20	0.89
108	E1	I-Beam	1.56	5.50	0.28	8.18	8.25	0.99	12.75	13.20	0.97
108	B1	Neutron Shield Panel	5.86	6.60	0.89	7.80	9.90	0.79	12.43	14.40	0.86
108	B1	I-Beam	1.68	6.60	0.25	8.77	9.90	0.89	13.34	14.40	0.93

Note

(1) The load cases are numbered per Chapter 2, Table 2-8, except E1 and E2 are the enveloping horizontal transfer/seismic load cases as described in the main body of the appendix

Table 3.9.5-7
Weld Stress Result Summary for the Neutron Shield Panel model

TC	Load Case(1)	Weld #	Stress (ksi)	Allowable	Ratio	S (ksi)
125	E2	Transfer Cask Outer Shell to I-Beam Fillet Weld	9.0	13.4	66.9%	20.0
125	E2	Neutron Shield Panel and I-Beam Slot Weld	4.9	13.4	36.7%	20.0
125	E2	Neutron Shield Panel Support and TC Outer Shell	7.9	13.4	58.8%	20.0
135	E2	Transfer Cask Outer Shell to I-Beam Fillet Weld	9.6	13.4	71.5%	20.0
135	E2	Neutron Shield Panel and I-Beam Slot Weld	4.9	13.4	36.7%	20.0
135	E2	Neutron Shield Panel Support and TC Outer Shell	9.3	13.4	68.9%	20.0
108	A1	Neutron Shield Panel Inner and I-Beam	0.8	3.0	26.6%	5.5
108	A1	Neutron Shield Panel Outer and I-Beam	1.3	3.0	44.2%	5.5
108	E1	Neutron Shield Panel Inner and I-Beam	0.9	3.0	29.9%	5.5
108	E1	Neutron Shield Panel Outer and I-Beam	1.4	3.0	47.3%	5.5
108	B1	Neutron Shield Panel Inner and I-Beam	0.9	3.7	25.5%	6.0
108	B1	Neutron Shield Panel Outer and I-Beam	1.5	3.7	41.9%	6.0

Note

(1) The load cases are numbered per Chapter 2, Table 2-8, except E1 and E2 are the enveloping horizontal transfer/seismic load cases as described in the main body of the appendix

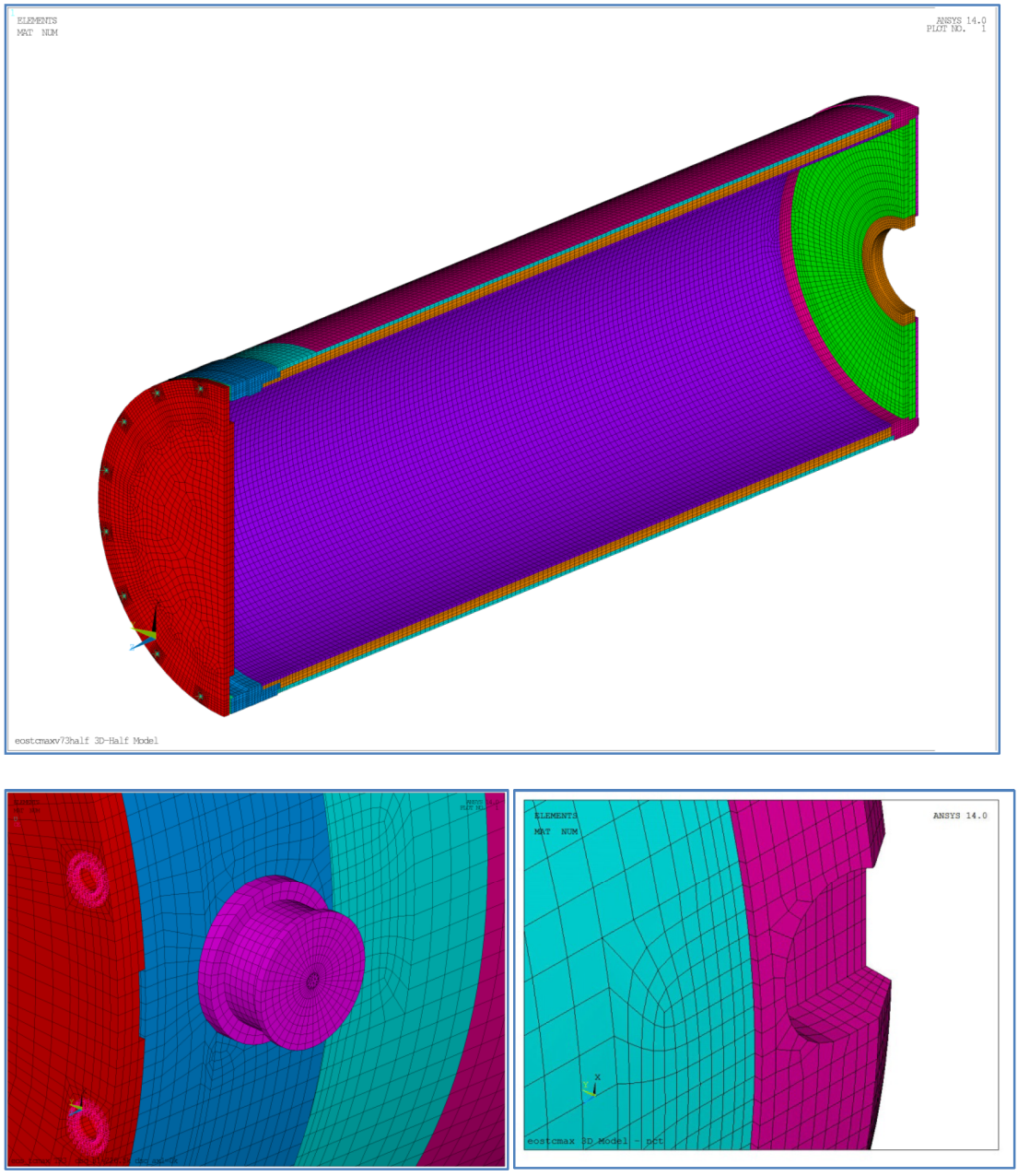

Figure 3.9.5-1
3D Half Symmetric Finite Element Model for Drop Loads

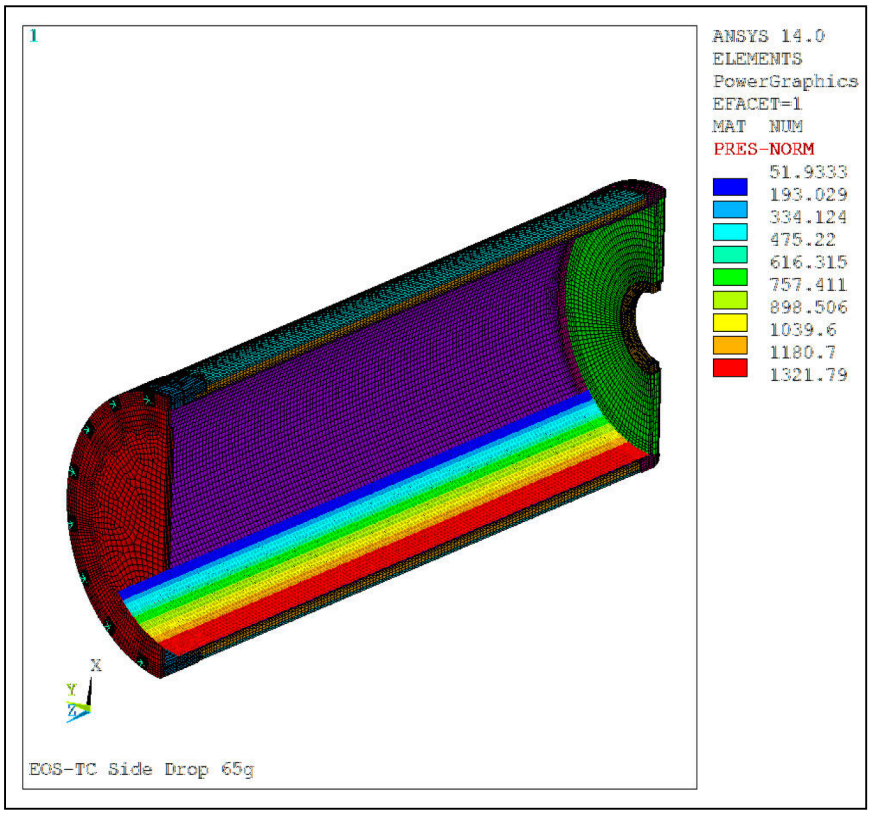

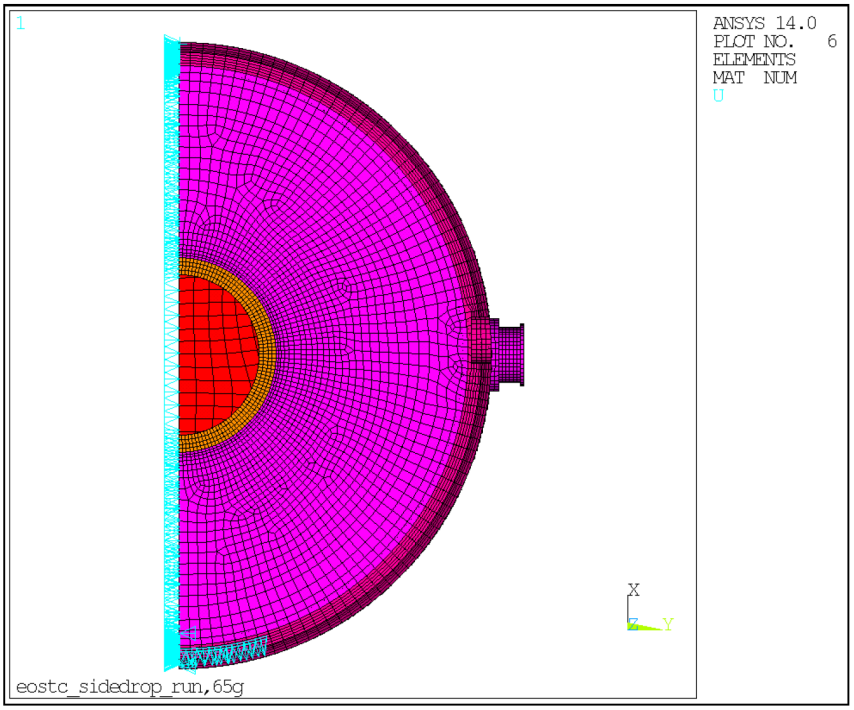

Figure 3.9.5-2
Pressure Load and Boundary Condition Plots – 65g Side Drop

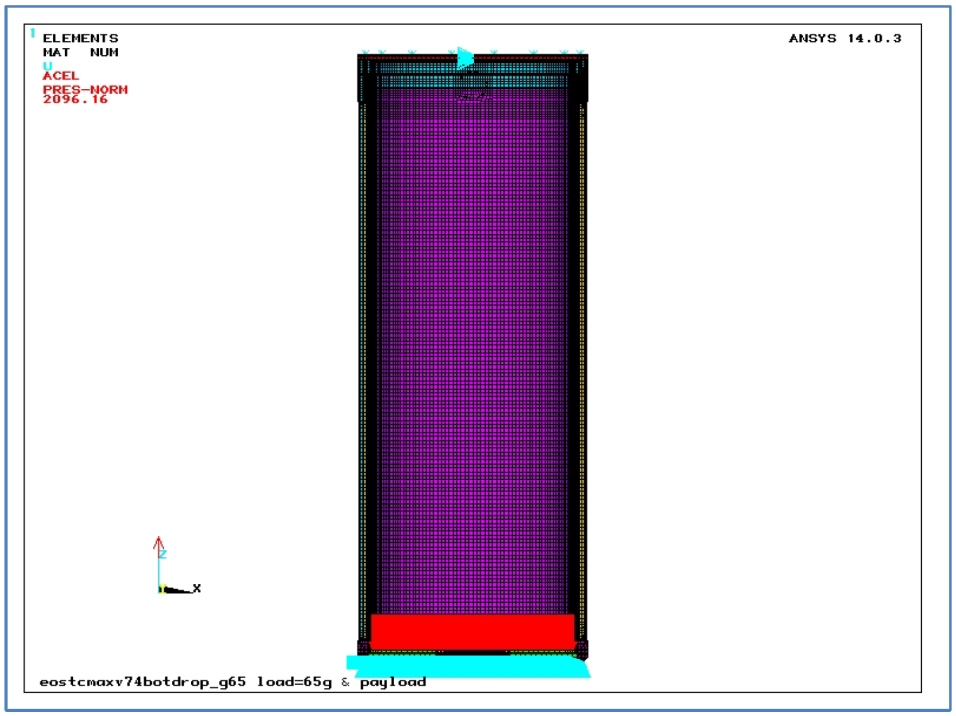

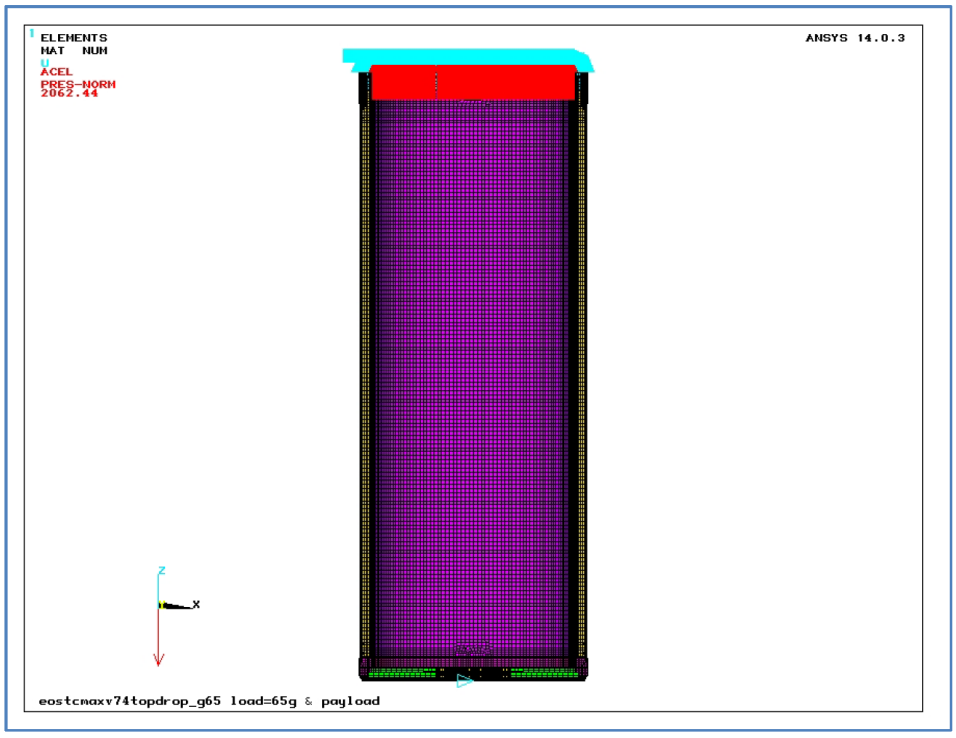

Figure 3.9.5-3
Pressure Load and Boundary Condition Plots – 65g End Drop

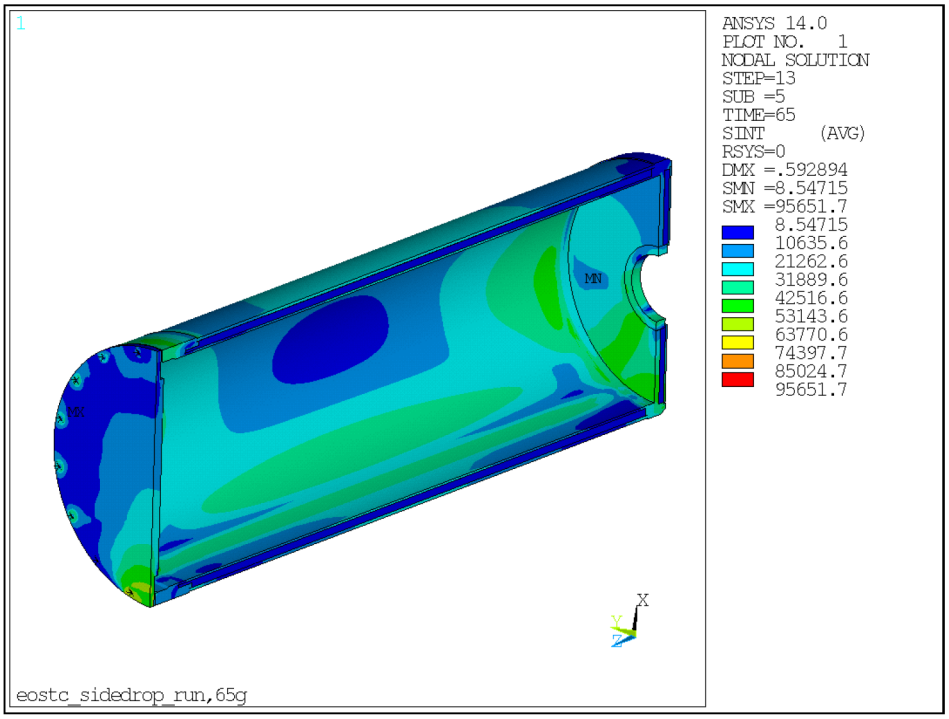

Figure 3.9.5-4
Stress Intensity (psi) plot for EOS-TCMAX – 65g Side Drop

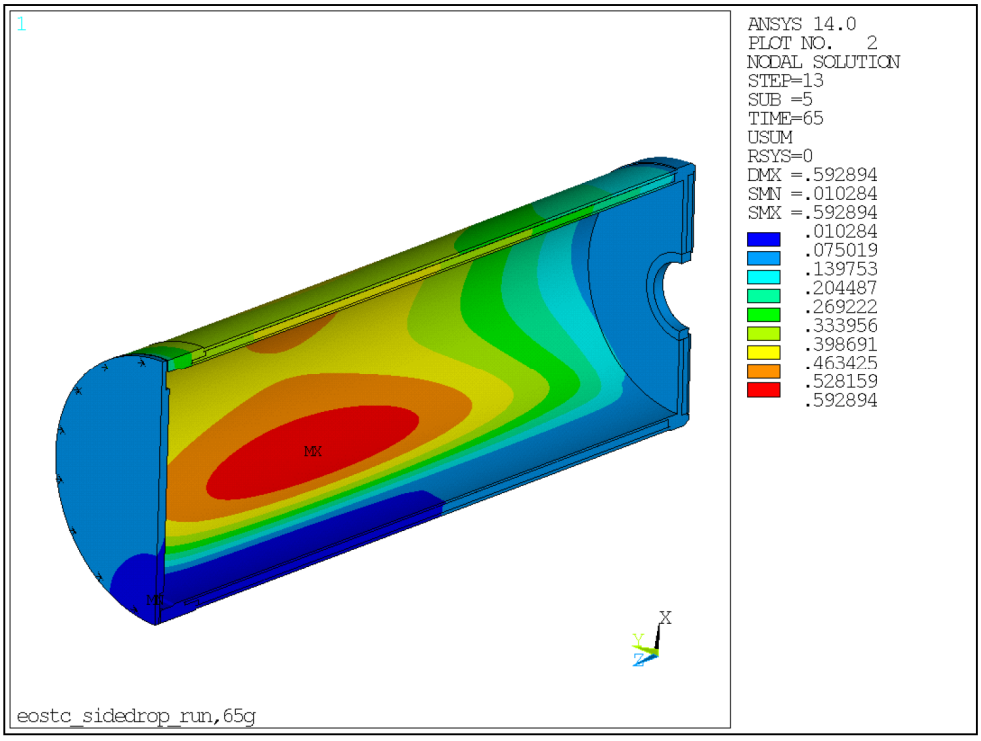

Figure 3.9.5-5
Deformation plot (in.) for EOS-TCMAX (scaled up) – 65g Side Drop

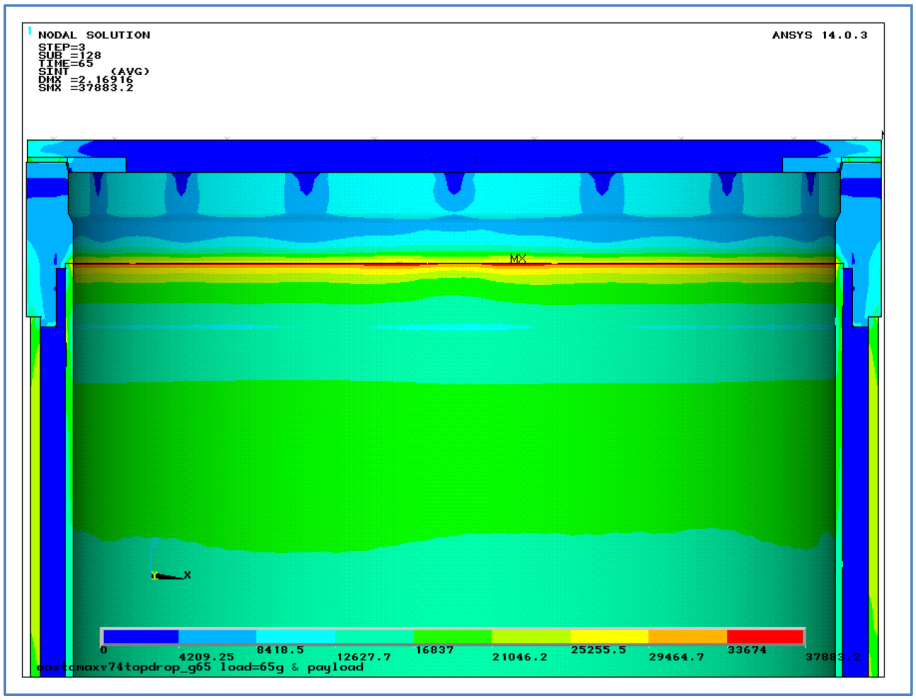

Figure 3.9.5-6
Stress Intensity (psi) plot for EOS-TCMAX – 65g Top End Drop

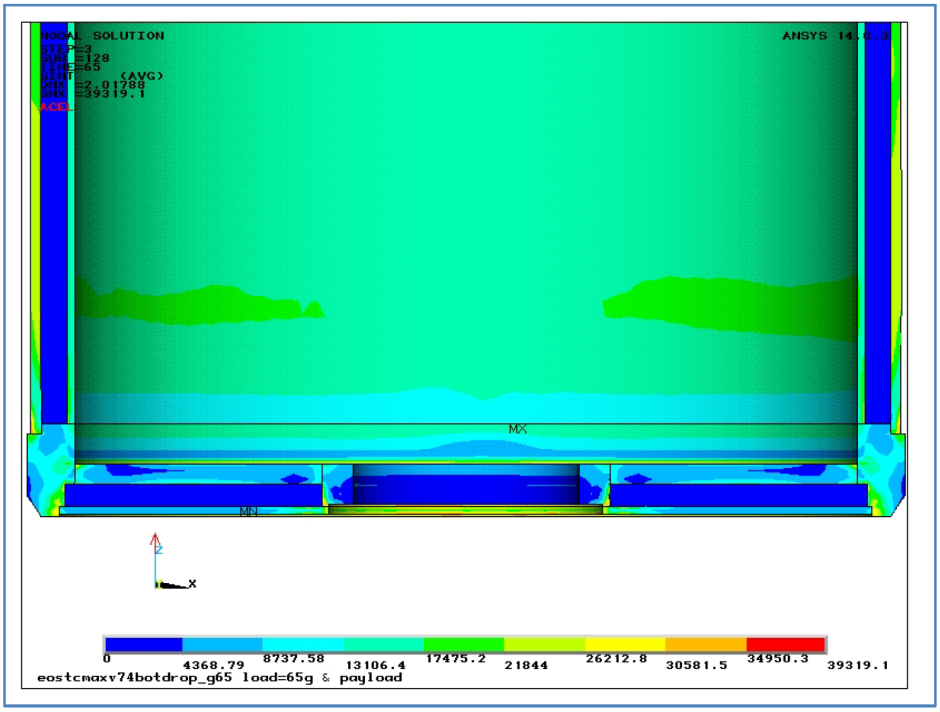

Figure 3.9.5-7
Stress Intensity (psi) plot for EOS-TCMAX – 65g Top End Drop

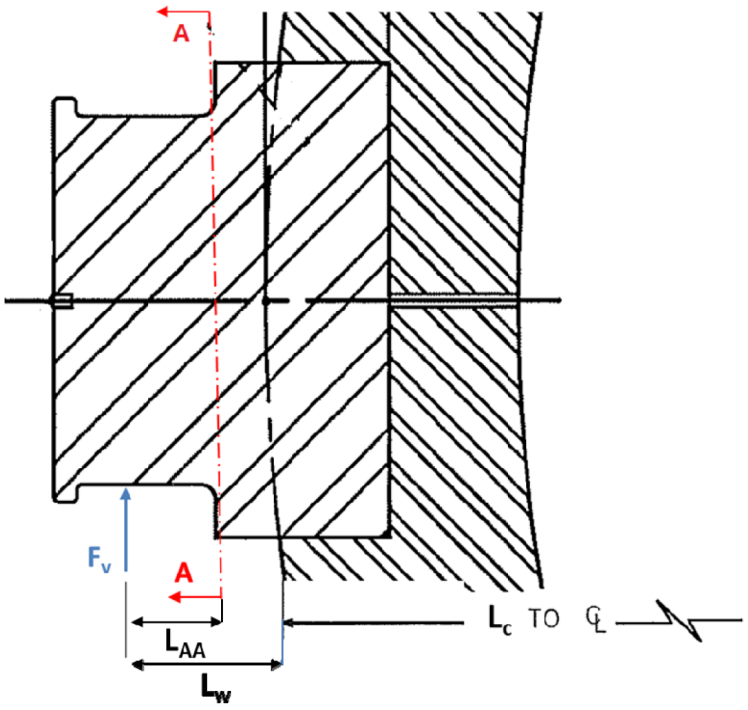

Figure 3.9.5-8
Upper Trunnion Sectional View

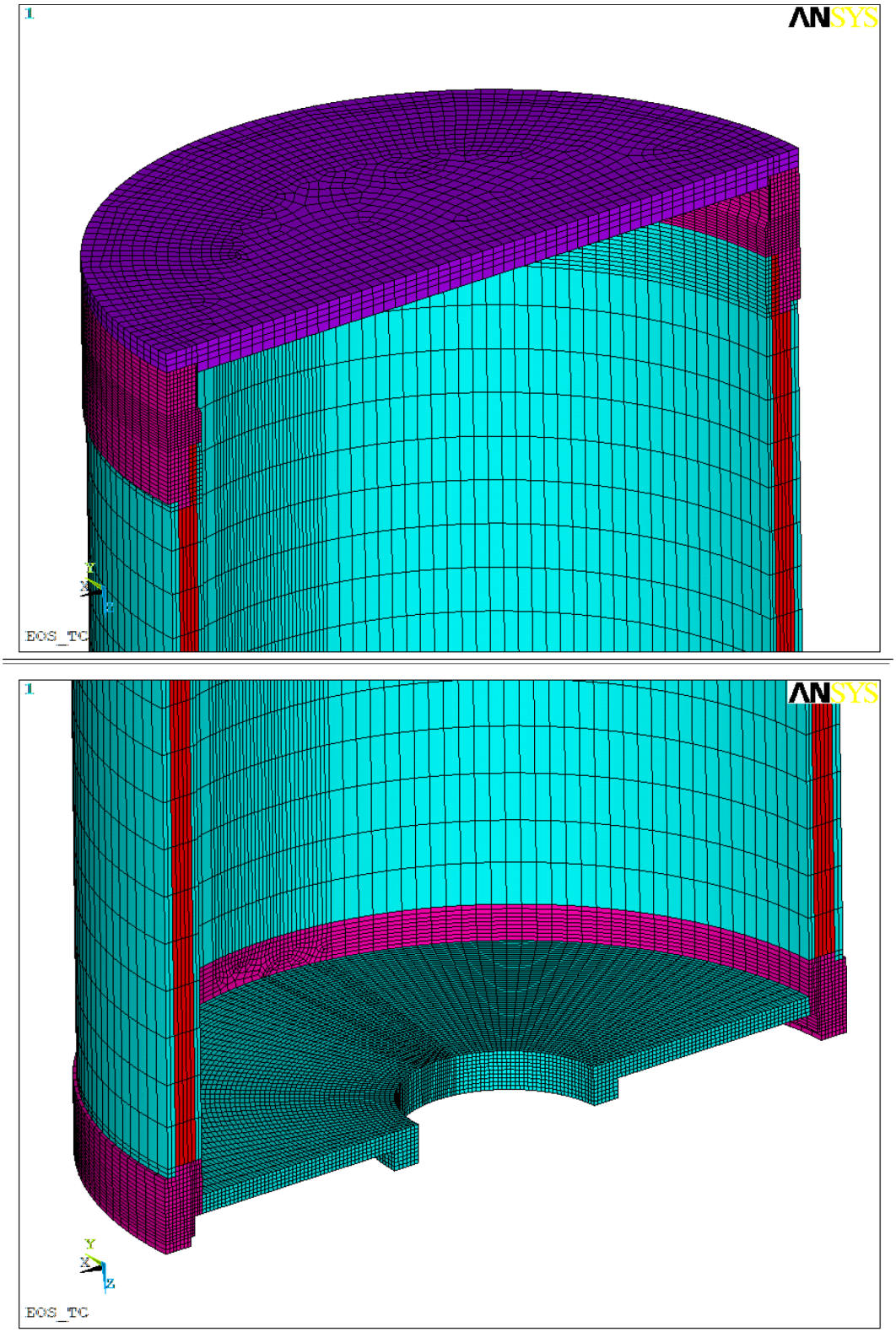

Figure 3.9.5-9
Cut Section Finite Element Model of EOS-TCMAX (Top and Bottom)

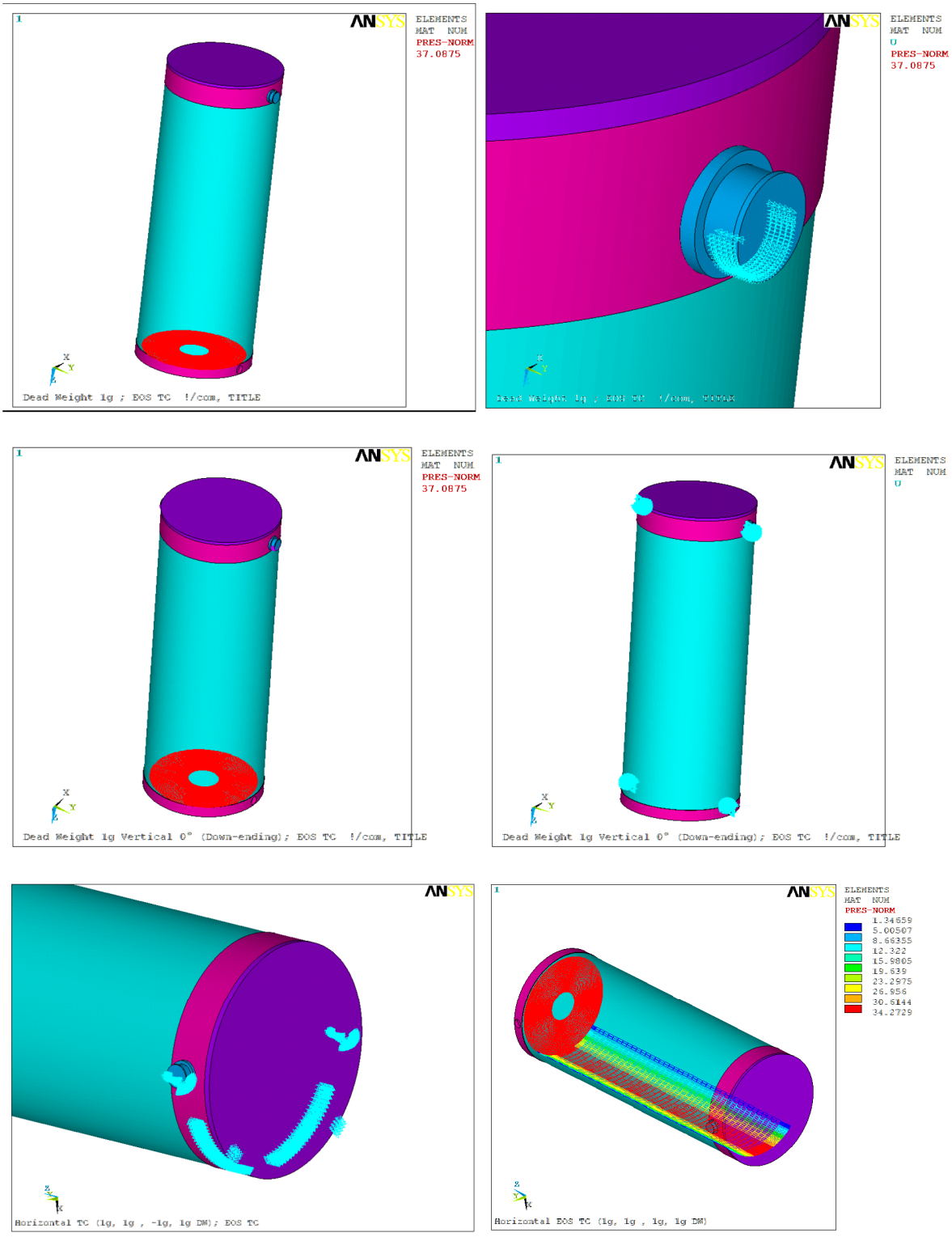

Figure 3.9.5-10
Pressure Load and Boundary Condition Plots

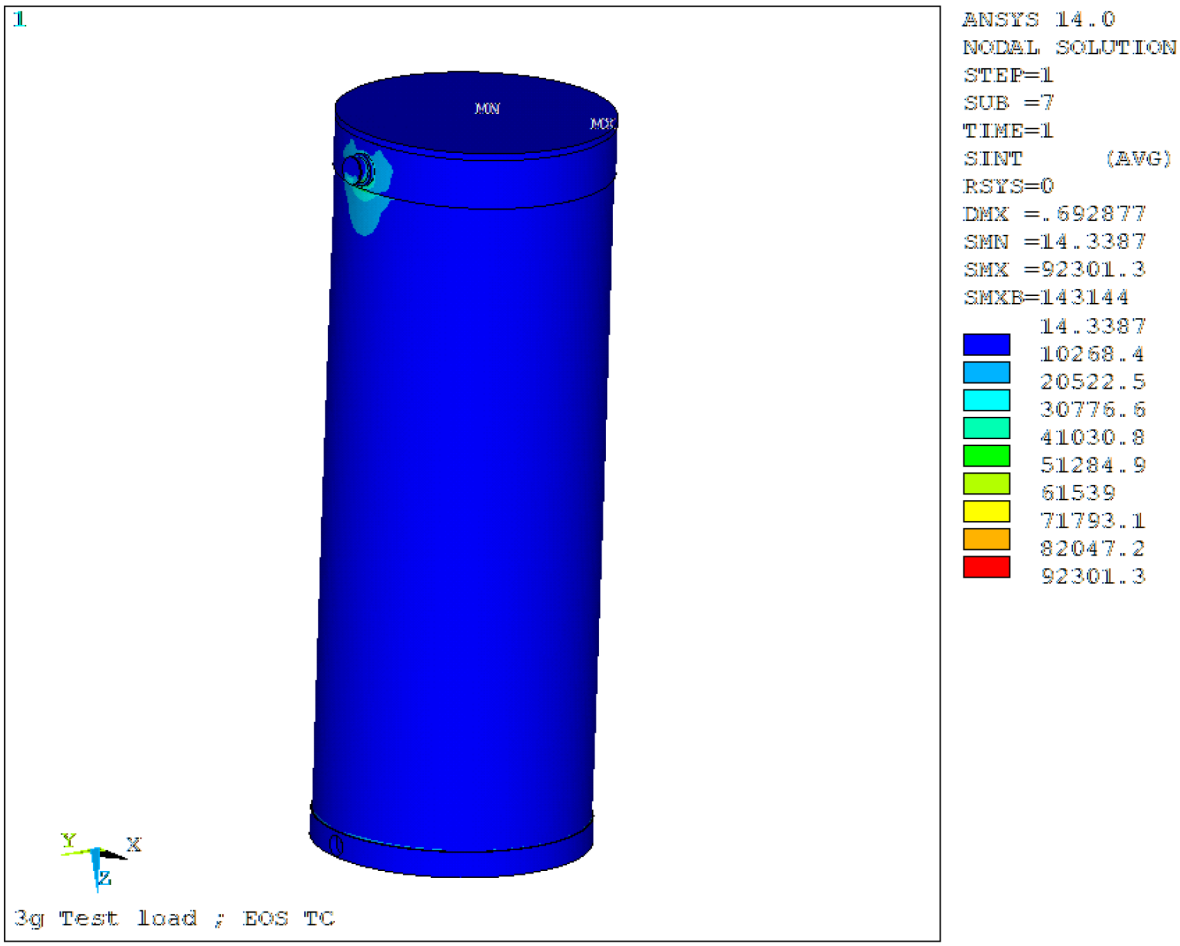

Figure 3.9.5-11
Stress Intensity (psi) Plot for Load Case 3g

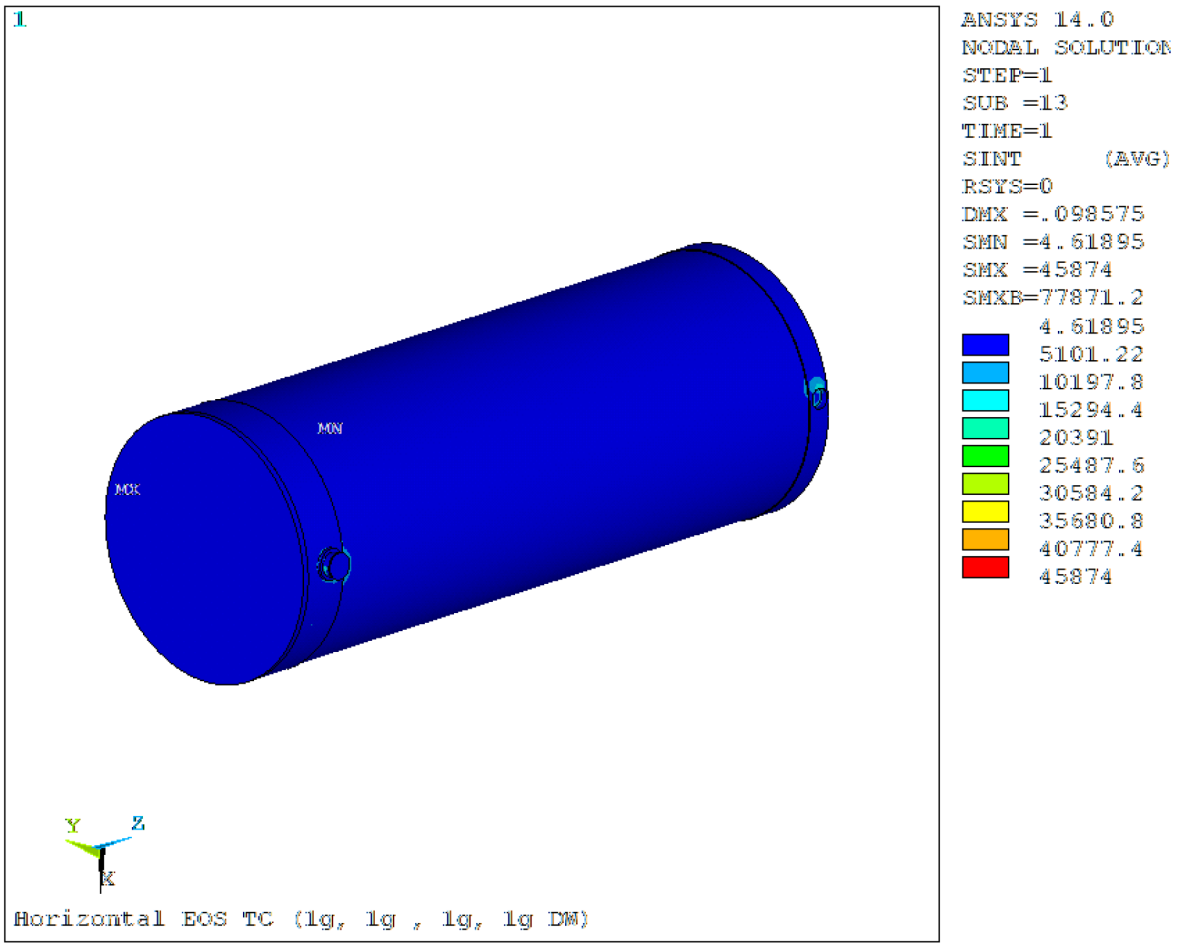

Figure 3.9.5-12
Stress Intensity (psi) Plot for Load Case Horizontal Transfer on Skid

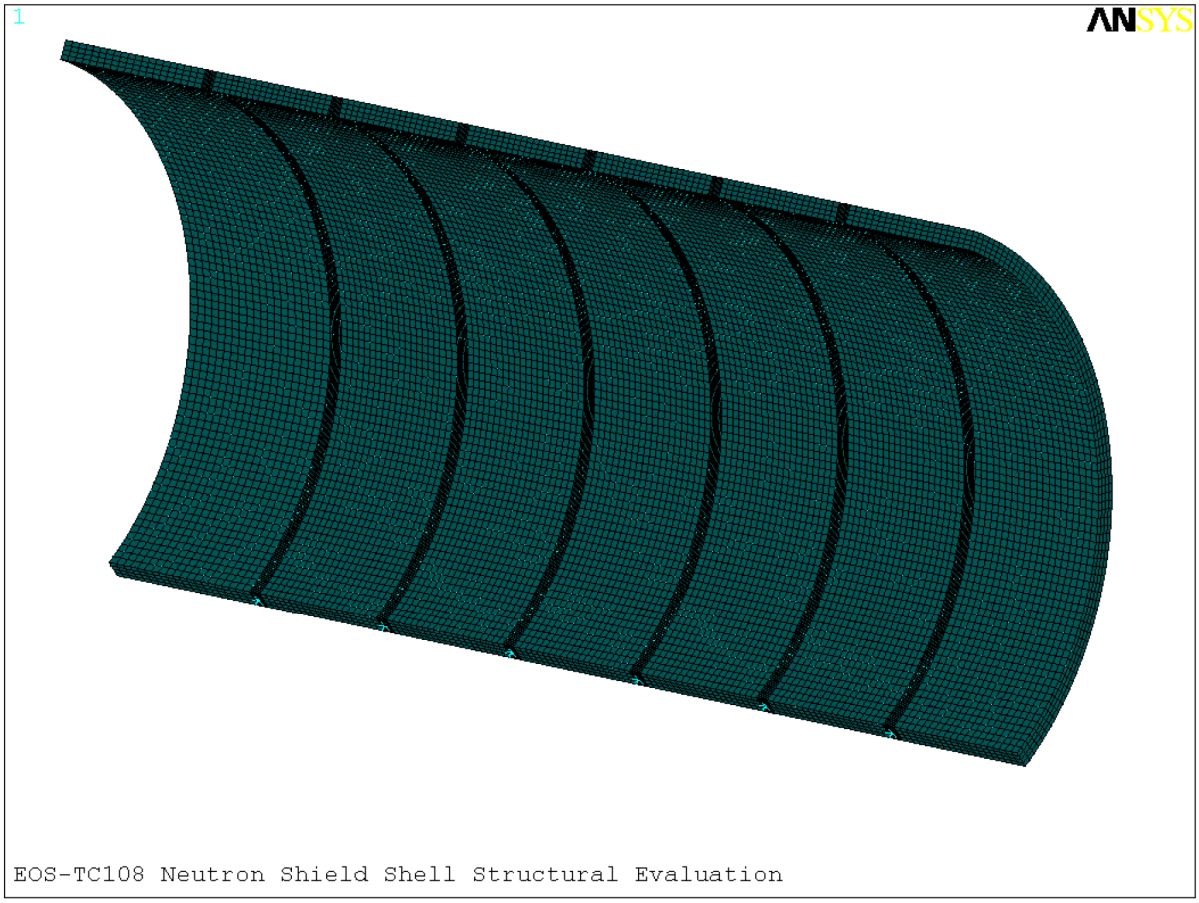

Figure 3.9.5-13
EOS-TC108 Meshed Model

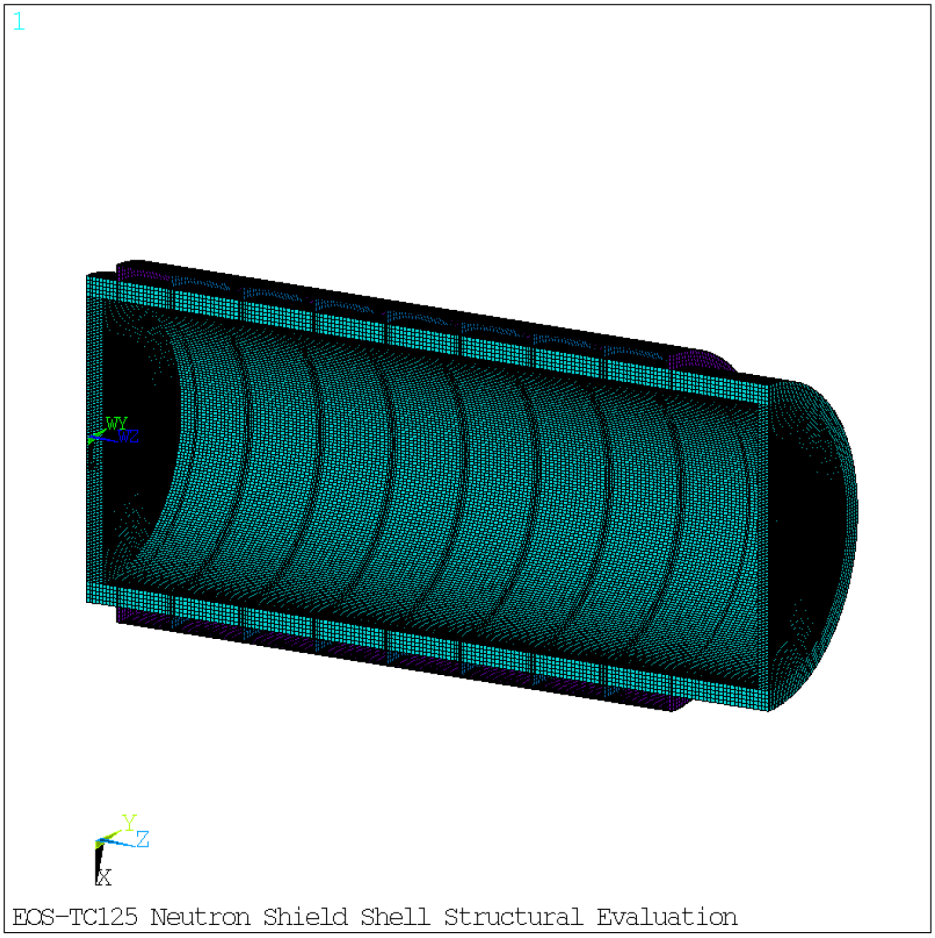

Figure 3.9.5-14
EOS-TC125 Meshed Model

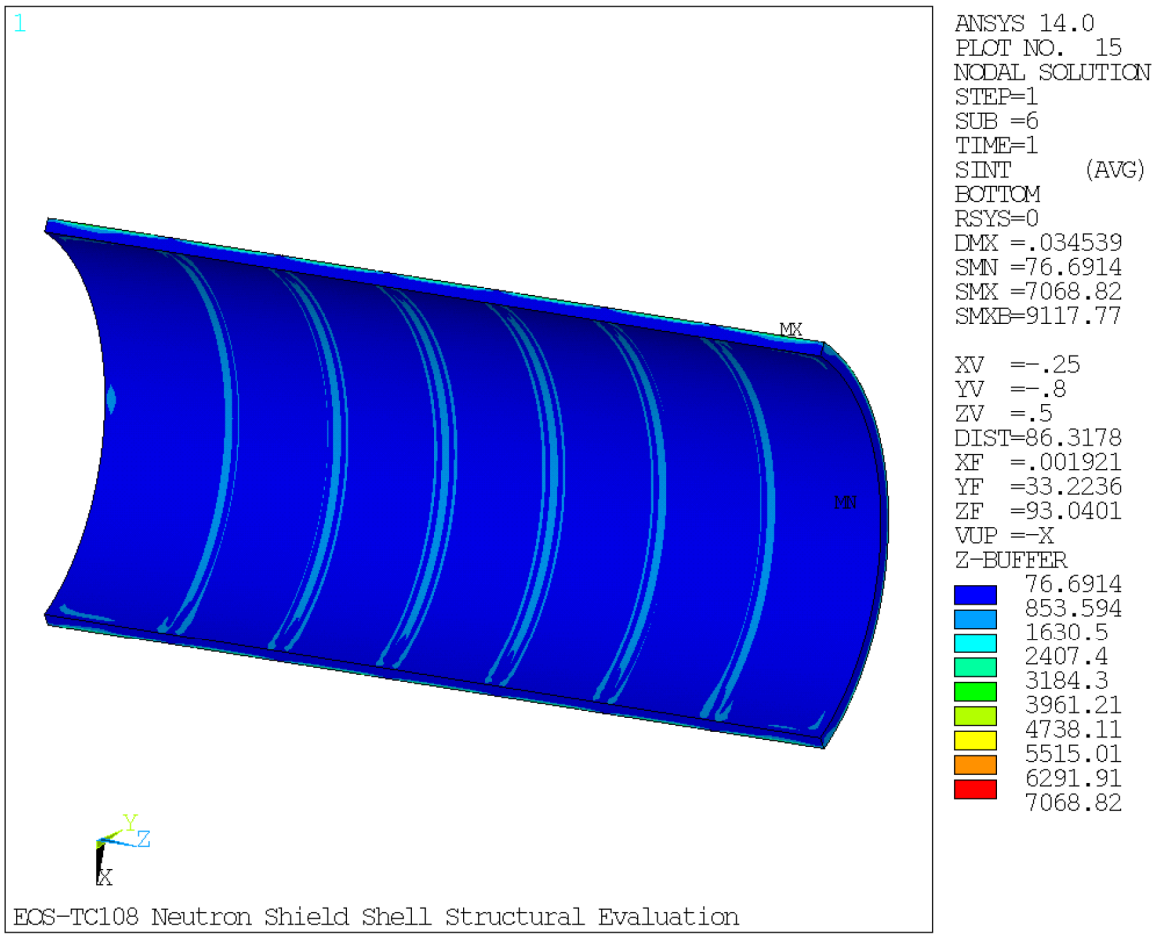

Figure 3.9.5-15
EOS-TC108 Neutron Shield Panel Stress Intensity (P_m+P_b) Plot Load Case E1

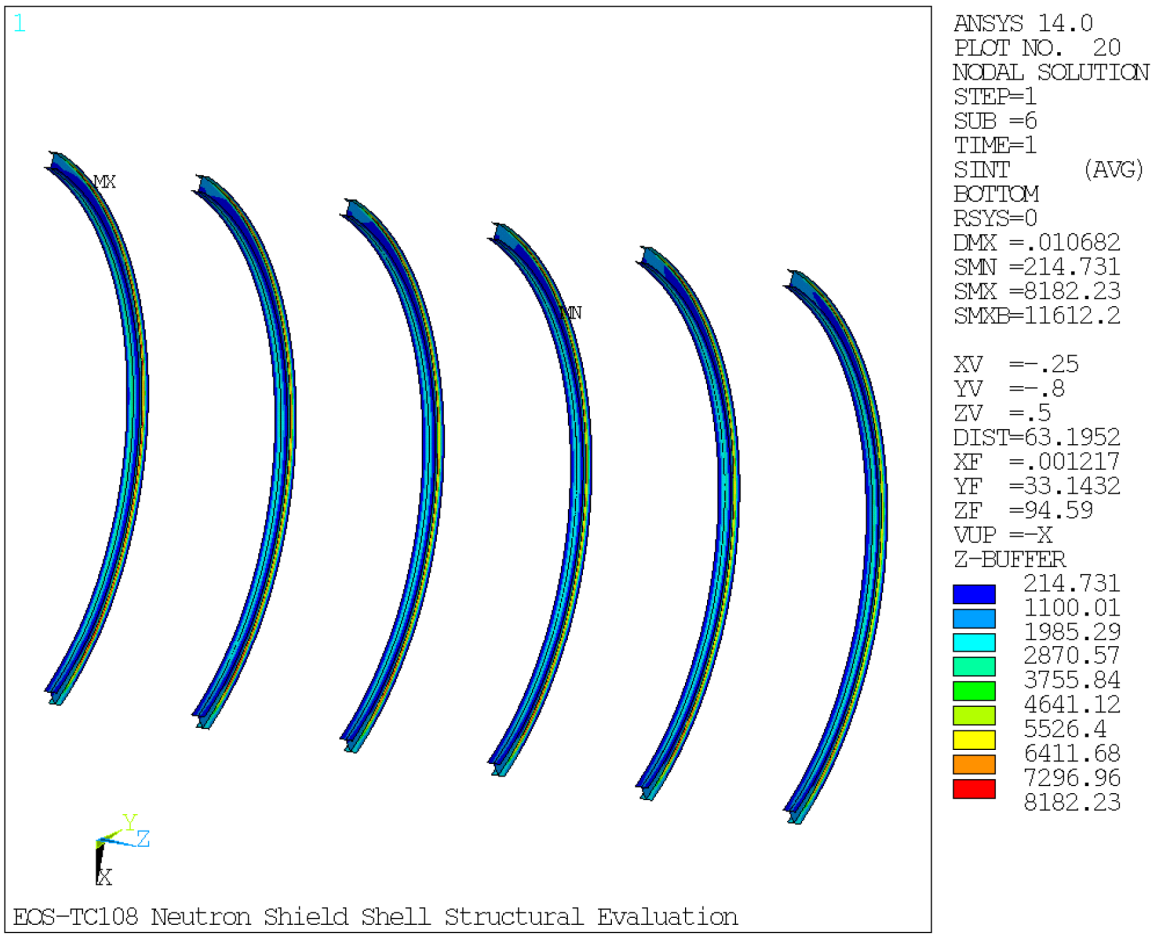

Figure 3.9.5-16
EOS-TC108 I-Beam Stress Intensity (P_m+P_b) Plot Load Case E1

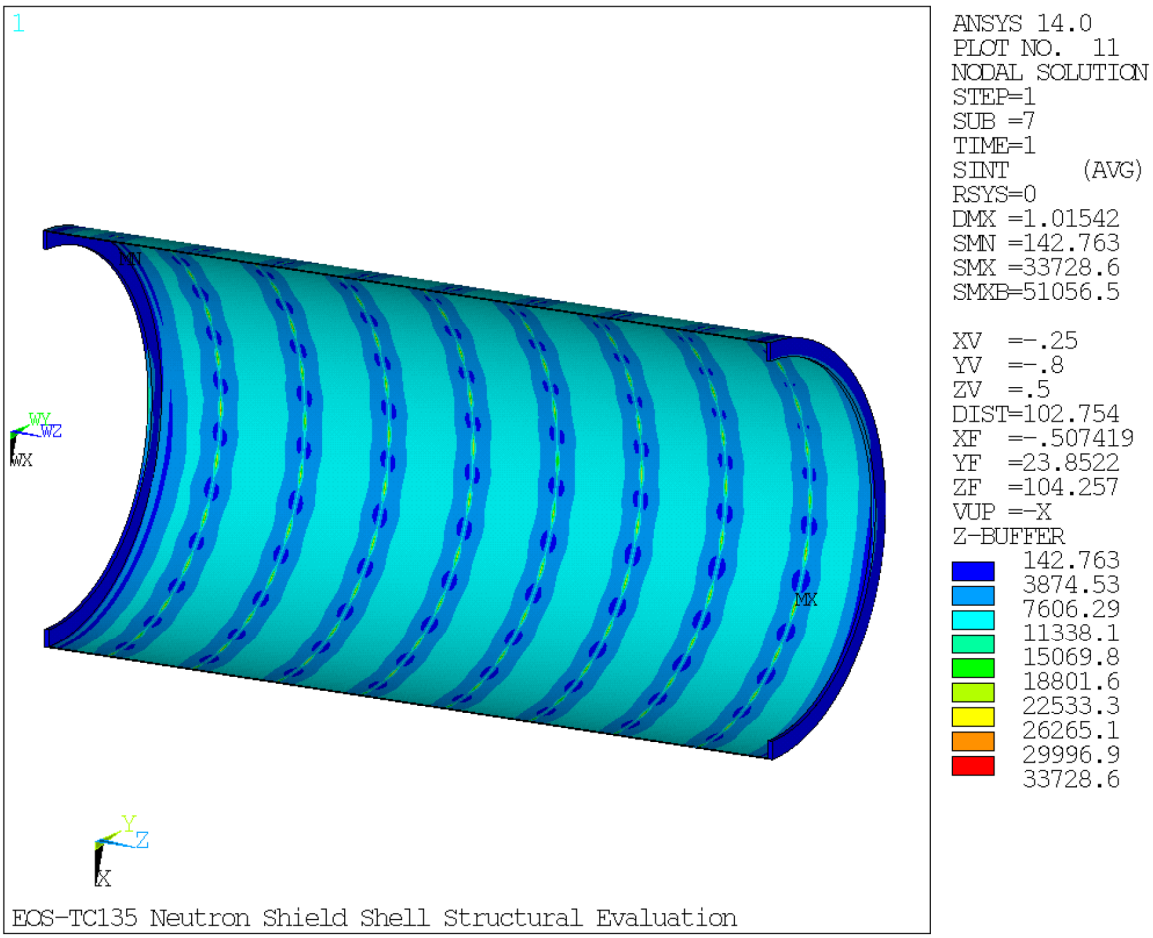

Figure 3.9.5-17
EOS-TC135 Neutron Shield Shell Stress Intensity Plot under Pressure Load (40 psig)

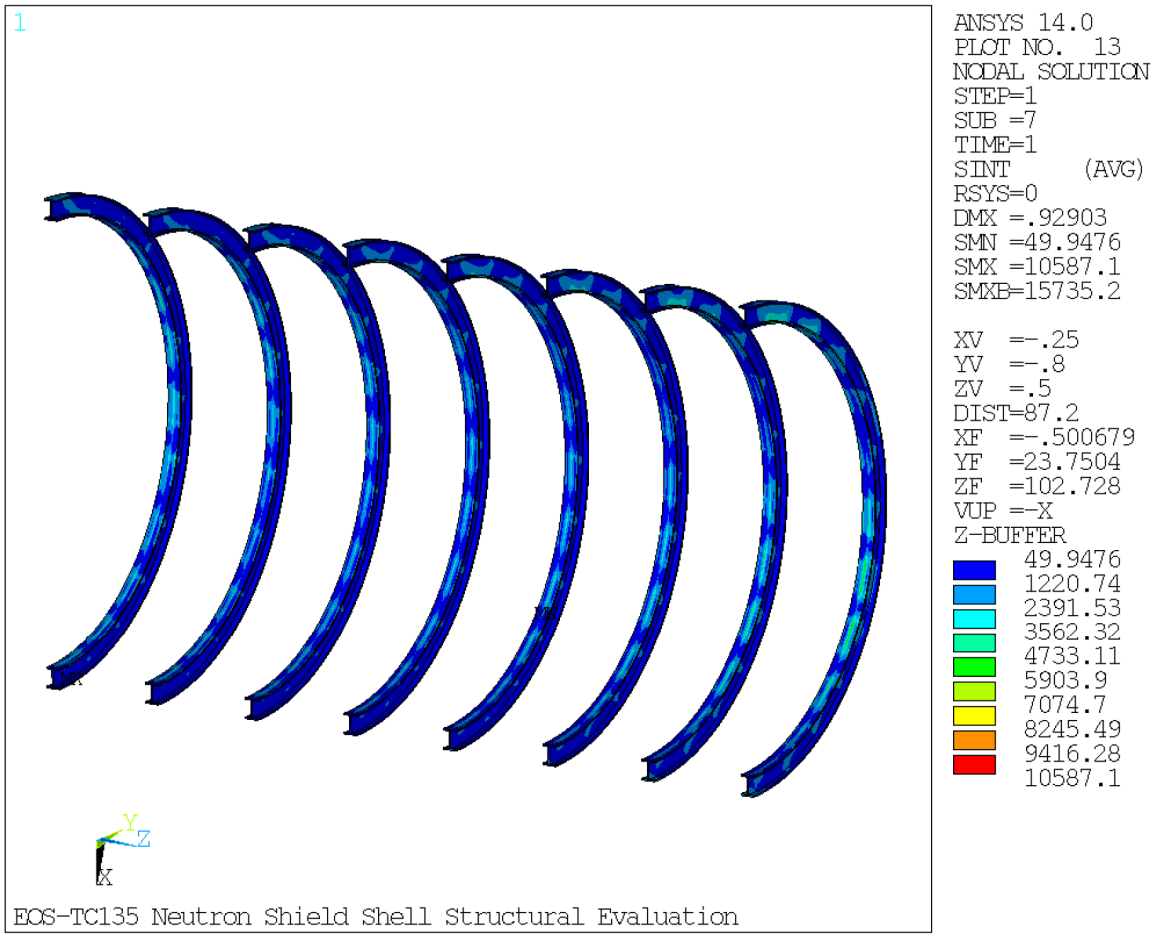

Figure 3.9.5-18
EOS-TC135 I-Beam Stress Intensity Plot under Pressure Load (40 psig)

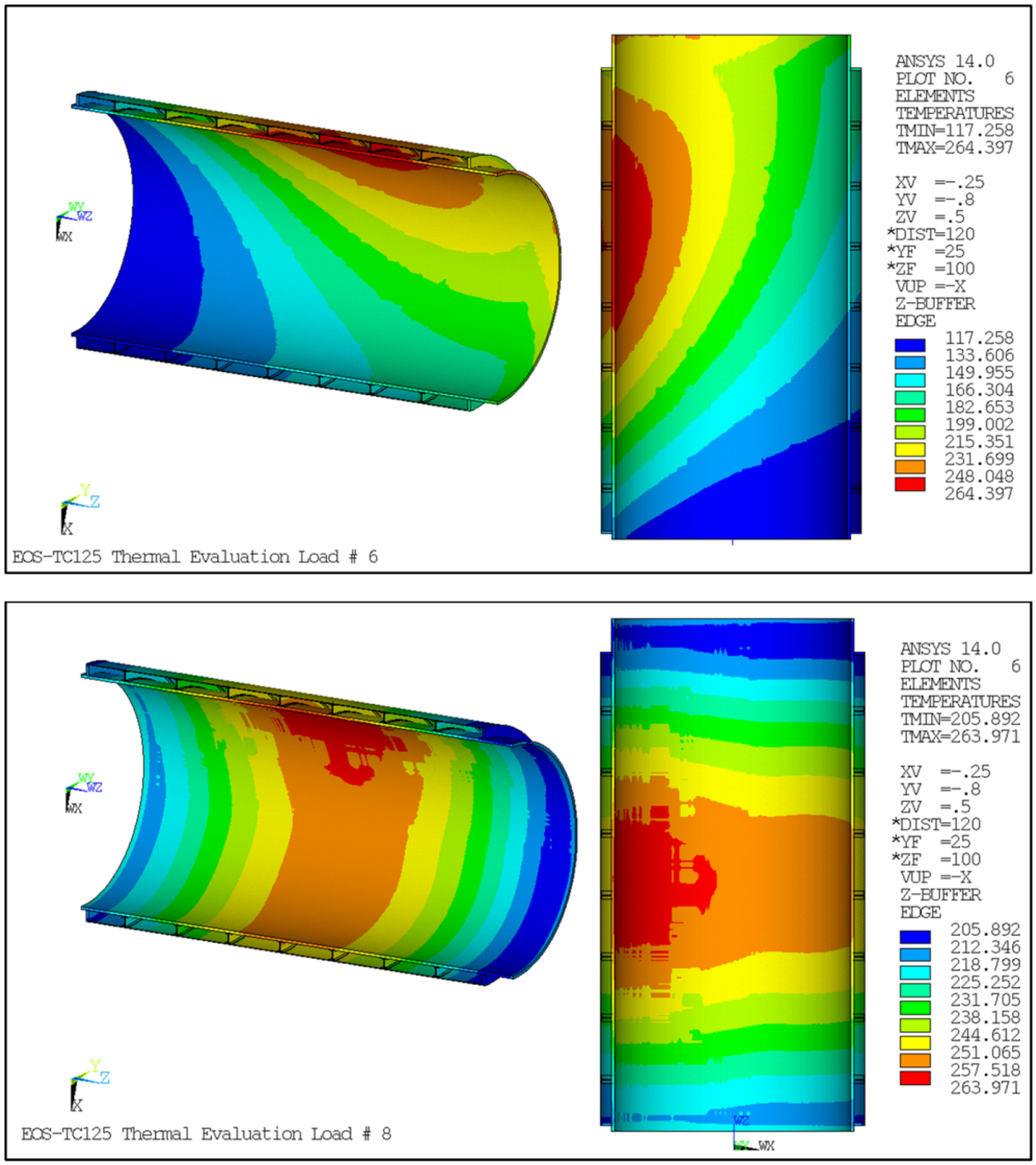

Figure 3.9.5-19
EOS-TC125 Temperature Distribution Plot

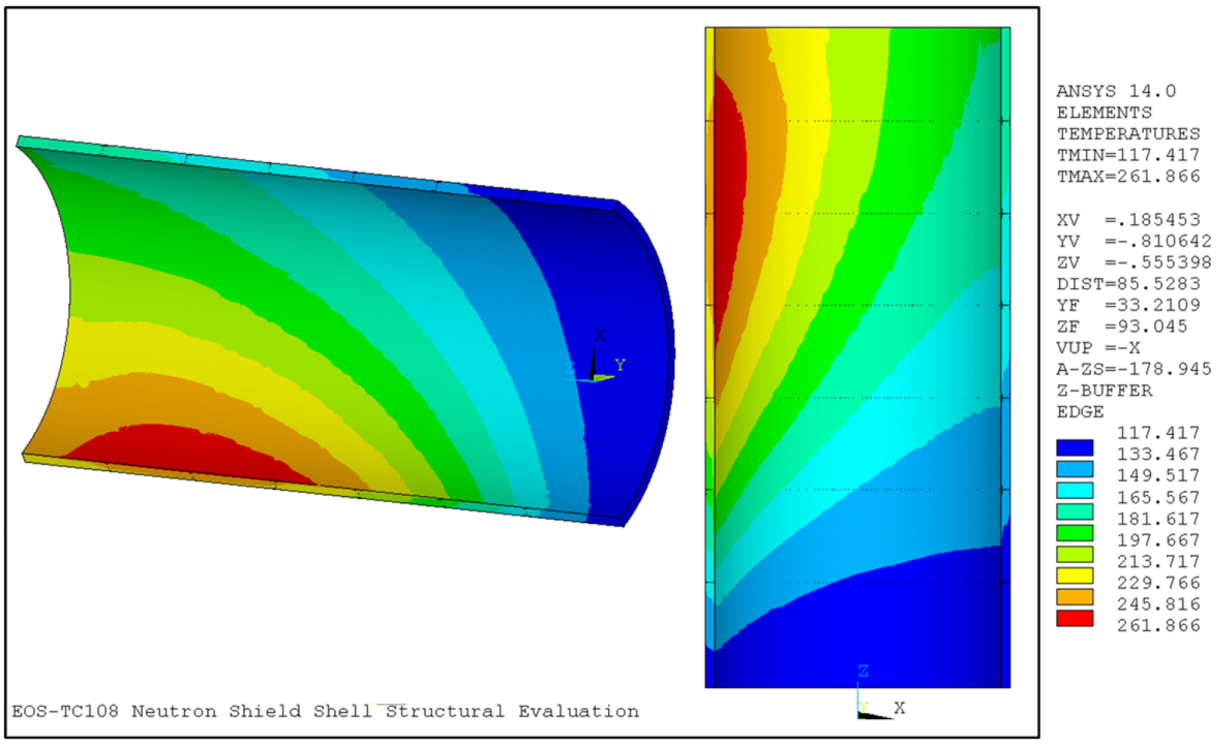

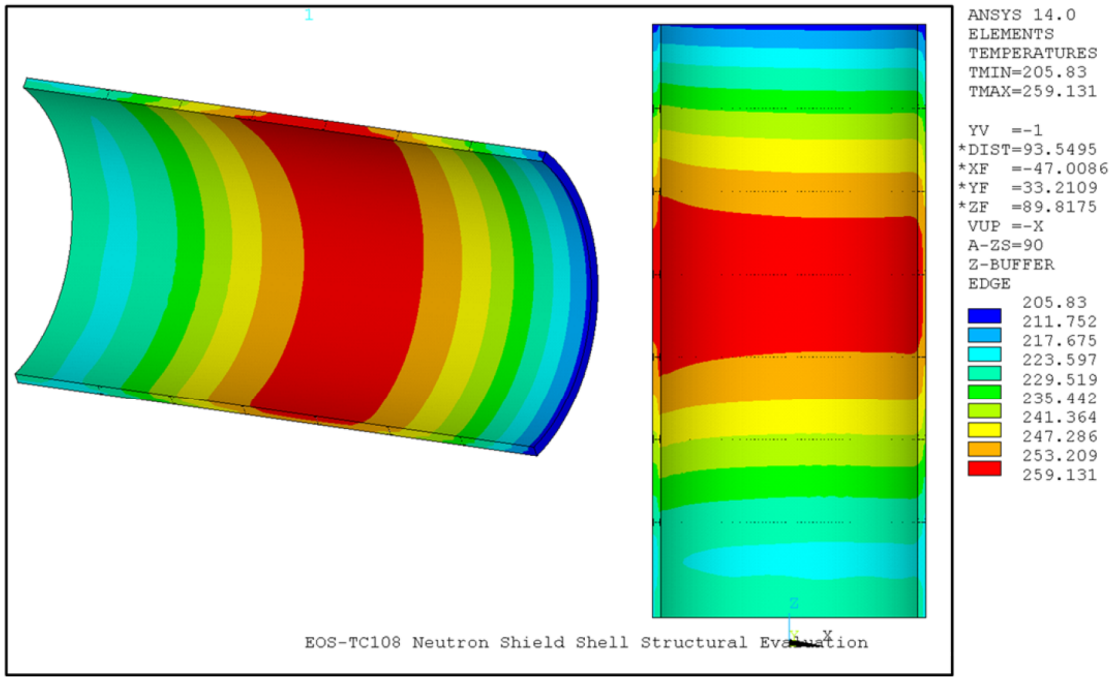

Figure 3.9.5-20
EOS-TC108 Temperature Distribution Plot

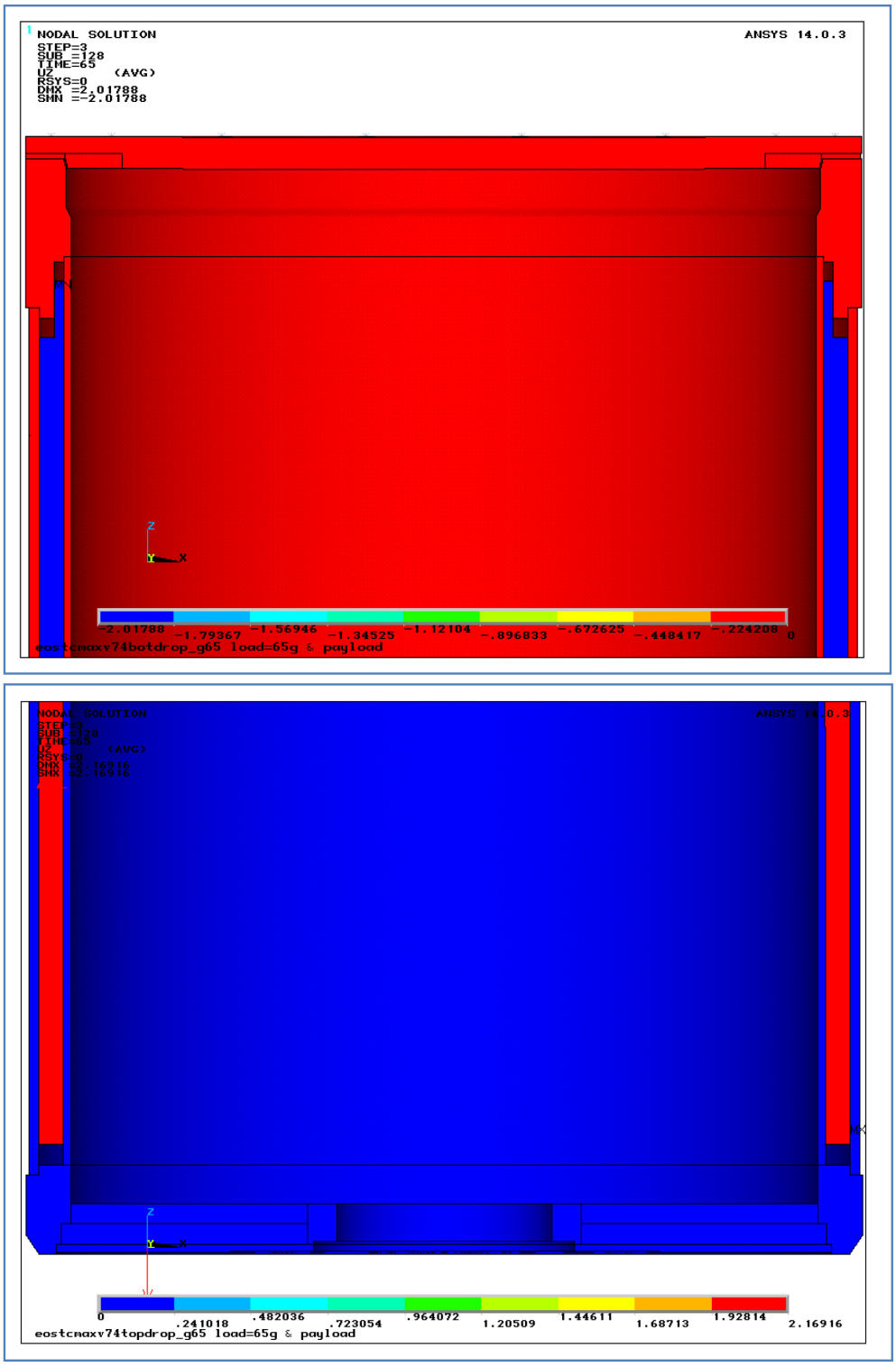

Figure 3.9.5-21
Bottom and Top, respectively, End Drops - Load 65g - Lead Slump Displacements

Proprietary Information on Pages 3.9.6-i through 3.9.6-iv and 3.9.6-1 through 3.9.6-55
Withheld Pursuant to 10 CFR 2.390

APPENDIX 3.9.7
NUHOMS® EOS SYSTEM STABILITY ANALYSIS

Table of Contents

List of Tables

List of Figures

3.9.7 NUHOMS® EOS SYSTEM STABILITY ANALYSIS

3.9.7.1 EOS-HSM Stability Evaluation

The sliding and overturning stability analyses due to design basis wind, flood, seismic, and massive missile impact loads are performed using hand calculations. The NUHOMS® EOS System consists of a reinforced concrete horizontal storage module (EOS-HSM) loaded with a dry shielded canister (DSC) (EOS-37PTH or EOS-89BTH).

3.9.7.1.1 General Description

The system consists of the dual-purpose (transport/storage) EOS-37PTH and EOS-89BTH DSCs, the EOS-HSM, and the onsite transfer cask (EOS-TC) with associated ancillary equipment. Each EOS-HSM is designed to store a DSC containing up to either 37 pressurized water reactor (PWR) or 89 boiling water reactor (BWR) spent fuel assemblies (SFAs).

The EOS-HSM storage modules can be arranged in both single-row or back-to-back-row arrays, with thick shield walls connected to the EOS-HSM at the ends of the arrays (end shield walls) and at the back end of the module (rear shield walls), if single-row arrays are used.

In the standard configuration, the EOS-HSM consists of two main segments: a base and a roof. The roof is installed on top of the base and is connected to it by bolts/embedments via four stiffened steel brackets located at each of the interior upper corners of the module's cavity. *Alternate designs of horizontal storage modules may be used in lieu of EOS-HSM as part of the NUHOMS® EOS System.*

The EOS-HSMS is a multi-segment design of a horizontal storage module, which consists of two segments of the base unit and a roof unit. The two segments of the base unit of EOS-HSMS are connected by grouted, high-strength, threaded bars/embedments, and the base and roof are connected in a similar way to that of EOS-HSM. An alternate Flat Plate Support Rail design of horizontal storage module, the EOS-HSM-FPS, may also be used in lieu of EOS-HSM as a part of the NUHOMS® EOS System. EOS-HSM-FPS is modified from the EOS-HSM to support the FPS DSC Support Structure with concrete pedestals spaced along the length of the DSC Support Structure. EOS-HSMS-FPS is a multi-segment design of the EOS-HSM-FPS, which consists of two segments of the base unit and a roof unit. The two segments of the base unit of EOS-HSMS-FPS are connected by grouted, high-strength, threaded bars/embedments, and the base and roof are connected in a similar way to that of EOS-HSM-FPS. EOS-HSM is used herein for all alternatives unless a unique situation is presented. EOS-HSM-FPS is used herein for both the EOS-HSM-FPS and EOS-HSMS-FPS unless a unique situation is presented.

3.9.7.1.2 Material Properties

The EOS-HSM assembly is constructed of reinforced concrete and steel. This analysis considers rigid body motions. Therefore, the mechanical properties of the materials are not used as design inputs in this evaluation.

3.9.7.1.3 Mass Properties

The mass properties of the EOS-HSM are listed in Table 3.9.7-1. Bounding values of concrete density (140 pcf, 150 pcf, and 160 pcf) are considered.

3.9.7.1.4 Friction Coefficients

The static analyses are performed using a concrete-to-concrete friction coefficient of 0.6.

3.9.7.1.5 Methodology

The stability of the EOS-HSM unit is evaluated for four load cases that may cause overturning and sliding of a single freestanding module. These four load cases are:

- Tornado-generated wind loads
- Massive missile impact loads
- Flood loads
- Seismic loads

3.9.7.1.6 Assumptions

1. The analyses assume that the dynamic coefficient of friction is equal to the static coefficient. This assumption maximizes the rocking uplift displacements of the EOS-HSM (particularly for the high friction coefficient analysis cases).

2. The differential pressure load caused by the tornado pressure drop does not affect the overall stability of the EOS-HSM and is ignored. The structure is vented, and so any differential pressure is very brief, while the internal and external pressures equilibrate. Since the structure is symmetric, the temporary internal pressure in the EOS-HSM caused by the negative tornado pressure does not cause any unbalanced loads on the EOS-HSM that would cause sliding and/or overturning.

3. This stability evaluation is applicable to both the standard EOS-HSM design, as well as the segmented EOS-HSMS design. The weight and inertia properties of the EOS-HSM and the EOS-HSMS are the same.

3.9.7.1.7 Loads and Boundary Conditions

3.9.7.1.7.1 Earthquake Input

The seismic stability evaluation is performed for a horizontal acceleration of 0.45g and vertical acceleration of 0.30g.

In addition, a 1.1 load factor is added to the seismic load.

3.9.7.1.7.2 Wind and Tornado Input

The EOS-HSM is evaluated for overturning and sliding due to the design basis tornado (DBT) specified in Chapter 2. The DBT is based on the NRC Reg. Guide 1.76 Region I Intensities. The maximum wind speed is 360 mph. The tornado loads are generated for three separate loading phenomena, as follows, which is combined in accordance with Section 3.3.2 of NUREG-0800 [3.9.7-1] (i.e. tornado wind load is concurrent with (additive to) tornado missile loads).

1. Pressure or suction forces created by drag as air impinges and flows past the EOS-HSM with a maximum tornado wind speed of 360 mph.

2. Suction forces due to a tornado generated pressure drop or differential pressure load of 3 psi.

3. Impact forces created by tornado-generated missiles impinging on the EOS-HSM.

Per NUREG-0800, the total tornado load on a structure is combined as follows:

$$W_t = W_p$$
$$W_t = W_w + 0.5W_p + W_m$$

Where,

W_t = Total tornado load
W_w = Load from tornado wind effect
W_p = Load from tornado atmospheric pressure change effect
W_m = Load from tornado missile impact effect

Note that W_p is not applicable to the stability analysis as discussed in Section 3.9.7.1.6. Thus, the load combination for tornado loading for this analysis is simplified to:

$$W_t = W_w + W_m$$

In addition, a 1.1 load factor is added to Dead weight + Tornado load.

The envelope of a range of missiles from Chapter 2 is used for the missile impact load.

As seen from Table 3.9.7-2 the automobile impact on to the EOS-HSM has the maximum momentum and is considered as bounding evaluation.

3.9.7.1.7.3 Flood Input

The EOS-HSM is evaluated for a flood height of 50 feet with a water velocity of 15 fps.

In addition, a 1.1 load factor is added to Dead weight + Flood load per Table 2-7 of Chapter 2.

3.9.7.1.8 Stability Analysis

The load categories associated with the EOS-HSM stability analysis are described in the previous section. The analysis steps and results for each load category are presented in this section.

3.9.7.1.8.1 Design Basis Tornado

The EOS-HSM is evaluated for forces created by drag as air impinges and flows past the EOS-HSM with a maximum tornado wind speed of 360 mph.

For sliding and overturning analysis, it is assumed that the module is subjected to the load due to 218 psf windward pressure loading acting on the end shield wall. The leeward side of the same module is subjected to a wind suction load of 154 psf. A suction of 326 psf is applied to the roof, including the top part of the shield walls. The loads are shown in Table 3.9.7-3.

In addition, missiles loads are combined with the tornado wind load per NUREG-800 [3.9.7-1].

3.9.7.1.8.1.1 Static Overturning Analysis due to Tornado Wind

The loaded EOS-HSM, the rear wall, one corner block, and one end shield wall rotates about B, shown in Figure 3.9.7-1. The other end shield wall and corner block rotates about point A, shown in Figure 3.9.7-1. Conservatively, the overturning of the loaded module with one end shield wall about point B is considered for the stabilizing moment.

In the overturning analysis of the EOS-HSM, the effects of tornado wind forces are first determined. An overturning moment is then calculated and is compared with a stabilizing moment. The minimum safety factor against overturning computed for all the three design lengths of EOS-HSM due to tornado wind is 1.59.

3.9.7.1.8.1.2 Dynamic Overturning Analysis of Tornado Wind Concurrent with Massive Missile Impact Loading

A dynamic analysis based on the conservation of energy is conducted for the combined effects of wind and concurrent massive missile impact loading. The effects of the concurrent massive missile impact loads are used in determining the initial angular momentum from the conservation of angular momentum equation using the wind loads from the previous section. Then the angle of rotation is determined from the conservation of energy of the concurrent loading.

The wind loads are calculated conservatively for EOS-HSM Long:

$$F_{hw} = (F_{windward} + F_{leeward})(L_{base})(h_{HSM+roof})$$

$$F_{vw} = (F_{roof})(L_{base})(w_{HSM+shield})$$

The concurrent wind loading is accounted for by reducing the inertia that resists motion in the denominator of the equation.

$$\omega_B = \frac{m_m \cdot d_m \cdot v_i}{m_m \cdot d_m^2 + I_{tot} - \left(\frac{F_{hw}}{g}\right)\left(\frac{h}{2}\right)^2 - \left(\frac{F_{vw}}{g}\right)\left(\frac{w}{2}\right)^2}$$

Where,

F_{hw} = Horizontal tornado wind load
F_{vw} = Vertical tornado wind load
ω_B = Angle of rotation
m_m = Mass of the missile
d_m = Distance from missile impact to floor
v_i = Initial missile velocity
I_{tot} = Total moment of inertia of HSM + Front end shield wall
h = Height of HSM + roof
w = Width of HSM + end shield wall

The conservation of energy is used for overturning.

Rotational Kinetic Energy = Change in Potential Energy – Work Done by Horizontal Wind force

$$\frac{I_{tot}\omega_B^2}{2} = (W - F_{vw}) \cdot r \cdot [\sin(\beta + \theta) - sin\beta] - F_{hw} \cdot r \cdot [\cos(\beta + \theta) - cos\beta]$$

Where,

θ = Angle of tipping
β = Angle from the horizontal to center of gravity (CG) of EOS-HSM (68.3°)

r = Diagonal distance from CG to point B
I_{tot} = Total moment of Inertia of HSM + Left end shield wall
W = Weight of the loaded HSM + Left end shield wall

The loaded EOS-HSM is stable against overturning as tip-over does not occur until the CG rotates past the edge (point B, Figure 3.9.7-1) of the HSM to an angle of more than 90°- 68.3° = 21.7°

A loaded EOS-HSM rotates a maximum of 0.7 degrees, which is less than the 21.7 degrees required to overturn the module.

3.9.7.1.8.1.3 Time-Dependent Overturning Analysis of Tornado Wind Concurrent with Massive Missile Impact Loading

In addition to the dynamic overturning analysis, a time dependent analysis is used to ensure the absence of any overturning.

An approximate relationship for the deceleration of an automobile impacting a rigid wall is given by:

$$-\ddot{x} = 12.5g \cdot x \qquad Eq.D-1\ of\ [3.9.7\text{-}4]$$

$-\ddot{x}$ = Deceleration (ft/sec^2)
x = Distance automobile crushes into target (ft)

A force time history is obtained:

$$F = 0.625 V_s W_m sin20t \qquad Eq.D-6\ of\ [3.9.7\text{-}4]$$

The overturning moment is:

$$M_{ot} = F \cdot d_m + \frac{F_{hw} h}{2}$$

Where,

d_m = Distance from missile impact to floor
h = Vertical height to the top of EOS-HSM and is a function of rotation

The stabilizing moment is:

$$M_{st} = (W_{HSM} - F_{vw}) \cdot r cos(\beta + \theta) + W_{end\ shield} \cdot r_{end} cos(\gamma + \theta)$$

Where,

W_{HSM}= Weight of the loaded EOS-HSM
r = Diagonal distance from CG to point B
θ = Angle of rotation
r_{end} = Diagonal distance from CG of end shield wall to point B
γ = Angle from horizontal to CG of end shield wall

The moment causing acceleration is:

$$M_{acc} = M_{ot} - M_{st}$$

The angular velocity is:

$$\omega_i = \left[\frac{M_{acc,i} + M_{acc,i-1}}{2} \cdot (t_i - t_{i-1})\right] / I_{tot} + \omega_{i-1}$$

Where,

i = Index for current time step
i-1 = Index for previous time step
I_{tot} = Total moment of Inertia of HSM + Left end shield wall

The angle of rotation is:

$$\theta_i = \left[\frac{\omega_i + \omega_{i-1}}{2} \cdot (t_i - t_{i-1})\right] + \theta_{i-1}$$

The angles of rotation resulting from these analyses are shown in Figure 3.9.7-2 through Figure 3.9.7-4. The governing angle of rotation is 3.12 degrees, which is less than the 21.7 degrees required to overturn the module.

3.9.7.1.8.1.4 Sliding Analysis for Tornado Wind Concurrent with Massive Missile Impact loading

The combined wind + missile impact case is considered for EOS-HSM sliding analysis based on the conservation of energy.

First, the conservation of momentum is used for the sliding analysis.

$$V = \frac{m \cdot v_i}{M/1.07 + m - F_{hw}/386.4}$$

Where,

V = Initial linear velocity of module after impact
v_i = Initial velocity of missile
m = Mass of the missile
M_1 = Mass of empty EOS-HSM Short
M_2 = Mass of end shield wall
M_3 = Mass of governing loaded EOS-89BTH DSC
M = Total mass = $M_1 + M_2 + M_3$
1.07 is the factor used to account for the uncertainty of the concrete density.

Then using the conservation of energy:

$$Friction\ Energy = Initial\ Kinetic\ Energy\ of\ System + Work\ done\ by\ Wind$$

$$\mu \cdot (gM/1.07 - F_{vw})d = \frac{(M/1.07 + m) \cdot V^2}{2} + F_{hw}d$$

Where,

μ	=	0.6 coefficient of friction for concrete-to-concrete surfaces
F_{vw}	=	Uplift force generated by DBT wind pressure on the roof
d	=	Sliding distance of EOS-HSM
F_{hw}	=	Sliding force generated by DBT wind pressure

The sliding distance of the EOS-HSM module is calculated to be 1.62 inches.

3.9.7.1.8.1.5 Time-Dependent Sliding Analysis for Tornado Wind Concurrent with Massive Impact Loading

In addition to the dynamic sliding analysis, a time dependent analysis is used to provide a bounding sliding displacement.

The total force causing sliding is:

$$F_{slide} = F + F_{hw}$$

The resisting force from friction is:

$$F_{resis} = \mu(W - F_{vw})$$

Therefore the force causing acceleration is:

$$F_{acc} = F_{slide} - F_{resis}$$

The velocity is:

$$v_i = \left[\frac{F_{acc,i} + F_{acc,i-1}}{2} \cdot (t_i - t_{i-1})\right] / m_{tot} + v_{i-1}$$

Where,

i	=	Index for current time step
i-1	=	Index for previous time step
m_{tot}	=	Total mass of loaded EOS-HSM and both end shield walls including adjustment for density uncertainty

The sliding displacement is:

$$x_i = \left[\frac{v_i + v_{i-1}}{2} \cdot (t_i - t_{i-1})\right] + x_{i-1}$$

The sliding displacements resulting from these analyses are shown in Figure 3.9.7-5 through Figure 3.9.7-7. The governing sliding displacement is 1.30 inches which is bounded by sliding distance of 1.62 inches resulting from dynamic sliding analysis as calculated in Section 3.9.7.1.8.1.4.

3.9.7.1.8.2 Flood Loads

The EOS-HSM is designed for a flood height of 50 feet and water velocity of 15 fps. The module is evaluated for the effects of a water current of 15 fps impinging on the side of a submerged EOS-HSM. Under 50 feet of water, the inside of the module is rapidly filled with water. Therefore, the EOS-HSM components are not evaluated for the 50 feet static head of water.

Calculation of the drag pressure due to design flood is shown in Appendix 3.9.4.

3.9.7.1.8.2.1 Overturning Analysis

The factor of safety against overturning of a single EOS-HSM with shield walls, for the postulated flooding conditions, is calculated by summing moments about the bottom outside corner of a single, freestanding EOS-HSM. The factors of safety against overturning for a single, freestanding EOS-HSM due to the postulated design basis flood water velocity are 1.14, 1.12, *1.11,* and 1.13 for the EOS-HSM Short, EOS-HSM Medium*, EOS-HSM-FPS Medium,* and EOS-HSM Long, respectively.

3.9.7.1.8.2.2 Sliding Analysis

The factor of safety against sliding of a freestanding single EOS-HSM due to the maximum postulated flood water velocity of 15 fps is calculated using methods similar to those described above. The effective weight of the EOS-HSM including the DSC and end shield wall acting vertically downward, less the effects of buoyancy acting vertically upward is calculated. The factors of safety against sliding for a single, freestanding EOS-HSM due to the postulated design basis flood water velocity are 1.12, 1.09, *1.08,* and 1.11 for the EOS-HSM Short, EOS-HSM Medium*, EOS-HSM-FPS Medium,* and EOS-HSM Long, respectively.

3.9.7.1.8.3 Seismic Load

The EOS-HSM is evaluated for maximum values for seismic accelerations of 0.45g in the horizontal direction and 0.30g in the vertical direction. Both the loaded EOS-HSM and the empty EOS-HSM are considered for these loads. The EOS-HSM and one end shield wall rotate about B, shown in Figure 3.9.7-1. The other end shield wall, corner blocks and rear shield walls are conservatively ignored.

The combination of 100% of horizontal acceleration and 40% of vertical acceleration is used.

3.9.7.1.8.3.1 Static Overturning Analysis of the EOS-HSM due to Seismic Load

The stabilizing and overturning moments are calculated and compared, and the case considering the bounding 140 pcf concrete density and the minimum DSC weight to minimize the stabilizing moment is shown below. The stability overturning analysis shown is for the governing EOS-HSM Long model. A factor of 1.07 (150 pcf/140 pcf) reduces the considered mass to the 140 pcf lower bound case. The 160 pcf upper bound is also considered, but not shown here.

Stabilizing Moment = $M_{st} = (W_{HSM} + W_{DSC}) \times d_{HSM-B} + W_{end\_shield\_wall} \times d_{end\_shield\_wall-B}$

$$M_{st} = \left(\frac{330kip}{1.07} + 134kip\right) \times (48in) + \left(\frac{187.1kip}{1.07}\right) \times (124in)$$

$M_{st} = 42{,}900$ kip-in

Where a factor of 1.07 (150pcf/140pcf) is used to account for the uncertainty of the concrete density.

Overturning Moment =

$$M_{ot} = 0.4a_v \times \left(W_{HSM}x_{HSM} + W_{DSC}x_{DSC} + W_{wall}x_{wall}\right) + a_h(W_{HSM}y_{HSM} + W_{DSC}y_{DSC} + (W_{wall}h_{wall})/2)$$

$$M_{ot} = 0.4 \times 0.30g \times \left[\frac{330kip}{1.07} \times 48in + 134kip \times 48in + \frac{187.1kip}{1.07} \times 124in\right] + 0.45g \times \left[\frac{330kip}{1.07} \times 126.5 + 134kip \times 106in + \frac{187.1kip}{1.07} \times 111in\right]$$

M_{ot} = 37,800 kip-in

Where,

W_{HSM}, W_{DSC}	=	Weight of empty HSM and DSC = 330 kip, 134 kip respectively
d_{HSM-B}	=	respective distance between the CG of the HSM and the point of rotation B (Figure 3.9.7-1) =116 in./2 - 10 in. = 48 in.
$d_{end\ shield\ wall-B}$	=	respective distance between the CG of the end shield wall and the point of rotation B (Figure 3.9.7-1) = 36 in./2 + 116 in. - 10 in.= 124 in.
a_v, a_h	=	vertical and horizontal seismic accelerations
x_{HSM}	=	horizontal distance between the CG of the HSM and the point of rotation B = 48 in. (Figure 3.9.7-1)

x_{DSC} = horizontal distance between the CG of the DSC and the point of rotation B = 48 in. (Figure 3.9.7-1)

x_{wall} = horizontal distance from the CG of the end shield wall to the point of rotation B = 124 in. (Figure 3.9.7-1)

y_{HSM} = vertical distance from the CG of the HSM and the point of rotation B = 126.5 in. (Figure 3.9.7-1)

y_{DSC} = vertical distance from the CG of the HSM and the point of rotation B = 106 in. (Figure 3.9.7-1)

h_{wall} = vertical distance from the CG of the end shield wall to the point of rotation B = 111 in. (Figure 3.9.7-1)

The maximum acceptable acceleration values before tipping occurs are calculated below:

$$\mathrm{M}_{st} = 42{,}900kip \cdot in \geq 1.1M_{ot} = 1.1\left\{0.4_{a_v} \times \left[\frac{330kip}{1.07} \times 48in + 134kip \times 48in + \frac{187.1kip}{1.07} \times 124in\right] + a_h\left[\frac{330kip}{1.07} \times 126.5 + 134kip \times 106in + \frac{187.1kip}{1.07} \times 111in\right]\right\}$$

And assuming $a_v = \frac{2}{3}a_h$

$a = 0.46g, a_v$=0.31g

The safety factor of $M_{st}/1.1M_{ot}$ = 1.03 and is greater than 1 and is the governing safety factor for all load cases. Therefore, it is concluded that the EOS-HSM is stable for seismic loads of up to 0.45g horizontal and 0.30g vertical.

3.9.7.1.8.3.2 Static Sliding Analysis of the EOS-HSM due to Seismic Load

The resisting friction force and horizontal seismic force are calculated and compared and the case considering the bounding 140 pcf concrete density and the minimum DSC weight to minimize the resisting friction force is shown below. The static sliding analysis is shown for the governing EOS-HSM Long model. Cases where the EOS-HSM is loaded versus empty and has one end shield wall versus no shield walls are also considered.

Friction force resisting sliding = $F_{st} = \mu(W_{HSM}+W_{DSC})(1\text{-}0.40\ a_v)$

$$F_{st} = 0.6 \times \left(\frac{330kip}{1.07} + 134kip\right) \times (1 - 0.40 \times 0.30)$$

$\mathrm{F_{st}} = 233\,\mathrm{kip}$

Applied horizontal seismic force = $F_{hs} = a_h\ (W_{HSM}+W_{DSC})$

$$F_{hs} = 0.45 \times \left(\frac{330kip}{1.07} + 134kip\right)$$

$F_{hs} = 199\text{kip}$

Where,

μ = friction coefficient = 0.6
a_v, a_h = vertical and horizontal seismic accelerations = 0.30g, 0.45g respectively
x, y = are the horizontal and vertical distance between the CG and point of rotation B

The maximum acceptable acceleration values before sliding occurs are calculated below:

$$F_{st} = 0.6 \times \left(\frac{330kip}{1.07} + 134kip\right) \times \left(1 - 1.1 \times 0.40_{a_v}\right) \geq 1.1F_{hs}$$
$$= 1.1a_h\left(\frac{330kip}{1.07} + 134kip\right)$$

And assuming $a_v = \frac{2}{3}a_h$

$a = 0.47g, a_v = 0.32g$

The safety factor of $F_{st}/1.1F_{hs}$=1.07 and is greater than 1 and is the governing safety factor for all load cases. Therefore, it is concluded that the EOS-HSM is stable for seismic loads of up to 0.45g horizontal and 0.30g vertical.

3.9.7.1.8.3.3 Seismic Stability of the DSC on DSC Support Structure inside the EOS-HSM

This evaluation is performed for the DSC resting on the support rails inside the EOS-HSM, which includes the stability of the DSC against lifting off from one of the rails during a seismic event and potential sliding off of the DSC from the support structure. The horizontal equivalent static acceleration of 0.45g is applied laterally to the center of gravity of the DSC. The point of rigid body rotation of the DSC is assumed to be the center of the support rail. The applied moment acting on the DSC is calculated by summing the overturning moments.

The stabilizing moment, acting to oppose the applied moment, is calculated and compared with the overturning moment to obtain the maximum acceleration to preclude sliding and overturning of the DSC.

Weight of the DSC = W (kip)

DSC outer radius = R = 75.5"/2 = 37.8"

Angle $\theta = 30^{\circ}$

$Z = 37.75\sin(30^\circ) = 18.88"$

$Y = 37.75\cos(30^\circ) = 32.69"$

Vertical Seismic Acceleration = 0.30g

Horizontal Seismic Acceleration = 0.45g

Vertical seismic force (kips) = $W \times 0.30 \times 0.4 = 0.12W = F_v$

Horizontal seismic force (kips) = $W \times 0.45 = 0.45W = F_h$

The overturning moment =
$1.1F_h \times Y = 1.1 \times 0.45W \times 32.69 = 16.18W$ kip-in

The stabilizing moment =
$(W - 1.1F_v) \times Z = (W - 1.1 \times 0.12W) \times 18.88 = 16.39W$ kip-in

Therefore, the margin of safety (*SF*) against DSC lift off from the DSC support rails inside the HSM obtained from this analysis is:

$$SF = \frac{M_{st}}{M_{ot}} = \frac{16.39W}{16.18W} = 1.01$$

The safety factor of M_{st}/M_{ot}=1.01 is greater than 1. Therefore, the DSC is stable against lifting off the DSC support rails in the EOS-HSM. The evaluation to determine the maximum seismic acceleration before any uplift of the DSC occurs is shown.

$$M_{st} = (W - 1.1 \times 0.4a_vW) \times 18.88 \geq M_{ot} = 1.1 \times a_hW \times 32.69$$

And assuming $a_v = \frac{2}{3}a_h$

$a_h = 0.46g, a_v = 0.30g$

Therefore, the maximum horizontal and vertical acceleration are determined to be 0.45g and 0.30g, respectively.

3.9.7.1.8.4 Interaction of EOS-HSM with Adjacent Modules

For the overturning and sliding analyses due to tornado wind plus missile and flood loading, a single module with one end shield wall is considered. For the seismic sliding and overturning analyses in Section 3.9.7.1.8.3, the cases both with and without an end shield wall are considered, where the same weight and moment of inertia is consistently used for sliding force/overturning moment and for friction force/stabilizing moment in each case.

In the actual scenarios, there is either an end shield wall on one side and another module on the other side, or one module on each side. In the case of sliding, the tornado wind plus missile impact loads the end shield wall plus the HSM module and incur a displacement. The maximum displacement is already obtained in Sections 3.9.7.1.8.1.4 and 3.9.7.1.8.1.5 assuming no resisting force from the adjacent module. With the presence of the adjacent module, the displacement can be transferred into a load onto the adjacent module and result in the maximum displacement if it is perfectly elastic (coefficient of restitution = 1). Then this displacement can be transferred into a load for the next adjacent module with a maximum displacement. However, concrete has a much lower coefficient of restitution (COR) of about 0.1. Energy absorption due to contact (due to the low COR=0.1) results in less critical sliding and overturning results. Impact due to sliding would be distributed over the large side/rear wall surface areas. Impact due to tipping would be localized at the free edges/corners of the modules. Any local damage in these corners or edges would not affect the structural, thermal, or shielding performance of the EOS-HSM. Therefore, the displacement of the adjacent module cannot reach the maximum displacement since there is some energy loss. Thus, the maximum displacement obtained in Sections 3.9.7.1.8.1.4 and 3.9.7.1.8.1.5 is conservative and bounding. This conservatism also applies to overturning and the cases due to flood loads.

3.9.7.1.9 Results

For the maximum seismic acceleration of 0.45g horizontal and 0.30g vertical, no sliding will occur. Also, there will be no overturning at this set of seismic accelerations.

For flood, wind, and missile impact, it is also determined that the uplift values are small and so the DSC remains stable on the support rails. For seismic loading, it is also determined that there is no uplift of the DSC.

In the case of an uneven surface of the concrete pad, shims under the end and rear shield walls can be placed to restore the HSM to its horizontal configurations.

Table 3.9.7-4 shows a summary of the bounding results from the analyses in Section 3.9.7.1.8. Thus, a maximum horizontal acceleration of 0.45g and a vertical acceleration of 0.30g can be exerted on the EOS-HSM before any uplift or sliding occurs. Also there is no DSC lift-off due to this seismic loading.

3.9.7.2 EOS Transfer Cask Missile Stability and Stress Evaluation

3.9.7.2.1 General Description

The stability, stresses, and penetration resistance of the EOS-TCs (TC108, TC125 and TC135) due to design basis tornado and missile impact are evaluated in this section.

3.9.7.2.2 Material Properties

The material properties of the cask outer shell, and top cover plate at 400 °F are taken from Chapter 8.

3.9.7.2.3 Assumptions

1. The gust factor value of 0.85 is taken from Section 6.5.8.1 of ASCE 7-05 [3.9.7-5].

2. The bolted bottom cover plate assembly is protected by transfer equipment attached to skid assembly during the transfer operations, and therefore DBT and missile load is not consider for bottom cover plate.

3. The impact between massive missile and EOS-TC is assumed to be perfectly plastic impact and the missile mass is attached to EOS-TC after impact.

4. The stresses in trunnion/saddle due to DBT and missile impact are bounded by seismic loads. The evaluations of trunnions are performed separately in Appendix 3.9.5.

3.9.7.2.4 Design Input/Data

The most severe tornado-generated wind and missile loads specified by Regulatory Guide 1.76 [3.9.7-6] are selected as the design basis.

3.9.7.2.4.1 DBT Velocity Pressure

The DBT Region I intensities are utilized since they result in the most severe loading parameters. For this region, the maximum wind speed is 230 mph, the rotational speed is 184 mph, and the maximum translational speed is 46 mph. The radius of the maximum rotational speed is 150 feet, the pressure drop across the tornado is 1.2 psi and the rate of pressure drop is 0.5 psi per second.

The maximum velocity pressure, q_z, evaluated at height z based on the maximum tornado velocity (v) is calculated using the relationship given in [3.9.7-5].

$$q_z = 0.00256 K_z K_{zt} K_d I (v)^2$$

The maximum tornado wind speed, V, is the resultant of the maximum rotational speed (184 mph) and the translational speed (46 mph) of the tornado.

The design wind force, F, on the EOS-TC due to this velocity pressure, q_z, is $F = q_z G C_f A_f$ lb Section 6.5.15 of Ref. [3.9.7-5]

Where,

G = gust-effect factor =0.85 (Assumption 1)
C_f = Force coefficient = conservatively taken as 0.82 (by linear interpolation of h/D value of 1.69) from Figure 6-21 of [3.9.7-5],
A_f = Projected area normal to the wind and geometry considered is shown in Figure 3.9.7-9 and is calculated for Case E of Table 3.9.7-6. This has a maximum projected area that is conservative.

Projected area of the cask = (Length of the cask, L_c) x (Diameter of the cask, D_c)

Projected area of the skid = (Length of the Skid, L_s) x (Height of the skid, H_s)

Projected area of the trailer = (Length of the trailer, L_t) x (Height of the Trailer, H_t)

Total projected area (Cask +Skid +Trailer),

Design wind force F = 22.36 kips

3.9.7.2.4.2 DBT Generated Missile Parameters

The tornado-generated missile impact evaluation is performed for a spectrum of missiles and are summarized in Table 3.9.7-5.

3.9.7.2.5 Methodology

The following analyses are performed for the cask and components using hand calculations:

- Stability analysis
- Stress analysis
- Penetration analysis

A load factor of 1.1 is applied to the tornado and seismic loads for stability analyses.

3.9.7.2.5.1 Combined Tornado Effects

Individual DBT, missile load, and combination of these loads are calculated assuming these act simultaneously and are shown in Table 3.9.7-8. Since the EOS-TC is vented, the differential atmospheric pressure is neglected.

3.9.7.2.6 Structural Evaluation

3.9.7.2.6.1 Design Basis Wind Pressure Loads

3.9.7.2.6.1.1 Stability Analysis due to DBT Wind Pressure Load

Total weight of the assembly (EOS-TC, skid and the trailer), W_C = Weight of (cask +skid + trailer)

The restoring moment is least for the assembly with minimum weight. Assuming the trailer and skid remain the same, the minimum weight of all the possible EOS-TC and DSC combinations per Table 3.9.7-6, is bounding for the stability analysis.

Considering the minimum weight of EOS-TC108 loaded with EOS-89BTH DSC (Case B, Table 3.9.7-6) is minimum (199.289 kips), a conservative weight of 170 kips is used for the evaluation.

Thus, the restoring moment, M_{st} = (Total weight) x (Half width of the trailer)

Conservatively assuming that the combined geometry of the cask/skid/trailer has a solid vertical projected area and ignoring the reduction in total wind pressure due to the open areas and shape factor, the maximum overturning moment, M_{ot}, for the cask/skid/trailer due to DBT wind pressure is:

$$M_{ot} = 2F \times H$$

Where,

H = Center of the cask/skid/trailer height
F = Design wind pressure
Accounting for the load factor of 1.1 on the overturning moment:

Factor of safety against overturning $= 1.1 \times \frac{M_{st}}{M_{ot}} = 3.92$

3.9.7.2.6.1.2 Stress Analysis

3.9.7.2.6.1.2.1 Stresses in the Cask Shell due to DBT Wind Pressure Load

Assuming the cask is simply supported and subjected to a uniform load, p, over the entire length, thus using Case 8c, Table 13.3 of Ref. [3.9.7-7], Page 650:

Circumferential membrane stress = $\sigma_2 = 0.492 B p R^{\frac{3}{4}} L^{\frac{-1}{2}} t^{\frac{-5}{4}}$

Circumferential bending stress = $\sigma_2' = 1.217 B^{-1} p R^{\frac{1}{4}} L^{\frac{1}{2}} t^{\frac{-7}{4}}$

Axial membrane stress $\sigma_l = 0.1188 B^3 p R^{1/4} L^{1/2} t^{-7/4}$

Total force = F = 22.36 kips (Section 3.9.7.2.4.1)

Force per inch, p, is maximum for the minimum length of the cask, thus the bounding minimum length, L (EOS-TC108, Case A Table 3.9.7-6) is taken conservatively

p = F / L

B = $[12(1-\nu^2)]^{1/8}$, where ν is the Poisson's ratio (= 0.3 for stainless steel)

Circumferential membrane stress is maximum for the minimum cask length as it is inversely related to the cask length, whereas circumferential bending stress and axial membrane stress is maximum for the maximum cask length since they are directly related to the cask length.

Also, circumferential membrane stress, circumferential bending stress and axial membrane stress are maximum for the maximum cask radius since they are directly related to cask radius:

Bounding minimum cask length = (EOS-TC108, Case A, Table 3.9.7-6)

Bounding maximum cask length = (EOS-TC135, Case E, Table 3.9.7-6)

Bounding maximum cask radius = (EOS-TC135, Case E, Table 3.9.7-6)

Circumferential membrane stress σ_2 = 0.086 ksi

Circumferential bending stress, σ_2 = 3.85 ksi

Axial membrane stress, σ_1 = 1.25 ksi

Primary membrane stress intensity = σ_1 = 0.135 ksf = 0.0009 ksi

Membrane plus bending, S.I. = 5.19 ksi

3.9.7.2.6.1.2.2 Stresses in Top Cover Plate due to DBT Wind Pressure Load

Assuming the plate is simply supported at edges and subjected to a uniform load, q, (load per unit area) over the entire area, thus using Case 10a, Table 11.2 of Roark's Formula for Stress and Strain [3.9.7-7], Page 488 and 509:

$M_c = qa^2 L_{17}$, where $L_{17} = \frac{1}{4}\left\{1 - \frac{1-v}{4}\right\}$ for $r_o = 0$.

Thus, $M_c = \frac{qa^2(3+v)}{16}$

$q = 0.135$ ksf M_c = 0.37 kip-in/in

$\sigma = \frac{6M_c}{t_1^2}$ = 0.21 ksi

Primary membrane stress intensity = σ_m = 0.135 ksf = 0.0009 ksi

Membrane plus bending, S.I. = 0.21 ksi

3.9.7.2.6.2 Massive Missile Impact

3.9.7.2.6.2.1 Stability Analysis due to Massive Missile Impact Load

Stability analysis is done to analyze the most critical impact (Missile B, Table 3.9.7-5) when the missile hits the cask on the side. However, it is conservatively assumed that the missile hits the top most part of the cask as shown in Figure 3.9.7-10.

Using Table 3.9.7-6 and from conservation of momentum,

$$(H_i)_o = (H_a)_o$$

Where,

$(H_i)_o$ is the angular momentum about point O before impact $= R_1 v_i M_m$

$(H_a)_o$ is the angular momentum about point O after impact
$= R_1^2 \omega_i M_m + (I_c)_o \omega_i$

R_1 is the distance from point O to the impact point
v_i is the impact velocity of the missile
M_m is the mass of the missile
M_c is the mass of the cask assembly
ω_i is the angular velocity of the missile about point O just after the impact
$(I_c)_o$ is the mass moment of inertia of the cask about an axis through point O

Therefore, by conserving the momentum before and after the impact:

$$R_1 v_i M_m = R_1^2 \omega_i M_m + (I_c)_o \omega_i$$

$$\omega_i = \frac{R_1 v_i M_m}{R_1^2 M_m + (I_c)_o}$$

From the conservation of energy, $KE_i + PE_i = KE_f + PE_f$

Where,

KE_i is the initial kinetic energy of the cask and missile $= \frac{(I_c)_o \omega_i^2}{2} + \frac{R_1^2 \omega_i^2 M_m}{2}$

KE_f is the final kinetic energy of the cask and missile $= \frac{(I_c)_o \omega_f^2}{2} + \frac{R_1^2 \omega_f^2 M_m}{2}$

PE_i is the initial potential energy of the cask and missile = 0
PE_f is the final potential energy of cask and missile = (weight of the cask) x (change in height of the C.G.)

Therefore:

$$\frac{(I_c)_o \omega_i^2}{2} + \frac{R_1^2 \omega_i^2 M_m}{2} = \frac{(I_c)_o \omega_f^2}{2} + \frac{R_1^2 \omega_f^2 M_m}{2} + w_c h$$

$$\omega_f^2 = \frac{[(I_c)_o + R_1^2 M_m]\omega_i^2 - 2w_c h}{[(I_c)_o + R_1^2 M_m]}$$

From Figure 3.9.7-10 $h = R_2[\sin(\phi + \theta) - \sin(\phi)]$

Hence, $\omega_f^2 = \frac{[(I_c)_o + R_1^2 M_m]\omega_i^2 - 2w_c R_2[\sin(\phi+\theta) - \sin(\phi)]}{[(I_c)_o + R_1^2 M_m]}$

The cask stops rotating when the angular velocity, $\omega_f = 0$ and $\omega_i = \frac{R_1 v_i M_m}{R_1^2 M_m + (I_c)_o}$

Thus, $\sin\phi\cos\theta + \sin\theta\cos\phi = \frac{(R_1 v_i M_m)^2}{2w_c R_2[(I_c)_o + R_1^2 M_m]} + \sin\phi$

$(I_c)_o = (I_c)_{CG} + M_c R_2^2$ (From parallel axis theorem)

Where,

$(I_c)_{CG}$ is the mass moment of inertia of the cask about center of gravity of EOS-TC.

Conservatively, the bounding (maximum) loaded cask weight from Case B (EOS-TC108 with EOS-89BTH DSC) of Table 3.9.7-6 (i.e., 199.29 kips) is taken, which is further decreased to 170 kips such that it is more conservative, because this results in maximum impact force and hence, the maximum primary membrane stress, circumferential membrane and bending stress intensity.

Hence, the total weight of the TC (EOS-TC, Skid and the Trailer), W_c = 170 + 10+ 35 = 215 kips

So the total mass of the TC assembly (EOS-TC, Skid and Trailer), M_c = (215*1000)/32.2 = 6,677.02 lbm

$(I_c)_{CG} = \frac{M_c R_c^2}{2}$ = 43,991.21 ft^2 lbm

$M_c R_2^2$ = 698,769.51 ft^2 lbm

$(I_c)_o$ = 7.43 x 105 ft^2 lbm

By substituting the parameters of cask and stability geometry in above equation, Sin (θ +φ) = 0.015+0.8433 = 0.8583,

Angle of Cask CG about pivot "O" relative to horizontal ,φ = tan-1 (L1/R) where R is the half width of trailer (5.5 ft assumed) and L1 is calculated to be 43 in. +17in. + (87/2) = 103.5 in. = 8.63 ft (See Figure 3.9.7-10). Therefore, φ = 57.49 and Solving above equation, θ = Sin^{-1}(0.8583)-57.49 = 59.13-57.49 = 1.64°

The maximum angle for the tip over the cask occurs when the CG is directly above the point of rotation.

i.e. $\theta_{tip} = 90^\circ - \phi = 32.52^\circ$ $\theta_{tip} = \tan^{-1} {}^{R}/_{R_2} = \tan^{-1} {}^{5.5}/_{10.6} = 27.42^\circ$

Accounting for the load factor of 1.1 on the tornado missile load by increasing the angle of rotation:

Since $\theta_{tip} >> 1.1 \times \theta$, the tip over of the cask does not occur.

3.9.7.2.6.2.2 Stress Analysis

3.9.7.2.6.2.2.1 Stresses in Cask Shell due to Massive Missile Impact Load

The missile impact is analyzed by taking Automobile 16.4 feet x 6.6 feet x 4.3 feet (Case B of Table 3.9.7-5) for evaluation of stresses in cask shell and top cover plates. The stresses in the cask shell due to the massive missile impact will be highest for an impact at the cask mid length. The impact force due to the massive missile is calculated by determining the work done in elevating the cask center of gravity the vertical distance corresponding to the angle of rotation (1.64°) resulting from impact.

The angle of rotation of the cask due to the massive missile impact is 1.64°, therefore, the impact force (*P*) including a dynamic load factor of 2.0 is given by:

P=2.0 x W_c x cos (90°-θ)

Total weight of cask, W_c (EOS-TC, Skid and the Trailer) = 253.30 +10 + 35 = 298.30 kips (Table 3.9.7-6 for enveloping EOS-TC weight)

W_c is considered to be approximately 300 kips, resulting in 17.17 kips

Assuming the cask is simply supported and subjected to a concentrated load, p, over short length 2b (Conservatively taken as 4.3 feet), thus using Case 8b, Table 13.3 of Roark's Formula for Stress and Strain [3.9.7-7], Page 650:

Circumferential membrane stress, $\sigma_2 = 0.130 BpR^{\frac{3}{4}} b^{\frac{-3}{2}} t^{\frac{-5}{4}}$

Circumferential bending stress, $\sigma_2^{'} = 1.56 B^{-1} p R^{\frac{1}{4}} b^{\frac{-1}{2}} t^{\frac{-7}{4}}$

Axial membrane stress, $\sigma_1 = 0.153 B^{3} p R^{\frac{1}{4}} b^{\frac{-1}{2}} t^{\frac{-7}{4}}$

Force per inch, p, is maximum for the minimum length of Automobile 16.4 feet x 6.6 feet x 4.3 feet (Case B of Table 3.9.7-5):

P = F / minimum dimension of Automobile
B = $[12(1-v^2)]^{1/8}$, where v is the Poisson's ratio (= 0.3 for stainless steel)

Also, circumferential membrane stress, circumferential bending stress and axial membrane stress are maximum for the maximum cask radius since they are directly related to cask radius:

Bounding maximum cask radius = EOS-TC135, Case E of Table 3.9.7-6

Circumferential membrane stress σ_2 = 0.39 ksi

Circumferential bending stress σ_2 = 10.03 ksi

Axial membrane stress, σ_1 = 3.27 ksi

Primary Membrane Stress Intensity = 3.27+0.39 = 3.66 ksi

Membrane plus Bending, $S.I. = \sigma_2 + \sigma_2^{'}$ = 13.69 ksi

3.9.7.2.6.2.2.2 Stresses in Top Cover Plate due to Massive Missile Impact Load

The impact on the top cover plate is assumed to be perfectly inelastic impact (Assumption 10) and the automobile (massive missile) is assumed to attach to the EOS-TC after impact.

Let

v_s= Striking velocity of the automobile normal to EOS-TC
w_{mssile}= Weight of missile

The impact force acting on the EOS-TC due to the massive missile automobile will be

W_m =0.625xv_s x w_{mssile} x sin (20t) lbs (Bechtel topical Report, Ref. [3.9.7-4])

Where,

t = time from the instant initial impact (sec)
w_m= 337500 lbs = 337.5 kips

Assuming the plate is simply supported at edges and subjected to a uniform load 'q' (load per unit area) over the entire area, thus using case 10a, Table 11.2 of Ref. [3.9.7-7], Page 509:

$M_c = qa^2 L_{17}$, where $L_{17} = \frac{1}{4}\left\{1 - \frac{1-v}{4}\right\}$ for $r_o = 0$.

Thus, $M_c = \frac{qa^2(3+v)}{16}$

$$M_c = \frac{p}{\pi a^2}\frac{a^2(3+v)}{16} = \frac{p}{\pi}\frac{(3+v)}{16}$$

$$\sigma = \frac{6M_c}{t^2} = \frac{6}{t^2}\frac{p}{\pi}\frac{(3+v)}{16} = 12.59 \text{ ksi}$$

Primary Membrane Stress= Total force acting on the EOS-TC due to massive missile automobile/ Area of top cover plate = 0.06 ksi

Therefore, Primary membrane + bending stress in the top cover plate will be 0.06 +12.59 = 12.65 ksi

3.9.7.2.6.3 Missile Penetration Resistance Analysis

3.9.7.2.6.3.1 Penetration Analysis

In order to evaluate the system for resistance towards the missile penetration, the minimum thickness required to resist the bounding missile (Case A, Table 3.9.7-5) is calculated using two different relations:

- Nelm's formula [3.9.7-8] is used to determine the minimum required thickness for puncture resistance.
- The Ballistic Research Laboratory formula is used to calculate the missile penetration distance and the minimum required thickness for puncture resistance.

It is assumed that the missile is rigid and the mass and velocity of the missile for the evaluation is taken from Table 3.9.7-5.

Nelms' Formula (page 54 of Reference [3.9.7-8])

$E_F / S = 2.4 d^{1.6} t^{1.4}$

Where,

E_F is the incipient puncture energy of the prismatic cask jacket (inch-lbs)
S is the ultimate tensile strength of the jacket material (cask outer shell) (ksi)

t is the thickness of the jacket material (inch)
d is the diameter of the punch/missile (6.625 inch)

Assuming all the kinetic energy of the missile is getting converted to the incipient puncture energy of the prismatic cask jacket.

$$E_F = \frac{1}{2} M_m v_m^{\ 2}$$

Where,

M_m and v_m are the mass and velocity of the missile, respectively.

$$E_F / S = 2.4 d^{1.6} t^{1.4}$$

$$t^{1.4} = 0.281 \Rightarrow t = 0.404 \text{ inch}$$

Ballistic Research Laboratory Relation (page 2-3 of [3.9.7-4])

$$T = \frac{\left(\frac{MV_s^{\ 2}}{2} \right)^{2/3}}{672D}$$

Where,

T is the steel plate thickness to just perforate (inch)
D is the diameter of the punch/missile (= 6.625 inch)
M_s is the mass of the striking missile (= 8.91 lbs.sec^2/ft)
V is the velocity of the striking missile normal to target surface (=135 fps)
T = 0.421 inch

The thickness t_p, of a steel barrier required to prevent perforation should exceed the thickness for threshold of perforations. It is recommended by [3.9.7-4] to increase the thickness, T, by 25 percent to prevent perforation.

Thus, minimum thickness of the barrier should be, $t_p = 1.25T$ inch = 0.526 inch

Out of the thickness calculated by the two methods, the threshold thickness evaluated by Ballistic Research Laboratory relation is bounding. Thus the minimum thickness required to prevent perforation in the EOS-TC is 0.526 inch.

Thickness of the cask outer shell (1 inch) >> 0.526 inch

Thickness of the top cover plate (3.25 inch) >> 0.526 inch

Since the cask shell, and top covers are much thicker than the depth of penetration; demonstrating that during a DBT, the cask is not be penetrated by the missiles specified in Table 3.9.7-5, thus protecting the DSC.

3.9.7.2.6.3.2 Localized Peak Stress Analysis due to Missile Impact Load

In order to evaluate the localized peak stresses occurring due to the missile impact on to the cask, impact force is calculated as follows:

$$F\Delta t = G_f - G_i$$

Where,

Δt is the time of contact =0.05 sec (more conservative than impact time 0.075 sec [3.9.7-4])
G_f is the linear momentum at time $t = t_f = mv_f$
G_i is the linear momentum at time $t = t_i = mv_i$
v is the velocity
m is the mass

Subscripts i and f represent initial and final states, respectively.

$$F = \frac{m(v_i - v_f)}{(t_f - t_i)} = \frac{m(v_i - v_f)}{(\Delta t)}$$

Assuming that the system stops after the impact, i.e. $v_f = 0$

$$F = \frac{m(v_i)}{(\Delta t)} = 24.1 \text{ Kips}$$

The impact force is dynamic as calculated using the rate of change of momentum; hence a dynamic load factor is not required.

3.9.7.2.6.3.2.1 Localized Peak Stresses in the Cask Shell due to Missile Impact Load

Assuming the cask is a cylindrical shell with closed ends and end support, subjected to a uniform radial load, p, over a small area A, thus using Case 8a, Table 13.3 of Roark's Formula for Stress and Strain [3.9.7-7], Page 649:

$$\frac{R}{t} = 43.5$$

r = 3.3125-in. radius of Schedule 40 Pipe (Case A, Table 3.9.7-5)

The localized peak stress region is taken at '2t' away from impact, hence r =5.3125 inches is used to simulate the peak stress region.

$$\frac{A}{R^2} = \frac{\pi(5.3125)^2}{43.5^2} = 0.0469$$

By interpolation,

$$\sigma_2'\left(\frac{t^2}{F}\right) = 0.74$$

$$\sigma_2' = 0.74\left(\frac{F}{t^2}\right) = 0.74\left(\frac{24.1}{1^2}\right) = 17.83 \text{ ksi}$$

By interpolation,

$$\sigma_2\left(\frac{Rt}{F}\right) = 6.37$$

$$\sigma_2 = 6.37\left(\frac{F}{Rt}\right) = 6.37\left(\frac{24.1}{43.5\times 1}\right) = 3.53 \text{ ksi}$$

Force applied by the missile on to the cask = 24.1 kips

Area of missile striking face = $\frac{\pi}{4}\times 6.625^2 = 34.47\, in^2$

Therefore, radial membrane stress $\sigma_3 = \frac{24.1}{34.47} = 0.70\, ksi$

As the weight of the missile (287 lb) is much less than the weight of the overall cask, thus stresses in the axial direction (σ_1) will be negligible.

Therefore, conservatively Primary Membrane stress

$\sigma_m = \max(\sigma_1 + \sigma_2, \sigma_2 + \sigma_3, \sigma_3 + \sigma_1) = 3.53 + 0.70 = 4.23\, ksi$

Primary Membrane plus Bending stress, $\sigma_m + \sigma_b = 4.23 + 17.83 = 22.06\ ksi$

3.9.7.2.6.3.2.2 Localized Peak Stresses in Top Cover Plate due to Missile Impact Load

Assuming the top cover plate is a circular plate simply supported at the edges and subjected to a uniform load over a small area A of radius r_o, thus using case 16, Table 11.2 of Roark's Formula for Stress and Strain, Page 514 [3.9.7-7]:

$$M_{\max} = \frac{W}{4\pi}\left[(1+\nu)\ln\left(\frac{a}{r_o'}\right)+1\right] \text{ at r = 0}$$

Where, a is the plate outer radius = 43.5 inch

r_o = 5.3125 inches
W is the load = 24.1 kips
t is the thickness of the top cover plate = 3.25 inches
M_{max} = 7.16 Kip-in/in

$$\sigma = \frac{6M_{max}}{t^2} = 4.07 \text{ ksi}$$

Force applied by the missile onto the cask = 24.1 kips
Area of missile striking face = 34.47 in^2
Therefore, radial membrane stress = 24.1/34.47 = 0.70 ksi
Primary membrane plus bending stress = 4.07+ 0.70 = 4.77 ksi

3.9.7.2.6.4 Stability Analysis for EOS-TC due to Seismic Load

During any seismic event in a loaded EOS-TC in the horizontal position on the skid and the trailer, it will be subjected to overturning moment. The peak ground acceleration in the horizontal (a_h) and the vertical direction (a_v) due to seismic event is 0.45 g and 0.30 g, respectively.

An overturning moment due to seismic load is calculated assuming the seismic load is acting on the cask center from the ground. The vertical seismic load is combined with the horizontal load using the 100-40-40 combination method (i.e., 40% of the vertical component acting simultaneously with 100% of the horizontal component). The stability analysis due to seismic overturning moment is performed below:

The overturning moment produced in the cask due to seismic effect is:

$$M_{ot} = a_h \times W \times L_1 + 0.4a_v \times W \times R$$

This overturning moment is resisted by the restoring moment:

$$M_{st} = W \times R$$

The variables are defined as follows:

a_h = horizontal seismic acceleration = 0.45g

W = weight of cask (results are independent of cask weight)

L_1 = vertical location of cask center of gravity = $\frac{\left(17+43+\frac{87}{2}\right)}{12} = 8.63$ feet
(Figure 3.9.7-9 and Figure 3.9.7-10)

R = horizontal distance from point of rotation to cask center of gravity = $\frac{11ft}{2} = 5.5$ feet (Figure 3.9.7-9 and Figure 3.9.7-10)

The factor of safety against overturning, including a load factor of 1.1 on the overturning moment is:

$$\frac{M_{st}}{1.1M_{ot}} = \frac{W \times R}{1.1(a_h \times W \times L_1 + 0.4a_v \times W \times R)} = \frac{5.5}{1.1(0.45 \times 8.63 + 0.4 \times 0.30 \times 5.5)} = 1.10$$

The maximum acceptable acceleration value before tipping occurs is calculated below:

$$a_v = \frac{2}{3}a_h$$

$$M_{st} > 1.1M_{ot} \rightarrow W \times R > 1.1\left(a_h \times W \times L_1 + 0.4\frac{2}{3}a_h \times W \times R\right)$$

$$\frac{R}{1.1} > a_h\left(L_1 + 0.4\frac{2}{3} \times R\right)$$

$$a_h < \frac{R}{1.1\left(L_1 + 0.4\frac{2}{3} \times R\right)} = \frac{5.5}{1.1(8.63 + 0.267 \times 5.5)} = 0.49g$$

$$a_h = 0.49, \quad a_v = 0.33g$$

The safety factor against overturning is 1.10 based on the design basis accelerations and including a load factor of 1.1 on the overturning moment. The EOS-TC can have up to 0.49g horizontal seismic acceleration and 0.33g vertical seismic acceleration before the cask can start to overturn. Therefore, the EOS-TC will maintain its stability during the seismic event.

3.9.7.2.6.5 Analysis of Cask for DBT Wind Load and DBT Missile Load Combination

Per NUREG-0800, the total tornado load on a structure is combined as follows:

$W_t = W_p$
$W_t = W_w + 0.5W_p + W_m$

Where,

W_t = Total tornado load
W_w = Load from tornado wind effect
W_p = Load from tornado atmospheric pressure change effect
W_m = Load from tornado missile impact effect

Note that W_p is not applicable to the stability analysis as discussed in Section 3.9.7.1.6. Therefore, the load combination for tornado loading for this analysis is simplified to:

$W_t = W_w + W_m$

The envelope of a range of missiles listed in Table 3.9.7-5 is used for the missile impact load evaluation. The automobile missile, with a size of 16.4 ft x 6.6 ft x 4.3 ft (Case B of Table 1), impact on to the EOS-TC has the maximum momentum and is considered as the bounding case.

3.9.7.2.6.5.1 Overturning Analysis due to Concurrent Tornado Loads

A dynamic analysis for the combined effects of wind and concurrent massive missile impact loading is conducted. The effects of the concurrent missile impact loads are used in determining the initial angular momentum from the conservation of angular momentum equations using the wind loads from the previous section. Then the angle of rotation is determined from the conservation of the concurrent loading.

Angular velocity of the missile about point O just after the impact is:

$$\omega_i = \frac{R_1 v_i M_m}{R_1^{\,2} M_m + (I_c)_o}$$

The concurrent wind load is accounted for by reducing the inertia that resists motion in the denominator of the equation of angular velocity of the missile about point O just after the impact

$$\omega_i = \frac{R_1 v_i M_m}{R_1^{\,2} M_m + (I_c)_o - W_w \times L_1^{\,2}}$$

Where R_1, v_i, M_m and $(I_c)_o$ are defined in Section 3.9.7.2.6.2.1

Using the relation presented in Section 3.9.7.2.6.2.1 and reducing the inertia that resists motion in the denominator of the equation,

$$Sin(\theta + \phi) = \frac{(R_1 v_i M_m)^2}{2 w_c R_2 [(I_c)_o + R_1^{\,2} M_m - W_w \times L_1^{\,2}]} + \sin\phi$$

$$Sin(\theta + \phi) = 0.0174 + 0.8433$$

$$(\theta + \phi) = Sin^{-1}(0.8607) = 59.40°$$

$$\theta = 59.40° - 57.49° = 1.91°$$

The maximum angle for the tip over of the cask occurs when the CG is directly above the point of rotation. The maximum angle for tip over calculated in Section 3.9.7.2.6.2.1 is $\theta_{tip} = 32.51°$. Since $1.1\theta \times < 1/3\ \theta_{tip}$, tip over of the EOS-TC cask will not occur.

3.9.7.2.6.5.2 Time-Dependent Overturning due to Concurrent Tornado Loads

In addition to the dynamic overturning analysis, a time dependent analysis is used to ensure the absence of any overturning.

An approximate relationship for the deceleration of an automobile impacting a rigid wall is given by:

$$-\ddot{x} = 12.5g * x \quad [3.9.7\text{-}4]$$

Where,$-\ddot{x} = 12.5g \cdot x$Eq. D-1of[3.9.7-4]

$-\ddot{x}$ = Deceleration (ft/sec^2)
x = Distance automobile crushes into target (ft)

A force time history is obtained:

$$W_m = 0.625 \times v_s \times w_{missile} \times \sin(20t)$$

The overturning moment is:

$$M_{ot} = W_m \times L + q_z \times L_\theta^{\ 2} \times L_T$$

Where,

L_θ = Height to the top of the cask system, which is dependent on rotation θ.
L = Initial height of the cask system
L_T = Length of the trailer
q_z = DBT velocity pressure

And the stabilizing moment is:

$$M_{st} = W_c * R_2 * Cos(\phi + \theta)$$

The moment causing acceleration is:

$$M_{acc} = M_{ot} - M_{st}$$

The angular velocity is:

$$\omega_i = \frac{\left[\frac{M_{acc,i} + M_{acc,i-1}}{2} * (t_i - t_{i-1})\right]}{(I_c)_o} + \omega_{i-1}$$

Where,

i = index for the current time step
$i-1$ = index for the previous time step

The angle of rotation is:

$$\theta_i = \left[\frac{\omega_i + \omega_{i-1}}{2} * (t_i - t_{i-1})\right] + \theta_{i-1}$$

Accounting for the required load factor of 1.1 on the design basis tornado, the angle of rotation resulting from the analysis is shown in Figure 3.9.7-11. The governing angle of rotation is 7.55 x 1.1 = 8.31 degrees, which is less than the (1/3) x tip angle (Θ_{tip}) = (1/3) x 32.51° = 10.84°. The factor of safety against tipping is 10.84/8.31 = 1.30. Therefore, the EOS-TC will not tip over due to wind concurrent with massive missile impact load combination.

3.9.7.2.7 Results

The factor of safety against tip overturn is greater than 1 for the individual DBT wind pressure load and seismic load. Also, the angle of rotation (θ) due to massive missile impact load, concurrent tornado loads is less than critical tipping angle ($1/3x\theta_{tip}$). Therefore, EOS-TC remains stable on the trailer during transfer operations. The primary membrane intensity and combined membrane plus bending stresses due to DBT and missile impact are calculated to be below the allowable stresses. The maximum missile penetration depth is found to be 0.526 inch, which is less than the thickness of the EOS-TC outer shell and top cover plate of 1 inch and 3.25 inches, respectively.

The resultant stresses for the bounding individual DBT, missiles impact and combined tornado load are summarized in Table 3.9.7-7 and Table 3.9.7-8, respectively.

3.9.7.3 References

3.9.7-1 NUREG-0800, Standard Review Plan, "Missiles Generated by Natural Phenomena", Revision 2, U.S. Nuclear Regulatory Commission, July 1981.

3.9.7-2 American Society of Civil Engineers, ASCE 7-10, "Minimum Design Loads for Buildings and Other Structures."

3.9.7-3 Raymond C. Binder, "Fluid Mechanics," Prentice-Hall, Inc, 1943.

3.9.7-4 Bechtel Report BC-TOP-9A Rev. 2, "Topical Report – Design of Structures for Missile Impact," September 1974.

3.9.7-5 American Society of Civil Engineers Standard, ASCE 7-05, "Minimum Design Loads for Buildings and Other Structures," (Formerly ANSI A58.1).

3.9.7-6 U.S. Nuclear Regulatory Commission, Regulatory Guide 1.76, "Design Basis Tornado for Nuclear Power Plants," Revision 1, March 2007.

3.9.7-7 R.G Budynas and W.C Young, "Roark's Formula for Stress and Strain," Eighth Edition, McGraw-Hill Book Company.

3.9.7-8 H. A. Nelms, "Structural Analysis of Shipping Casks, Effects of Jacket Physical properties and Curvature on Puncture Analysis," Vol.3, ORNL TM-312, Oak Ridge National Laboratory, Oak Ridge Tennessee, June 1968.

Table 3.9.7-1
Sizes and Weight for Various EOS-HSM Models

EOS-HSM Module	Total Length of EOS-HSM (in.)	Nominal Weight of Empty HSM (lbs.)
EOS-HSM Short	228	292,000
EOS-HSM Medium	248	314,000
EOS-HSM-FPS Medium	*248*	*307,000*
EOS-HSM Long	268	330,000

Table 3.9.7-2
Missile Load Data for EOS-HSM Stability Analysis

Missile	Mass (lbs.)	Dimensions	Velocity (fps)	Momentum (lbs-fps)
Utility Wooden Pole	1,124	13.5-inch Diameter 35 feet Long	180	202,320
Armor Piercing Artillery Shell	276	8-inch Diameter	185	51,060
Steel Pipe	750	12-inch Sch. 40 15 feet Long	154	115,500
Automobile	4,000	20 ft^2 Contact Area	195	780,000

Table 3.9.7-3
Design Pressures for Tornado Wind Loading

Wall Orientation (1)	Velocity Pressure (psf)	Ext. Pressure Coefficient (2)	Int. Pressure Coefficient (3)	Max/Min Design Pressure (psf) (4)
Front	253.8	0.680	± 0.18	218
Left	253.8	-0.595		-197
Rear(5)	253.8	-0.425		-154
Right	253.8	-0.595		-197
Top	253.8	-1.105		-326

Notes:

1. Wind direction assumed to be from front. Wind loads from other directions may be found by rotating above table values to desired wind direction.
2. These values are calculated using the external pressure coefficients from Figure 27.4-1 of [3.9.7-2] times the gust effect factor (0.85) from Section 26.9 of [3.9.7-2].
3. Internal pressure coefficient from Table 26.11-1 of [3.9.7-2].
4. These values are computed based on Equation 27.4-1 of [3.9.7-2].
5. The bounding C_p of -0.5 from an L/B ratio of 0-1 is used for wind in all directions from Figure 27.4-1 of [3.9.7-2].

Table 3.9.7-4
Summary of EOS-HSM Sliding and Stability Results

Loading	**Tornado Wind + Missile**		**Flood**		**Seismic for Loaded EOS-HSM with End Shield Wall**	
Result	Maximum Sliding Distance (in)	Maximum Rocking Uplift[3] (°)	Safety Factor against Sliding	Safety Factor against Tipping	Maximum Acceleration before Sliding[1] (horiz / vert) (g)	Maximum Acceleration before Tipping[2] (horiz / vert) (g)
EOS-HSM Short	1.62	3.4	1.12	1.14	0.45 / 0.30	>0.45 / 0.30
EOS-HSM Medium	1.62	2.8	1.09	1.12	0.45 / 0.30	>0.45 / 0.30
EOS-HSM-FPS Medium	*1.62*	*2.7*	*1.08*	*1.11*	*0.45 / 0.30*	*>0.45 / 0.30*
EOS-HSM Long	1.62	2.4	1.11	1.13	0.45 / 0.30	>0.45 / 0.30

Notes:

1. Maximum acceleration to preclude sliding is 0.47g / 0.32g, but seismic load is limited to 0.45g / 0.30g based on static stability analysis of DSC on the support structure.
2. Maximum acceleration to preclude tipping is 0.46g / 0.31g, but seismic load is limited to 0.45g / 0.30g based on stability analysis of DSC on the support structure.
3. A 1.1 required factor is applied for the wind load to the angles from Figure 3.9.7-2 to Figure 3.9.7-4.

Table 3.9.7-5
Design-Basis Tornado Missile Spectrum and Maximum Horizontal Speed for EOS-TC Stability Analysis

Case #	Missile [1]	Weight (lbs)	Horizontal Impact Velocity [2] (fps)
A	Schedule 40 Pipe (ϕ 6.625 inch x 15 ft long) [5]	287	135
B	Automobile (16.4 ft x 6.6 ft x 4.3 ft) [3][4]	4000	135
C	Solid Steel Sphere (ϕ 1 inch)	0.147	26

Notes:

1. Missiles are assumed to strike at 90 degrees to the surface with the longitudinal axis of the missile parallel to the striking angle.
2. Vertical striking velocity is 67% of the horizontal.
3. Automobile missile (Case B) bounds all other cases for stability and stresses and therefore only Case B is evaluated for stability and associated stresses.
4. The automobile missile (Case B) considered to impact at all altitudes less than 30 ft above all grade levels within 0.5 mile of the plant structure.
5. Schedule 40 pipe (Case A) bounds all other items for penetration resistance and for local stresses and therefore Case A is evaluated for the penetration resistance.

Table 3.9.7-6
Cask and DSC Weights in Different Configuration and Their Geometric Properties

CASE	Configuration	Cask without NSP Assembly[1] (lbs)	DSC Weight[2] (lbs)	Minimum Weight (lbs)	Maximum Weight (lbs)	Cask Diameter[1] (inches)	Length[1] (inches)
A	TC108/37PTH	86,289	119,000	205,289	220,289	85.5	206.76
			134,000				
B	TC108/89BTH	86,289	113,000	199,289	206,289	85.5	206.76
			120,000				
C	TC125/37PTH	108,802	119,000	227,802	242,802	87	208.01
			134,000				
D	TC125/89BTH	108,802	113,000	221,802	228,802	87	208.01
			120,000				
E	TC135/37PTH	119,230	119,000	238,230	*253*,230	87	228.59
			134,000				

Note:

1. Weight of TC without NSP assembly and their geometric parameter in different configuration is taken from Section 3.2.
2. Weight of 37PTH and 89BTH DSC weights are taken from Section 3.2.

Table 3.9.7-7
EOS-TC Analysis Results

Load Description	Stress Category	Calculated Stress (ksi)		Allowable Stress (ksi)	Impact Force (kips)
		Cask Shell	Top Cover Plate		
Wind Pressure Loads	Primary Membrane	1.34	0	39	22.36
	Membrane + Bending	5.19	0.21	58.5	
Massive Missile	Primary Membrane	3.66		39	17.17
	Membrane + Bending	13.69		58.5	
	Primary Membrane		0.06	39	337.5
	Membrane + Bending		12.65	58.5	
Penetration Resistance	Primary Membrane	4.23	0.70	39	24.1
	Membrane + Bending	22.06	4.77	58.5	

Table 3.9.7-8
Combined Tornado Effect

Load Description	Stress Category	Combined Stress (ksi)		Allowable stress (ksi)
		Cask Shell	Top Cover Plate	
Wind pressure load + Massive Missile	Primary Membrane	5.0	0.06	39
	Membrane + Bending	18.88	12.86	58.5

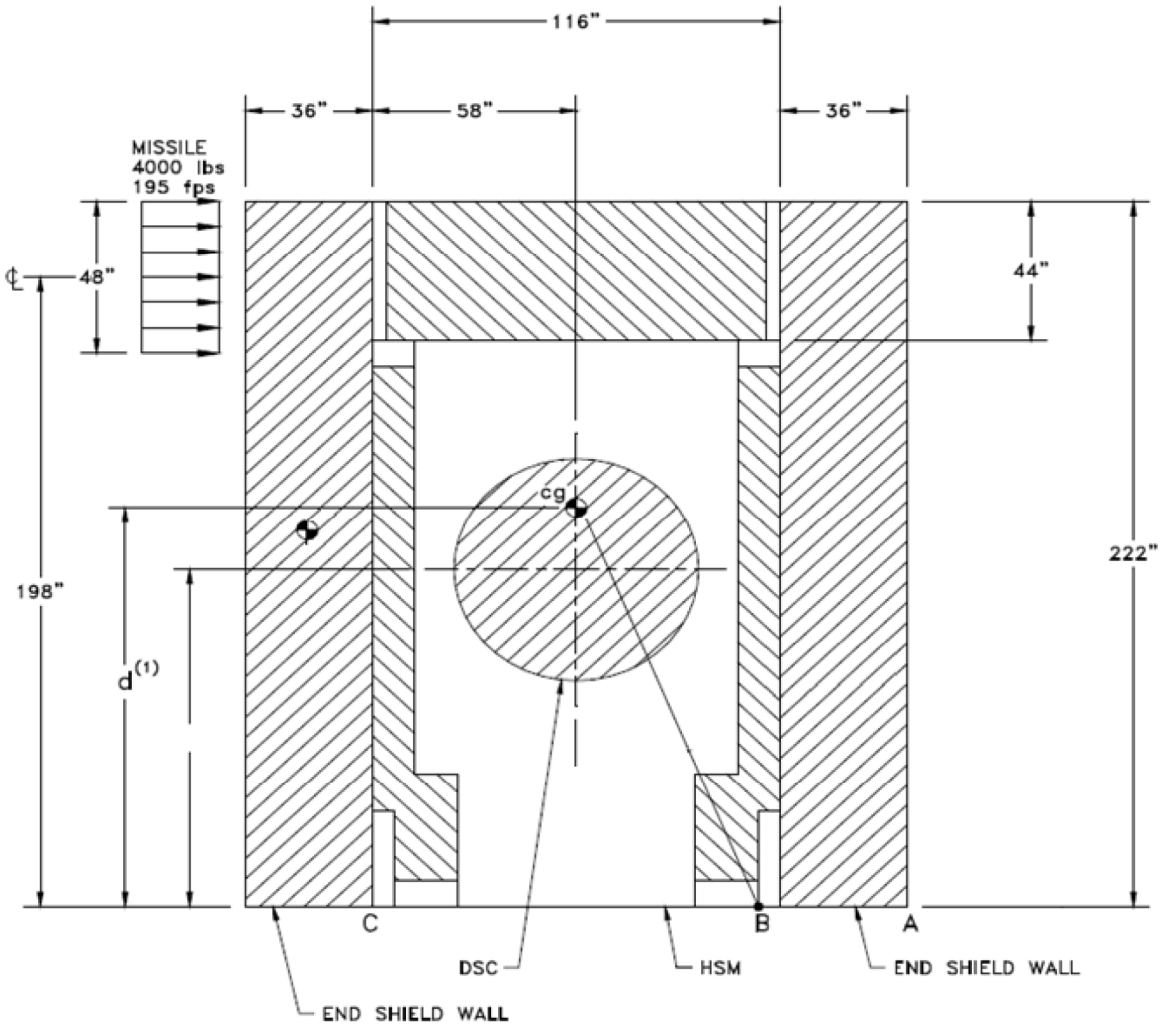

(1) d = distance to CG of EOS-HSM

Figure 3.9.7-1
EOS-HSM Dimensions for Stability Analysis

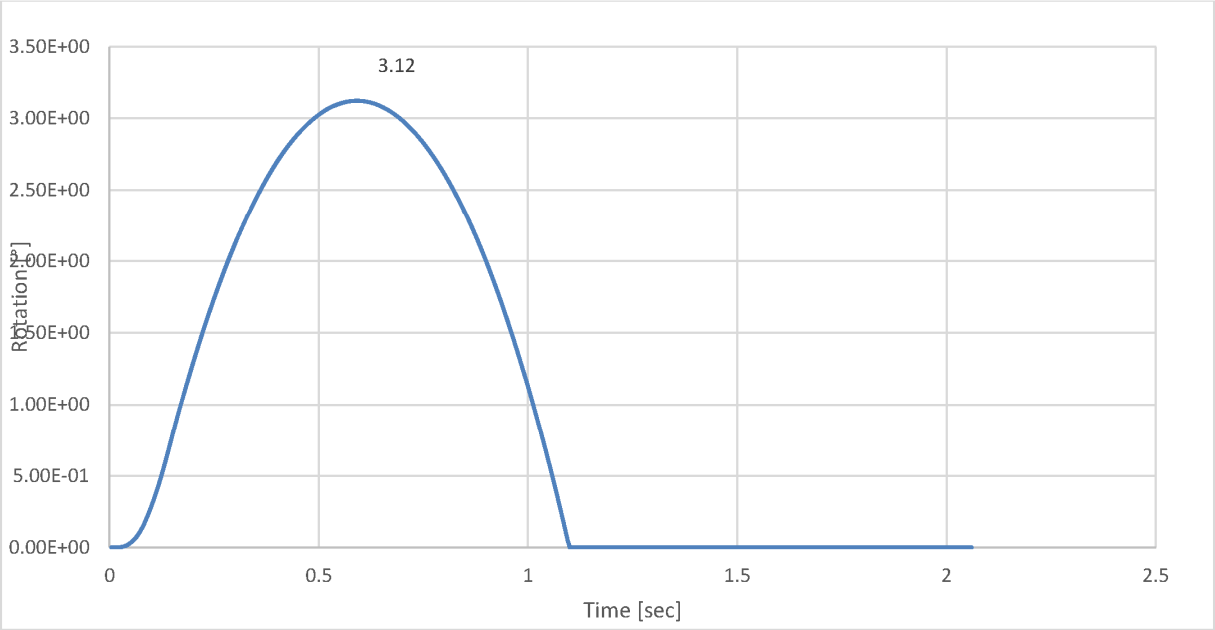

Figure 3.9.7-2
Angle of Rotation from Time-Dependent Analysis Due to Tornado Wind and Massive Missile Loading for EOS- HSM Short

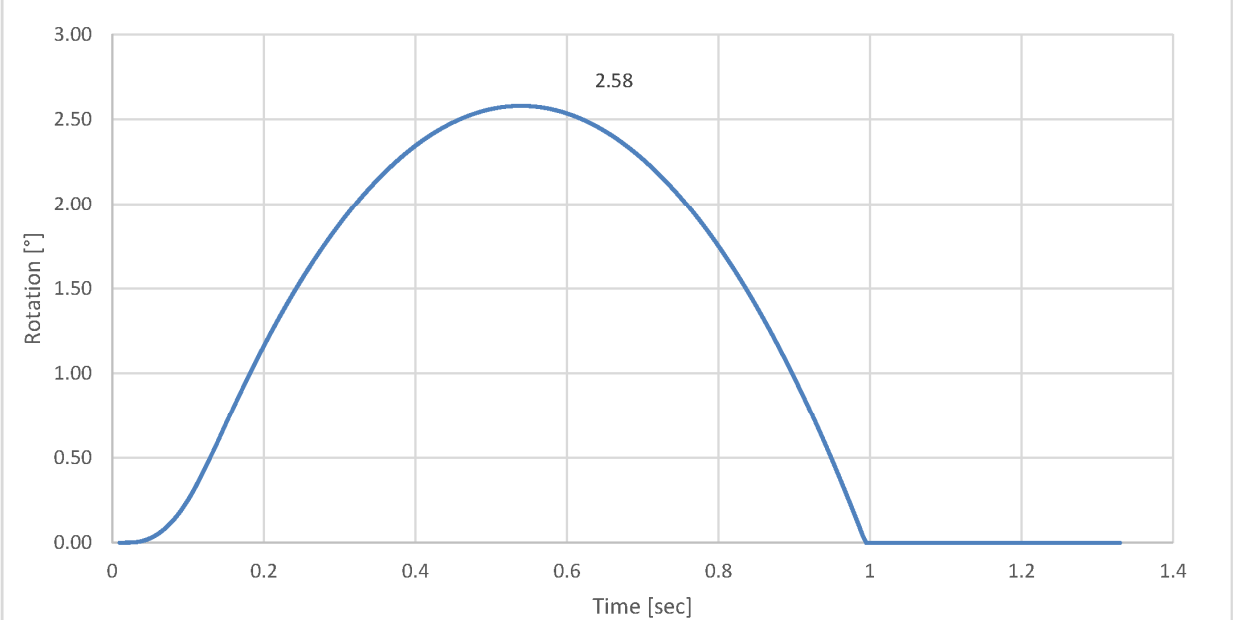

Figure 3.9.7-3
Angle of Rotation from Time-Dependent Analysis Due to Tornado Wind and Massive Missile Loading for EOS- HSM Medium

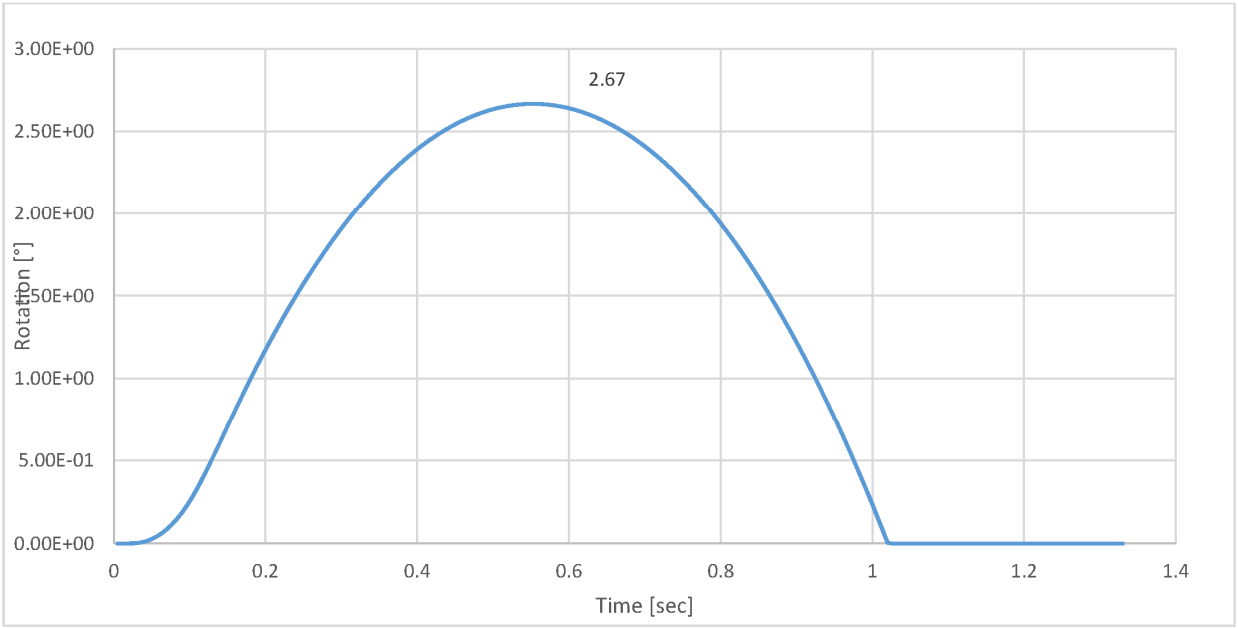

Figure 3.9.7-3a
Angle of Rotation from Time Dependent Analysis due to Wind and Massive Missile Loading for EOS-HSM-FPS

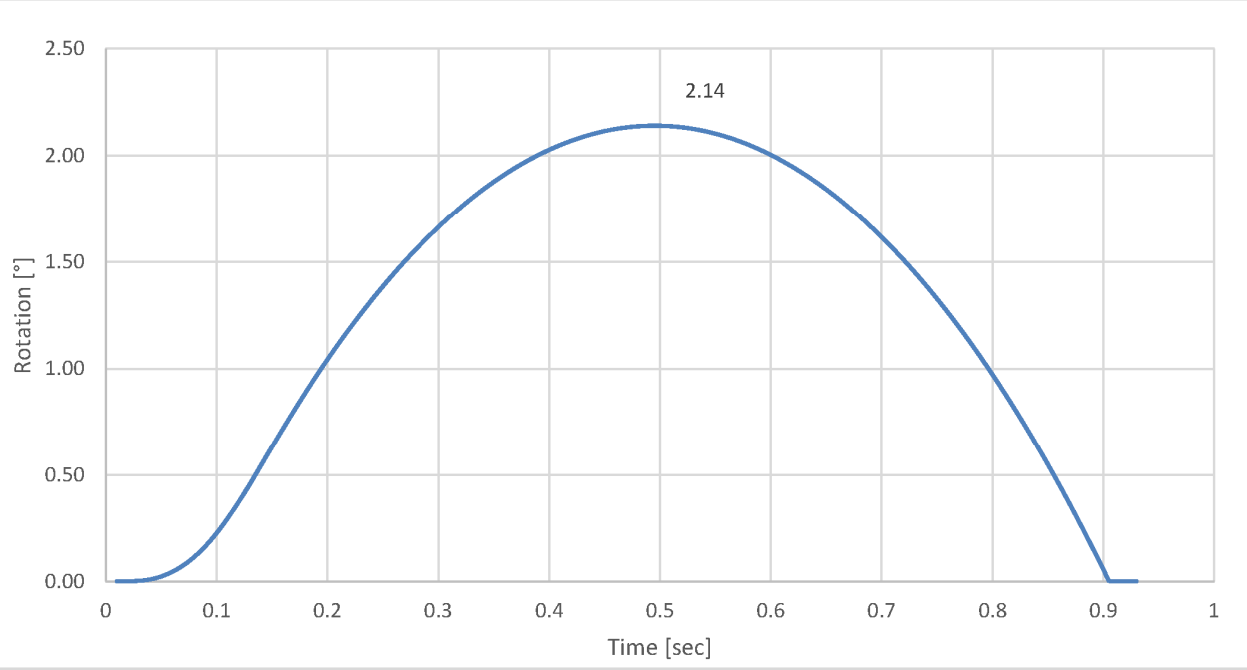

Figure 3.9.7-4
Angle of Rotation from Time-Dependent Analysis Due to Tornado Wind and Massive Missile Loading for EOS- HSM Long

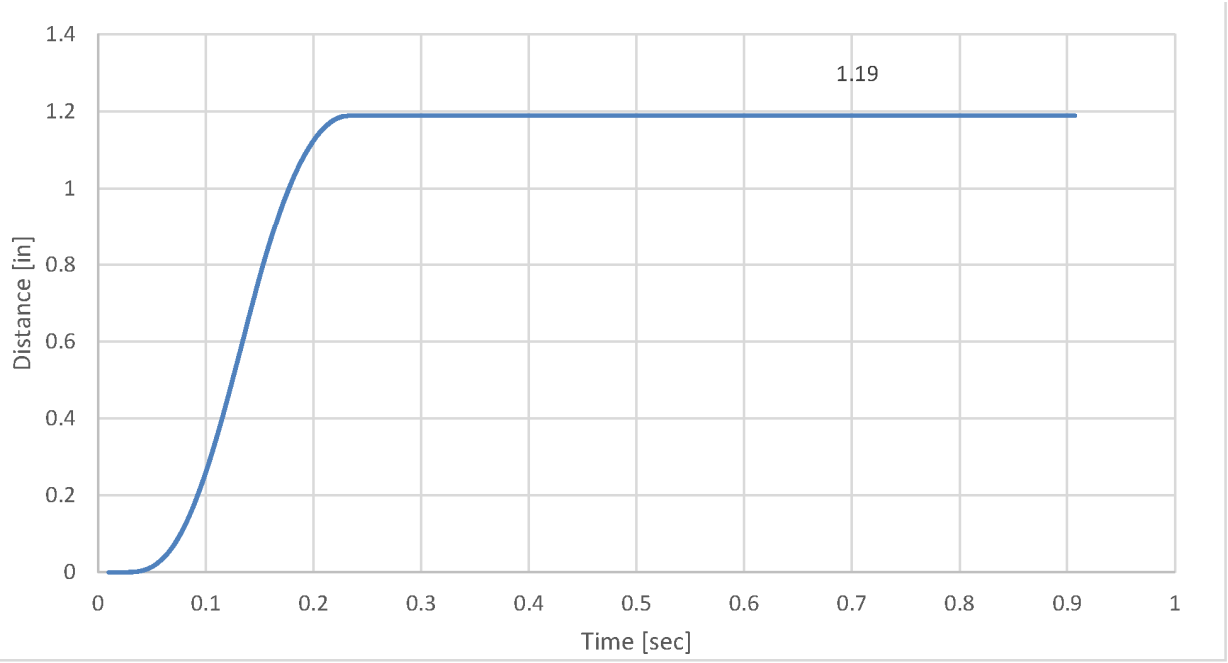

Figure 3.9.7-5
Sliding Displacement from Time-Dependent Analysis Due to Tornado Wind and Massive Missile Loading for EOS- HSM Short

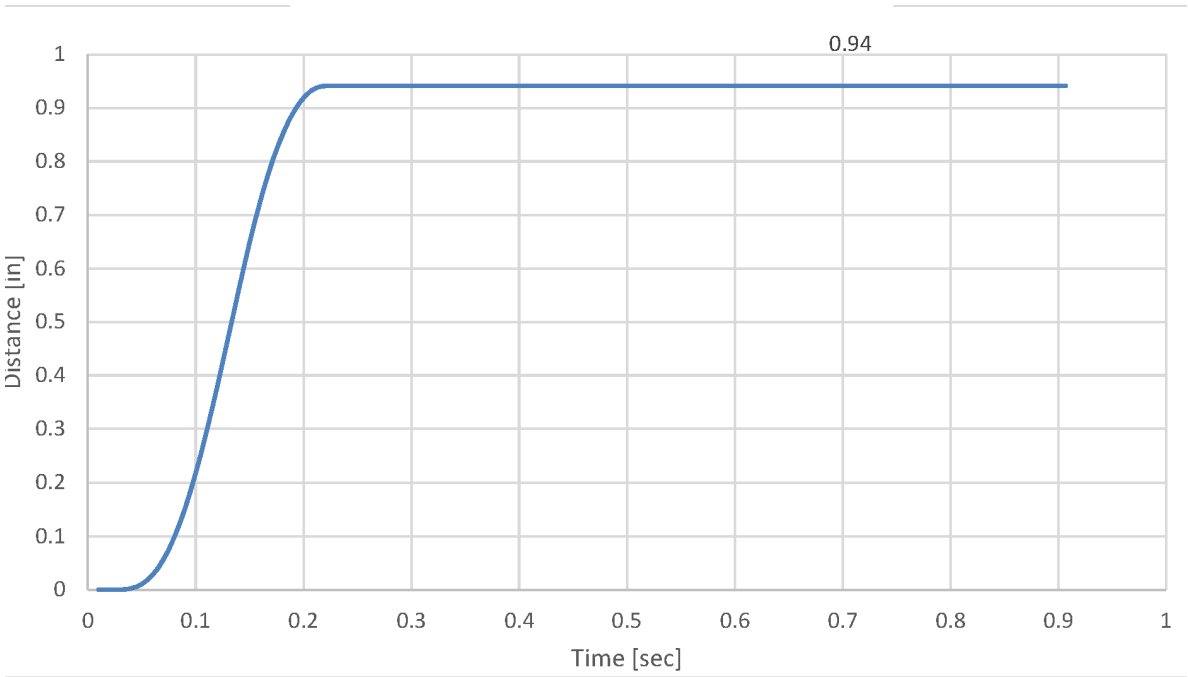

Figure 3.9.7-6
Sliding Displacement from Time-Dependent Analysis Due to Tornado Wind and Massive Missile Loading for EOS- HSM Medium

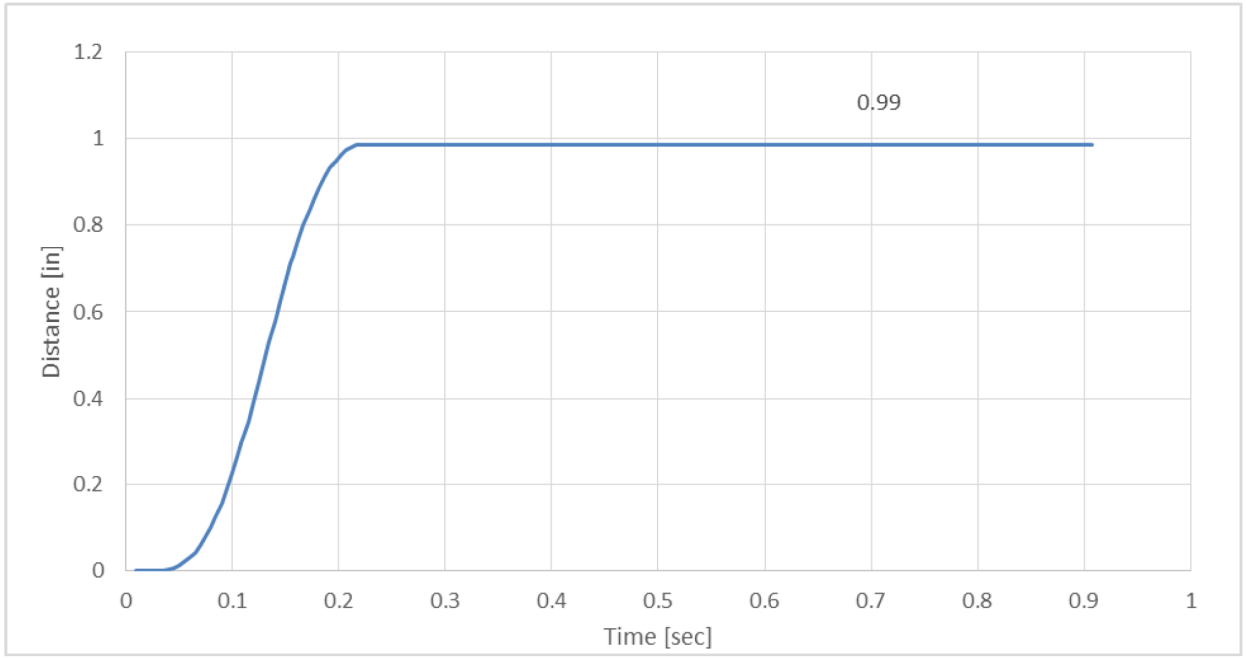

Figure 3.9.7-6a
Sliding Displacement from Time Dependent Analysis due to Wind and Massive Missile Loading for EOS-HSM-FPS

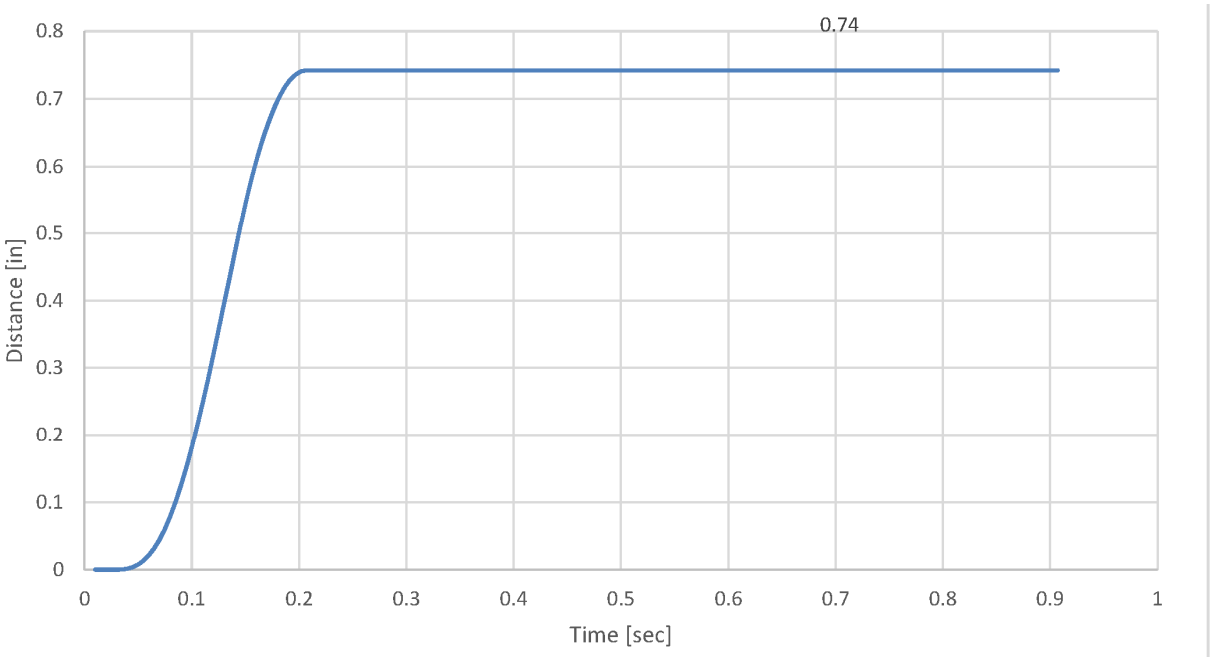

Figure 3.9.7-7
Sliding Displacement from Time-Dependent Analysis Due to Tornado Wind and Massive Missile Loading for EOS- HSM Long

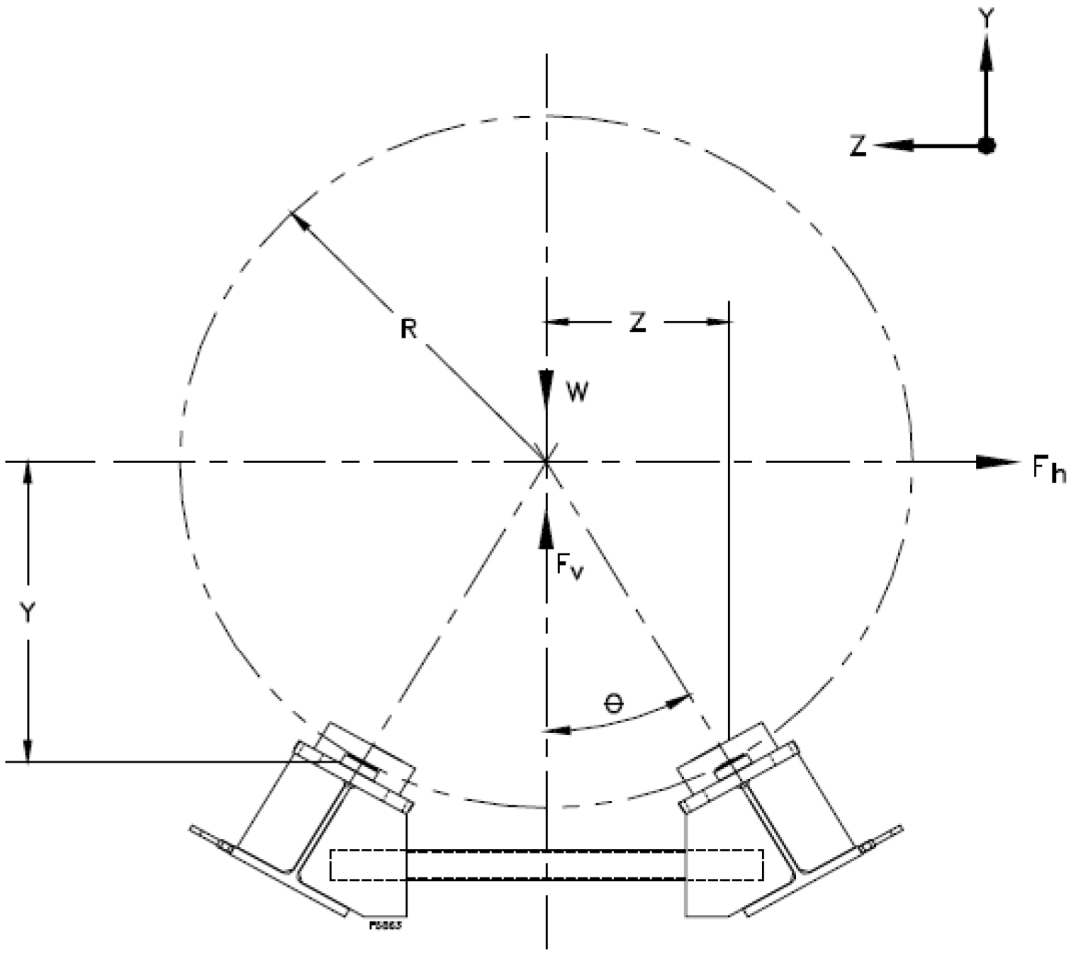

Figure 3.9.7-8
Stability of the DSC on the DSC Support Structure

Note: The EOS-HSM-FPS DSC support structure is not shown in this figure

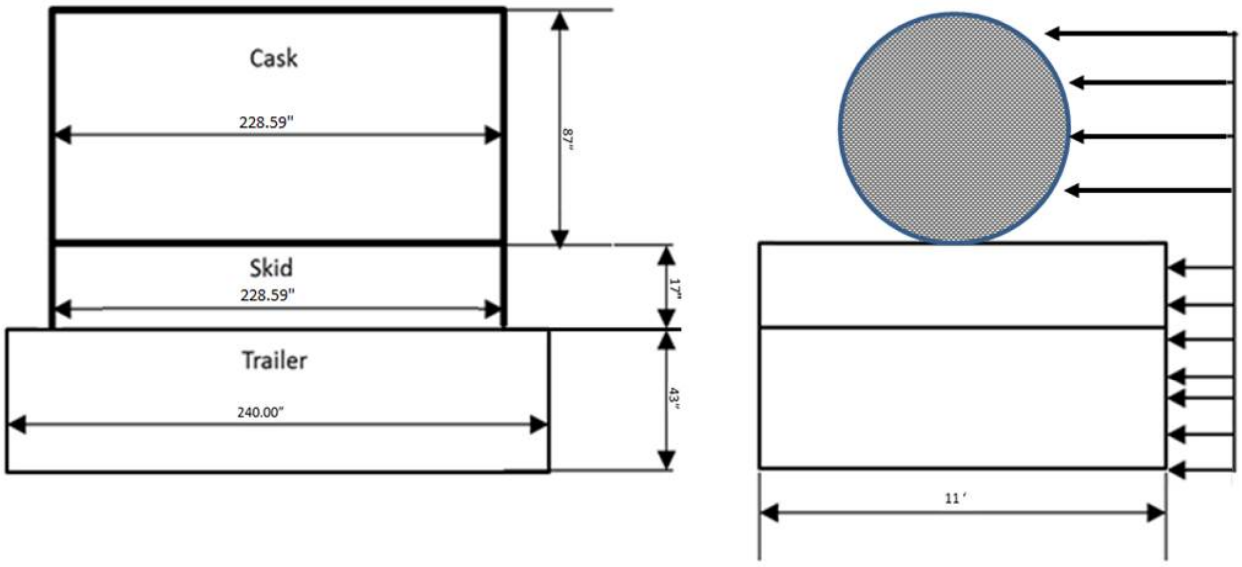

Figure 3.9.7-9
Arrangement of EOS-TC, Skid and Transfer Trailer at Rest

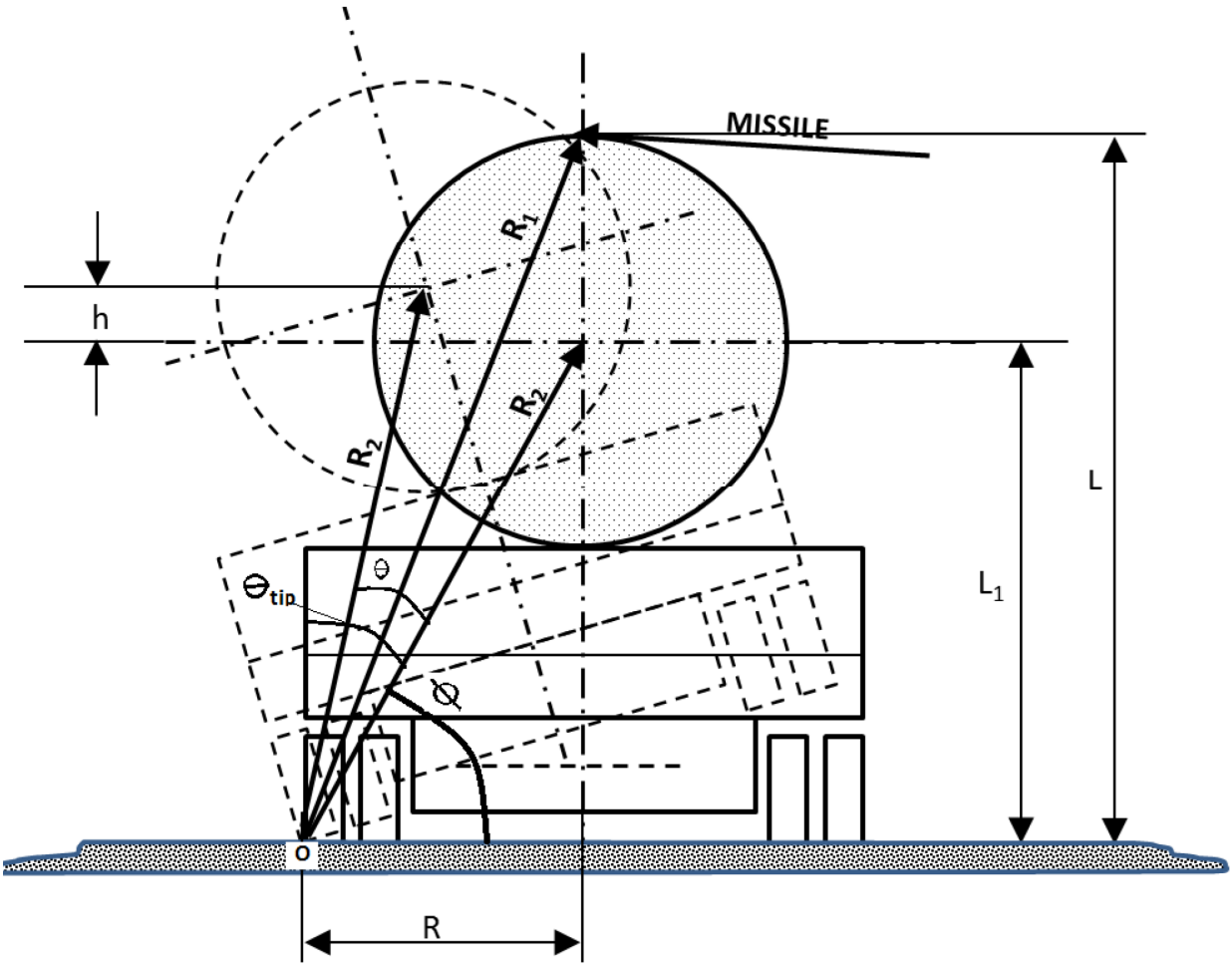

Figure 3.9.7-10
Stability Geometry of TC on Transfer Trailer

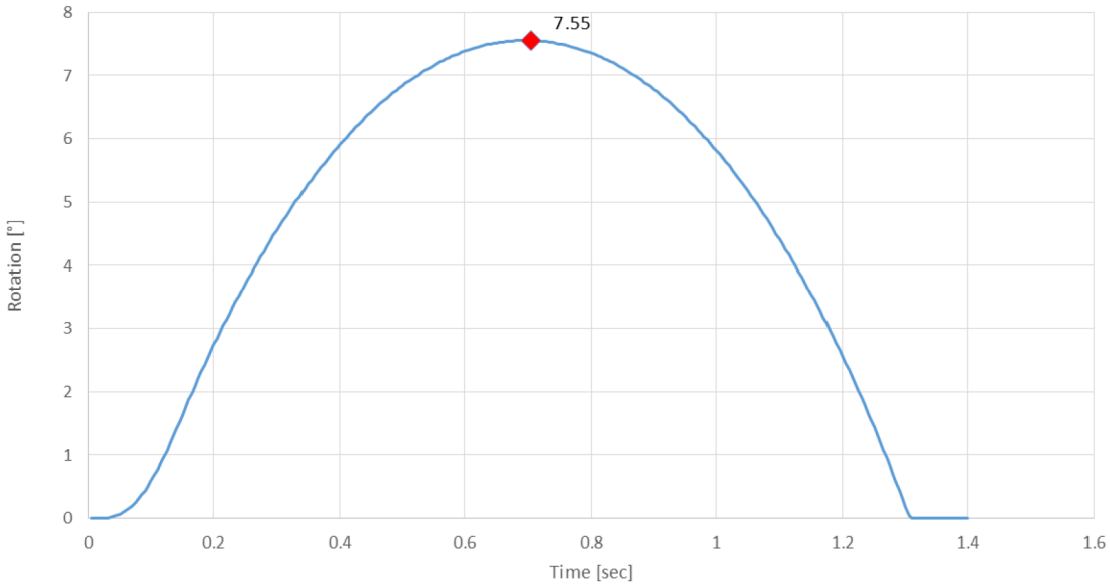

Figure 3.9.7-11
Angle of Rotation (Time-Dependent)-Wind and Missile Loading for EOS-TC